An investigation of plasma polymerization and copolymerization using fluoroaromatic compounds

Till, Clare

AN INVESTIGATION OF PLASMA POLYMERIZATION AND COPOLYMERIZATION USING FLUOROAROMATIC COMPOUNDS

by

Clare Till, B.Sc.(Hons.)

(Trevelyan College)

A thesis submitted

for the Degree of Doctor of Philosophy

to the University of Durham

1986

To

Kathleen, Dennis, Clive,

Diane and Sally-Anne,

With love

MEMORANDUM

The work described in this thesis was carried out in the University of Durham between October 1983 and August 1986. It has not been submitted for any other degree, and is the original work of the author except where acknowledged by reference.

Work in this thesis has formed the whole, or part, of the following publications:

1. An ESCA investigation of the inductively coupled RF plasma polymerization of fluoronaphthalene and fluoronaphthalene/hydrogen mixtures.
   H.S.Munro and C. Till, J.Polym.Sci.,Polym.Chem.Ed., 23(b), 1621 (1985).
2. ESCA studies of metal containing plasma polymers. Pt. 1. Incorporation of Mercury into plasma polymerized perfluorobenzene.
   H.S.Munro and C. Till, J.Polym.Sci.,Polym.Chem.Ed., 22(12). 3933 (1984).
3. A preliminary ESCA investigation of the plasma copolymerization of tetramethyltin and perfluorobenzene.
   H.S. Munro and C. Till, Thin Solid Films, 131, 255 (1985).
4. An ESCA and optical emission study of the inductively coupled RF plasma copolymerization of naphthalene/octafluoronaphthalene mixtures.
   H.S. Munro and C. Till, J.Polym.Sci.,Polym.Chem.Ed., in press (1986).
5. An ESCA and plasma emission study of the plasma polymerization of 1-fluoronaphthalene and octafluoronaphthalene.
   H.S. Munro and C. Till, J.Polym.Sci.,Polym.Chem.Ed., 24, 279 (1986).

6. The surface photopolymerization and copolymerization of perfluorobenzene and perfluorobenzene/benzene.
H.S. Munro and C. Till, J.Polym.Sci.,Polym.Chem.Ed., in press (1986).

7. An ESCA investigation of the inductively coupled RF plasma polymerization of N vinyl pyrrolidone.
H.S. Munro and C. Till, Polymer, submitted (1986).

ACKNOWLEDGEMENTS

I would like to gratefully acknowledge all the help and encouragement which has gone into my stay in Durham. This is directed especially to Dr. Hugh Munro for his glowing guidance as supervisor over the (non) continuous period of data collection which involved nothing but exciting chemistry. Thank you, Hugh. This gratitude is also extended to Clive for his bright ideas, and to all those coffees!

Nitro man, McTickle and the army man are also thanked for their friendship down in the ESCA den; as are Heiner, Andy and Jeff, all departed from this lab. to a, perhaps, less stimulating life outside: to Remington Steele for a roof over my head, even if the stairs were missing!

I am indebted to S.E.R.C. for the provision of an IT award.

This acknowledgement would not be complete without mentioning the deciphering skills, and patience, of Marion in typing this great volume.

Finally, to all who contributed to dinner times over the road - Cheers!

AN INVESTIGATION OF PLASMA POLYMERIZATION AND COPOLYMERIZATION USING FLUOROAROMATIC COMPOUNDS

by

CLARE TILL

ABSTRACT

The work detailed in this thesis concerns polymers synthesised by R.F. inductively coupled plasmas excited in fluorine containing monomer vapours.

The structure and bonding in a series of polymers prepared from perfluoroaromatic monomers by plasma polymerization was investigated by ESCA. The composition and structural features of these films were compared and contrasted with each other and with plasma polymers derived from the same parent compounds with lower degrees of fluorination.

Optical emission spectra, ∿260-600nm, from these plasmas were recorded and a correlation made between certain species fluorescing in the gas phase and functional groups within the polymer. An association has also been made between the peaks at ∿280 and ∿510nm in the optical emission spectrum. Difluorocarbene is responsible for the peak at ∿280nm but the peak at 510nm has an unknown origin.

The effect of copolymerizing a fluoroaromatic compound with a second component on polymer composition has been examined, where the comonomer has ranged from an inert gas to an organic hydrocarbon analogue. Copolymerization resulted in a stabilisation of the rearrangement mechanisms normally associated with the plasma polymerization of a perfluoroaromatic compound; $CF{=}CF_n$ and CF_2 groups were greatly reduced in intensity in the copolymer. The binding energy of the $CF{-}CF_n$ peak indicated that the component peak was, in fact, due to $CF{-}CF_{aromatic}$, *i.e.* copolymerization had also resulted in a greater retention of the aromatic nature of the parent fluorocompound.

Polymers were also prepared by irradiating the monomer vapour with wavelengths ≥130nm. Perfluorobenzene could not be polymerized with UV irradiation of wavelengths greater than 200nm, but could however be polymerized with wavelengths below 200nm. This produced a polymer whose composition, as determined by ESCA, was very similar to the composition of plasma polymers derived from the same monomer indicating that the mechanisms involved in both polymerizations are similar. Vibrationally excited ground state perfluorobenzene is thought to be involved in the reaction pathway.

CONTENTS

LIST OF ABBREVIATIONS

PFB	perfluorobenzene
1FB	1 fluorobenzene
OFN	octafluoronaphthalene
1FN	1 fluoronaphthalene
N	naphthalene
DFB	decafluorobiphenyl
OFB	octafluorobiphenyl
MFB	monofluorobiphenyl
NVP	N vinyl pyrrolidone
TMT	tetramethyltin
TMG	tetramethylgermanium
TMS	tetramethylsilane
DMP	dimethylpropane
FWHH	full width half height
VUV	vacuum UV

CHAPTER ONE

AN INTRODUCTION TO PLASMA POLYMERIZATION

1.1 Introduction

The term plasma describes the state of an ionized gas (see below) whilst plasma polymerization refers to the formation of polymeric materials under the influence of a plasma.

By definition a plasma refers to the partially ionized gaseoue state consisting of molecules, atoms and ions in both ground and excited states (including metastable states) and electrons such that the concentration of positively and negatively charged species result in dose to overall electrical neutrality.

Historically, the use of gas discharges really began in the 18th century. Both the work of Crookes (1879) and Thomson (1897) on the properties of cathode rays emitted from discharge tubes were connected with the discovery of the induction coil by Ruhemkroff in 1851.[1] These initial experiments opened up the pathway for research into the nature of such discharges. The role of the electron causing ionization (of the gas molecules) and conduction and the nature of other charged species present were established by the early 1900s. In 1928 Langmuir[2] coined the word plasma to denote the state of ionized gases formed in an electrical discharge.

Plasmas are characterised by their electron density and the average electron energy; numerous forms of plasmas can be found, both in nature and in the laboratory dependent on these two parameters.[3] Figure 1.1 indicates the variety of plasmas known. Two types of plasma are of most interest to chemists, these are the 'hot' and 'cool' plasmas.

The 'cool' - a non-equilibrium-plasma found in a glow discharge experiment,is characterised by electron densities

PLASMAS FOUND IN NATURE AND IN THE LABORATORY

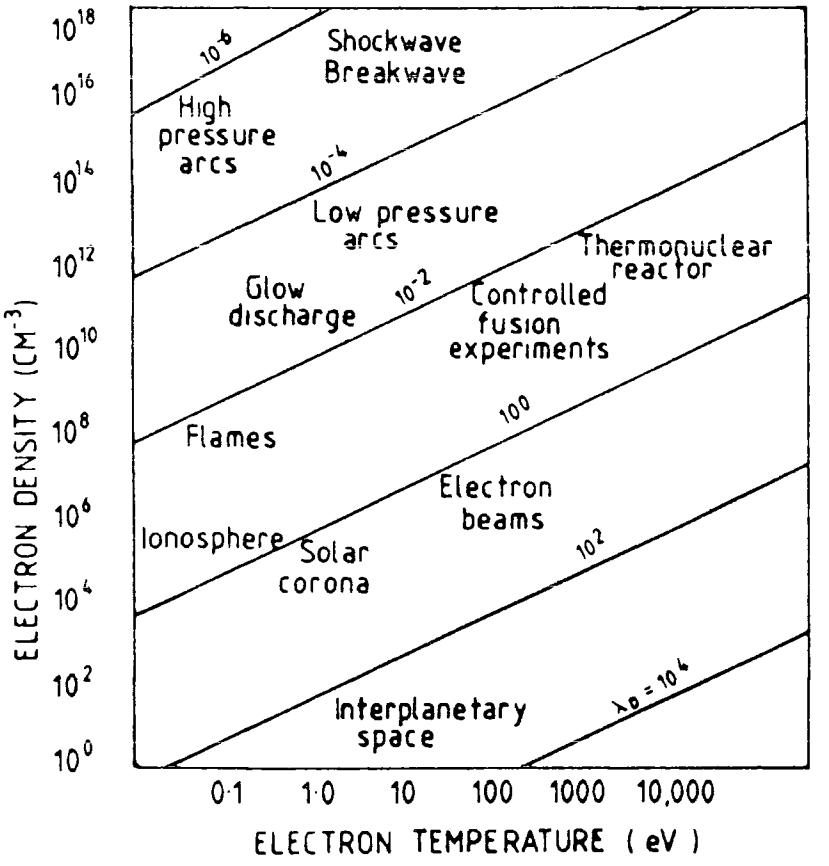

FIGURE 1.1 Characterization of Plasmas by their electron temperatures and electron densities

in the range 10^{9}-10^{12} cm^{-3} with average electron energies in the range 1-10eV. These plasmas are characterized by electron temperatures which are some two orders of magnitude greater than the Boltzmann temperatures of the ions and molecules which are roughly ambient.

This is in contrast to the 'hot' or equilibrium plasmas of similar electron densities. This class of plasma is characterized by a very high gas temperature which is equated approximately to the electron temperatures. Due to the low thermal stability of organic molecules, this type of plasma finds its use in the compositional analysis of materials. The sample of interest is fed into the high temperature plasma where destruction of the material occurs to form atoms; atomic

absorption is then followed by an associated emission, where analysis is achieved through the spectral analysis of this emission.[4] This analytical technique is known as inductively coupled Plasma-Optical Emission Spectrophotometry (ICP-OES), and can be applied to the analysis of inorganic and metal[5] systems as well as organic systems (which may include biological tissue).

The 'cool' plasma has found a use in several areas of applications:

(i) Synthetic Organic/Organometallic Chemistry

The work in this area has been dominated by Suhr[6] and coworkers. Initial experiments were hampered by the very small yields obtainable through plasma synthesis; more success was achieved by the selection of experimental plasma conditions which avoided high electron energies and elevated temperatures, which reduced the amount of damgge tothe organic molecule. All organic vapours, liquids or solids react in a glow discharge to some extent, so an almost infinite number of organic plasma reactions are possible, although percentage yields may vary from very small to almost a 100% conversion . This, together with the amount of energy available from the plasma in comparison to conventional and photochemical techniques (>10eV *cf.* 4 and 6eV respectively[7]) - which means that super-excited states can be obtained which are beyond the reach of other synthetic methods - makes synthesis within a plasma so appealing.

(ii) Surface Modification

A second major area of interest is the application of plasma techniques to the surface modification of polymers. This interest falls into three groups:

(a) Surface grafting[8] where the polymer surface is exposed to a plasma to create reactive sites. This activation of the surface initiates a conventional free radical polymerization process at the surface when the graft monomer is introduced into the reactor (no plasma). For example, attention has been placed on the modification of surfaces of fibres for improving wettability[9] and flame retardancy[10] purposes.

(b) In the second group surface modification is effected by direct and radiative energy transfer from plasmas excited in inert gases. This is known as CASING - crosslinking by activated species of inert gases - and has been used to improve adhesive bonding,[11] wettability,[12] and printability of polymers.

(c) A third technologically important area of the use of 'cool' plasmas for surface modification is in the microelectronics industry, where the plasma, particularly oxygen and halogenated gases, are used to selectively etch or remove organic polymeric phases[13] in the production of integrated circuit chips. This is a particularly active area of research with the current trend towards a totally vacuum lithographic process.

(iii) Polymer Synthesis

The third area of application, one which perhaps equals the interest of polymer modification, is that of *in situ* polymer synthesis.[14] The plasma polymerization of organic and organometallic compounds has been a particularly active area of research, especially since the process offers several advantages over conventional polymer synthesis; not least the

often superior nature of the deposited thin film in both physical and chemical properties. Starting compounds do not need to contain functional groups normally associated with conventional polymerization and this coupled with the one step synthesis in a 'clean' environment makes plasma polymerization a particularly attractive method of polymer synthesis. It is in this area of application that the work in this thesis has been devoted to.

1.2 Fundamental Aspects of Plasmas

Theoretically a plasma - "afourth state of matter" - by definition must be electrically neutral, a condition which is satisfied when the dimensions of the discharged column are significantly greater than the Debye length[3] λ_D,

$$\lambda_D = \left(\frac{E_o kTe}{ne^2}\right)^{\frac{1}{2}}$$

which defines the distance over which a charge imbalance may exist, where E_o is the permitivity of free space

k is the Boltzmann constant

Te is the electron temperature

n is the electron density

and e is the charge in the electron.

The ionization of molecules within the plasma zone is essential if the discharge is to be initiated and maintained. Electrons within the plasma are accelerated by the electric field and produce further ionization by collisions with other species. Collisions between an electron and a gas molecule result in one of two states; an elastic collision in which very little energy is lost or transferred by the electron,[3]

or an inelastic collision which results in the transfer of usable energy from the electron to the molecule. When the electron does not have enough energy to cause ionization of the molecule, the transfer of energy in an inelastic collision results in the production of a higher energy state of the molecule where the excess energy can be stored in rotational, vibrational and/or electronic excitation. It is from such inelastic collisions, of major importance in plasma polymerization, that electron energy is continuously lost. After collision the electron gains energy from the electric field, the amount of kinetic energy picked up before further collision is dependent on the mean free path of the electron in the gas[15] which is connected to the pressure of the system; at too high a pressure, the mean free path is very short and the amount of energy gained by the electron in between collisions is not very large. Too low a pressure results in a long mean free path such that gas collisions are not important. This results in a typical working pressure range for plasma polymerization of 0.05-10 torr. At charge densities of around 10^{10} cm^{-3} it has been calculated that the average lifetime of an electron against recombination is around a millisecond.[16]

The average velocity, $\bar{c}$ of an electron between collisions is given by:[17]

$$\bar{c} = \left(\frac{Me^2E\lambda}{m^3}\right)^{\frac{1}{4}}$$

where M is the mass of the heavier particle

e is the electron charge

E is the electric field

λ is the electron mean free path

and m is the electronic mass .

Expressions describing the electron energy distribution in terms of energy input, discharge dimensions and gas pressure lead to a Maxwellian distribution[16] of electron energies shown in Figure 1.2. Such numerical solutions are only possible

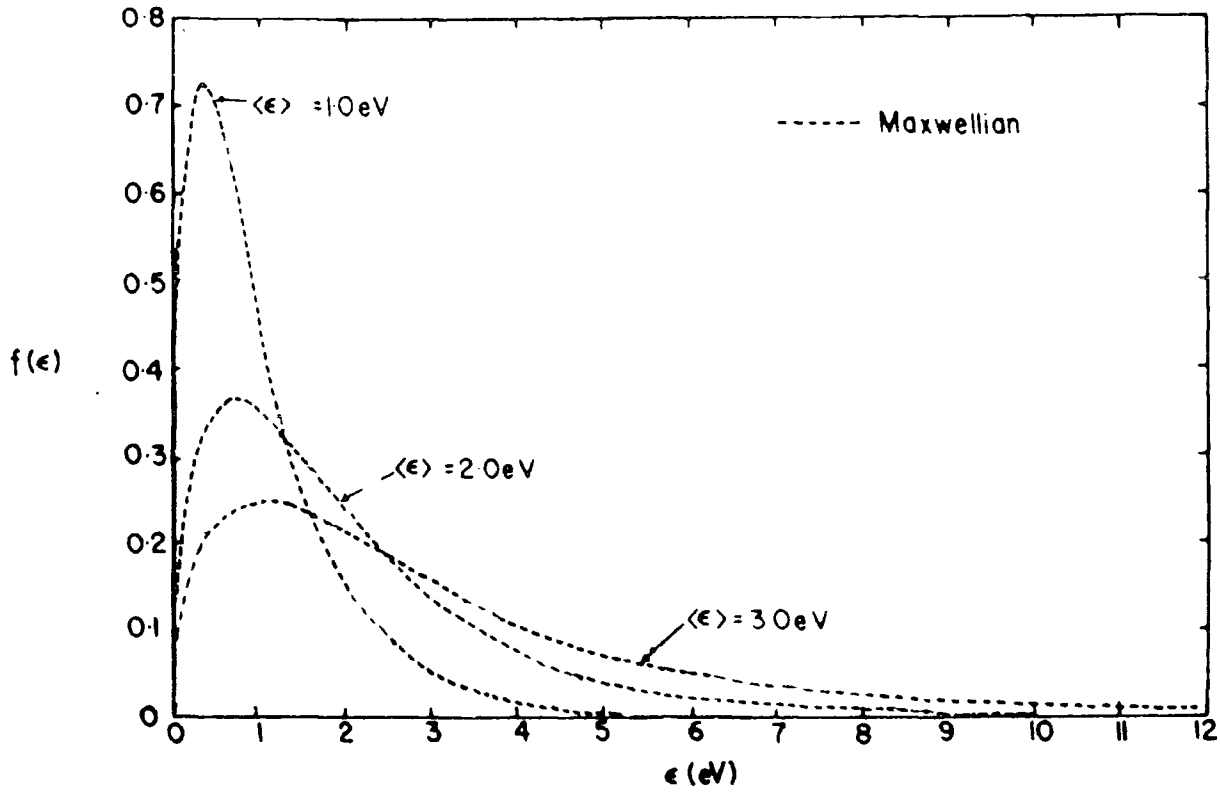

FIGURE 1.2 Maxwellian energy distributions of electrons in an inert gas

for simple systems, but the form of the distribution has been analysed experimentally by probe measurements[18] and direct electron sampling.[19] From Figure 1.2 it can be seen that the average electron energy will be in the order of 2-3eV,[15] *i.e.* the electron energy distribution is such that it is more effective in producing excitation than ionization. The degree of ionization is, in fact, low 10^{-4}-10^{-7} cm^{-3} with neutral species predominating in a non equilibrium plasma.[6] Since only the electrons in the tail of the distribution will be effective in causing ionizations, where ionization potentials are typically 10 + eV, it may be expected that some of the major chemistry

occurring within a plasma is connected, not with ionization, but with excitation; since typical bond dissociation energies of organic compounds lie well below 10eV - see below. This aspect is examined further in Chapter Seven, where the photopolymerization of PFB, with energies below the ionization potential of the molecule, is discussed.

TABLE 1.1 Energies associated with a glow discharge and some typical bond energies

Energies (eV) associated with a glow discharge:	
Electrons	0-20
Ions	0-2
Metastables	0-20
Visible/UV	3-40

Bond energies (eV):			
C-H	4.3	C=O	8.0
C-F	4.4	C-N	2.9
C-C	3.4	C=C	6.1

The collision process, shown in Figure 1.3, results in the emission of electromagnetic radiation as de-excitation of the various excited species occur. Some of this output is in the visible region, this has led to the term 'glow discharge' and gives rise to the characteristic colours for plasmas excited in a given system. However, most of the intensity of the emission is, in fact, in the UV/vacuum UV region as has been shown for Ar plasmas.[20] It is this component of the electromagnetic spectrum, together with electrons, which are of most use in the direct surface modification of polymers.

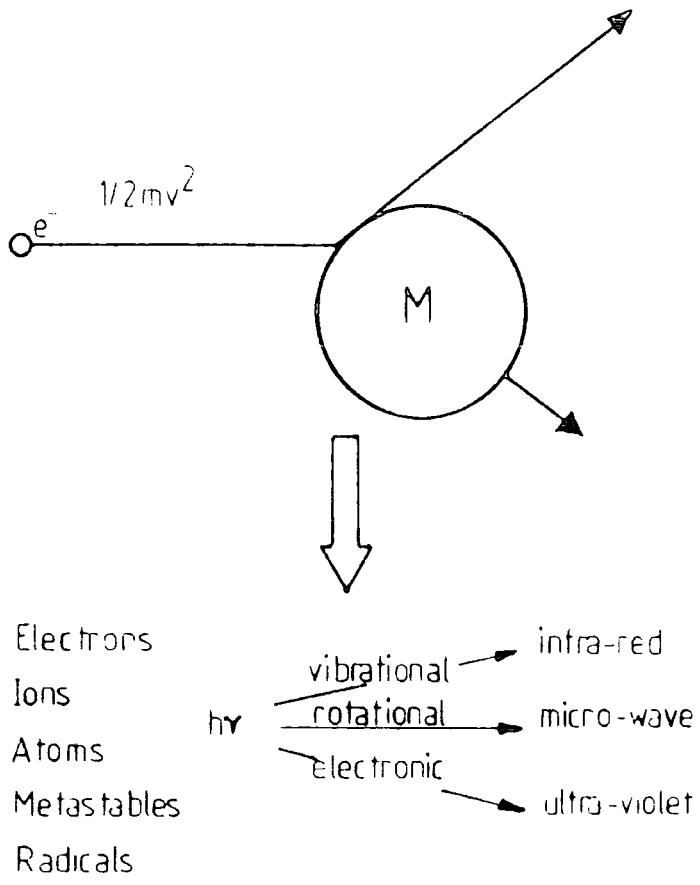

FIGURE 1.3 Collision Processes in a Plasma

Both the IR and visible components are absorbed, but the IR radiation - which can be strongly absorbed - is dissipated through thermal reactions which produce heat.[12]

1.2.I Reactive Species in Plasmas

The reactive species in a plasma resulting from ionization, fragmentation and excitation processes resulting from electron impact include ions, neutral species, atoms, metastables and free radicals (either ground or excited states). It should be remembered, however, that a non equilibrium plasma is only a partially ionised gas, in fact it has been stated that at 1 torr the concentration of neutrals is $10^{16} cm^{-3}$.[6] which is some 4-6 orders of magnitude greater than the number of ionic species. Together with the electrons and the electromagnetic radiation previously noted, a typical plasma constitutes

a relatively complex entity, providing a variety of energetically available mechanisms for reactions within the plasma which result in polymerization. The variety of species present in a plasma present a whole host of reactions which are possible between the various species, the importance of each depends on the vapour in which the plasma is excited. It should be remembered that since a plasma is electrically neutral, the number of positive species must balance the number of negative species in the steady state plasma, *i.e.* the formation of charge and its removal which occur independently but simultaneously must balance.

The reactive intermediates involved in polymer formation are such that extensive molecular rearrangements are seen to occur in the perfluoroaromatic[21] compounds where the films produced are highly cross-linked. Although there may be complex interactions between the reactive intermediates generated in a plasma, under a given set of conditions a plasma excited in a given monomer[†] will produce a well characterized product or series of products.

1.2.II Plasma Reactions

Although the present knowledge of reactions occurring within plasmas excited in organic/organometallic compounds is rather incomplete, it is possible to give general types of reactions which are common. This knowledge is based on various kinds of investigation based mainly on analysis of

---

[†] The term monomer is used here as the generic name for the low molecular weight starting material. Due to the complex nature of the processes occurring in a gas plasma, it is often not possible to readily identify the true precursors to polymerization.

the product gas trapped out downstream of the reactor. Typical reactions which occur in a glow discharge can be summarized as follows:[7]

(a) Generation of reactive species - under suitable conditions the recombination of atoms formed in a discharge is so slow that it is possible to study their reaction with organic compounds outside of the discharge zone.[22] Whilst products obtained in plasmas of aromatic compounds have led workers to suggest the intermediate presence of arynes.[23]

(b) Isomerization - *e.g.* the *trans* isomer of stilbene when subject to a glow discharge yields both the *cis* and *trans* isomers.[24]

(c) Oligermerization and dimerization - *e.g.* benzene has been reported as being converted mainly into biphenyl under the action of a plasma[25] (under certain conditions).

(e) Elimination - *e.g.* partially halogenated hydrocarbons show elimination of hydrogen halide.[26]

In general most plasma reactions can be described as:

$$M \xrightarrow{\text{Excitation}} M^{*} \xrightarrow{\text{Bond Breakage}} I \xrightarrow{\text{Stabilization}} \text{Product}$$

Where M^{*} is the excited neutral or ionic species and I is the neutral or ionic intermediate.

1.3 Plasma Techniques

In general there are three distinct aspects which are of interest; namely the source of electrical power used to sustain the plasma, the coupling mechanism and what can loosely be termed the plasma environment. This is illustrated schematically in Figure 1.4.

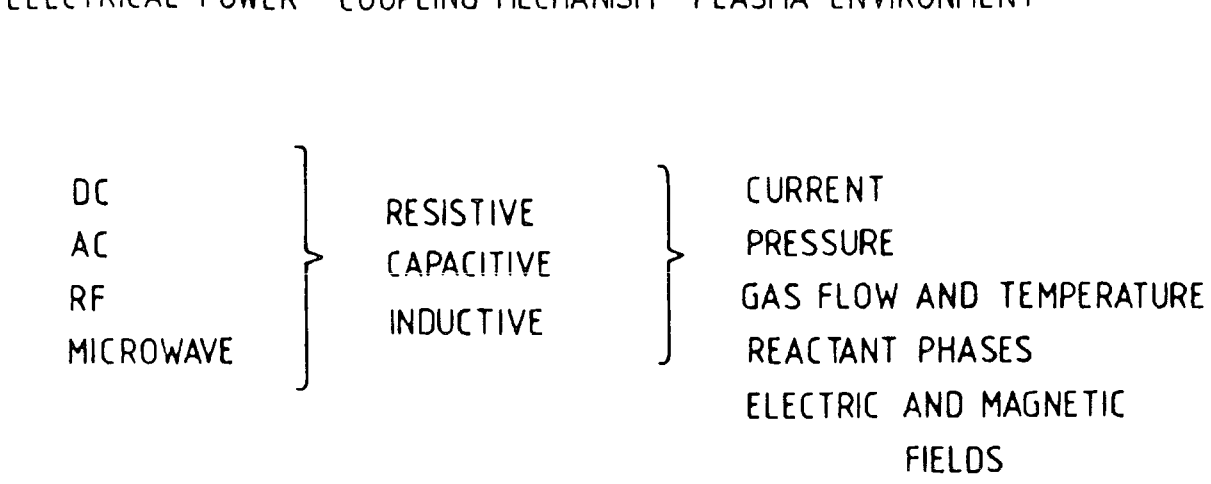

FIGURE 1.4 Elements of a glow discharge experiment

From Figure 1.4 it can be seen that there are two main types of coupling mechanisms, *i.e.* direct and indirect.[22] In the direct method - resistive coupling - the glow discharge is initiated between electrodes, and thus the electrodes are part of the plasma environment. As such, they may be involved in the plasma reactions, and polymer deposition if it occurs is on to the electrodes. The indirect method - capacitive and inductive coupling - allows the plasma to be formed such that the coupling mechanism is isolated from it. This is achieved by means of electrodes placed externally to be reactor or by a copper coil - electrodeless discharge - wound round the external surface of a cylindrical reactor respectively. The greater flexibility and closer control over operating parameters has led to the choice of the latter coupling mechanism for the work contained within this thesis. Electrodeless

microwave discharges may also be excited inductively using tuned cavities.

Indirect coupling mechanisms can only be used however using frequencies higher than 1MHz;[6] below this frequency, direct contact of the electrodes with the plasma is necessary for sufficient energy transfer to take place to sustain the plasma. With internal electrodes, and low pressures, experiments have been performed over a wide range of frequencies from AC to the RF region. Yasuda[27] *et al* have employed frequencies of 60Hz (AC), 10kHz (AF) and 13.56MHz (RF). Since it is well known, however, that some polymers produced by plasma polymerization are particularly system dependent[27] (*e.g.* power and pressure), there have been surprisingly few studies carried out to characterize the product/s of a given plasma sustained by different energy sources, to determine the nature of the effect of exciting frequency on the product.

The main operating parameters of a glow discharge experiment are those of power input and operating pressure, where power may vary from 0.1 watt to a few kilowatts and pressure for $\sim$0.01 torr to atmosphere depending on experimental conditions.

Operating pressures using an RF discharge can range from $\sim$0.01 to 1.0 torr whilst the power range is from 0.1W to 150W utilizing commercially available equipment. Low power levels (<1.0W) are generally difficult to sustain, but when using RF power a stable plasma can be accomplished by pulsing the power input. Typical parameters used in the work herein were 5-50W and 0.075 torr.

Microwave discharges are less stable at low pressures.

The use of an increased pressure leads to an increase in the gas temperature which can cause decomposition of organic species and is therefore not a method commonly used for plasma polymerizations. At higher power levels (>50W), especially when working with DC discharges some special cooling systems are necessary for the electrodes, although the use of D.C. does allow pressures of up to 1 atmosphere, but as with the microwave discharge, a higher pressure will lead to a higher temperature which again limits its applications in plasma chemistry. Although the above discussion relates to all types of microwave discharges it is particularly applicable to a small microwave cavity, thermolysis of organic compounds does not seem to be such a problem when using very large volume plasmas - Leybold-Hareaus have a pilot plant in operation for plasma polymerization based on microwave excitation.

Low frequency and DC discharges are generally characterized in terms of the voltage and current supplied to the electrodes. Typical operating voltages are in the range ∿10-100V, and ∿1A at pressures of ∿1 torr. For RF and microwave plasmas the situation is less straightforward, the requisite instrumentation is needed to measure the power in the plasma, and to match the impedence of the generator with that of the coil volume such that maximum power is transferred to the plasma.

1.4 Plasma Polymerization

Polymer formation within a plasma may be achieved by either injecting an organic or organometallic vapour into an inert gas discharge, such as argon, or by creating a plasma

in the organic/oragnometallic vapour, where the vapour may be pure or may consist of a mixture of gases. Under such conditions, the deposition of polymeric material onto surfaces exposed to the plasma is often observed.

Although the formation of polymers in a glow discharge has been known for many years[28] - (indeed the first polymers were thought of as a by-product of the discharge experiment which caused many problems due to polymer removal caused by their inertness and insolubility[29]), the detailed mechanism of polymer formation is still not understood. The process of plasma polymerization has been classified by Yasuda into 'plasma-induced' polymerization and 'plasma-state' polymerization.[30] The former process requires monomers to contain polymerizable structures, *e.g.* olefinic double bond, triple bonds or cyclic structures, and mechanistically is essentially the same as conventional addition polymerization where the plasma is used to initiate polymerization either by direct or indirect contact.[31] This is in contrast to 'plasma-state' polymerization which occurs only under plasma conditions. Although when conventional monomers, such as vinyl compounds, are used in plasma polymerization, both plasma state and plasma induced polymerizations can, and may, occur.[32]

Under plasma conditions, the final product is determined by the competing processes, *i.e.* ablation and polymerization which occur within the plasma. This has been termed Competitive Ablation and Polymerization[32] (CAP) and is represented schematically in Figure 1.5. As an extreme example plasmas excited in CF_4 do not form polymer films due to the domination of ablative processes over polymerization reactions, caused

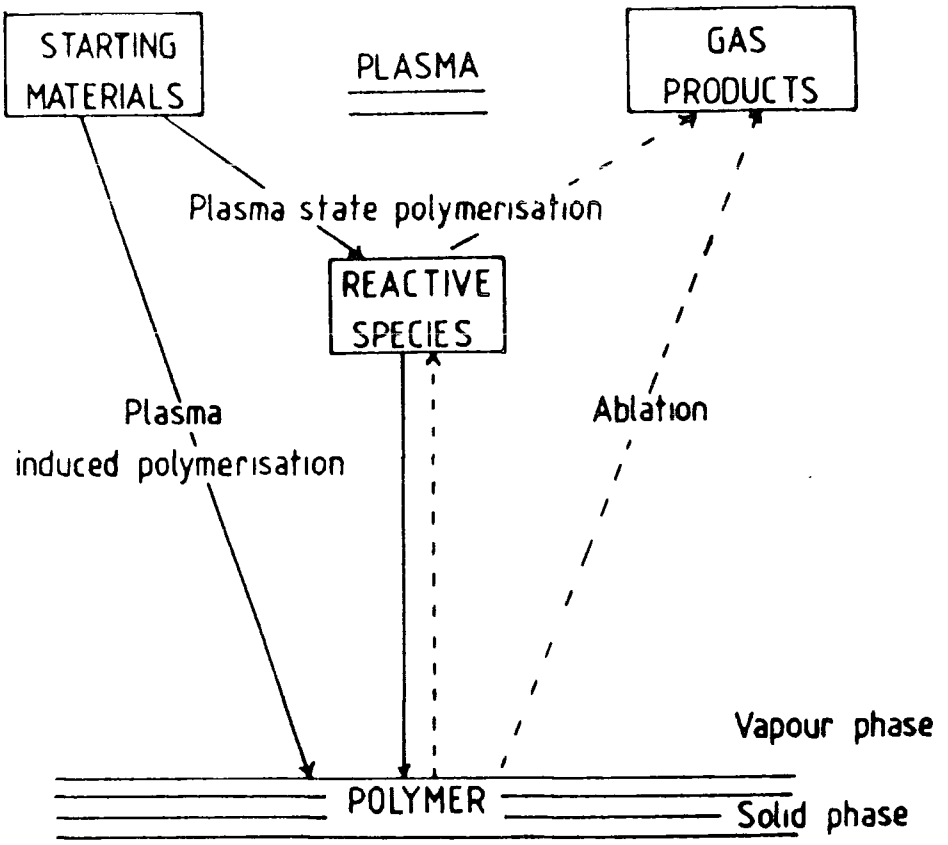

FIGURE 1.5 Competitive ablation and polymerization in glow discharge polymerization

by the abundance of reactive fluorine species created in the plasma, such that etching proceeds more rapidly than deposition.[33] The polymers produced by fluorocarbon plasmas are thus the result of a balance between these two processes; a greater fluorine content favouring ablation whilst a higher hydrocarbon content favours polymer deposition. In the preceding example, deposition was observed by the introduction of hydrogen into the monomer flow system only to be followed by etching when the hydrogen flow was stopped.[33]

It has been noted that the overall CAP mechanism of polymer formation is extremely dependent on the discharge conditions.[32] Yasuda has suggested the use of a composite

parameter, $^{W}/_{FM}$, relating the discharge power to the unit mass of monomer which may be used to correlate the polymerization processes occurring in the glow discharge.[34]

Where W is the discharge power (watt), this generally determines the amount of fragmentation of the monomer; a higher power causing more fragmentation.

F is the monomer flow rate, this determines the residence time of the monomer in the reactor, together with the pressure (and hence pumping speed) and M is the molecular weight of monomer.

This parameter allows a comparison to be made between different monomers in terms of the energy input per unit mass in relation to the rate of deposition of the end product. For this comparison to be valid, however, the polymerization must be performed under identical experimental dimensions, *i.e.* the reactor configuration also plays a part in determining polymer product. The nature and distribution of the polymer formed also strongly depends on other experimental parameters such as the geometrical arrangement of monomer inlet and outlet in relation to the region of energy input,[32] and the reactivity of the starting material.

An excellent review on the work of Yasuda *et al* has appeared in book form[32] and covers such topics as a comparison of plasma polymerization with conventional polymerization and and mechanistic aspects of plasma polymerization, along with a chapter on general characteristics of plasma polymers. This review forms a valuable addition to the present literature on plasma polymerization and the serious reader is urged to peruse this volume even with the foreword that all interpretations presented are strictly those in accordance with the authors' view.

1.5 Plasma Diagnostics

Comparatively little is known about the processes occurring within a plasma despite the increasing technological importance of plasma chemistry, especially in the field of micro electronics. Yet the success of a particular process leading to a desired end product can often depend critically on a delicate balance between the experimental variables inherent in a plasma process. It is for this reason that plasma diagnostic techniques are currently an important, and popular, area of research.

Diagnostic techniques can conveniently be divided into three groups dependent upon the position of, and interference caused by, the analytical probe, *i.e. in situ* non-intrusive, *in situ* intrusive and *ex situ*. Although most techniques perturb the plasma to a greater or lesser extent, perhaps the most non-intrusive method is based on analysis of the spectral output of a plasma which is why optical techniques in plasma chemistry are so popular.[35a]

Optical emission spectrophotometry (OES) involves the analysis of the optical emissions, ranging from the vacuum-UV to the far infrared which are emitted by most gaseous plasmas. One important example of the use of OES is in the end point detection of etching of the exposed surface of silicon oxide in the fabrication of silicon microcircuits using a CF_4-O_2 plasma.[35b] Three principal species were found to be responsible for the main emission, F and O atoms and CO molecules; the authors concluded that F and O were active in the etching process, since in the presence of silicon wafers the emission from these two atoms was drastically reduced, but that CO

was not. In fact only F is responsible for silicon etching, the oxygen caused an increase in etching by reacting with CF_4 to liberate more free fluorine atoms.

The use of OES has also been used to monitor deposition in the plasma polymerization of halocarbons with the simultaneous sputtering of gold or aluminium.[36] It was seen that the ratio of emission intensities of Au/CF_2 and Al/Ar can be used as processing parameters in the preparation of metal doped polymer films. Similarly the emission, and hence the gas phase composition, in a copolymerization experiment has been shown to be very important with regard to the composition of the deposited polymer film.[37] This will be discussed in much greater detail in Chapters Three and Four on the copolymerization of fluoroaromatic monomers with their hydrocarbon analogues, and with the tetramethyl compounds of group IV.

However, this apparently very useful tool does have its limitations. One of the main drawbacks is that only electronically excited states in the gas phase which relax by the emission of photons can be monitored. Also, whilst being qualitatively very useful, the technique can only give semi-quantitative information since the intensity of emission from a species is not directly proportional to its concentration. This arises due to problems in determining probabilities for excitation and emission under a particular mode of excitation for the species under examination.[35a]

Laser induced fluorescence (LIF), however, has the advantage of being able to probe directly the ground state (or metastable state) populations of the plasma, particularly radicals and ions. This probe has been used to monitor $[CF_2]$ in various

discharge environments in $CF_4/O_2/H_2$ plasmas.[38] As a function of applied power, the CF_2 concentration was found to increase, which was in agreement with the work carried out by Hargis and Kushner.[39] It was seen that $[CF_2]$ had an inverse relationship to the $[O_2]$ and was directly proportional to $[H_2]$. As expected, $[CF_2]$ decreased as O_2 was added to the plasma due to oxidation reactions of CF_4 to form CO and CO_2 and form free fluorine atoms. In the presence of hydrogen, however, an increase in abstraction reactions occurred which resulted in HF formation and an increase in $[CF_2]$. CF_2 concentration has also been examined as a function of the parent fluorocarbon, hexafluoroethylene was found to generate about four times as much difluorocarbene as tetrafluoromethane plasmas.[39]

LIF, as with OES, has its limitations. Significantly, the species to be detected must fluoresce with a reasonable quantum efficiency - which is usually the case for atoms and diatomics in a low pressure environment. However, it need not be the case for larger polyatomic molecules which can return to the ground state non radiatively, or possibly photo-dissociate in the electronic excited state.

Another *in situ* probe is in the use of infrared spectroscopy, to monitor the absorption of ground state species. This method has been used to monitor air plasmas,[40] and to investigate the decompostion of CF_4 and C_2F_4 in plasmas.[41] This technique, suffering the same limitations as OES, is typically a much less sensitive technique requiring either a high concentration of absorbing species or a long optical path length.

An example of an *in situ* intrusive technique is that used to sample the plasma medium directly to gain information about

electron energy distributions.[18] Here the probe is inserted into the plasma environment and causes perturbations to it.

A common characteristic of *ex situ* techniques is that a sample of the plasma zone is analysed outside of the plasma region. For example, a differentially pumped mass spectrometer has been mounted downstream of various fluoro and fluorohydrocarbon plasmas to analyse the gaseous effluent.[42] A major disadvantage to these techniques is readily apparent, namely that there is always a doubt about the accuracy of the results in relation to the real plasma environment, *i.e.* that what is detected at the probe has been formed after leaving the plasma zone. Since the sample contains many highly reactive species-ions, free radicals, *etc.* - there is always the possibility that there has been some reaction, either inter- or intramolecular, or change in energy distribution during the journey from the reactor.

From the above discussion it can be seen that no one technique is adequate to characterise plasma chemistry. Ideally a combination of diagnostic tools should be available to the plasma chemist to obtain the maximum amount of information about the system under study. Great care and caution must be used, however, in interpreting the diagnostic data. This can be especially important when trying to determine the influence or importance of a particular species in a plasma process.

An example is seen in the plasma polymerization of fluorocarbon systems where, due to the presence of CF_2 in the gas phase of all fluorocarbon plasmas, CF_2 has been suggested as being an important polymer precursor. Whilst this indeed may

be so, the presence of a particular species does not mean that it is involved in polymer formation - it may even be a by-product of the process under study. This will be discussed in more detail in context of the optical emission data obtained from copolymerizing PFB with another monomer (see Chapters Two and Three).

1.6 Polymer Properties and Characterization Techniques

Following the preceding discussions on the principles and techniques involved in the application of gas plasmas to organic polymer film formation, the following section on the analytical techniques which have been used to characterize these materials is essential: without this section the chapter would be incomplete, for without an analysis of the polymer to date information regarding the behaviour of an organic in a plasma would be missing, *e.g.* the rearrangement rather than elimination behaviour shown by perfluoroaromatic molecules in the processes leading to deposition.

The techniques used to study plasma polymers can be broken down into two groups: those used to study bulk properties and those used to characterize the surface of the film. Table 1.2, although not comprehensive, gives a list of the analytical methods which have provided the most insight into the structure, both physically and chemically, of these materials.

The bulk property analysis techniques will be examined briefly here for the sake of completeness, the surface characterization techniques will however be considered in more detail as appropriate to this thesis. The analysis of the plasma

TABLE 1.2 Analytical Techniques used to study Plasma Polymers

A. Bulk Properties

Micro analysis

Electron Spin Resonance Spectroscopy

Nuclear Magnetic Resonance

Dielectric Properties

Infra-red Spectroscopy

Differential Scanning Calorimetry and Thermal Gravimetric Analysis.

B. Surface Properties

Contact Angles

Microscopic Studies

Reflectance I.R.

ESCA - Electron Spectroscopy for Chemical Applications

SIMS - Secondary Ion Mass Spectroscopy.

---

polymer produced by N Vinyl Pyrrolidone will be used as an example in the appropriate places.

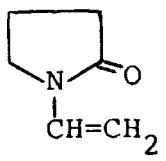

N Vinyl Pyrrolidone (NVP)

Plasma polymerized films have been shown to be of a reproducible nature both in terms of composition and properties if the plasma polymerization experiment is repeated under identical conditions, *i.e.* the plasma processes leading to deposition are highly system dependent. It is for this reason that although various papers, written by other authors may have been referenced throughout the thesis, the data contained therein can only be used as an independent interesting observation,

rather than for a direct comparison of, the work detailed within this thesis. This should be borne in mind by the reader.

One of the most important bulk properties of plasma polymers is that a large quantity of free radicals are often trapped within the polymer matrix. These arise during film formation. A steady state concentration of activated species is not reached in a plasma such that those quenched in film formation (or by production of gas phase products which leave the reactor as exhaust gases) are not balanced by the quantity formed. Thus, the rapidly growing film incorporates free radicals by the reaction of one part of a diactivated species with the forming film, the other part - the free radical - does not have time to react before it is trapped unquenched within the crosslinking matrix. These trapped radicals convey a reactive nature upon the polymer film and may affect the performance of these films in a particular application, since the film can 'age' by gradual reaction of these trapped species with oxygen, water, *etc*. The use of ESR to determine spin density,[43] has shown the quantity of trapped free radicals to be related to the chemical structure of the monomer; saturated aliphatic hydrocarbons yield the lowest quantity whilst highly unsaturated monomers produce the highest level of trapped free radicals in the produced polymer films.[32]

Infra red spectroscopy has been used to examine the polymer derived from NVP as a function of power of the plasma. The complex nature of plasma polymers makes the precise interpretation of their IR spectra difficult. However, useful information concerning the general nature and perhaps mode of reaction

(when more than one reactive functional group is present) can often be derived. Figure 1.6 shows the spectra produced by films formed in 8 and 50W NVP plasmas respectively, all other variables were constant. Also shown in Figure 1.6 is the

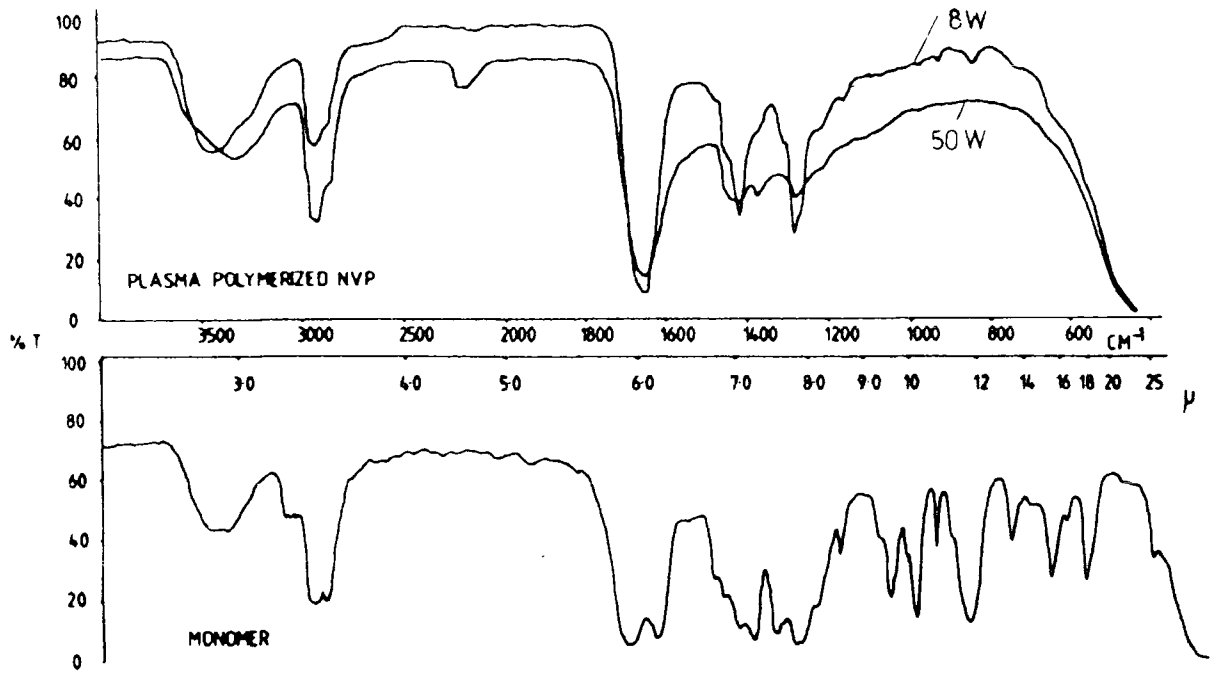

FIGURE 1.6 Infra-red spectra of plasma polymerization NVP at 8 and 50W cf.contact spectra of NVP monomer

'contact' spectrum of the liquid monomer. In general, the IR spectra of both of the plasma polymers contain most of the major peaks associated with the parent monomer above 1200 cm^{-1}. Not surprisingly, most of the peaks in the 'fingerprint' region of NVP have been lost, or greatly reduced in intensity, in the polymers. One of the most interesting features of the polymer spectra is the loss of one of the major peaks, cf. the parent monomer, in the 1600-1750 cm^{-1} region. The two peaks, at $\sim$1620 and 1690 cm^{-1} respectively, arise from C=O and C=C groups in NVP and are replaced by the appearance of a peak at $\sim$1655 cm^{-1} in the spectra of both plasma polymers. This is

suggestive of the lack of C=C unsaturation present in the polymer, *i.e.* polymerization reactions in the plasma would appear to be mainly through opening of the C=C bond in the NVP monomer.

A number of important differences are apparent between the IR spectra of the two plasma polymers; namely as the power input, and hence plasma density increases, the peaks broaden out considerably and become less well resolved indicating the greater amount of similar environments, *i.e.* the greater amount of cross-inking which has occurred in the 50W plasma polymer. The greater fragmentation at 50W may be inferred by the presence of a new peak in the spectrum of this polymer; the peak at 2,200 cm^{-1} which may have arisen from the formation of C≡N, N=C=O or C≡C groups during film formation - none of these groups are present in the parent molecule.

The spectra of the 50W plasma polymer was recorded again 4 hours later (not shown in Figure 1.6). On the whole, the two spectra were very similar, there were however slight changes. One alteration was in the intensity of the C=O peak which had increased slightly in the aged polymer sample and the other difference was in the formation of broad shoulders, of unknown origin, in the 1850 and 2600 cm^{-1} regions.

The increase in the carbonyl peak may be due to the reaction of oxygen or water with the free radicals present in the polymer film, *i.e.*

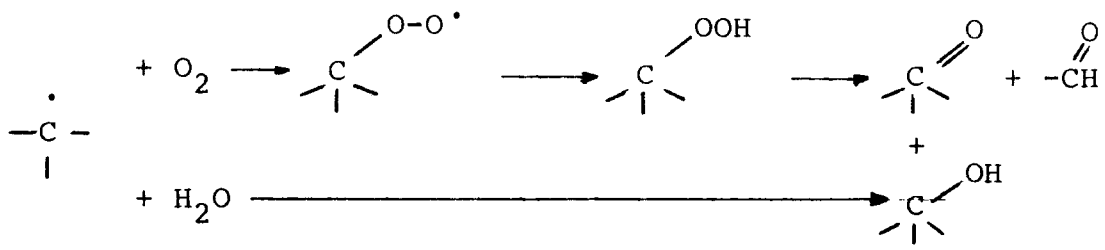

FIGURE 1.7 Reaction of a Free Radical with Oxygen or Water

The correlation between the decrease in free radical concentration and the subsequent increase in the carbonyl and possibly the hydroxyl group as a function of time has been reported.[44]

One of the problems associated with plasma polymers with regard to their analysis by conventional techniques is the insolubility of the polymers to most organic solvents, which arises from the highly crosslinked inert nature of the film. Thus, techniques which require the analysis of a solution will be practically useless - included in this group is solution phase NMR - and as such cannot be directly applied to the analysis of the structure of plasma polymers. Solid state NMR, however, is a technique which is growing in popularity[45] as a means of obtaining structural information of plasma polymers, where both saturated and unsaturated environments can be distinguished. This technique has also been used to study plasma polymers prepared from ^{13}C labelled compounds. In this instance, two carbon compounds were chosen, *i.e.* ethane, ethylene and acetylene, (only 1 carbon was labelled) such that information regarding each carbon type could be derived from the NMR spectra.[46] Five resolved spectral bands were apparent and were assigned to $=C\langle$, $=\overset{|}{C}H$ and $=CH_2$, $\rangle C\langle$, $\geq CH$ and $>CH_2$, and finally $-CH_3$ groups. The high degree of branching and crosslinking was implied by the high number of carbons, both unsaturated and saturated, which were not directly bonded to hydrogen. The degree of unsaturation present in the polymer films was found to be in the order ethane<ethylene<acetylene.[46]

Other properties of plasma polymers which greatly hampers the use of conventional analytical tools are the ultrathin

nature of these films which are often strongly adherent to the substrate. Because of this excellent bonding, the collection of polymer material for micro analysis often requires the film to be 'scratched' away from the substrate (unless experimental conditions can be found where deposition is such that the films physically come away from the substrate, or deposition takes the form of powders rather than coherent films). Thus the results of any such elemental micro analysis must be regarded with a certain amount of caution, since material belonging to the substrate rather than the polymer may have been included in the sample analysed.

Differential scanning calorimetry has shown that plasma polymers have no phase transition point where decomposition starts to occur, rather that there is a very gradual decomposition of the polymer with increasing temperature and is a reflection, on the whole, of the thermal stability of these materials.[47] A much more detailed and complete discussion of the bulk properties of plasma polymerized materials can be found in the relevant literature,[48] together with an excellent review on the dielectric properties of plasma polymers.[49]

The second analytical approach, those given in Section B of Table 1.2, is to rely on the surface analysis of these materials. Here, the top surface layers - often less than 100Å - provide direct information about the composition and/or surface energy state of the polymer film.

Contact angle determinations have been used to investigate the polarity of these surfaces[50] and the properties have been shown to reflect those of their conventional counterparts. Plasma derived fluorocarbon films are of low surface free

energy, *i.e.* exhibit large contact angles as are the surfaces of regular fluorocarbon polymers. On the other hand, oxygen containing surfaces exhibit a wettability appropriate to a high energy surface similar to those of conventional oxygen containing polymers.

The surface energy of polymer films derived from NVP have been shown to be directly related to the flow rate of the monomer and the power input to the plasma. A higher flow rate (1.3×10^{-4} cm^3_{STP} min^{-1}) gives a highly hydrophilic polymer surface whose contact angle with water is less than 5^{o}. On decreasing the flow rate to 6.9×10^{-5} cm^3_{STP} min^{-1}, the surface energy is decreased and the surface of the plasma polymer becomes more hydrophobic giving a contact angle of $\sim 55^{o}$ with water. This same trend, *i.e.* an increase in contact angle indicating a decrease in surface energy, is apparent on increasing the plasma power in the case of the high flow rate of monomer, at 5 and 10W the deposited polymers are very hydrophilic but quickly change to give a contact angle of $\sim 56^{o}$ as the power is increased to 15W. There is no effect in the surface energies of the films deposited at a low flow rate as a function of power.

The application of SIMS to polymeric surfaces[51] is still in its infancy and more studies are required to enable the full potential of this technique to be realised. It will be apparent, however, by the following results and discussions on plasma polymerized NVP that this surface technique is complementary to, rather than an alternative to, ESCA (see later Section).

To investigate the apparently different polymers prepared

by the plasma polymerization of NVP with two different flow rate conditions positive ion FAB/SIMS (fast atom bombardment SIMS) data were collected on a Kratos SIMS 800 system. The spectra obtained for the high and low flow rate polymers are shown in Figures1.8I and II respectively. In both spectra, fragments of mass greater than 100 AMU only appear at very low intensities, this arises in part from the greater instability of higher mass fragments, and the greater sensitivity of the quadropole to lower mass fragments (a preset condition). Experimental conditions were not completely optimised, moreover, for analysing insulating polymer samples.[51b]

From a cursory glance at both spectra there is a remarkable degree of similarity between the fragmentation patterns produced by both polymer films, which at first sight may appear identical. A closer look will show that the fragmentation patterns of three groups of peaks (at 27 28 29, 41 42 43 and 55 56 57 AMU) are not constant between the two spectra. Although it is not the intention of this discussion to undertake a comprehensive analysis of the spectra but rather to highlight certain features which can be used as a monitor for the differences between the two plasma polymers, a possible peak assignment for the peaks of interest is given in Table 1.3.

Peak assignment is complicated by the presence of Na^+, Al^+ and K^+ ion contaminants which are invariably present in SIMS spectra and give rise to peaks at 23, 27 and 39 AMU. Since the relative intensity of the peak at 27, which is of special interest in the present case, is not in question the problem due to contamination is of no consequence in the interpretation of the data. It should be noted however that the peak at 27 is most likely to be due mainly to organic $\overset{+}{H}C{=}CH_2$ groups.

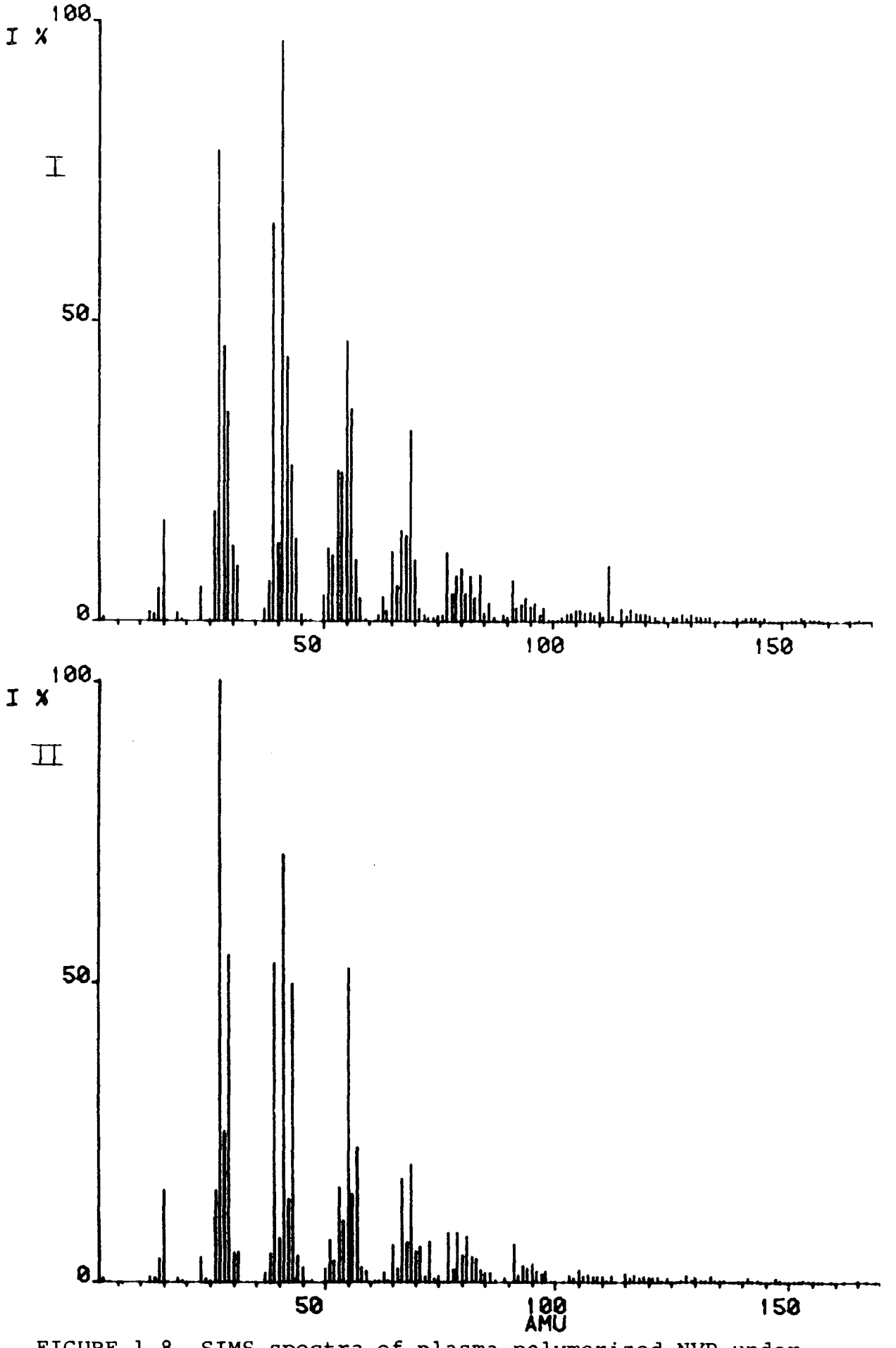

FIGURE 1.8 SIMS spectra of plasma polymerized NVP under high (I) and low (II) flow rate conditions

TABLE 1.3 Possible fragments arising from positive ion SIMS spectra of plasma polymerized NVP

	Peak/AMU	Possible Assignment for Positive Fragments
Group 1	27	$HC{=}CH_2$
	28	CH_2N CO
	29	CHO, C_2H_5, NH_2, CH_3N
Group 2	41	$CH_2C{=}N$, C_3H_5, C_2HO, C_2H_3N
	42	C_2H_2O, C_2H_4N
	43	CHNO, C_2H_3O, C_2H_5N, C_3H_7
Group 3	55	C_2HNO, C_3H_3O, C_3H_5N, C_4H_7
	56	C_2H_2NO, C_3H_4O, C_3H_6N, C_4H_8 (CN_2O, CH_2N_3, C_2O_2)
	57	C_4H_9, C_3H_7N, C_3H_5O, C_2H_3NO, (C_2HO_2 N_4H, CHN_2O)

From the small variation in the fragmentation pattern of these three groups of peaks it is apparent that the change produced in the plasma polymer by altering the flow rate condition of the monomer is subtle rather than dramatic. This subtle change is mirrored by the ESCA analysis of the two plasma polymers derived from the different plasma conditions.

The application of ESCA to the study of structure and bonding in polymer surfaces has been excellently demonstrated by Clark *et al.*[52] Its application in the analysis of plasma polymers has proved itself invaluable since the inherent properties associated with these materials, which create problems for conventional analytical techniques, do not affect the analysis of the surface of the polymer film by ESCA (the Kratos ES300 spectrometer routinely requires a solid sample to be inserted into the spectrometer).

As a summary, some of the important information levels available from ESCA studies - which are used routinely in the analysis of the plasma polymers prepared herein - are listed below.

1. Elemental analysis - by a comparison of the various core level areas (together with a knowledge of the sensitivity factors - see Appendix Two).
2. Functional group analysis - structural features can be determined by a knowledge of the chemical binding energy shifts produced in a particular core level spectrum, especially the C_{1s} core level, by the different functional groups containing that element.
3. Shake-up studies to investigate mainly short range unsaturation. In fluoropolymer systems, the energy separation of the shake-up satellite from the direct photoionisation peak can also give an insight into the amount of fluorination of the polymer.
4. Angular studies - by increasing the electron take-off angle, surface features can be enhanced. Thus by the judicious choice of two different take-off angles a certain amount of depth profiling can be achieved.

Returning to the problem of the 'different' plasma polymers derived from NVP, the C_{1s} envelopes plus component peak analysis of each polymer film deposited in the coil region, under the two different monomer flow rates, are shown in Figure 1.9. The N_{1s} and O_{1s} core levels are not depicted here, but are strikingly similar to those displayed in Chapter Seven, Figures 7.2 and 7.3 for NVP derived films, polymerized with wavelengths greater than 130nm, under the two different flow rate conditions.

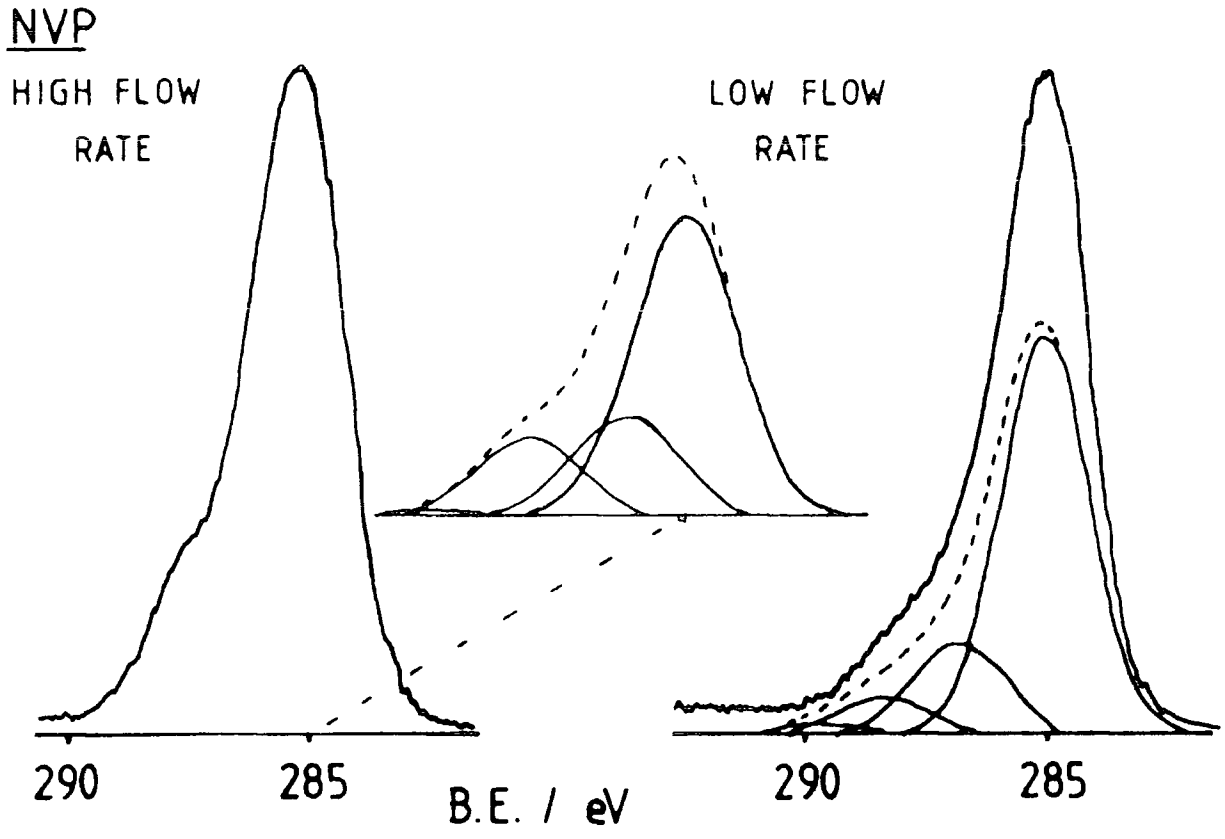

FIGURE 1.9 C_{1s} envelopes, plus component peak analysis, of plasma polymerized NVP under high and low flow rates

As with the SIMS spectra, an initial observation on the shape of the C_{1s} envelope indicates a very strong similarity between the two different polymers. A more detailed analysis of the component peaks shows the subtle differences in both the binding energy and intensity of each component peak. Due to the similarity in chemical shifts exhibited by both oxygen and nitrogen containing groups in similar environments, the functional groups giving rise to the component peaks in the C_{1s} envelopes of NVP derived polymer films have only been tentatively assigned (CH, C-O/C-N, O=C-N and O=C-O). Thus the differences in composition of the higher flow rate polymer giving rise to smaller chemical binding energy shifts and a reduced intensity of the peak at 288.7eV can not really be discussed in terms of functional groups. This difference, however, is real and

reproducible. One very interesting observation on polymer composition is in the trends shown, by increasing the power in the higher flow rate system in the sample deposited in the coil region. On increasing the power from 5 to 15W there is a dramatic increase in the amount of the hydrocarbon component from 62 to 72%, this increase in C-H is accompanied by a large decrease of 7% in the component at 287.4eV from 16-9%. (There is also a 2% increase in the component peak at 288.7eV with a 4% increase in the peak at 286eV - see Figure 1.10). This sharp increase in the intensity of the C-H component mirrors the effect of power in the contact angle of the film with water over the same power range, namely a sharp increase from <5° to 65°.

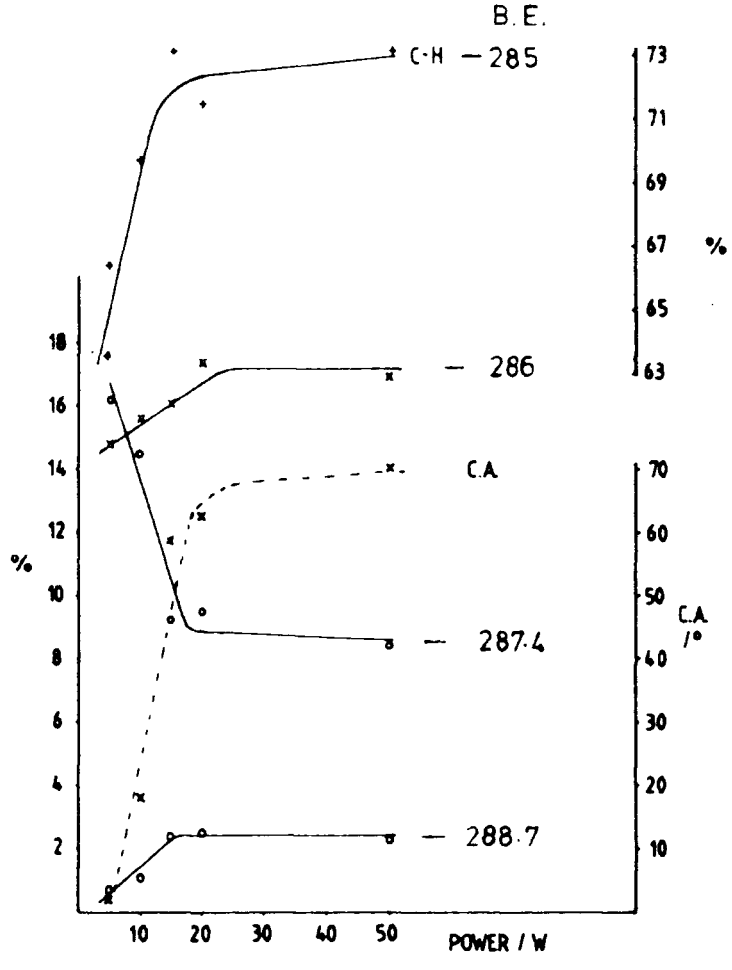

FIGURE 1.10 Effect of increasing power input to plasma on component analysis of C_{1s} envelope of NVP film (deposited in coil region using higher flow rates) and contact angle of the films with water

The same trends do not occur in the lower flow rate polymer film where contact angles increase linearly from 50-55^{o} over the 5-50W power range.

The use of ESCA in investigating the structure and bonding exhibited in plasma polymers has been extensively discussed and reviewed by Clark,[52] as are the information levels available from the ESCA spectra. A detailed analysis of the instrumentation and the theory behind the ESCA experiment is not reproduced here, rather the reader is referred to some of the excellent articles available in the literature.[53]

1.7 Fluorocarbon *versus* Hydrocarbon Plasma Polymerization

An investigation into the comparison of the behaviour shown by hydrocarbons with their analogous fluorocarbons has been attempted by Yasuda *et al*[54]. They concluded that two effects were predominantly important within each plasma:

(i) the abstraction of hydrogen or fluorine

(ii) the competitive etching effect of the product gas.

The abstraction of hydrogen has been shown to be of importance to hydrocarbon plasma polymerization using closed system experiments with subsequent analysis of the gas phase, where hydrogen was found to be one of the major product gases. However, repeating the same experiment with an analogous fluorocarbon showed that the yield of fluorine gas was generally much less.[54] This has been attributed to two different phenomena: the first is in the bond strength of F-C (116kcal/mol) in comparison to H-C (99kcal/mol). The fluorine-carbon bond is

stronger, in fact it is also stronger than a C-C bond (83kcal/mol). This would suggest that the breakage of C-C bonds are more favourable than the abstraction of fluorine in perfluorocarbon plasmas; such bond breakages are usually degradative, which would agree with the observation that fluorine containing compounds generally do not polymerize as well as their corresponding hydrocarbon.[32]

The second effect is the reactive nature of the product gas: hydrogen is relatively stable whilst the reactivity of diatomic fluorine is such that it reacts with the growing polymer, etching it away. As such, ablation is in direct competition with polymer formation. CF_4 is a well known gas which causes etching but not polymer formation, within a plasma due to the large quantity of reactive fluorine formed. However, the introduction of a small quantity of hydrogen ensures the efficient removal of fluorine from the system by the formation of a much more stable HF molecule, allowing polymer formation to proceed.[33]

In the case of perfluorobenzene, *cf.* benzene plasmas, the amount of fluorine product gas was found to be not only one order of magnitude less than the amount of H_2 product gas but also gave the smallest yield of F_2 in all of the perfluoro carbons examined.[54] This suggests that polymer etching by fluorine should play a relatively minor role in the plasma polymerization of perfluorobenzene. It also indicates that elimination of fluorine is not favourable in the perfluoroaromatic which is in agreement with the compositional analysis of the PFB derived polymer films which show a retention of monomer stoichiometry.[21]

1.8 Plasma Copolymerization *versus* Plasma Codeposition

Compositional analysis of plasma polymers, to date, has been based mainly on polymers produced by pure gas plasmas. As examples, perfluorobenzene has been shown to undergo extensive rearrangement in a plasma, resulting in a polymer composition rich in functional groups not present in the monomer; whilst TMT gives rise to films which are rich in oxygen due to the oxidation of the tin containing species.[55]

Plasma codeposition resulting from a mixed PFB/TMT plasma would be expected to result in a polymer film which retained the characteristics of each individual component, *i.e.* the high oxidation associated with TMT, and the production of C-CF, CF_2 and CF_3 functional groups as in plasma polymerized PFB. Moreover, the composition of the film would reflect the individual deposition rates of each component. In this instance a PFB/TMT polymer would be expected to be much richer in the organometallic component due to the much higher deposition rate of TMT compared to PFB. In other words, codeposition would result from the simultaneous independent plasma polymerization of each individual component. No interaction would be expected to occur between the comonomers. Such an example is seen in the independent sputtering of gold in the presence of a depositing organic plasma;[56] the resultant film contained elemental metal held, but not bound, within the polymer matrix.

Copolymerization on the other hand would result in the deposition of a film whose nature and composition have been altered by the presence of the second monomer. Although compositional analysis is very similar to a pure PFB derived

polymer, plasma polymerization of PFB in the presence of elemental mercury caused the formation of organo-metal bonds to be formed within the polymer film.[57] A better example is seen in the copolymerization of PFB/TMT.[55] The composition of the copolymer does not reflect individual deposition rates nor does the structural features evident in the polymer strongly resemble those of the individual plasma polymers. Copolymerization results in (1) a much greater retention of the aromatic nature of the PFB monomer and inhibits the oxidative tendencies of the metal, and (2) the copolymer composition shows an effectively 1:1 incorporation of the two monomers.[55]

1.9 Industrial Applications of Plasma Polymerized films

Plasma polymerized films show a widespread promise in a variety of applications. The very unique and superior nature of the polymer film, good adhesion to substrate, uniform film coverage, and strong resistance to chemicals, *etc*. lends itself particularly well to use in the coatings industry where these characteristics are extremely important. Here a sample with the required bulk properties can be used as a substrate for the plasma polymerization experiment and thus may acquire surface properties which would not otherwise be compatible with the bulk properties.

The use of plasma polymer films as protective coatings, *e.g*. for KBr optical windows[58] relies on the pinhole-free nature of the film together with the highly crosslinked polymer network having a good adhesion to the substrate. The particular properties of plasma polymerised films make them ideal for thin film capacitors,[59] insulating films[60] and corrosion protecting coatings of electronic devices.[61]

Coating a certain substrate with a conventional polymer requires several steps: (1) Polymerization of the monomer to form either the intermediate polymer (needs further processing), or the polymer (2) preparation of coating solution, (3) cleaning and/or conditioning of substrate surface, (4) application of coating, (5) drying of coating (6) curing.

In plasma polymerization, however, all these functional steps are replaced by an essentially one-step process starting from a relatively simple gas or mixture of gases with the added advantage that the monomer to be polymerized need not contain conventional reactive groups. Further, processing is carried out on a 'clean' environment of a partial vacuum minimising faults arising from contamination such as dust. The problems associated with the use of potentially toxic chemicals, *i.e.* safety and disposal, not to mention the associated costs, are eliminated, and the processing time is greatly reduced.

Polymer deposition in a plasma has the further advantage that it is not greatly affected by the nature of the substrate, *e.g.* polymer, metal or glass.[62] The process is therefore not restricted by the choice of substrate materials. Neither does the shape of the substrate affect the character of the thin polymer film which retains its integrity and uniformity throughout. This allows for the controlled deposition of a thin film onto a substrate of the users choice. Further, plasma polymerization may be relied upon to give compositions and surface properties to a high degree of reproducibility.

1.10 Disadvantages

The greatest disadvantage in using plasma technology is the imcomplete understanding of mechanisms which occur within the plasma zone, and the exact influence of the variables, *e.g.* reactor configuration, substrate temperature, *etc.* inherent in a plasma polymerization experiment. This means that a specific predetermined polymer stoichiometry cannot be produced - polymer tailoring - nor can the behaviour of a specific monomer be predicted prior to its polymerization.

Work in this thesis, however, has attempted to help resolve both of these problems; to tailor polymer films by the use of a second monomer - either polymerizable or non-polymerizable in its own right - and to gain an insight into the probable behaviour of a monomer in a plasma through an examination of its photochemistry.

REFERENCES - CHAPTER ONE

1. S.C. Brown, in 'Gaseous Electronics', Vol.1, M.N. Hirsh, H.J. Oskan (Eds.), Academic Press, N.Y. (1978).

2. L. Tonks and I. Langmuir, Phys.Rev., 33, 195 (1929).

3. A.T. Bell, in 'Techniques and Applications of Plasma Chemistry', J.R. Hollahan, A.T. Bell (Eds.), Wiley, N.Y. (1974), Chapter 1.

4. R.M. Barnes and P. Fodor, Spectrochim.Acta, Pt.B., 38B(9), 1191 (1983).

5. R. Carpenter and C. Till, Analyst (London), 109(7),881 (1984).

6. H. Suhr, Applications of Non-equilibrium Plasmas to Organic Chmistry, in ref. 3 and references therein.

7. H. Suhr, Plasma Chem. Plasma Processing, 3, 1, 1983.

8a. C.I. Simonescu, F. Dénes, Cellulose Chem.Technol., 14, 285, (1980).

8b. A.E. Pavlath and K.S. Lee, J. Macromol.Sci.Chem.A., 10, 579 (1976).

9. M.M. Millard, K.S. Lee and A.E. Pavlath, Text.Res.J., 42, 307 (1972).

10. D.M. Soignet, R.J. Berni and R.R. Banerito, J.Appl.Polym. Sci., 20, 2483 (1976).

11. M.M. Millard and A.E. Pavlath, Text.Res.J., 42, 460 (1972).

12. M. Hudis in ref. 3, Chapter 3.

13. R.W. Kirk, Applications of Plasma Technology to the Fabrication of Semiconductor Devices, in ref. 3 and references therein.

14. H. Yasuda, in 'Contemporary Topics in Polymer Science'. M. Shen (Ed.), 103, Plenun (1979).

15. F. Kaufman,in 'Chemical Reactions in Electrical Discharges', R.F. Gould (Ed.), American Chem.Soc., Advances in Chemistry Series 80, Washington, D.C. (1969), Chapter 3.

16. W.L. Fite in ref. 15, Chapter One.

17. J.M. Meek and J.D. Craggs (Eds.), 'Electrical Breakdown of Gases', Wiley, Chicester, (1978), Chapter One.

18. P. Brassem and F.J.M.J. Massen, Spectrochimica Acta, 29B, 203 (1974).

19. D.T. Clark and A. Dilks, 'Characterization of Metal and Polymer Surfaces', Vol.2, L.H.Lee (Ed.), Academic Press, N.Y. (1977).

20. D.T. Clark and A. Dilks, J.Polym.Sci., Polym.Chem.Ed., 18, 1233, (1980).

21. D.T. Clark and D. Shuttleworth, J.Polym.Sci., Polym.Chem. Ed., 18, 27 (1980).

22. F.K. McTaggart, 'Plasma Chemistry in Electrical Discharges', Elsevier, Amsterdam (1967), Chapter One.

23. H. Suhr and A. Szabo, Ann.Chem., 752, 73, (1971).

24. H. Suhr and U. Schücker, Synthesis, 431 (1970).

25. C. Boelhouwer and H.I. Waterman, Research (London), 9. 5511 (1956).

26. Y.I. Shmykov, S.N. Shorin, A.L. Suris, N.L. Volodon, V.T. Dyatlov, Y.V. Irzinger and A.M. Tukhvatullin, Khim.Vys.Energ., 11, 371 (1977).

27a. N. Morosoff and H. Yasuda in 'Plasma Polymerization', M.Shen, A.T. Bell (Eds.), ACS Symp.Series 108, Washington D.C. (1979). Chapter Ten.

27b. N. Morosoff and H. Yasuda, in ref. 27a, Chapter 17.

28. J. Goodman, J.Polym.Sci., Lett.Ed., 44, (144), 551 (1960).

29a. P. De Wilde, Ber., 7, 352 (1874).

29b. P. Thenard, Compt.Rend., 78, 218 (1874).

30. H. Yasuda and T. Hsu, Surf.Sci., 26, 232 (1976).

31. Y. Osada, , M. Takase an Y. Iriyama, Polym.J.(Tokyo), 15(1), 81 (1983).

32. H. Yasuda, 'Plasma Polymerization', Academic Press,N.Y.(1985).

33. E. Kay, Invited Pap.Int.Round Table Plasma Polym.Treat., IUPAC Symp. Plasma Chem. (1977).

34. H. Yasuda,and T. Hirotsu, J.Polym.Sci.,Polym.Chem.Ed., 16, 743 (1976).

35a. R.A. Gottscho and T.A. Miller, Pure Appl.Chem.,56(2), 189,(1984).

35b. W.R. Marshberger, R.A. Porker, T.A. Miller and P. Norton, Appl.Spectrosc., 31, 201 (1977).

36. L. Martinu and H. Biederman, Plasma Chem.Plasma Processing, 5,(1), 81 (1985).

37. H.S. Munro and C. Till, J.Polym.Sci.,Polym.Chem.Ed., in press (1986).

38. S. Pang and S.R.J. Brueck, in 'Laser Diagnostics and Photochemical Processing for Semiconductor Devices', R.M.Osgood, S.R.J. Brueck and H.R. Schlossberg (Eds.), North-Holland,N.Y.(1983

39. P.J. Hargis,Jr. and M.J. Kushner, Appl.Phys.Lett., 40, 779, (1982).

40. H. Sakai, P. Hansen, M. Esplin, R. Johansson, M. Peltola, and J. Strong, Appl.Opt., 21, 228 (1982).

41. H.U. Poll, D. Hinze, and H. Schlemm, Appl.Spec.36, 445 (1982).

42. A. Dilks and E. Kay, Macromolecules, 14, 855 (1981).

43. H. Kobayashi, M. Shen, and A.T. Bell, J.Macromol.Sci.,Chem., 8, 373 (1974).

44. H. Yasuda, H.C. Marsh, M.O. Bumgarner and N. Morosoff, J. Appl.Polym.Sci., 19, 2845 (1975).

45. A.Dilks and S. Kaplan, J.Polym.Sci.,Polym.Chem.Ed., 21, 1819 (1983).

46. A. Dilks, S. Kaplan and A. Vanhaelen, J.Polym.Sci.,Polym. Chem.Ed., 19, 2987 (1981).

47. L.F. Thomson and K.J. Mayhan, J.Appl.Polym.Sci., 16, 2991 (1972).

48a. A.N. Mearns, Thin Solid Films, 3, 201 (1969).

b. 'Plasma Chemistry of Polymers', M. Shen (Ed.), M. Dekker, N.Y.,(1976).

c. J.P. Wightman and N.J. Johnson, Adv.Chem.Ser.,80, 322 (1969).

d. H. Yasuda, Chapters 10/11 in ref. 33.

49. H. Yasuda and M. Gazicki, Plasma Chem.,Plasma Process, 3(3), 279 (1983).

50a. B.D. Washo, J. Macromol.Sci.,Chem., A(10),(3), 559 (1976).

b. P.J. Dynes and D.H. Kaeble, J.Macromol.Sci.,Chem., A(10),(3) 535 (1976) and references therein.

51a. M.R. Ross, Diss.Abstr.Int.B., 42(6), 2357 (1981).

b. A. Brown and J.C. Vickerman, Surf.Interface Anal., 8, 75 (1986) and references therein.

52a. D.T. Clark in 'Photon, Electron and Ion Probes of Polymer Structure and Properties', T.J. Fabish, D. Dwight, H.R. Thomas, (Eds.), ACS Symposium Series, No.162, Am.Chem.Soc., Washington, D.C., (1979).

b. D.T. Clark in 'Polymer Surfaces', D.T.Clark, W.J. Feast (Eds.), Wiley, London, 1978 and references therein.

c. D.T. Clark, Structure and Bonding in Polymers as revealed by ESCA, in 'Electronic Structure of Polymers and Molecular Crystals', J. Lallik, J.M. Andre (Eds.), Plenum Press, N.Y. (1975).

53. egs. D. Shuttleworth, Ph.D. Thesis, Durham University,UK,(1978).
D.R. Hutton, Ph.D. Thesis, Durham University, UK, (1983).

54. H. Yasuda and T. Hsu, Surf.Sci., 76, 232 (1978).

55. H.S. Munro and C. Till, Thin Solid Films, 131, 255 (1985).

56. E. Kay, M. Hecq., J. Appl.Phys., 55, 370 (1984).

57. H.S. Munro and C. Till, J.Polym.Sci.,Polym.Chem.Ed., 22, 3933, (1984).

58a. B.L. Weigand, Govt.Rep.Announce.(U.S.), 75(6), 179, (1975).

b. T. Wydeven and C.C.Johnson, Polym.Prep.Am.Chem.Soc.,Div. Polym.Chem., 21(2), 62 (1980).

59. J.C. Dubois, Fr.patent 2,379,889 (1978).

60. M. Kobale and H. Pachonik, Ger.patent, 2,105,003 (1972).

61. W.D. Freitag, H. Yasuda and A.K. Sharma, Org.Coat.Appl. Polym.Sci.Proc., 47, 449 (1982).

62. A.B. Gilman, L.S. Tuzov, V.M. Kolotrykin and V.K. Polapov, Vysokomol., Soedin.,Ser.B., 24(4), 315 (1982).

CHAPTER TWO

THE PLASMA POLYMERIZATION OF FLUOROAROMATIC COMPOUNDS

2.1 Introduction

The use of fluorinated organic compounds as starting materials in a plasma polymerization experiment is very attractive. The incentives to produce fluoropolymers are based on the following unrelated facts:

(i) the academic and industrial importance of fluoropolymer systems, and

(ii) a greater ease of interpretation of ESCA data.

The first practical and industrial application of fluorinated organic compounds was the introduction of fluoroderivatives of methane and ethane into refrigeration.[1] With the increasing ease of synthesis of fluorocompounds, the use of such materials have spread into many diverse areas of applications such as lubricants, water and oil repellants finishes in textiles, adhesives, fire extinguishers, anaesthetics and anti inflammatory drugs.[1] Despite the very many uses of fluorocompounds the industrially important areas remain in refrigerants, propellants and fluorinated polymers.

One of the most well known fluoropolymers is polytetrafluoroethylene (PTFE) which owes its popularity to the fact that PTFE is one of the most chemically and thermally stable addition polymers known,[2] with a multitude of applications ranging from self lubricating bearings, electrical insulation, and laboratory glassware, to non-stick coatings in pans and bakeware.

One of the main disadvantages associated with the usage of fluoropolymers, however, is in the cost of manufacture. Since many applications result from the surface properties

exhibited by fluoropolymers, *i.e.* their very low surface free energy and low coefficients of friction, attempts have been made to convert conventional polymers to fluorinated polymers by post treatment with fluorine.[3] This suffers from the inherent disadvantages associated with the use of a chemically very reactive element. However plasma polymerization provides an attractive alternative method of producing uniform surface coatings, with the desired characteristics, on bulk polymer substrates. This also has the added advantage of being a single step *in situ* polymerization process, carried out at ambient temperatures in a clean environment of a partial vacuum.

The glow discharge synthesis of polymers has been a particularly active area of research due to the particular advantages of producing pin-hole free, uniformly thin films which exhibit superior physical, chemical, electrical and mechanical properties.[4] The generally cross-linked nature of polymers produced in this manner does, however, lead to a number of difficulties in analysis. The insoluble nature of these films preclude the use of conventional wet techniques, and the thin nature of plasma polymers presents difficulties in bulk sample analytical techniques.

ESCA has been proved to be an ideal spectroscopic tool for investigating structure and bonding within plasma polymers.[5] The use of fluoromonomers has the advantage that it allows compositional information on the structure of the fluoro plasma polymer to be obtained from an ESCA C_{1s} spectrum. This benefit is derived from the electronegativity of the fluorine atom and the chemical shifts induced in carbon atoms in different fluorinated environments. The shift in core

binding energies for the C_{1s} levels of fluoropolymer systems is large and well documented and provides a convenient means of establishing structural features.[6]

The fluorobenzenes have, in particular, been the subject of an extensive investigation into their plasma polymerization behaviour with the subsequent ESCA analysis of the surface composition of the deposited film.[6c,e-h] The work presented in this chapter forms an extension to this investigation by examining the surface composition of plasma polymers prepared from other fluorinated aromatic compounds under a variety of conditions. This study also forms the basis of work carried out on copolymerization which is presented in the following chapters.

2.2 Experimental

2.2.1 Plasma Polymerization

Plasma polymerizations were performed in tubular pyrex reactors. Two main designs were used and these are shown in Figure 2.1. The shorter reactor was used mainly for copolymerization work, when a glass side was inserted along the length of reactor. Aluminium substrates were then placed at various distances along this shelf for 'collection' of deposited polymer samples. The larger reactor was principally used for substrate temperature studies (and other work in this chapter) when the aluminium substrates were placed on the top of the glass oil bed. This oil bed was connected to a thermostatically controlled silicon oil bath to give a temperature range from room temperature to 200°C.

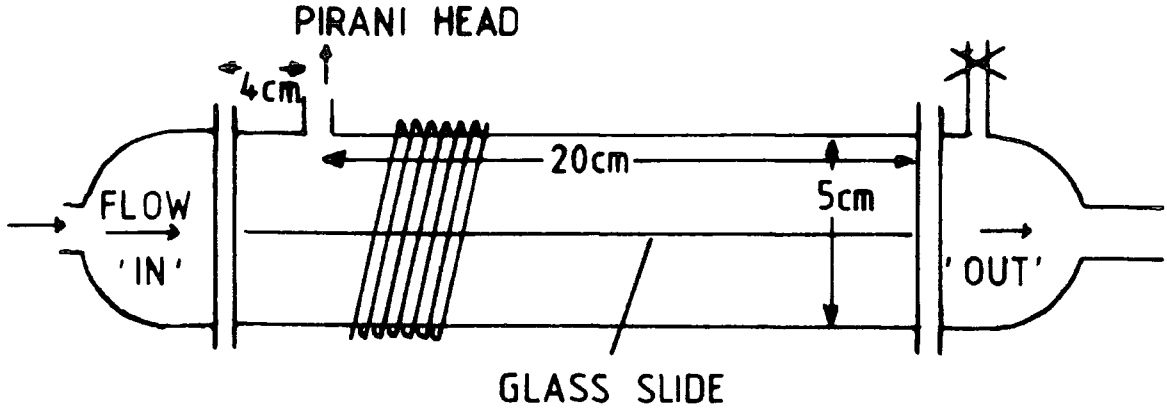

Reactor Configuration for Substrate Temperature Studies

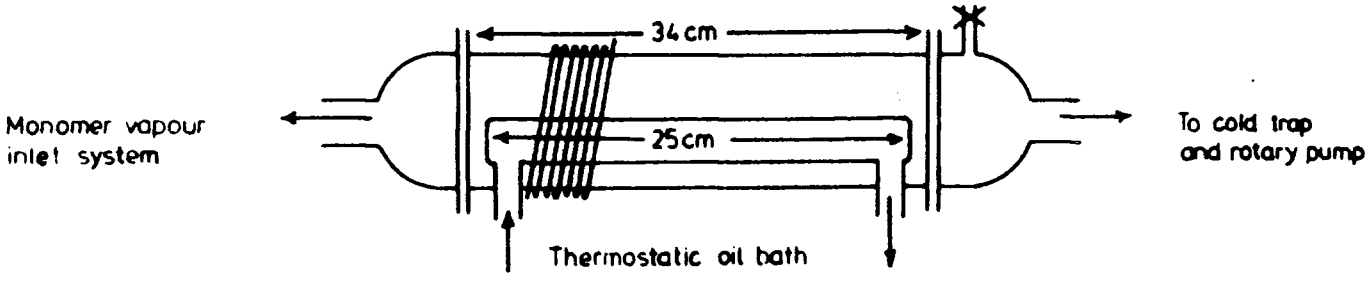

FIGURE 2.1 Experimental reactor configurations

The reactor was inserted in an all glass, grease-free vacuum line. Flanged joints and the cold trap were sealed with Viton O rings whilst all other connections were made with Cajon ultra torr couplings on ground glass. Vacuum taps were sealed with PTFE stoppers.

A schematic of the experimental configuration is shown in Figure 2.2. An Edwards ED2M2 $2\ell s^{-1}$ mechanical rotary pump was used to evacuate the vacuum line. The cold trap, itself acting as a pump, was used with liquid air both to trap out reactive/waste products before reaching the pump and to stop any backstreaming of pump oil from occurring. This pumping system gave a typical base pressure of *ca.* $2x10^{-2}$mb. Pressure measurements were made using a Pirani thermocouple gauge.

Before each deposition involving a new 'monomer' the reactor and end caps were cleaned with a hard nylon brush using acetone, detergent and salt, washed thoroughly with water/distilled water and then acetone before baking in a vacuum oven. The needlevalve assembly was also disassembled and placed in the oven to remove any traces of the organic monomer and so preventing any 'memory' effects from occurring.

Prior to the start of each experiment, the leak rate of the vacuum line was tested, by closing off the pumping and measuring the rise of pressure in the reactor over a period of time, to ensure that the leak rate was acceptable. (A high leak rate can cause an unacceptable amount of oxygen and/or nitrogen to be incorporated into the polymer film during polymerization). The monomer vapour was then 'leaked'

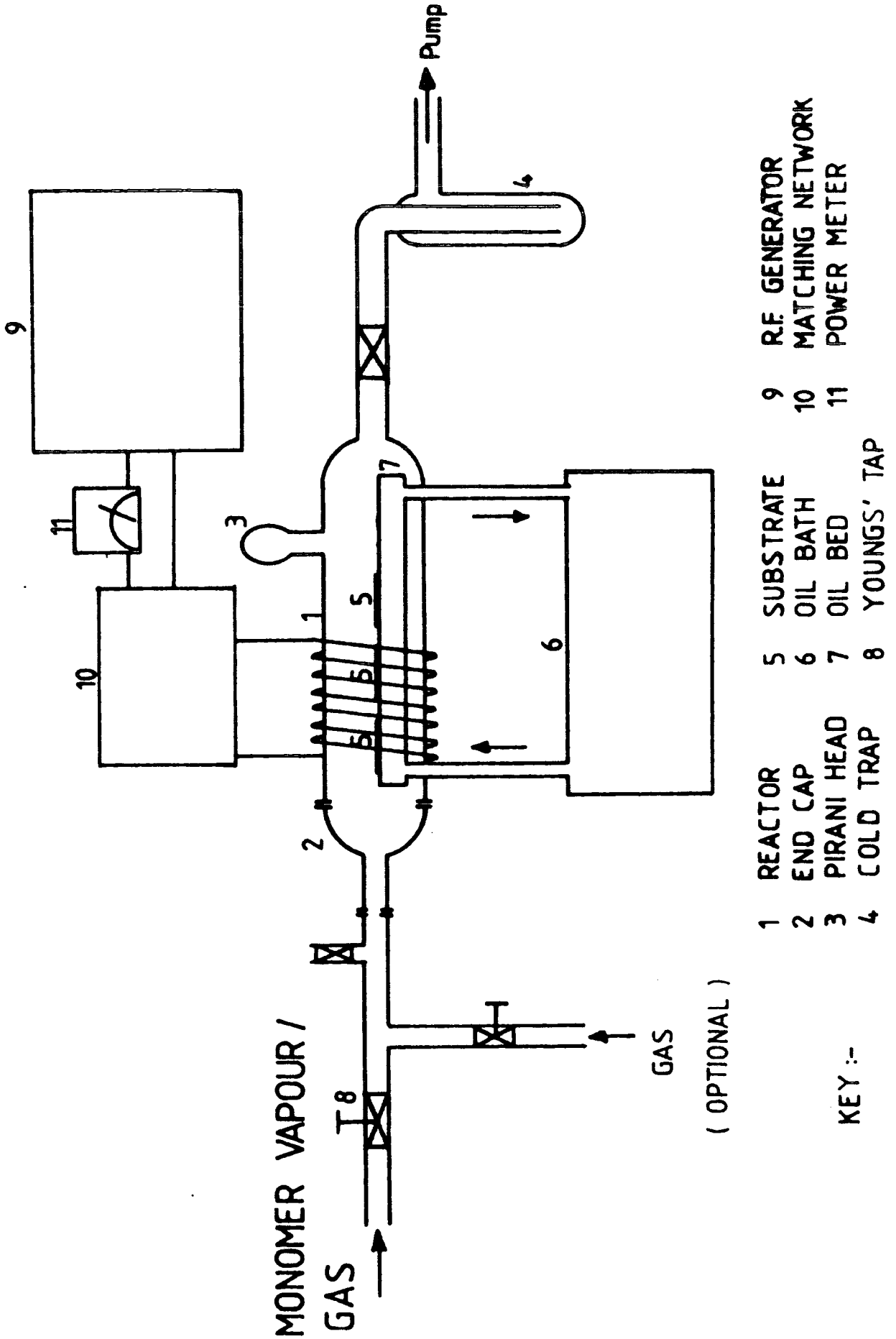

FIGURE 2.2 Experimental configuration of vacuum line/RF generator and associated equipment

through an Edwards needlevalve to the desired pressure and its flow rate measured. This was achieved by closing off the pumping to the system and monitoring the increase of pressure due to the unaided flow of the organic vapour into the reactor. All plasma polymerization experiments were performed with a dynamic flow of monomer vapour through the reactor, *i.e.* the reactor was open to the pumping system during the period of experiment.

The r.f. power supplied by an r.f. (13.56MHz) generator was inductively coupled to the reactor *via* an externally wound 9 turn copper coil, and capable of delivering from 0.1 -150 Watts. The generator was matched to the external inductive load *via* an L-C matching network. A DIAWA SW110A meter was used to measure the standing wave ratio and r.f. power (Figure 2.2). Maximum power transfer, to the external circuit occurs when the standing wave ratio is at a minimum, the optimum value being 1.

All monomers, except for the biphenyls and the naphthalenes, were degassed by alternate freeze-thaw cycles prior to use. The biphenyls and naphthalenes were used as bought. All were supplied by the following commercial sources:

Aldrich - 4-Fluoro- and 2-fluorobiphenyl (97%), Decafluorobiphenyl (99+%), Octafluorobiphenyl (98%).

Bristol Organics Ltd. - Perfluorobenzene (99.5%), Octafluoronaphthalene (99.5%).

Koch Light Laboratories - 1-Fluoronaphthalene (>99%).

For the polymerization of the naphthalene and biphenyls, a sample of the solid was crushed and then placed in a tube, sealed at one end, and connected directly to the

reactor end cap. Hence flow rates/pressures could only be very crudely 'controlled' by heating the sample and so increasing the rate of sublimation.

After each deposition period, of *ca.* 10 minutes, the reactor was let up to atmosphere using argon or nitrogen. The sample was then transferred through air to the spectrometer for analysis. All samples were analysed almost immediately after deposition.

2.2.2 ESCA Analysis

Samples were mounted onto a three sided probe tip, measuring approximately 19mm by 6mm, by double sided Scotch adhesive tape. The tip was then mounted onto the end of a probe and inserted into the spectrometer. All analyses were carried out on a Kratos ES300 spectrometer, with $Mg_{K\alpha_{1,2}}$ irradiation, of 1253.6eV energy, using an electron take-off angle of 35^{o}. Depth profiling was achieved by using a higher take-off angle of 70^{o}.

The ES300 spectrometer is controlled by the Kratos DS300 data system which is based on an LSI-11 minicomputer running under RT-11. Data acquired is stored on floppy disc, and the repeated scanning of up to 10 regions is allowed. The data analysis package provides for, amongst others, the addition, comparison, subtraction, differentiation and integration of spectra, the subtraction of satellites and a peak fitting/synthesis routine.

Component analyses were achieved, following linear background subtraction by using gaussian peaks with a constant

full width at half height. C_{1s} component peak positions were assigned by reference to the experimentally determined binding energies of the various functionalities in standard samples and are constant to within ±0.3eV. The one variable parameter is that of peak height. This was altered to get the best chemical fit.

2.2.3 Optical Emission Analysis

Optical emission spectra were recorded using an E.G. and G.OMA III system with a polychromator and diode array detector. The diode array detector was intensified over the main scan region and this should be remembered when looking at the optical emission spectra. The use of a polychromator and diode array detector during data acquisition can be very important when looking at the emission from a plasma. If the rate of polymer deposition is fairly fast, as in the perflurooaromatic plasmas, then emission through the window will quickly be attenuated and stopped by polymer deposition onto the window. A scanning monochromator may not be sufficiently fast enough to scan through the required wavelengths before the plasma polymer seriously interferes with the light emitted from the plasma. Unfortunately increasing the data acquisition time does not provide a solution since the continued deposition of polymer will lead, sooner or later, to a total block of light transmission through the window. Spectra were recorded, using a scan time of 20 milliseconds with two resolutions. A wide scan using a low resolution covered the region from ∿230-600nm. A high resolution scan was then obtained over the 250-300nm region.

The reactor configuration, of similar dimensions to the oil bed reactor, consisted of a quartz glass window mounted, prior to the coil, on the reactor's side. This window was demountable, facilitating the removal of plasma polymer in between each plasma analysis.

The spectra shown in this chapter were acquired using 5,000 scans, *i.e.* an acquisition time of 100 seconds.

2.2.4 Calculation of Flow Rate

Working in the vacuum range, *i.e.* the range used in plasma polymerizations, gases and vapours can be considered ideal gases and as such obey the ideal Gas Law[7]:

$$pV = nRT$$

where n = no. of moles of gas; R = gas constant; T = absolute temperature (K)

p = pressure (torr) and V = volume of the system (m^3).

Based on this Law, the quantity of gas in a system can be expressed by the volume of gas at the standard state, *e.g.* cm^3_{STP} and the flow rate as cm^3_{STP}/sec.

$$\text{flow rate} = \frac{dn}{dt} = \frac{dP}{dt}\,\frac{V}{RT} = x \quad \text{mol sec}^{-1}$$

as $$1\ cm^3_{STP} = \frac{1}{22{,}414}\ \text{mol} = 4.46 \times 10^{-5}\ \text{mol}$$

the quantity of gas given in cm^3_{STP}/min is:

$$\text{flow rate} = \frac{x \times 60}{4.46 \times 10^{-5}}\ cm^3_{STP}\ \text{min}^{-1}$$

2.2.5 Calculation of Leak Rate

The leak rate is given by the equation:

$$\text{Leak rate} = \frac{V\ (L) \times \Delta P\ (\text{torr})}{R.T(K).\text{Time}\ (s)} = \text{mol sec}^{-1}$$

To obtain an accurate flow rate, the leak rate value is taken away from that calculated for the flow rate. However, this is based on the assumption that the leak rate is independent of pressure - that the leak rate determined at base vacuum is the same as the leak rate of the system with the desired monomer pressure - in most cases this approximation is sufficiently accurate since the flow rate value will be an order or two of magnitude greater than the leak rate.

2.3 Results and Discussions

2.3.1 Plasma Polymerized Perfluorobenzene (PFB)

Typical examples of the C_{1s}, F_{1s} and O_{1s} core level spectra from plasma polymerized perfluorobenzene are shown in Figure 2.3. As has already been noted in previous studies[6c] of this polymer, the overall band profiles of each of the levels studied, and their relative area ratios, remain essentially constant over a wide range of operating parameters so no mention is made here of the experimental variables resulting in this particular plasma polymer. However, these core level spectra will serve as suitable examples to explain some of the phenomena associated with plasma polymerization and the subsequent analysis of the polymers by ESCA.

The O_{1s} core level, present in nearly all plasma polymers[6] albeit at a very low level ($C_1:O_{0.03}$) is situated at approximately 533.5eV. The spectrum is usually a broad complex band made up of at least two components due to

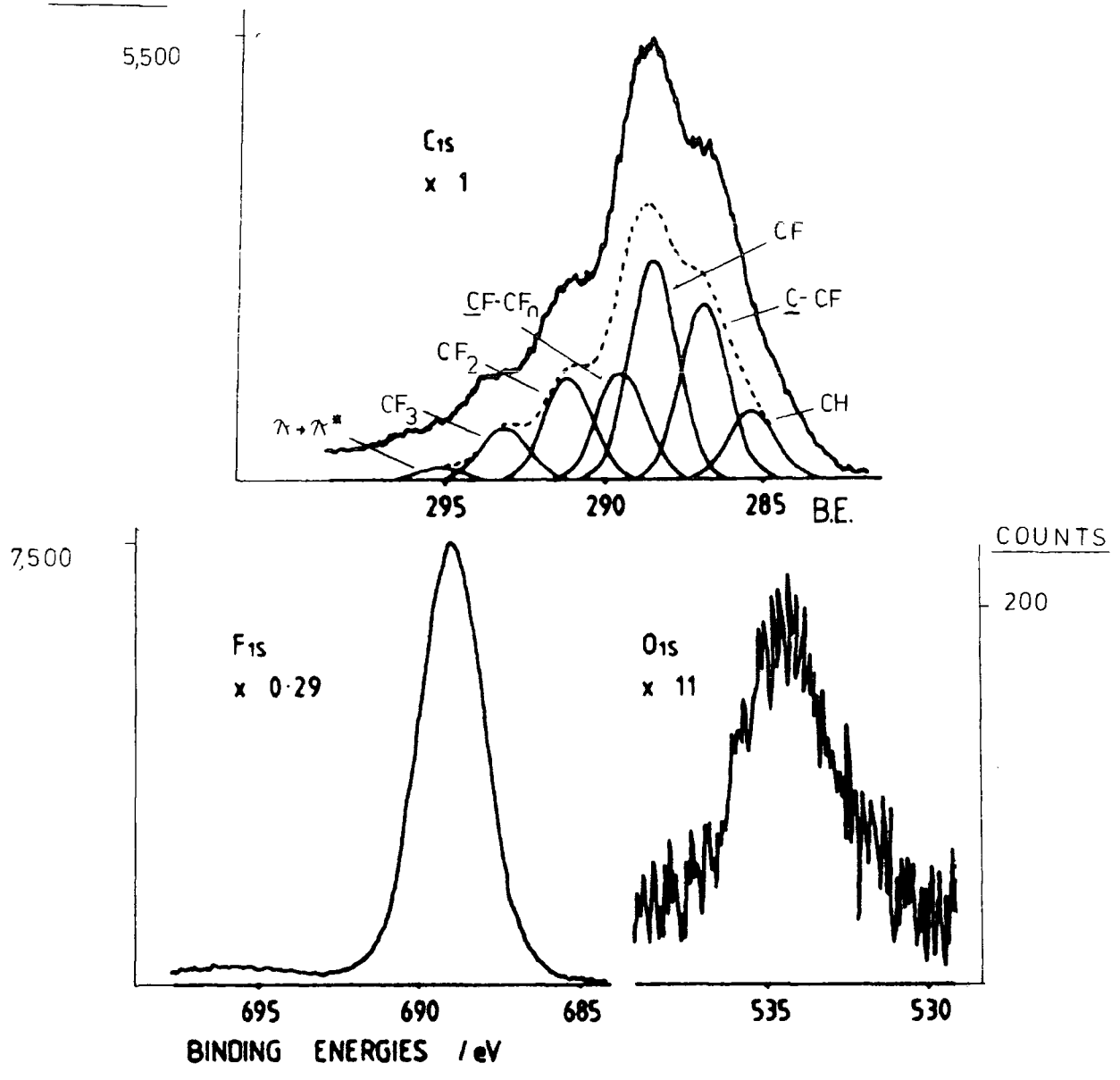

FIGURE 2.3 Typical core level spectra from plasma polymerized PFB

$-\overset{|}{\underset{|}{C}}-O-$, and $\overset{|}{\underset{|}{C}}=O$ functionalities[6c] and possibly in more highly oxygenated systems, also $\overset{|}{\underset{O}{\overset{|}{C}}}=O$ and $\overset{|}{\underset{O}{\overset{O}{C}}}-O-$. This oxygen contamination is thought to arise from two possible sources. The first source is due to any small leak in the vacuum line. It has been demonstrated that even if plasma polymerization is carried out *in situ*, *i.e.* the plasma reactor is connected directly to the electron spectrometer so the sample does not 'see' atmosphere that there is still a small signal from the O_{1s} core level.[6g] Due to the highly

cross-linked nature of the plasma polymer it is known that during polymeization this matrix can 'trap out' products of the plasma reaction.[8] The resultant freshly prepared polymer will then contain a large number of unpaired spins, *i.e.* radicals. These trapped radicals, being very reactive, can then react with oxygen in the atmosphere.[8] However, this source of contamination was not a serious problem with the fluorinated aromatics as can be seen by the very low level of oxygen associated with the polymer after being transferred through air to the spectrometer; so no special precautions were taken.

The second source of oxygen contamination has also been thought to be due to the desorbtion of low molecular weight oxygen containing species from the reactor walls.[6b] It has been stated that in the plasma polymerization of perfluorobenzene, as the power is increased the relative amount of oxygen content increased.[6g] From the work carried out for this thesis, there did seem to be some trend towards an increased oxygen content at higher power. However since this became only apparent at relatively very higher powers, *i.e.* around 50W - which is higher than the normal experimental range used - this did not cause any problems.

The F_{1s} core level is a symmetrically shaped peak centred at around 689.0eV. This line shape is not characteristic of a single fluorine environment but due to a range corresponding to the species identified in the C_{1s} profile. As the chemical shifts in the F_{1s} binding energy are not very large, a broad symmetrical peak is observed for sufficiently 'thick' films; (when the Al_{2p} signal is not visible by ESCA).

The spectrum thus consists of one quassian† peak due to covalently bonded fluorine environments.[6] However, when the aluminium substrate is 'visible' a second peak appears in the F_{1s} core level at lower binding energies. This is thought to be due to the interaction of perfluorobenzene at the interface between the plasma polymer and the substrate, and is discussed in more detail in Chapter Seven.

In highly fluorinated samples in which there is a high amount of unsaturation, the F_{1s} main photoionisation peak is accompanied by the presence of a small $\pi \rightarrow \pi^*$ shake-up satellite some 7 to 8eV removed to higher binding energies.[6c-h] Thus the presence of this peak in an ESCA spectrum is characteristic of unsaturation within the plasma polymer, and originates from transitions accompanying core ionization of $=\underline{C}\text{-}F$[6c-h] groups.

The C_{1s} core level is very broad and complex, exhibiting much structure, and demonstrates the wide variety of different carbon environments present in the plasma polymer of perfluorobenzene. Detailed analysis of this envelope reveals that extensive molecular rearrangement has taken place to produce component functionalities which are not present in the parent monomer, namely CF_2 and CF_3 groups.[6]

The process of component peak analysis of the C_{1s} envelope for fluoro polymer samples was developed by Clark *et al.*[6] Using the chemical shift spacing discussed in the literature for the plasma polymer of perfluorobenzene,[6c,g] this gives rise to component peaks at 285, 286.6, 288.3, 289.5 291.2, 293.3 and 295.2eV. These are due to C-H, $\underline{C}$-CF, CF,

---

† The actual peak shape is made up of a gaussian peak with some Lorenztian character in the tail region.[9]

$\underline{C}F\text{-}CF_n$, CF_2, CF_3 and $\pi \rightarrow \pi^*$ shake-up satellite environments respectively. Since the hydrocarbon peak, used as the energy reference, is the smallest component of the C_{1s} envelope and therefore difficult to locate precisely, the binding energies given are approximate to ±0.3eV.[10]

The hydrocarbon peak is present due to contamination of the plasma polymer. This arises from a combination of three effects: (i)athin layer film being deposited on top of hydrocarbon contamination in the substrate,[6c] (ii) the deposition of hydrocarbon onto the plasma polymer whilst it is being transferred to the spectrometer[6], or (iii) the formation of a hydrocarbon overlayer during analysis in the spectrometer.[6g] For samples of perfluorobenzene prepared '*in situ*',[6g] the initial absence of hydrocarbon indicated the second source of hydrocarbon contamination. However, after a period within the spectrometer the same sample would then show an appreciable build-up of hydrocarbon contamination. It has been shown that a major source of this contaminant is due to hydrocarbon 'boiling off' the X-ray cap and window,[11] and by equipping the X-ray cap with a cooling jacket using either cold water or liquid nitrogen, that this method of contamination can be greatly inhibited.[11]

For the work carried out in this thesis, this modification to the X-ray cap was not employed. Hence contamination of these plasma polymers is due to the latter two methods only, the rate of polymer deposition for perfluorobenzene is so rapid that after a typical deposition period of ten minutes the films are visible and appear yellow/gold coloured.

The $\pi \rightarrow \pi^*$ shake-up satellite is characteristic of unsaturation present in the plasma polymer[6] and arises from processes which occur on the same time scale as the photoionisation event. The removal of a core electron is accompanied by substantial reorganisation of the valence electrons. This perturbation yields a finite probability for photoionisation to be accompanied by the simultaneous excitation of a valence electron from an occupied to a higher unoccupied state. Short range unsaturation, *e.g.* a pendant phenyl[12] group in polystyrene gives rise to a defined satellite whilst long range unsaturation, *e.g.* in a conductor produces an asymmetric tailing of the main peak,[13] as the number of available transitions increase and each satellite becomes less distinct.

The shake-up processes derive the energy from the single electron process thus lowering the KE of the primary photoelectron and therefore all calculations on photoionisation peak intensity need to include shake-up satellite intensity, if these are present.

The typical energy separation between the primary photoionisation peak and the shake-up satellite is about 7-8 eV removed to higher binding energies and depends on the degree of fluorination of the parent monomer.[14] A hydrocarbon system produces a peak around 7eV from the main photoionisation peak which increases to 8eV for a fully fluorinated aromatic compound.[14]

The broad nature of each of the component peaks in the C_{1s} envelope, typically a full width at half height

(FWHH) of 1.8-1.9eV represents the complexity of a plasma polymer. A carbon core level in a regular polymer will have a FWHH of *ca.* 1.3eV,[15] the increased width of the peaks in the plasma polymer indicating the number of closely related functionalities with similar, but not identical, electronic environments. The value of the FWHH† is proportional to the lifetime of the core hole state which is typically of the order of 10^{-13} to 10^{-16} seconds.[16] Since, in the polymer these states will all have similar lifetimes the C_{1s} envelope was fitted with peaks all of the same FWHH.

Due to the use of unmonochromatic radiation as the photon source, the $Mg_{K\alpha_{3,4}}$ radiation caused two more peaks to appear in the spectrum some eight and ten eV removed to lower binding energies of the main photoionisation peak due to $Mg_{K\alpha_{1,2}}$ radiation. These are not shown in any diagrams and will not be referred to again.

The insulating nature of organic plasma polymer films is seen in the shift of the binding energies of the peaks on ESCA analysis, the extent of charging is determined by the shift from 285.0eV by the CH component, *i.e.* energy calibration is achieved using the hydrocarbon component peak. This apparent increase in binding energy is due to the rapid build up of positive charge on the surface of the polymer upon X-ray irradiation. The energy required to remove an electron is now that much greater due to the retardation caused by the positive surface. Various methods of reducing or eliminating this charging effect have been studied and include

---

† The FWHH also depends on the natural linewidth of the photon source, the natural linewidth of the core hole and on aberrations of the analyser. These, however, when using the same irradiation source, will be kept constant.

the use of a low energy electron flood gun[17] or by IV irradiation of the sample by a low pressure low power mercury arc lamp.[18] All energy values quoted throughout the thesis have been corrected for charging.

Elemental stoichiometry is obtained by a ratio of the appropriate peak areas multiplied by a sensitivity factor. This sensitivity factor takes into account the sensitivity of the spectrometer for a particular core level and includes such factors as electron mean free path† and analyser response to the electron energy. Sensitivity factors can either be determined experimentally[19] or theoretically,[20] a list of sensitivity factors used throughout - and the calculations used to determine them - are presented in Appendix Two. A second method of calculating the F:C atomic ratio of fluoropolymer systems is available. Here the contribution of each component peak in the C_{1s} envelope which has one or more fluorines directly attached to the carbon is summed,

i.e. $$\frac{[\%CF] + [\%CF\text{-}CF] + 2[\%CF_2] + 3[\%CF_3]}{100} = C:F$$

For the work presented in the following chapters, stoichiometries are based on peak area ratios although the consistency is checked by comparing the values obtained by both methods. It should be noted here that the value obtained from a calculation involving the C_{1s} core level can be slightly higher than that obtained by using the ratio of peak areas. The C_{1s} core level, acquired first, has a larger mean

---

† Mean free path, λ, of an electron is defined as the distance in the solid that electrons of a given energy can travel before $1/e$ of them have not suffered energy loss through inelastic collision. The sampling depth, from which 95% of the signal for a given core level is derived is given as $3\lambda\cos\theta$ (θ represents the angle of escaping electrons with respect to a direction normal to the samples surface).

free path than F_{1s} (15Å *c.f.* 8.3Å).[21] The signal from the F_{1s} core level is therefore more highly attenuated by the contaminant hydrocarbon layer than the signal from the C_{1s} core level.[6] However, the discrepancies between the two F:C stoichiometric values are usually very small and can effectively be ignored.

In the present example, the C:F atomic ratio calculated from a peak area ratio is close to that of the starting monomer, *i.e.* C_1:F_1. This illustrates the importance of non-elimination reactions occurring in the plasma which are involved in polymer formation.

(I) Substrate Temperature Study

The effect of elevated substrate temperatures on the composition of a deposited plasma polymer is an area which has not received much attention to date.[22] It has been alluded to as being of importance in influencing the plasma polymers of hexamethyldisiloxane and hexamethyldisilazane.[23] ESCA studies of the composition of the deposited film from acrylonitrile[24] have shown a startling contrast in the two polymers deposited as a function of substrate temperature, over the power range of 1 to 55W; the most significant feature being shown in the nitrogen composition within the coil region. At room temperature the extent of nitrogen incorporation went through a minimum value at ∿35W. This is the opposite to that which occurred at a substrate temperature of 150°C, *i.e.* a maximum value was obtained at ∿30W.

The physical properties, surface texture and morphology of plasma polymerized tetrafluoroethylene have been

reportedly controlled by varying the substrate temperature up to 200°C.[25]

To examine the effect of substrate temperature on the composition of the plasma polymer produced from perfluorobenzene, initial studies were carried out by varying the power over the range of 5-30W, for samples deposited at a substrate temperature of 150°C. Plasmas were excited in 0.1mb PFB.

A graph of component peaks† of the C_{1s} envelope (in percentages) *vs.* the applied power is shown in Figure 2.4. The perfluorobenzene had a preplasma pressure of 0.1mb and all samples were deposited in the coil region for 10 minute periods. The corresponding graph for deposition at room temperature is shown in Figure 2.5.

Both graphs are very similar in appearance. In both of the substrate temperature depositions, the amount of $\pi \rightarrow \pi^*$ shake-up shows a linear decrease with increasing power. This has been noted before[6g] and is not entirely unexpected. This goes hand in hand with the increase in CF_2 which shows an increasing linear trend at a high substrate temperature, but appears to level off at room temperature. As the available power to the plasma increases, the proportion of electrons with a higher energy content may have increased. Thus, a greater degree of (fragmentation) reactions resulting in loss of unsaturation might be expected which would result in a decrease in the $\pi \rightarrow \pi^*$ shake-up satellite. The behaviour of the C-CF component peak, with power, mirrors that of the CF_2 peak at both substrate temperatures.

---

† Due to the ambiguity of assignment of intensity between the CF and $CF\text{-}CF_n$ peaks - these are summed to give a total CF content which is the value plotted. Peak intensities of the various component peaks have different reproducibility values. These have been assessed as being ±5% for C-CF, CF and CF_2, ±10% for CF_3, and ±25% for the $\pi \rightarrow \pi^*$ shape-up. These are represented as error bars.

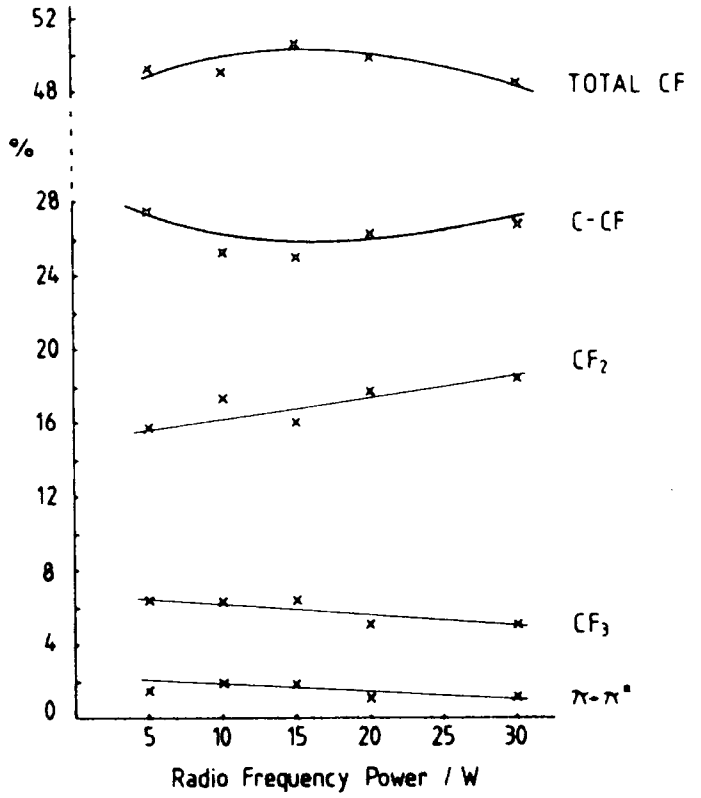

FIGURE 2.4 Component peak analysis of the C_{1s} envelope as a function of power at 150°C

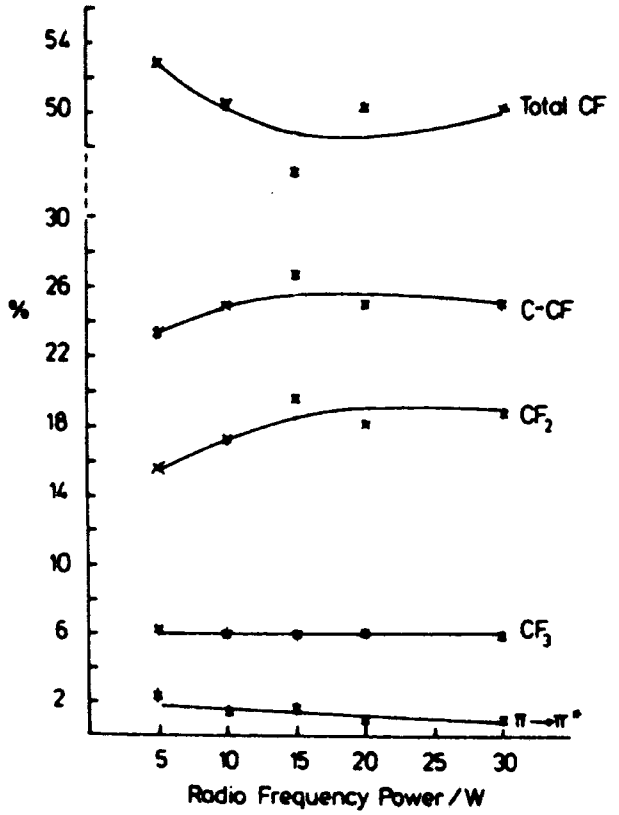

FIGURE 2.5 Component peak analysis of the C_{1s} envelope as a function of power at 23°C

The one main subtle difference would appear to be in the amount of CF. At room temperature, this would appear to pass through a minimum value at 15W whilst for a higher substrate temperature the amount is moreor less constant. However, the variance between the two sets of values are so slight that it is difficult to be sure of any real difference.

For both polymers at each substrate temperature the F:C stoichiometry is the same and close to unity, again emphasising the importance of rearrangement mechanisms as opposed to elimination reactions in the plasma polymerization mechanism.

The percentage composition of each of the component peaks in the C_{1s} envelope are very similar as illustrated in Table 2.1.

TABLE 2.1 Effect of substrate temperature on the percentage Composition of the C_{1s} envelope

Temperature	C-CF	Total CF	CF_2	CF_3	$\pi \rightarrow \pi^*$
23°C	26	50	17	6	1
150°C	25	49	18	6	2

PFB - 10W, 10 minutes 0.1mb pressure.

This similarily would tend to suggest the absence of any real effects due to an increased substrate temperature.

Although the rate of deposition of the plasma polymer, with distance in the reactor at a substrate temperature of 150°C, was not measured, the variation in deposition rate quickly became apparent. The colour of the plasma, *i.e.* the emission from the plasma in the visible region, appeared to change in going from the inlet to the outlet of the reactor.

This was simply due to the variance in deposition rate causing films of different thicknesses to be deposited on the reactor walls which altered the transmission characteristics of the emitted light. Deposition was fastest in the coil region.

The surface composition of the polymer as a function of distance in the reactor, using a 150°C substrate temperature has also been examined. Four different regions were looked at: before the coil, in the coil region, 2cm after the coil region and finally at the end of the reactor. Graphs of component peak intensity (not shown) against position in the reactor show the same effects as those shown in the coil region by increasing the power (see Figure 2.5). That is, the increasing loss of unsaturation, shown by a decrease in the $\pi \rightarrow \pi^*$ shake-up satellite, together with an increase in CF_2 functionalities, as a function of increasing distance. Again there is no variation in the overall atomic ratio which is constant at around $C_1:F_1$ for all four of the positions sampled. The reason for this variation is not at all clear as yet.

It has been suggested that a study of the polymer produced in the non-glow region - the area downstream of the visible glow - will give an indication of the nature of the most long lived species within the gas plasma.[6c] Clark and Shuttleworth have examined the structure of perfluorobenzene in the glow and non-glow region,[6c] with deposition onto a 'room temperature' substrate, and found that the polymer produced in the non-glow region was distinctly different from that produced in the glow region of the plasma. The dominant

peak in the C_{1s} envelope was no longer due to $\underline{C}$-F but $\underline{C}$-F_2. This CF_2 component had a similar binding energy to the CF_2 component in tetrafluoroethylene.[15] It was pointed out that in a recent publication,[26] CF_2CF_2 had been found to be present in the highest yield of low molecular weight material produced in a Tesla discharge in perfluorobenzene. The conclusion was that the precursors to polymerization in the non-glow regions were higher in CF_2 content than those in the glow region. It should be pointed out here that in the present study, the glow region extended to the end of the reactor and thus all samples were present in the visible plasma region. The composition and gross structural features of the core level spectra remained essentially the same over the distance studied.

(II) Optical Emission

Emission from a plasma arises from excited states - caused mainly by electron impact - in the gas phase relaxing and losing their excess energy through fluorescence. A second mode of relaxation is also available, by chemical reaction, however, when this method predominates fluoresence does not occur. Emission from the gas phase therefore only gives an insight into the excited state species which do not undergo chemical reaction but relax by fluorescence.

A low resolution spectra of the emission from the visible pale blue plasma of perfluorobenzene from 260-600nm is shown in Figure 2.6. Although wavelengths have been assigned manually to the various features present in the spectrum, these values should not be taken as absolute values and may vary by about ±20nm, due to the difficulties in

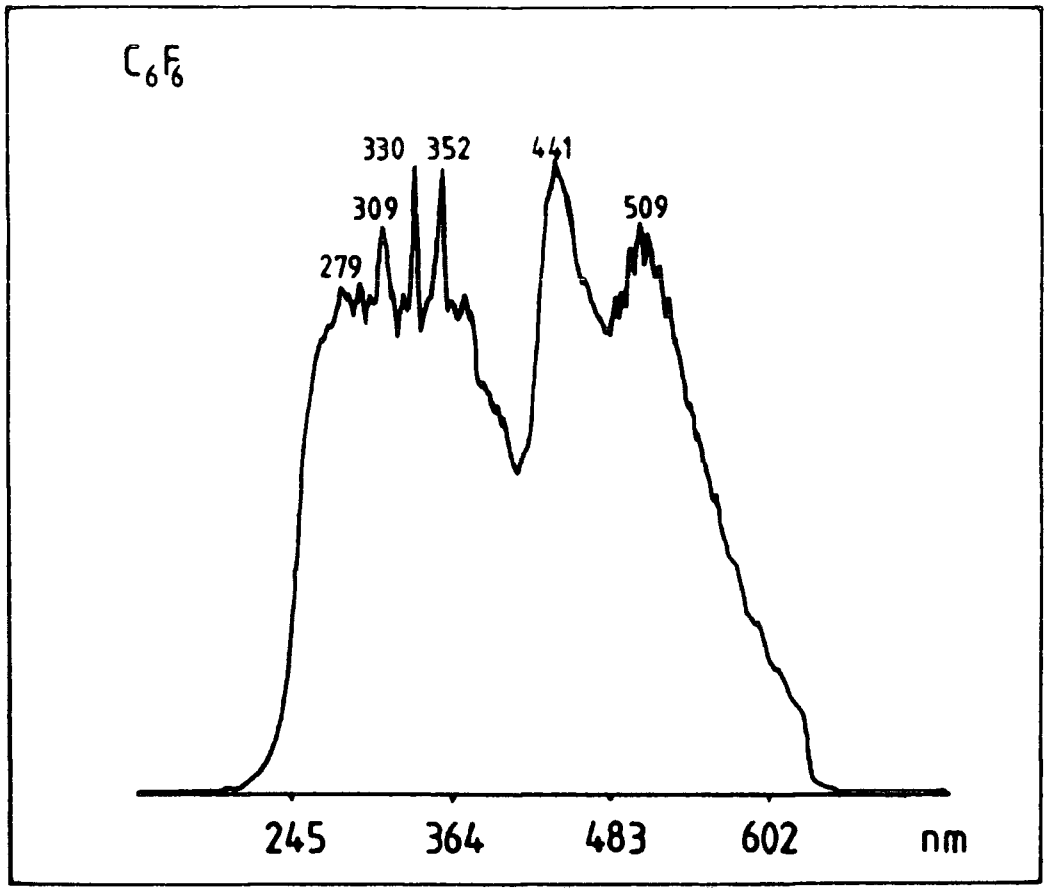

FIGURE 2.6 Optical emission spectrum from a PFB plasma

calibration of the spectrometer and to the crude 'ruler and pencil' assignment of peak energies.

The plasma emission is very broad and shows much structure. Two distinct peaks are apparent at ∿440nm and ∿510nm. The former has been attributed to the $\tilde{B} \rightarrow \tilde{A}, \tilde{X}$ electronic transition of a radical cation[27] of PFB and is the major contributor to the visible colour of the plasma. Maier *et al*[27] have studied the radiative relaxations of the excited electronic states of the radical cations of the fluorobenzene formed by low energy (20-30eV) electron beam excitation of low pressure gaseous samples. The fluorescence of a radical

cation, $C_6F_6^+$, was seen to occur from ∿465nm. This emission is due to the fluorescent decay of an excited state radical cation dropping to lower energy states, the wavelength of emission being proportional to the energy separation of the different states involved.

That a radical cation exists, as shown by the peak at ∿400nm, clearly demonstrates that the energy available to the molecule from the plasma is in excess of 10eV, since the first ionization potential of C_6F_6 is 9.97eV.[28] However a distribution of electron energy with relative populations, a Maxwellian distribution, shows that the majority of electrons have an energy value far less than this - the average ẽ energy is *c.a.* 2.0eV[6f] - and that the majority of collisions in a plasma will involve excitation rather than ionisation which is caused by electrons in the tail of the distribution peak, and that the chemistry involved in a plasma will mirror this fact. Thus radical cations would not be expected to play a large role in plasma polymerization. This is explored in more detail in Chapter Seven.

In the plasma polymerization studies of fluorobenzenes by Gilbert and Théorêt[29] it was found that 1FB has a plasma emission corresponding to that of $S_1 \rightarrow S_0$ emission of the monomer and for PFB, emission arising from CF_2 was dominant.[29] These emission characteristics may be associated with the different film compositions. The $S_1 \rightarrow S_0$ transition of the PFB molecule was not detected, but it was suggested that the emission from CF_2 radicals, over the 235-350nm, probably obscured the $\pi \rightarrow \pi^*$ molecular emission,[29] since the value of the fluorescence quantum yield for perfluorobenzene is very low.

Gilbert and Théorêt found in their study that as the degree of fluorination of the benzene molecule increased the quantum deficit increased.[29] Quantum deficit is defined by $1-(\phi S_1 + \phi T_1)$, where ϕS_1 and ϕT_1 represent the luminescence quantum yields of the first excited singlet and triplet states respectively. As this value gets higher photochemical reactions of the first excited state become increasingly important as the means of releasing the excess energy.

Thus, since photochemical reactions of the first excited state of perfluorobenzene are dominant, the amount of fluorescence seen is expected to be very small.

A high resolution scan of the region around 280nm is shown in Figure 2.7. This broad band shows the fine structure of the CF_2 radical and is of the same structure as that reported by Gilbert and Théorêt[29] which has over 60 bands.

The origin of the other bands is as yet uncertain, including the peak at 510nm which is as dominant as the emission from the radical cation.

2.3.2 Plasma Polymerized Octafluoronaphthalene (OFN)

Naphthalene has previously been plasma polymerized and its polymer found to act as a composite gas separation membrane when deposited onto a microporous substrate. The permeability of this membrane to He and H were studied, no mention is made of the composition of the plasma polymer.[30]

The C_{1s}, F_{1s} and O_{1s} core level spectra for plasma polymerized octafluoronaphthalene are displayed in Figure 2.8, and represent samples removed from the coil region of a 30W,

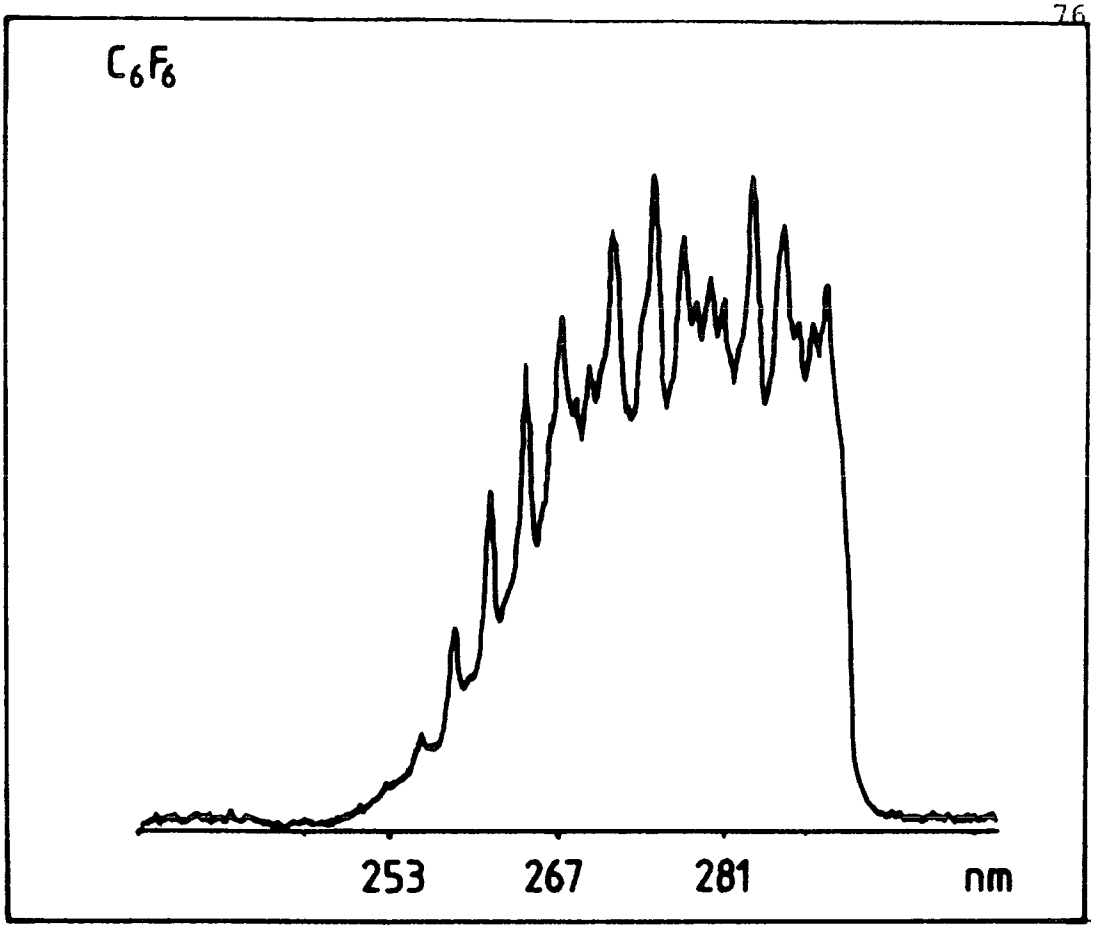

FIGURE 2.7 High resolution spectrum of the plasma emission of PFB around 260nm

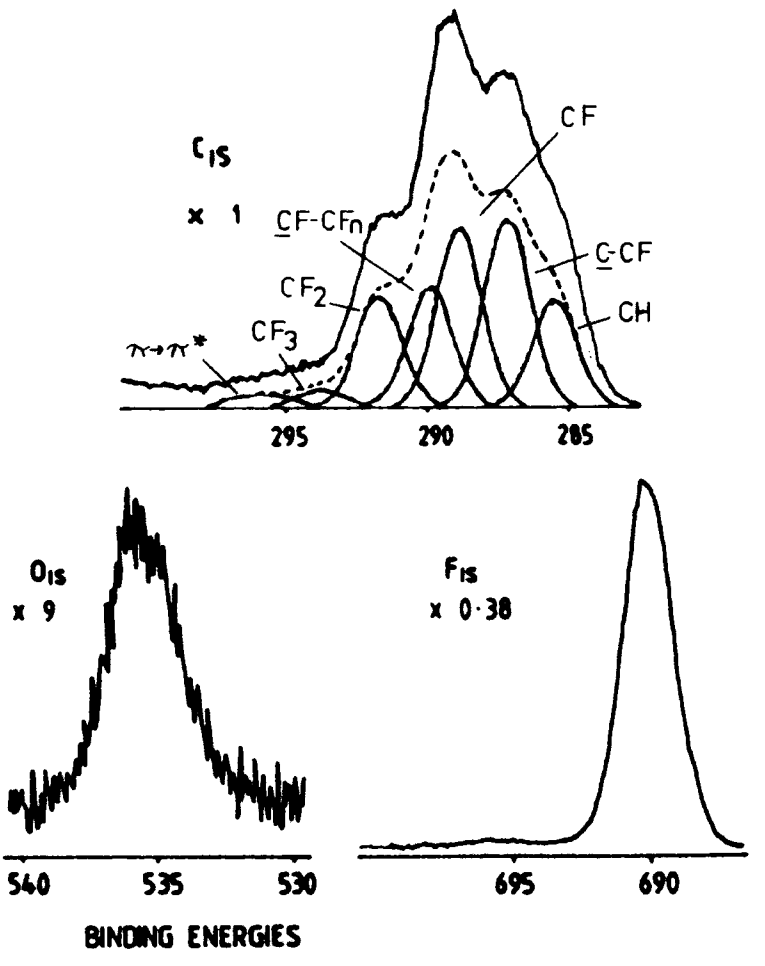

FIGURE 2.8 Typical core level spectra from plasma polymerized OFN and component peak fit of the C_{1s} envelope

0.07mb plasma. The C_{1s} envelope, as for perfluorobenzene, is broad and structured. A component peak analysis is also shown in Figure 2.8. This reveals peaks at 286.45, 288.2, 289.15, 291.1, 293.7 and 295.8eV arising from the same functionalities as are present in the plasma polymer of perfluorobenzene, $\underline{C}$-CF, CF, $\underline{C}F$-CF_n, CF_2, CF_3 and $\pi \rightarrow \pi^*$ shake-up satellite with percentage intensities of 30, 29, 19, 17, 3 and 2% respectively. Thus the predominant peaks in the C_{1s} envelope are those due to $\underline{C}$-CF and CF functionalities. Extraneous hydrocarbon contamination gives rise to the peak at 285.0eV.

The F_{1s}/C_{1s} area ratio gives a stoichiometry of $C_1:F_{0.7}$, *i.e.* essentially that of the monomer.

The strong similarity of the ESCA data from plasma polymerized OFN and PFB suggest that the polymerization processes involved follow similar pathways, *i.e.* rearrangement processes are more important than elimination. If the mechanisms of plasma polymerization of OFN are related to those of PFB then similarities in the respective photochemistries should be expected. The involvement of valence isomerisation reactions of the benzene nucleus of tetrafluorobenzene[6f] during plasma polymerization has been extensively discussed by Clark and Abraham as a possible explanation for the appearance of CF_2 and CF_3 moieties. The formation of these isomers are energetically more favourable than the elimination of HF from the corresponding benzene. Cycloaddition reactions of the fulvene, benzvalene and hexadienyne systems with the monomer molecule can then give rise to complex cross-linked material.[6f] The photochemical valence isomerisation of naphthalene and some of its derivatives to form hemi-Dewar naphthalene have been reported;[31] thus suggesting the possible formation of the valence isomer of OFN in the plasma is not unreasonable.

(I) Substrate Temperature Study

The effect of increasing the substrate temperature to 150°C on the composition of the film deposited in the coil region was examined. The increased heat in the reactor caused the pressure to rise to 0.1mb as a consequence of increased sublimation of the octafluoronaphthalene. However, since the fluoroaromatic compounds seem to be rather insensitive overall to small changes in experimental conditions, this fact did not cause concern.

The gross structural features of the core levels were very similar to those acquired from a polymer deposited at room temperature. The carbon to fluorine peak area ratio did show however a slight tendency towards a higher fluorine content at the higher temperature, and also resulted in a slight variation in the composition of the C_{1s} envelope. As already discussed, this difference does not occur in polymerised films of perfluorobenzene (see Table 2.1 *c.f.* Table 2.2).

TABLE 2.2 Effect of Substrate temperature on the composition of the C_{1s} envelope

Temp.	C-CF	total CF	CF_2	CF_3	$\pi \rightarrow \pi^*$
23°C	27	52	15	4	2
150°C	31	49	17	2	1

OFN, 30W, 10 min. ∿0.1mb Plasma

As with the slightly increased C:F ratio, these variations may be more apparent than real.

(II) Optical Emission

The plasma emission spectrum from an OFN plasma is shown in Figure 2.9, this gives a low resolution scan of

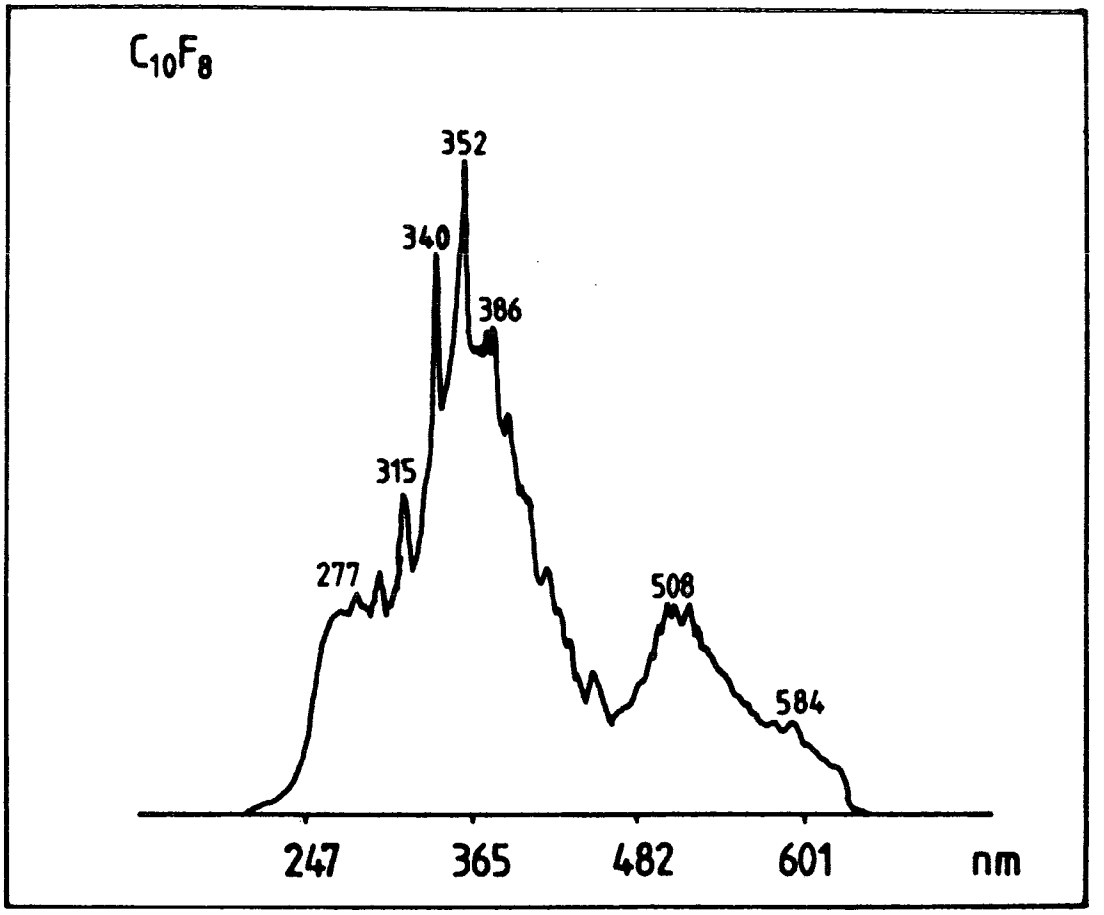

FIGURE 2.9 Optical emission spectrum from a OFN plasma

the 250-600nm region. As with the emission from perfluorobenzene, the spectrum is complex and displays some structure.

The main regions of interest are centred at ∿280, ∿350 and ∿510nm. The latter region is similar to that found in the emission from a PFB plasma, and as in that case, its intensity equals that due to the difluorocarbene radical, at ∿280nm. A high resolution scan of this latter region produced a many banded spectrum identical to that shown for perfluorobenzene, confirming the original of the band in the emission from octafluoronaphthalene.

Examination of the relevant valence photoelectron spectrum for OFN[32] in the search for possible states of the radical cation giving rise to emission reveals that no such transition should occur at the wavelength.[32] The lack of emission from the octafluoronaphthalene cation formed by electron impact has already been noted.[33] It is quite possible that the band at ∿510nm may be associated with a rearrangement or fragmentation product. The emission at ∿350nm is associated with the $S_1 \rightarrow S_0$ transition of the neutral molecule.[34]

Studies of the energy relaxation processes for the excited states of the fluorobenzene by Gilbert and Théorêt revealed that as the extent of fluorination increased the quantum deficit increased and photochemical reactions of the first excited state become increasingly important as the means of releasing the excess energy.[29]

Evidence for a similar situation occurring in the naphthalenes may be taken from the relevant solution phase luminescence quantum yields.[34] On going from naphthalene to the perfluorinated compound the quantum deficit is increased by a factor of ∿2, *i.e.* photochemical pathways, *e.g.* isomerisation, polymerization are more important as a means of relaxation than in naphthalene or 1-fluoronaphthalene.

2.3.3 Plasma Polymerized 1-Fluoronaphthalene (1FN)

Due to the very low vapour pressure of 1FN only one pressure of 0.06mb could be used. Figure 2.10 shows typical C_{1s}, F_{1s} and O_{1s} core level spectra for plasma polymerised 1FN.

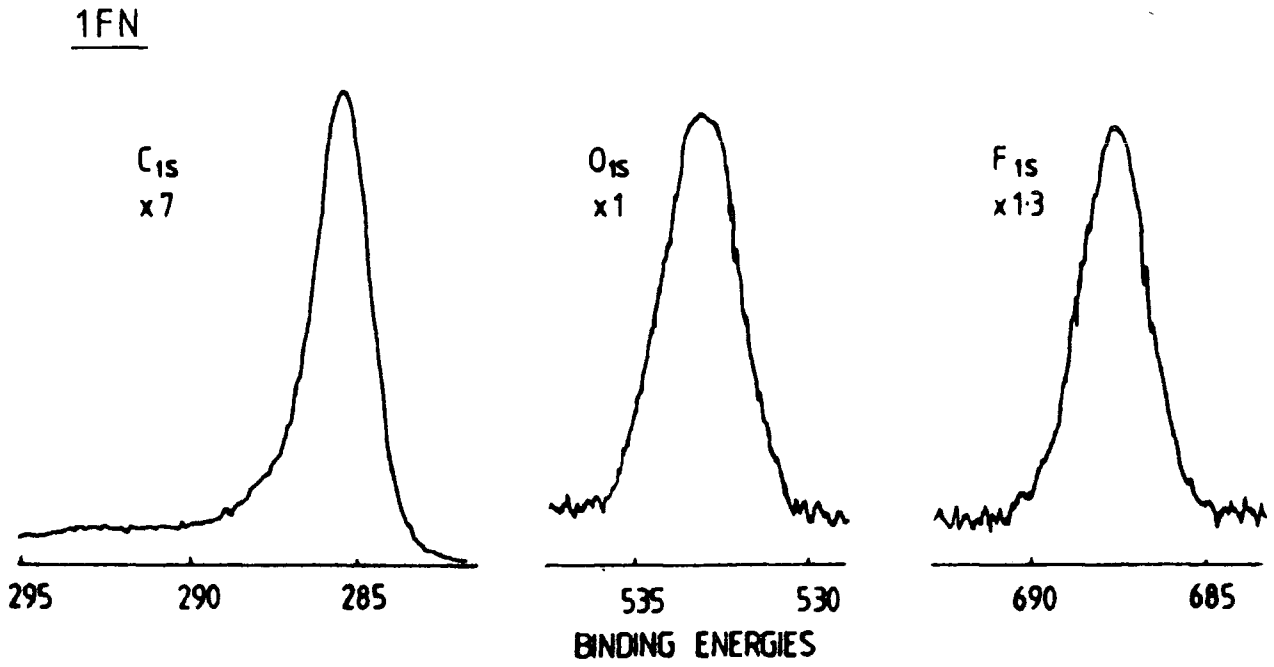

FIGURE 2.10 Typical core level spectra from plasma polymerized IFN

The C_{1s} envelope has a main photoionization peak centred at 285.0eV arising from carbons not bonded to fluorine or oxygen. A shoulder to higher binding energy is evident and indicative of the presence of functional groups other than C-H. By using standard peak fitting techniques already mentioned components are found at binding energies of *ca.* 286.6, 288.2, 289.7 and 292.0eV. The assignment of these peaks is not straightforward. The complication arises from the fact that the C-O and C=O groups have similar chemical shifts as C-CF and C-F, and therefore the component peaks may arise from both fluorine and oxygen environments. As has been discussed in the plasma polymerization of perfluorobenzene,

oxygen incorporation is a common feature of plasma polymerization,[6] but due to the low level of fluorine in the deposited films, it is unlikely that the components at higher binding energies, *i.e.* greater than 288.0eV will arise from significant contributions due to CF_2 and CF_3. Therefore, the peak at 292.0eV has been assigned to $\pi \rightarrow \pi^*$ shake-up of the main photoionisation peak.[35] The separation of 7eV of the shake-up satellite from the main photoionisation peak in hydrocarbon systems has already been reported.[14]

It should be noted at this stage that the C_{1s} envelope displays a distinct asymmetry, *i.e.* a step in the background counts on going from the high to low binding energy side of the main photoionization peak. This asymmetry will be discussed in greater detail in the next chapter.

Due to the difficulties outlined above in peak assignment of the C_{1s} envelope, only total peak area ratios are considered. For plasma polymerized 1FN this gives a value of $\sim$1:0.04 for the C:F stoichiometry of a sample in the coil region.

From the plasma polymerization studies of the fluorinated benzenes,[6e-h] it has been shown that as the degree of fluorination decreases in the parent monomer, there is a concomitant decrease in the level of fluorine in the deposited film. This would suggest that in lowly substituted benzenes elimination reactions are an important pathway in the deposition of plasma polymers. This trend seems to be apparent in the behaviour of the fluoronaphthalenes, *i.e.* the perfluoro compound shows a retention of configuration, but with associated rearrangement whilst the 1-fluoro compound shows ex-

tensive elimination. The atomic ratio of the 1FN monomer is $C_1:F_{0.1}$.

The intensity of the O_{1s} core level is greater than might be expected from previous experience with the perfluorinated monomers. However, from the work carried out on the fluorobenzenes,[6e-h] the extent of oxygen uptake can be related to the fluorine content of the deposited film, *i.e.* as fluorine content increases the oxygen content decreases. Oxygen uptake is not necessarily associated directly with fluorine elimination. Rather that the elimination of fluorine moieties could make the polymer precursosrs and the deposited films more susceptible to oxidation than those involved in the perfluoro case. It is less likely that oxidation is the primary cause of fluorine elimination. If this were the case then the amount of fluorine retained in the polymer film for any monomer would vary, and be associated with the leak rate of the reactor. However, this is not seen and the results are very reproducible suggesting that the former is responsible for the higher oxygen content.

The increase in the fluorine content of the deposited plasma film of 1FN as the sample is taken from further down the reactor (although still just in the glow region) has still to be explained. As with studies on the composition of the C_{1s} envelope as a function of distance along the reactor for plasma polymerized benzenes and naphthalenes, the composition profile of the fluorine-containing species needs to be obtained. It may be the case for 1FN that the reactive fluorine moieties are able to migrate further down the reactor or that the available energy required to initiate fluorine

elimination is less the further removed from the coil region from which the sample is taken. It is certainly to be expected that the highest energy region will be associated with the coil. Support for this statement can be obtained from the power loading dependence on the extent of fluorine elimination. The extent of fluorine loss increases rapidly as the power is increased from 5-20W. At higher loadings an approximately constant level of fluorine is present in the film.

The effects of power on the $^{F}/_{C}$ ratio (excluding the sensitivity factor) is shown in Figure 2.11 whilst the effect of position in the reactor is shown in Figure 2.12.

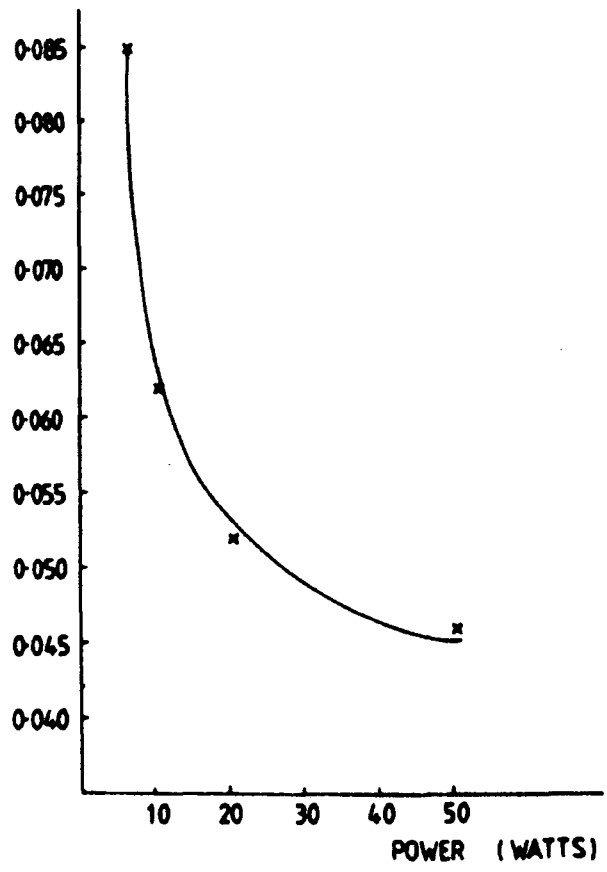

FIGURE 2.11 Peak area ratio of F_{1s} to C_{1s} envelopes as a function of power at 4-6cm.

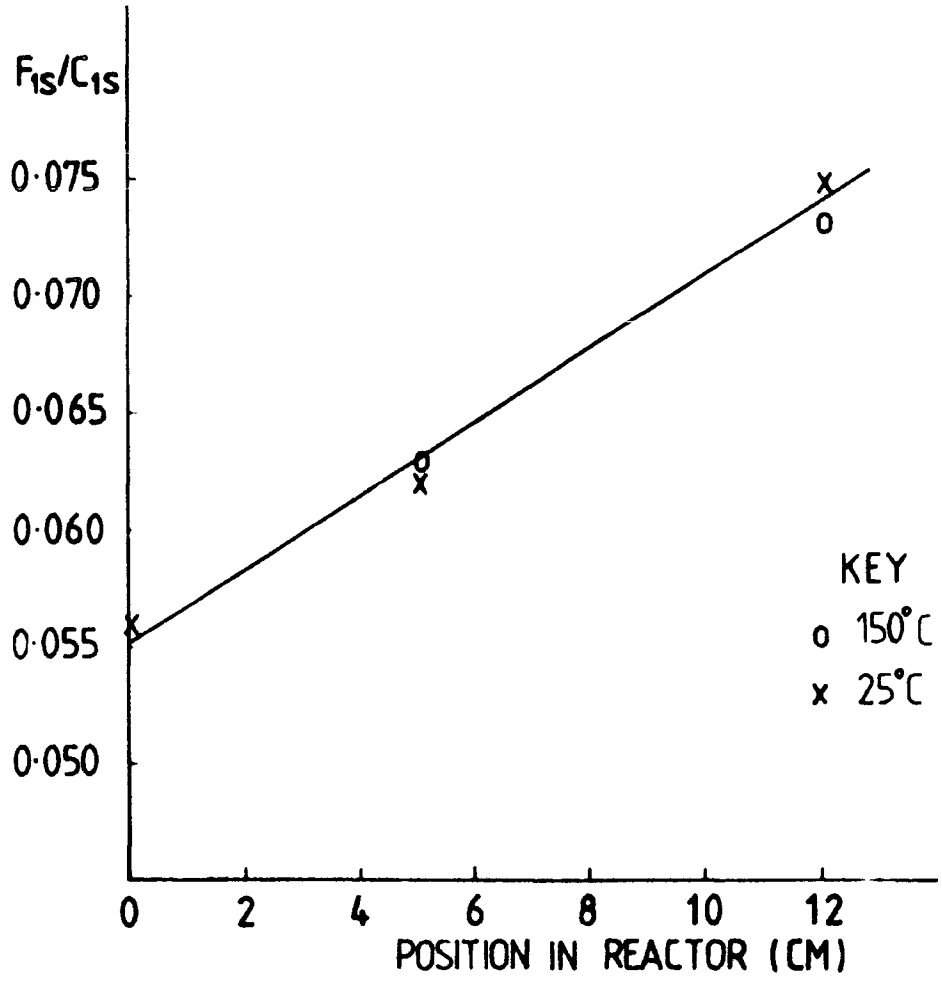

FIGURE 2.12 Peak area ratios of F_{1s} to C_{1s} envelopes as a function of position at 25 and 150°C substrate temperatures at 10W

(I) Substrate Temperature Study

From Figure 2.12, which also shows the effect of position on the $^{F}/_{C}$ ratio using a substrate temperature of 150°C, it can be seen that there is no real difference between the two temperatures. This follows the behaviour shown by the other fluoroaromatic compounds and is not really surprising considering the well known stability of fluoropolymers.[1]

(II) Optical Emission

The optical emission from a 1-fluoronaphthalene plasma is shown in Figure 2.13. The wide scan shows an emission band centred at ∿335nm and is essentially featureless.

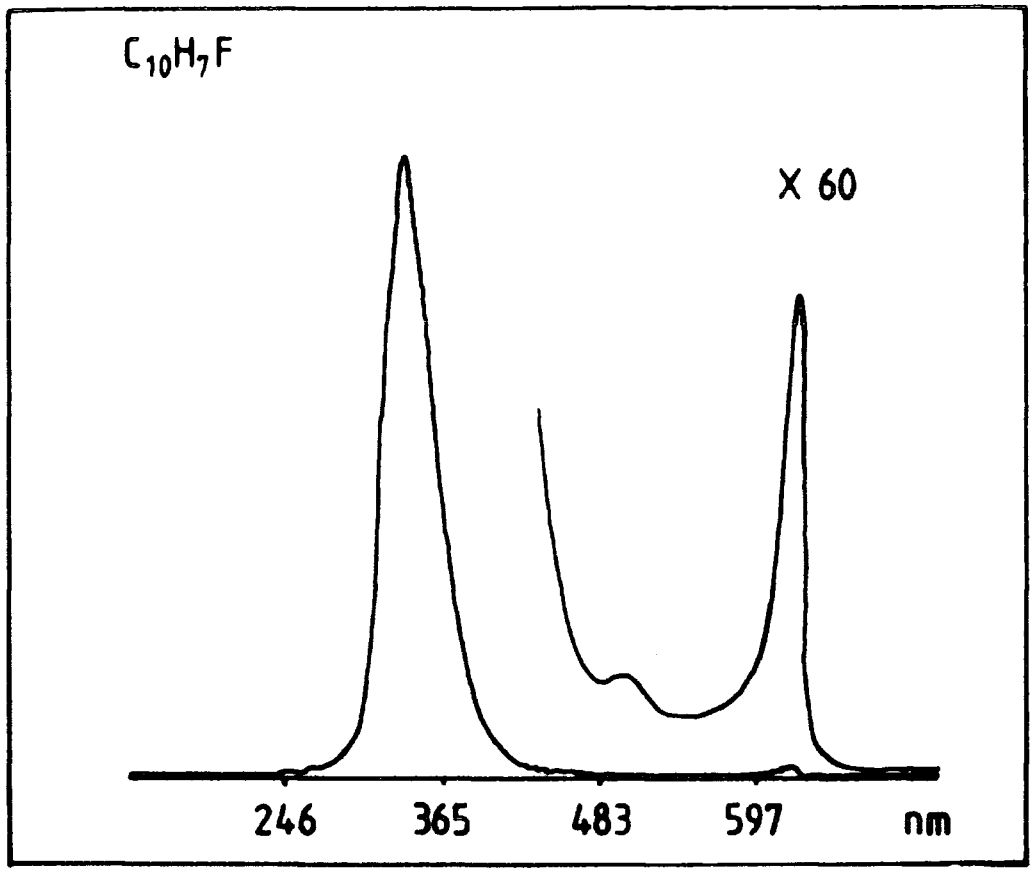

FIGURE 2.13 Optical emission spectrum from a 1FN plasma

This arises from the $S_1 \rightarrow S_o$ transition of the first excited state of the molecule.[34] The X60 expansion shows a small peak, of unknown origin, to longer wavelengths of the main band. An expansion of the 270nm region revealed that there was no emission present from CF_2. This spectrum is shown in Appendix 1.

2.3.4 Plasma Polymerized Fluorobiphenyls

Due to the limited data on the plasma polymerization of the fluorobiphenyls, the deca, octa and monofluorobiphenyls are all considered here. The importance of the position of the fluorine in monofluorobiphenyl is con-

sidered by looking at the plasma polymerization behaviour of 2 different positions of the fluorine:

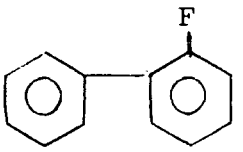

and

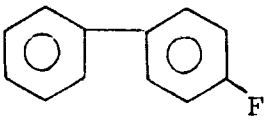

2-fluorobiphenyl 4-fluorobiphenyl

Studies of the biphenyls were limited to their sublimation pressure of *ca.* 0.065mb, and a sample position within the coil region using a power of 50W.

As with the other perfluoroaromatics the C_{1s} envelope derived from both the octa and decafluoro compounds is highly complex and shows very similar structure arising from the multiple environment of the various carbon atoms.[6c-i]

The C_{1s}, O_{1s} and F_{1s} core level spectra for decafluoro and octafluorobiphenyl plasma polymers, along with their respective C_{1s} component peak analyses, are shown in Figure 2.14.

The percentage contributions of the C-CF, CF, CF-CF_n, CF_2, CF_3 and $\pi \rightarrow \pi^*$ shake-up components of the C_{1s} envelope from the polymer produced from decafluorobiphenyl are 30, 18, 22, 22, 6 and 2 respectively, Table 2.4, demonstrating that a large amount of rearrangement has accompanied plasma polymerization. That this is not accompanied by fluorine elimination is demonstrated by the C:F stoichiometry of 1:0.79 which is very close to that of the starting monomer. One difference between the C_{1s} envelopes produced from the plasma polymer of decafluorobiphenyl compared with those produced by the polymers from perfluorobenzene and perfluoronaphthalene is evident. In the latter two polymers, the C-F

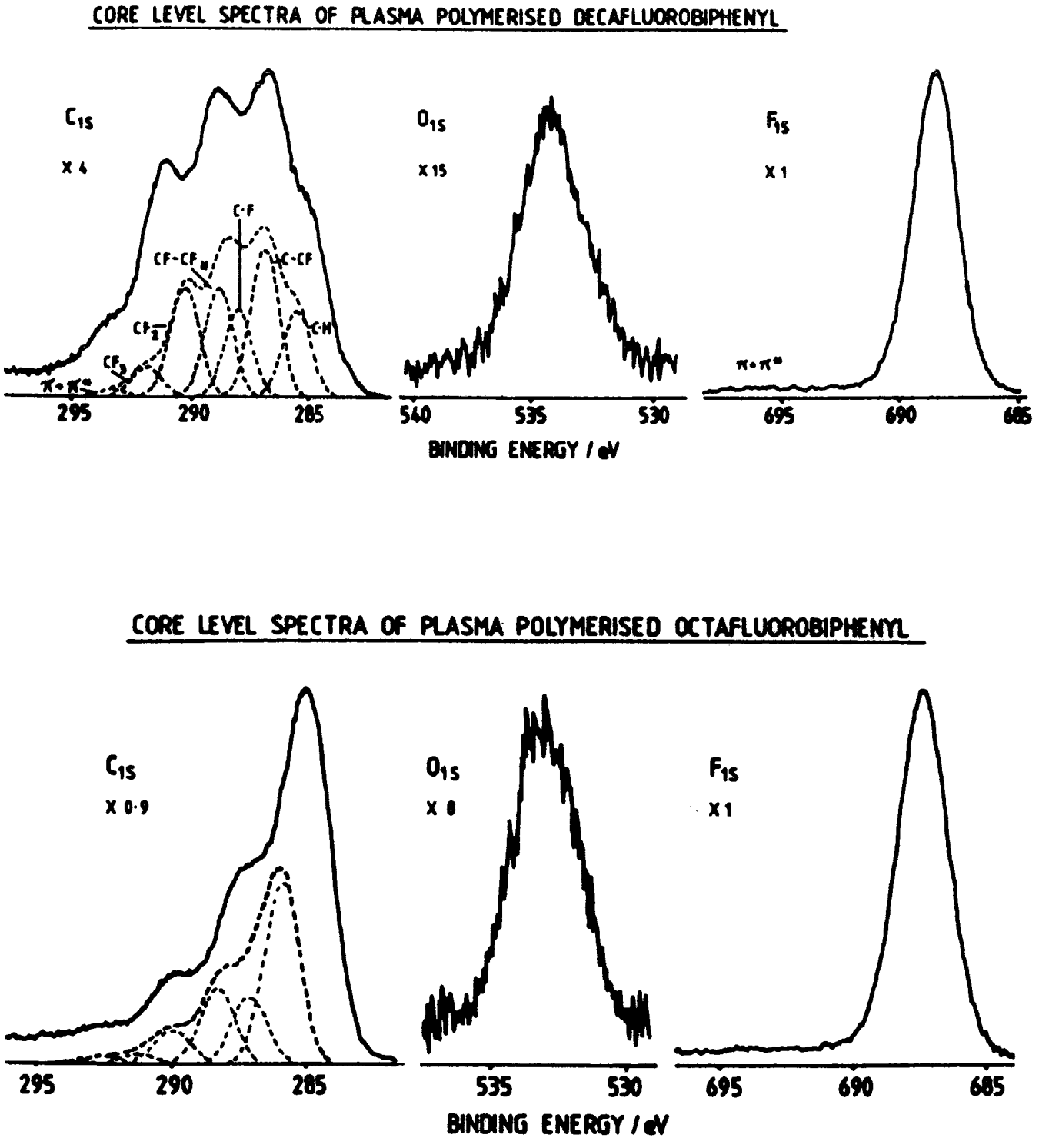

FIGURE 2.14 Typical core level spectra from plasma polymerized DFB and OFB

peak is the dominant peak of the envelope, however this is not the case for the polymer from decafluorobiphenyl. The most dominant peak here is C-CF which is followed in intensity by the peak produced by carbon in CF_2 environments. The unsaturation shown in the C_{1s} envelope is also demonstrated by the $\pi \rightarrow \pi^*$ [14] shake-up satellite in the F_{1s} core level spectrum.

As with the polymer produced from decafluorobiphenyl, the C:F ratio of the material derived from octafluorobiphenyl is also close to that of the starting material ($C_1:F_{0.66}$), but there has been some elimination of fluorine, to give a C:F stoichiometry of $C_1:F_{0.4}$ in the plasma polymer. This calculation was based on the total area of the C_{1s} envelope and as is evident from the C_{1s} core level spectrum, there is a large contribution towards the area from hydrocarbon. It is present in a quantity which would not be expected from the parent monomer. A calculation of the C:F ratio using the component peaks of the C_{1s} envelope agrees with the value obtained from the peak area ratio. This tends to suggest that the level of hydrocarbon is a 'real' effect due to the plasma polymerisation of octafluorobiphenyl, and is not to any marked extent due to hydrocarbon contamination.

The extent of unsaturation, as evidenced by the very low intensity $\pi \rightarrow \pi^*$ shake-up satellites both in the C_{1s} envelope and the F_{1s} core level, has decreased. The relative intensity pattern of the component peaks of the C_{1s} envelope has also changed from that in the decafluorobiphenyl derived material. After the hydrocarbon peak, the component due to CF is now the most prominent, similar to that in the C_{1s} core level from plasma polymerized perfluorobenzene.

There is also more oxygen incorporation, to give a C:O ratio of 1:0.05. This is almost double the amount present in the plasma polymer of the perfluoro compound, and is analogous to the situation in the plasma polymerization of fluorobenzenes and fluoronaphthalenes - as the fluorine content of the parent compound decreases, the oxygen content of the respective plasma polymer increases. This has been discussed in the section on the plasma polymerization of 1-fluoronaphthalene. From this result it would seem that the substitution of 2 hydrogen atoms in the perfluorobiphenyl molecule has quite an effect on the behaviour of the compound in the plasma. This is based on the dissimilarity of the C_{1s} core level envelopes of the resultant plasma polymers.

Since the core level spectra of the monofluorinated biphenyls are 'identical' only the spectra obtained from the 4-fluorobiphenyl are shown in Figure 2.15.

Peak fitting of the C_{1s} envelope which consists of the one main photoionisation peak at 285.0eV (due to C-H) with a shoulder to higher binding energies, reveals peaks at ∿286.6, 288.2, 289.7 and 292.0eV (Table 2.4). As is the case with the 1-fluoronaphthalene derived material peak assignment is not straightforward and has not been attempted for the peaks above 285eV. The extremely low level of fluorine present (C_1:$F_{0.02}$) strongly suggests that the latter two peaks are due to oxygenated carbon environments only, whilst the two former peaks will be due to both carbon-oxygen and carbon-fluorine environments. This assignment is backed up by the lack of emission from CF_2 in the optical emission spectrum from the plasma. The increased level of oxygen is reflected in the overall stoichiometry of C_1: $O_{0.07}$.

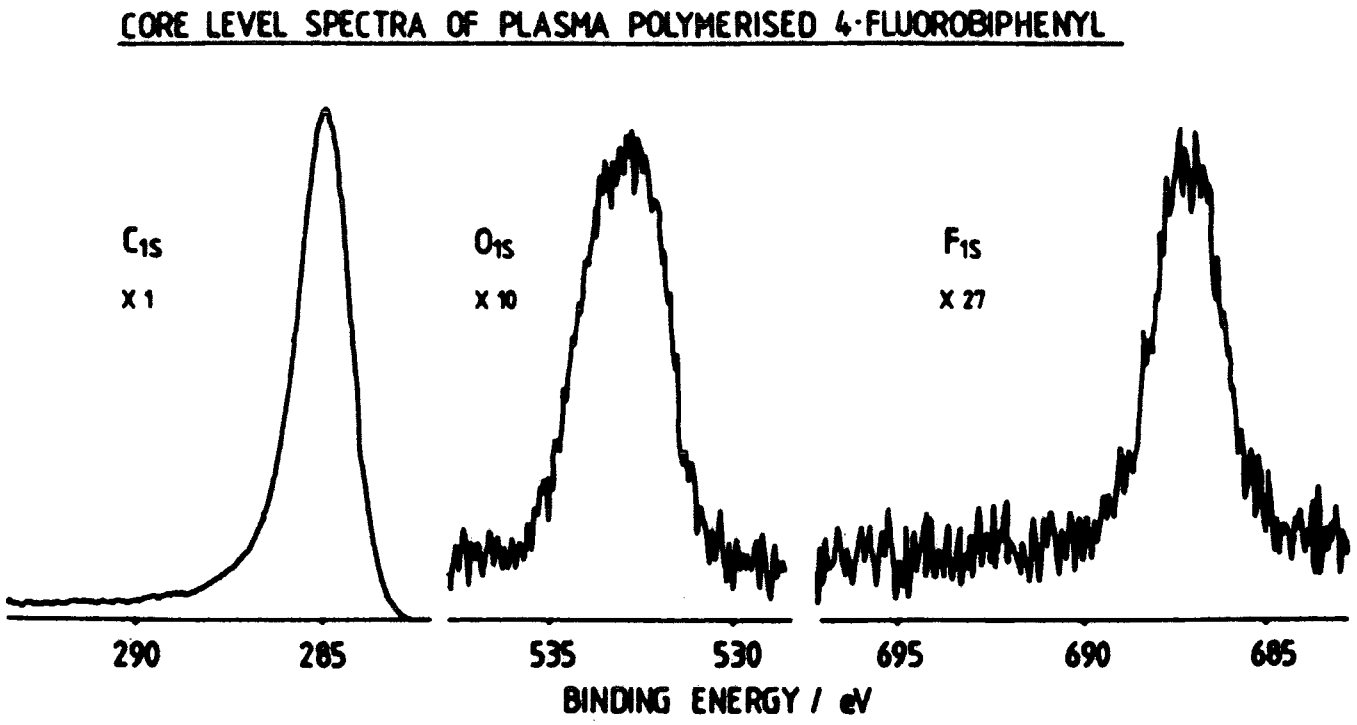

FIGURE 2.15 Typical core level spectra from plasma polymerized MFB

From the fluorine to carbon peak area ratio it can be seen that there has been extensive elimination of fluorine in the mechanisms resulting in deposition of the plasma polymer. This situation is analogous to that shown by the fluorobenzenes and fluoronaphthalenes. Perfluoro-aromatic compounds undergo plasma polymerization utilizing mechanisms that result in extensive rearrangement, but not elimination of fluorine to produce polymer which is not deficient in fluorine when compared with the parent compound.

In conclusion, Table 2.3 lists the C:F ratio of the parent monomer and the resultant plasma polymer together

with the O:C stoichiometry of the materials derived from the fluorobiphenyls.

TABLE 2.3 Elemental Ratios for the Polymers Produced from the Fluorinated Biphenyls

Monomer	$C:F_{monomer}$	$C:F_{polymer}$	$C:O_{polymer}$
2 $C_{12}F_1H_9$	1:0.08	1:0.02	1:0.06
4 $C_{12}F_1H_9$	1:0.08	1:0.02	1:0.07
$C_{12}F_8H_2$	1:0.66	1:0.40	1:0.05
$C_{12}F_{10}$	1:0.83	1:0.80	1:0.03

TABLE 2.4 Lists of Component Peaks of the C_{1s} envelope of the fluorobiphenyls in percentage areas

Monomer	CH	C-CF	Total CF	CF_2	CF_3	$\pi\rightarrow\pi^*$
$C_{12}F\ H_9$	84.1	?	?	?	?	-
$C_{12}F_8H_2$	-	35.0	57.0	5.0	3.0	-
$C_{12}F_{10}$	-	30.0	40.0	23.0	6.0	1

(I) Optical Emission

The optical emissions from decafluoro and monofluorobiphenyl plasmas are shown in Figures 2.16 and 2.17 respectively, both are wide scans covering the UV - visible region. High resolution scans of the ∿270nm region are shown in Appendix 1. Emission arising from the CF_2 radical has been shown to occur in the region[29] and its spectrum is typified by that shown in the plasma of decafluorobiphenyl. Hence emission in this region, by CF_2, is characteristic of rearrangement processes in the plasma. This high resolution scan is identical to scans obtained from the same region in both perfluorobenzene and perfluoronaphthalene plasmas. The surface composition of all three perfluoroaromatic plasma

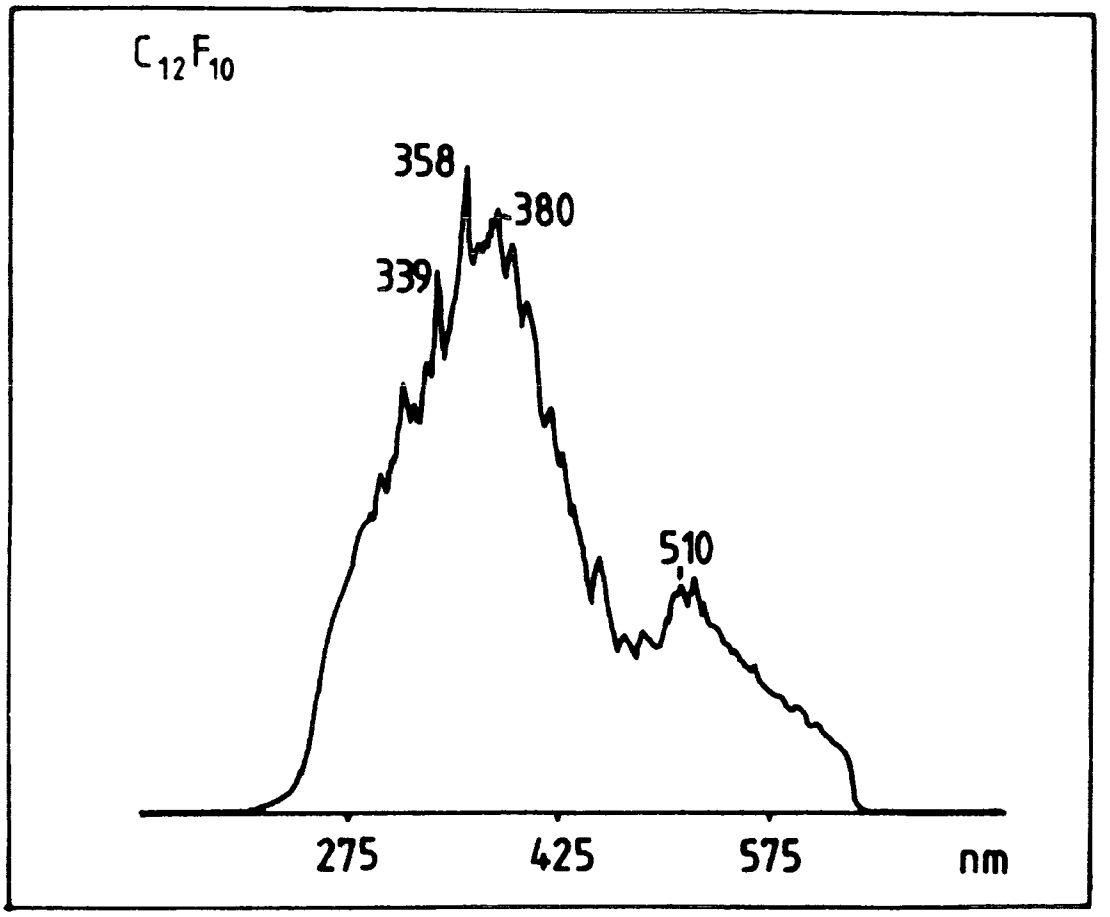

FIGURE 2.16 Optical emission spectrum from a DFB plasma

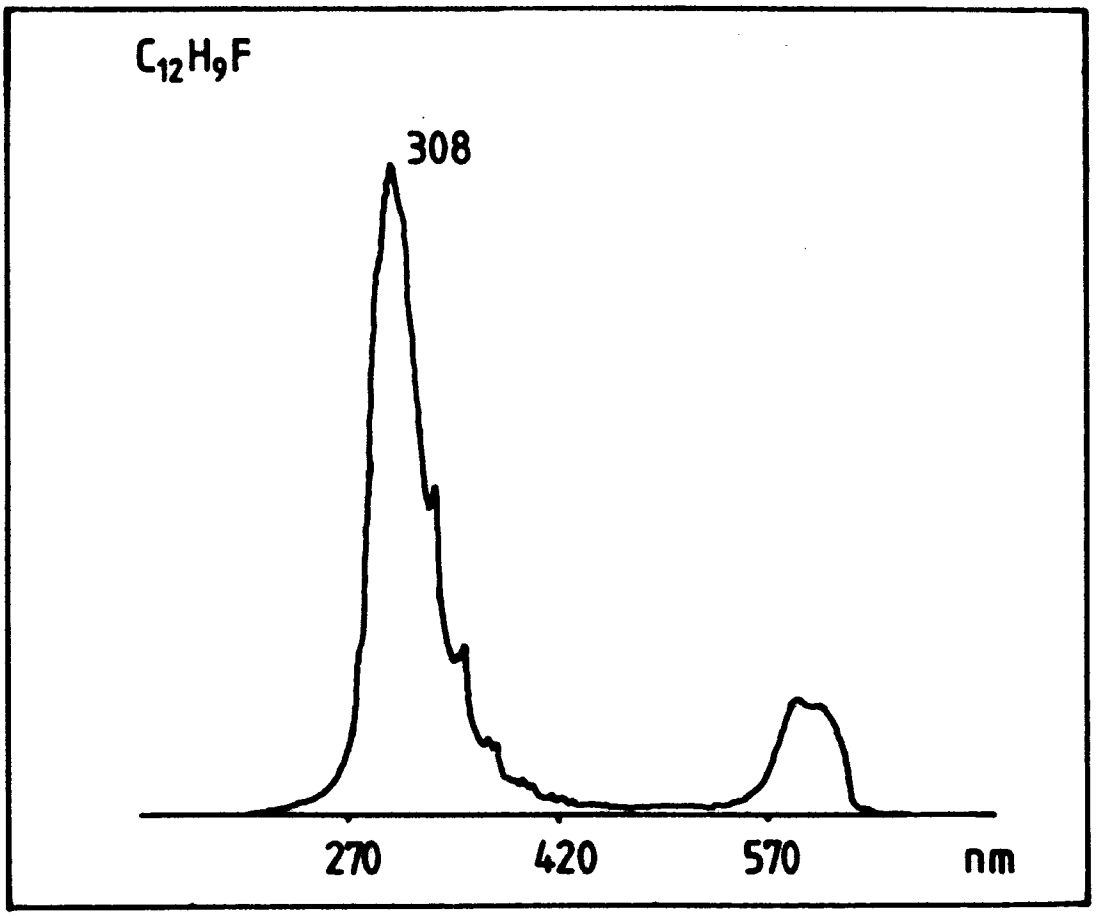

FIGURE 2.17 Optical emission spectrum from a MFB plasma

polymers reflecting the rearrangement mechanisms which must occur in the plasma leading to deposition. There is no emission from the CF_2 radical in the plasma of monofluorobiphenyl.

The emission from monofluorobiphenyl (Figure 2.17) is centred at ∿308nm and shows some fine structure on the higher wavelength side of the main peak which is thought to arise from an $S_1 \rightarrow S_o$ transition of the first excited state of the molecule. In contrast, the spectrum of decafluorobiphenyl is more complex. The main regions of interest are centred at ∿290nm, ∿350nm and ∿510nm. The latter region is similar to that found in the emissions from perfluorobenzene and octafluoronaphthalene plasmas. Its origin is at present uncertain but may be due to a precursor of CF_2 moieties. As with the aforementioned plasmas the intensity of the 510nm peak is of the same intensity as the peak at ∿290nm due CF_2.

2.4 Conclusion

The work detailed in the previous pages on the plasma polymerization of fluoroaromatic compounds, *i.e.* benzenes, naphthalenes and biphenyls can be summarised pointwise. For the fully fluorinated compound these are:

1. Plasma polymerization of the perfluorocompounds resulted in a retention of fluorine such that the overall stoichiometry of the polymeric film is essentially the same as the starting monomer.

2. The C_{1s} spectra revealed evidence of extensive molecular rearrangements with components appropriate to CF_3, CF_2 and C-CF components.

3. A low intensity peak arising from O_{1s} levels was observed in all cases (*ca.* $C_1:O_{0.03}$) as was a variable component at 285.0eV due to hydrocarbon contamination.

4. The optical emission from the plasma of the perfluorinated compounds all show a strong emission at ∿290nm, due to CF_2 species, and this is associated with an emission at ∿510nm of equal intensity whose origin is as yet unknown.

5. The overall band profile of the C_{1s} and F_{1s} core levels and their relative area ratios remained essentially constant over the range of conditions studied.

6. The composition of the deposited film is invariable with respect to increasing the substrate temperature to 150°C from room temperature.

7. The surface composition is reflected in the 'bulk' composition as far as ESCA can determine.

8. Over a 10 minute deposition period, the rate of production of film was so rapid that the substrate was not 'visible' to ESCA, *i.e.* at least a 70A thick film.

These last four points also apply to the lower fluorinated compounds, to which the following points also relate:

1. Plasma polymerization of the lower fluorinated compounds is accompanied by elimination of fluorine such that the plasma polymer may only contain $^1/_4$ of the amount of fluorine as the parent monomer.

2. With a decreasing amount of fluorine, an increased amount of oxygen is incorporated into the plasma polymer.

3. The C_{1s} spectra reveal a main photoionisation peak at 285.0eV with a shoulder to higher binding energies. Both fluorine and oxygen containing functional groups contribute to this shoulder.

4. The optical emission from the plasma of a monofluorinated compound lacks any emission from CF_2 at ∿290nm, or the associated peak at ∿510nm.

REFERENCES - Chapter Two

1. M. Hudlicky, 'Chemistry of Organic Fluorine Compounds - A Laboratory Manual', John Wiley and Sons (Publishers), New York, 2nd Ed. 1976 and references therein.

2. 'High Polymers Vol.XXV - Fluoropolymers', L.A. Wall (Ed.), Wiley Interscience, John Wiley and Sons, Inc.,New York,1972.

3. J.L. Margrave and R.J. Iagow, Chem.Eng.News., 48(2),40 (1970).

4a. N. Kogoma, T. Moriwaki and S. Okazaki, Proc.Int.Ion Eng. Congr., 3, 1499 (1983).

b. G. Legeay, J.J. Rousseau and J.C. Brosse, Eur.Polym.J., 21(1), 1 (1985).

c. J.A. Thornton, Thin Solid Films, 107(1), 3, (1983).

d. H. Yasuda, J.Membr. Sci., 18, 273 (1984).

e. M. Gazicki and H. Yasuda, Plasma Chem.Plasma Process. 3(3), 279, (1983).

5. D.T. Clark in 'Photon Electron and Ion Probes of Polymer Structure and Properties', T.J. Fabish, D. Dwight and H.R. Thomas, Eds., ACS. Symposium Series No.162, Am.Chem. Soc., Washington, D.C. (1979).

6a. D.T. Clark and D. Shuttleworth, J.Polym.Sci.,Polym.Chem.Ed., 16, 1093 (1978).

b. D.T. Clark and D. Shuttleworth, J.Polym.Sci.,Polym.Chem.Ed., 17, 1317 (1979).

c. D.T. Clark and D. Shuttleworth, J.Polym.Sci.,Polym.Chem,Ed., 18, 27 , (1980).

d. D.T. Clark and D. Shuttleworth, J.Polym.Sci.,Polym.Chem.Ed., 18, 407, (1980).

e. D.T. Clark and M.Z. AbRahman, J.Polym.Sci.,Polym.Chem.Ed., 19, 2129 (1981).

f. D.T. Clark and M.Z. AbRahman, J.Polym.Sci.,Polym.Chem.Ed., 19, 2689 (1981).

g. D.T. Clark and M.Z. AbRahman, J.Polym.Sci.,Polym.Chem.Ed., 20, 1717 (1982).

h. D.T. Clark and M.Z. AbRahman, J.Polym.Sci.,Polym.Chem.Ed., 20, 1729, (1982).

i. D.T. Clark and M.Z. AbRahman, J.Polym.Sci.,Polym.Chem.Ed., 21, 2907 (1983).

7. H. Yasuda, 'Plasma Polymerization', Academic Press Inc., Florida (1985).

8. D.T. Clark in 'Polymer Surfaces, D.T. Clark, W.J. Feast (Eds.) Wiley, London, 1978.

9. P.M.A. Sherwood in 'Practical Surface Analysis by Auger and X-ray Photoelectron Spectroscopy', D.Briggs, M.P. Seah (Eds.), John Wiley and Sons Ltd. (1983).

10. H.R. Thomas, Ph.D. Thesis, Durham University, U.K. (1977).

11. D.T. Clark, H.R. Thomas, D. Shuttleworth, A. Dilks, J.Electron.Spectrosc.Relat.Phenom., 10, 455 (1977).

12. D.T. Clark and A. Dilks, J.Polym.Sci.,Polym.Chem.Ed., 15, 15 (9177).

13. C.S. Fadley, in 'Electron Spectroscopy, Theory, Techniques and Applications', Vol.2, C.R. Brundle and A.D. Baker (Eds.), Academic Press, London, (1978).

14. D.T. Clark and D.B. Adams, Theoret.Chim.Acta (Berl.), 39, 321 (1975).

15. D.T. Clark and W.J. Feast, J.Macromol.Sci.Rev.Macromol. Chem. 12,191 (1975).

16. D.T.Clark, 'Structure and Bonding in Polymers as Revealed by ESCA', in 'Electronic Structure of Polymers and Molecular Crystals', J. Lallik and J.M. Andre (Eds.), Plenum Press, New York (1975).

17. D.A. Huchital and R.T. McKeon, Appl.Phys.Letts. 20, 158 (1972)

18. D.T. Clark 'ESCA applied to Polymers', in 'Advances in Polymer Science', Springer-Verlag, 24, 125 (1977).

19. D.T. Clark and H.R. Thomas, J.Polym.Sci.,Polym.Phys.Ed., 15, 2843 (1977), and references therein.

20. D.R. Penn, J.Electron.Spectrosc.Rel.Phenom., 9, 29 (1976).

21. D.T. Clark and D. Shuttleworth, Eur.Polym.J., 15, 265,(1979).

22. H. Yasuda, C.R. Wang, J.Polym.Sci.,Polym.Chem.Ed., 23(1), 87 (1985).

23. A.M. Wrobel, J.E. Klemberg, M.R. Wertheimer and H.P.Schreiber, J.Macromol.Sci.Chem., A15(2), 197 (1981).

24. H.S. Munro and H. Grunwald, J.Polym.Sci.,Polym.Chem.Ed., 23, 479 (1985).

25. G. Czornyj, Org.Coat.Appl.Polym.Sci.Proc., 47, 457 (1982).

26. G. Bieri, J.P. Stadelmann, F. Thommen, and J. Vogt, Helv. Chim.Acta, 61(1), 357 (1978).

27a. M. Allan, J.P. Maier, and O. Marthaler,Chem.Phys.26,131 (1977)

b. J.P. Maier and F. Thommen, Chem.Phys., 57, 319 (1981).

28. J.W. Robinson, Ed., C.R.C. Handbook of Spectroscopy,Vol.1, C.R.C. Press, Cleveland, OH. 1974.

29. R. Gilbert, A. Théorêt, J.Phys.Chem., 80, 1017, (1977).

30. P. Canepa, M. Nicchia, S. Munari and G. Bena, Chim.Ind. (Milan), 66(4), 238 (1984).

31. R.W. Franck, W.L. Mandella and K.J. Falci, J.Org.Chem., 40(3), 327 (1975).

32. C.R. Brundle, M.B. Robin and N.A. Kuebler, J.Am.Chem.Soc., 94,1451 (1872).

33. J.P. Maier, O. Marthaler and M. Mohrarz, J.Chim.Phys., 77, 661 (1980).

34. H.M. Rosenberg, and C.D. Carson, J.Phys.Chem., 72(10), 3531, (1968).

35. D.T. Clark, Pure and Appl.Chem., 54, 415 (1982).

CHAPTER THREE

THE PLASMA POLYMERIZATION OF FLUOROCARBONS IN THE PRESENCE OF NON POLYMERIZABLE GASES

3.1 Introduction

The effects of diluting the monomer with a carrier gas such as argon or other non-polymerizable gas has been explored in the hope of being able to synthesise tailor-made films by varying the composition of the gas phase.[1] Inert gases have also been used in numerous patents[2] to achieve the required pressure, *i.e.* they are used to boost the limited vapour pressure of the organic monomer,[3] or to cause the incorporation, by physical sputtering, of metal.[4]

Another application of the addition of simple gases to the plasma zone is in the field of plasma etching/plasma polymerization. The chemistry occurring in a fluorocarbon plasma has been determined as being critically dependent upon the effective fluorine/carbon ratio of active species in the reactor.[5] For fluorocarbons with a high F/C ratio, the predominant process is etching, while for fluorocarbons with a low F/C ratio polymerization and oligomerization are the dominant processes.[5] This ratio can be altered by the addition of 'simple' gases. An effective lowering of the F/C ratio can be achieved by the addition of hydrogen, this leads to the removal of fluorine by conversion to stable volatile fluorides.[6] The addition of oxygen causes the F/C ratio to shift in the other direction due to the formation of CO and CO_2 gases.[6] This dual effect of the F/C ratio has been used to incorporate metals into plasma polymerized fluorocarbons by the simultaneous etching and polymerization.[7] The metal to be incorporated forms one of the electrodes in a capacitively coupled reactor system. The metal is then entered into the gas phase by physical sputtering of the

cathode or by the plasma etching through the formation of volatile fluorides, or a combination of both. The composition of metal in the plasma polymer can be controlled by changing the relative rates of etching and deposition, *i.e.* increasing the F/C ratio such that etching, and hence metal incorporation, dominate over the deposition rate which decreases.[7] It should be noted that in experiments in which hydrogen or oxygen addition has been used to manipulate the effective F/C ratio, the polymer structure will be modified by the inclusion of hydrogen and oxygen functionalities.[8] This may affect the properties of the metal containing polymer.

Non polymerizable gases have also been copolymerized with organic monomers in the hope of inserting specific functional groups. It has been noted that oxygen containing organic monomers when subject to a plasma, lose oxygen due to the formation of CO.[9] In the hope, therefore, of incorporating carboxyl groups into the polymer, acrylic acid and carbon dioxide have been copolymerized.[10] It was reported that the copolymer formed contained both carboxyl and carbonyl groups. Similarly ammonia has been incorporated into a fluorocarbon polymer[11] when nitrogen functionalities, mainly in amido form were incorporated into the formed polymer. This changed the surface energy of the resultant copolymer to a high energy system, *i.e.* hydrophilic. The gas permeability, to oxygen and nitrogen, of the copolymer films was determined to be controlled by the concentration of ammonia in the plasma feed.[11]

By the use of oxygen and hydrogen, to alter the concenration of the various active species present in a fluorocarbon fed plasma, it has been concluded that the etch rate of

silicon depends only on the F atom concentration rather than on the various charged species and electron density.[12]

The addition of hydrogen has been found to result in an increased deposition rate of organic monomers,[13] under certain conditions of discharge power and ratio of inert gas/organic monomer. This is thought to be due to the reaction of the H atom with both monomer and F atoms to increase the free radical concentration in the plasma and to decrease the etch rate respectively.[13] In the copolymerization of hexafluoroethane and hydrogen, when the ratio was less than 1, no H could be detected in the resultant polymer. However, when the ratio was greater than 1, the H content increased abruptly.[14]

Discharges of mixtures of benzene with He, Ar or Xe have been examined by sampling the gas phase ions by mass spectroscopy.[15] It was concluded that there was no evidence of the rare gas altering the chemistry by the exchange of potential energy from either long-lived metastable states or by charge exchange. As it has already been pointed out, however, the results of such an investigation should be treated carefully. The sample volume of gas has been transferred away from the reactor zone to be analysed. Thus the relative concentrations and energy distributions of the various species could have altered during the journey to the spectrometer.

That the presence of the inert gas can change the properties of the plasma as well as the structure of the film is shown by the polymerization of siloxanes in the presence and absence of argon. Gas phase electron spin resonance measurements revealed that a higher concentration of free radicals

resulted when a rare gas was present.[16] Examination of the films by infrared spectroscopy indicated that the films formed in the presence of argon were more crosslinked than those prepared in the absence of argon.[16] This could be a result of the increased concentration of free radicals and/or due to the bombardment of the forming polymer film by Ar which increased the cross-linking density.

This chapter describes the results obtained by a study of the structure and bonding of polymers produced by the plasma polymerization of a fluorocarbon monomer in the presence of a non polymerizable gas: the plasma polymerization of 1 fluoronaphthalene with varying pressures of hydrogen, perfluorobenzene with varying pressures of Ar, and perfluorobenzene in the presence of iodine.

3.2 Experimental

Aluminium substrates were placed at various positions along the top of the oil bed within the reactor for the collection of polymer samples deposited during 1 fluoronaphthalene/hydrogen and perfluorobenzene/argon plasmas whilst samples were taken from the coil region only from the perfluorobenzene/iodine plasma.

A power loading of 10w and a deposition period of 15 minutes were used with the full vapour pressure of 1 fluoronaphthalene (with needlevalve fully open, 0.06 mbar). Diffusional mixing of the hydrogen and 1 fluoronaphthalene took place prior to entry into the reactor inlet *via* a 'T' piece, the amount of hydrogen adjusted until the desired total

pressure was reached.

Before collection of polymer samples deposited during the plasma polymerization of perfluorobenzene in the presence of argon, the reactor and substrates were precleaned with a 30min 50hr 0.2mb Ar plasma. A power loading of 6w and a deposition period of 10 minutes was used to obtain the polymer samples. As with 1 fluoronaphthalene/hydrogen mixes, perfluorobenzene and argon were mixed prior to entry into the reactor through a 'T' piece, the pressure of each being individually controlled by needlevalves.

Total pressures of the PFB/Ar system relate to the following flow rates of PFB and PFB/Ar:

PFB/Ar	Total Pressure (mb)	Flow rate PFB (cm^3 STP min^{-1})	Total Flow rate PFB/Ar (cm^3_{STP} min^{-1})
1:0	0.2	7×10^{-4}	-
1:0	0.1	7×10^{-4}	-
1:1	0.16	7×10^{-4}	8.0×10^{-4}
1:2	0.24	7×10^{-4}	1.2×10^{-3}
1:9	0.2	1.6×10^{-4}	1.6×10^{-3}
1:4	0.2	2.6×10^{-4}	1.6×10^{-3}
1:2.5	0.2	3.6×10^{-4}	1.6×10^{-3}

The above table contains a few representative examples of flow rates obtained. It is apparent that the flow rate of PFB, under the different variety of conditions, does not change drastically. In fact it was only found to vary from $1.6\text{-}7 \times 10^{-4}$ with total flow rates changing from 8.0×10^{-4} - 3.4×10^{-3} cm^3_{STP} min^{-1} (1:1 *cf.* 1:3 PFB/Ar)

The iodine was sublimed into the reactor by inserting some iodine into a U tube and connecting this to a 'T' piece immediately prior to the reactor inlet. The iodine was heated to 60°C to ensure the presence of sufficient iodine in the reactor. A pressure of PFB of 0.1mb was used together with a power of 6w for polymer formation collected over a 10 minute period. A flow rate of 8.9×10^{-5} cm^3_{STP} min^{-1} was used for the iodine, the combined PFB/I had a total flow rate of 4×10^{-4} cm^3_{STP} min^{-1}.

All samples were shown to be vertically homogeneous with respect to the F:C stoichiometry by using variable electron take-off angles (TOA) consequently the results reported here are those obtained using a 35° TOA.

3.3 Results and Discussion

3.3.1 The Plasma Polymerization of 1-Fluoronaphthalene/Hydrogen Mixes (PPFN/H_2)

Following the study on the plasma polymerization of perfluorobenzene-hydrogen mixtures, where hydrogen appeared to have a profound effect on the structure, composition and rate of deposition of the plasma polymer,[17] the presence of hydrogen on the plasma polymerization of 1 fluoronaphthalene was investigated.

Typical core level spectra for plasma polymerized 1 fluoronaphthalene are shown in Figure 2.10 and are not repeated here. Essentially, the polymer film contained a low level of both fluorine and oxygen functionalities. This was reflected in the C_{1s} core level which consisted of the main photoionisation peak at 285.0eV- due to CH - and a shoulder

to higher binding energies resulting from both C-CF, C-F, C-O, C=O and $\overset{O}{\overset{\|}{C}}$=O groups. Unsaturation in the polymer film was evidenced by the presence of a $\pi \rightarrow \pi^*$ shake-up satellite in the C_{1s} envelope[18] and the asymmetry, *i.e.* a step in the background counts on going from the high to low binding energy side of the main photoionisation peak,[19] of the same core level. The C:F stoichiometry of the plasma polymer showed that elimination of fluorine had taken place, the polymer no longer retained the starting C:F stoichiometry of the monomer. This is in contrast to the plasma polymerization of perfluoro-aromatic compounds in which the C:F ratio is retained.[20]

Under the experimental conditions employed in the present case the partial pressure of fluoronaphthalene could not be varied. Thus the change in fluoronaphthalene/hydrogen composition in the starting mixture is also reflected in an increase in total pressure. This is in contrast to the study by Clark and AbRahman in which the total pressure was kept constant throughout, but the partial pressure of per-fluorobenzene was varied.[17]

For a fixed fluoronaphthalene/hydrogen mixture (FN/H_2 - total pressure = 10^{-1}mb) and a power loading of 10w the variation in fluorine content as a function of sample position is shown in Figure 3.1.

This reveals a similar trend to that for pure PPFN, discussed in Chapter Two, except that the F_{1s}/C_{1s} area ratio is lower for $PPFN/H_2$. At sample position 2 PPFN has a F:C stoichiometry of 0.062:1 whereas for $PPFN/H_2$ it corresponds to 0.048:1. This clearly demonstrates that the inclusion of H_2 into the starting vapour facilitates the elimination of fluorine, and is in agreement with the study of

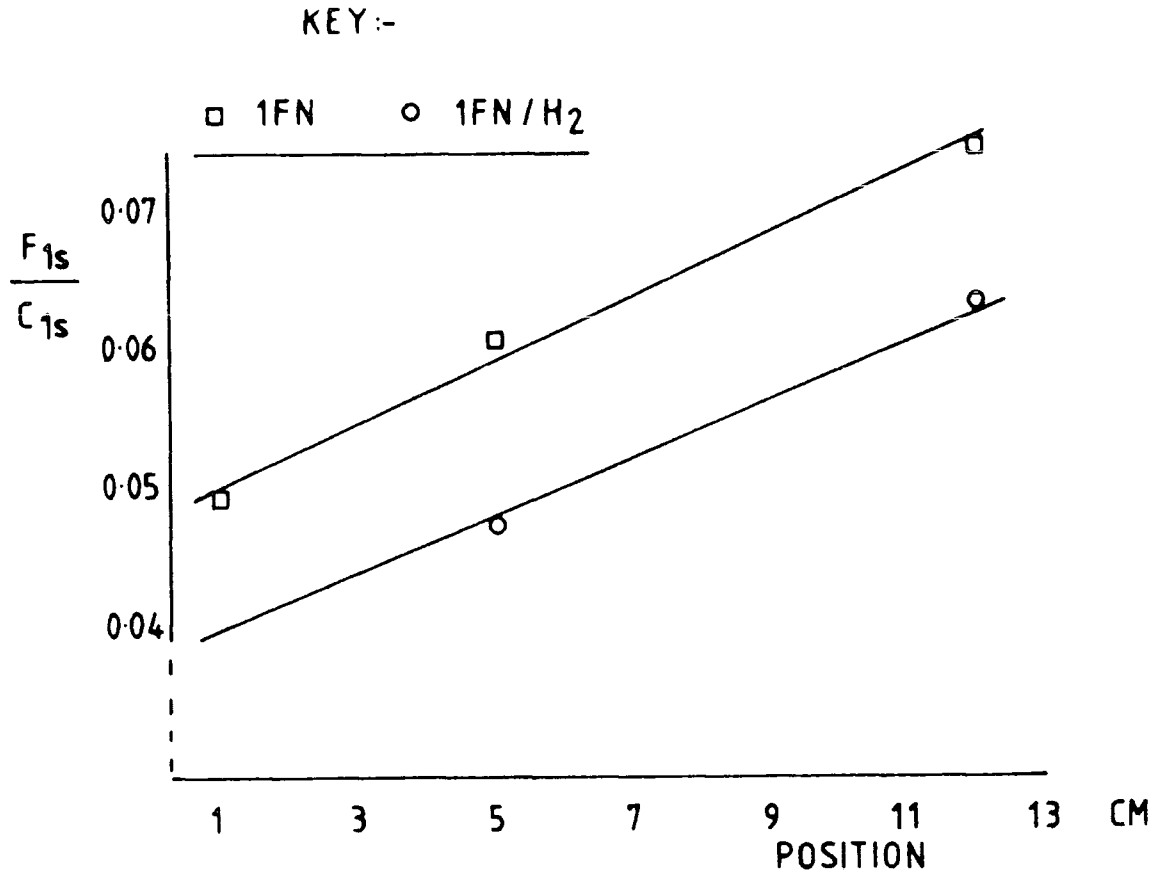

FIGURE 3.1 Peak area ratio F_{1s} to C_{1s} envelopes as a function of position for PPFN/H_2.

the plasma polymerization of perfluorobenzene/H_2 mixtures by Clark and AbRahman.[17] As with the homopolymer, there is a negligible effect of the substrate temperature in the F_{1s}/C_{1s} peak area ratio of the PPFN/H_2 copolymer as a function of sample position in the reactor (Fig.3.1). Deposition on to substrates at room temperature and 150°, result in the same variation in the F_{1s}/C_{1s} area ratio - an essentially linear increase in fluorine content of the film as the sample is taken from further down the reactor. This is an indication that the species present in the gas phase and participating in the polymerization reactions are very sensitive to position within the reactor.[21] It may be the case that the reactive fluorine moieties are able to migrate further down the reactor or that

the available energy required to initiate fluorine elimination is less the further removed from the coil region from which the sample is taken. It is certainly to be expected that the highest energy region will be associated with the coil[21] and the support for this latter process can be derived from the power loading dependence on the extent of fluorine from PPFN in Figure 2.11.

Further evidence for the elimination of fluorine with the inclusion of H_2 in the plasma feed is seen in Figure 3.2.

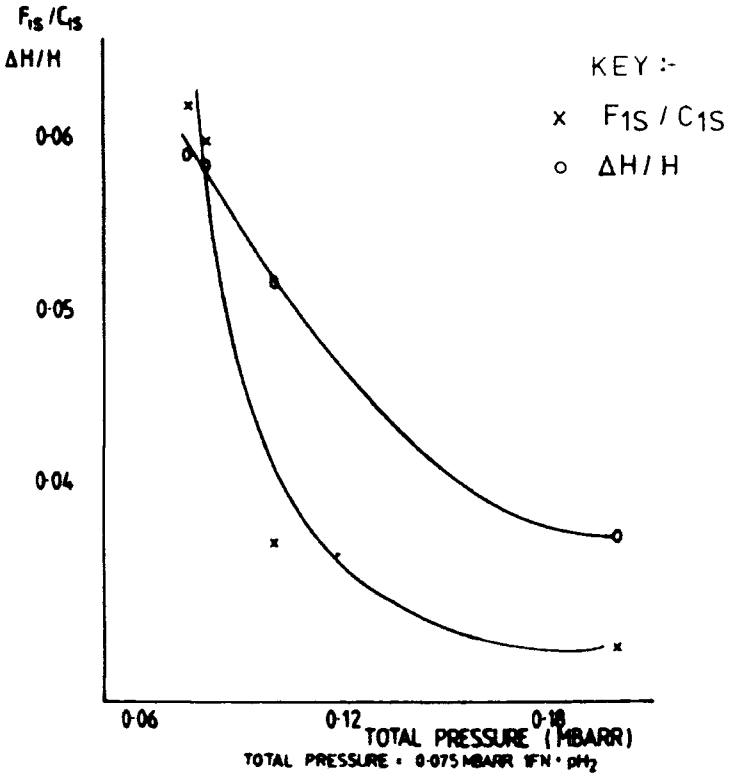

FIGURE 3.2 Height of step function in relation to total pressure and peak area ratio of F_{1s} to C_{1s} envelopes as a function of total pressure.

From the plot of F_{1s}/C_{1s} peak area ratio *versus* an increasing hydrogen pressure it can be seen that with an increase in pressure from 0.075 to ∿0.1 mb the fluorine content of the polymer has almost halved. However, even at relatively high hydrogen pressures not all the fluorine was eliminated.

In the present study the rate of deposition was not monitored. It was noticed by Clark and AbRahman[17] that there was a decrease in the rate of deposition, at a constant total pressure, on going from the pure perfluorobenzene plasma to the hydrogen/perfluorobenzene mixes. If, however, the data was viewed in terms of the partial pressure of the fluorocarbon, then the effect of hydrogen was to actually increase the rate of deposition. This is in agreement with other studies in the plasma polymerization of organic monomers with hydrogen.[13]

The asymmetry of the C_{1s} envelope of PPFN has also been recently observed in plasma polymerized acrylonitrile,[22] ferrocene, vinyl ferrocene, dimethylaminoferrocene,[23] cyclopentadienyl cobalt dicarbonyl,[24] octafluoronaphthalene, and naphthalene.[25] The C_{1s} envelope of the copolymer from tetramethylgermanium and perfluorobenzene also exhibits a very distinct asymmetry, or step- the 1:1 copolymerization of the latter two compounds is discussed in Chapter Five.

From the ESCA studies of a series of polycyclic aromatic compounds and ion bombarded polymers,[19] where similar asymmetries have been observed, it has been postulated that the step in the C_{1s} envelope is evidence for extensive unsaturation in the compound.[19] In polymers such as polystyrene discrete shake-up satellites are observed which are diagnostic

of the local unsaturation present in the pendant phenyl rings.[26] In polystyrene the conjugation length is small, however, as the conjugation length increases, *e.g.* in a system like polyacetylene, the number of allowed shake-up transitions also increases with the result that the shake-up intensity broadens out over a range of such transitions. In PPFN a shake-up satellite is still discernible above the asymmetry indicating the presence of both short and long range unsaturation effects.[27]

The ratio of step height to the height of the main photoionisation peak (ΔH/H as displayed in Figure 3.3) has been shown in a series of polycyclic aromatic compounds[19]

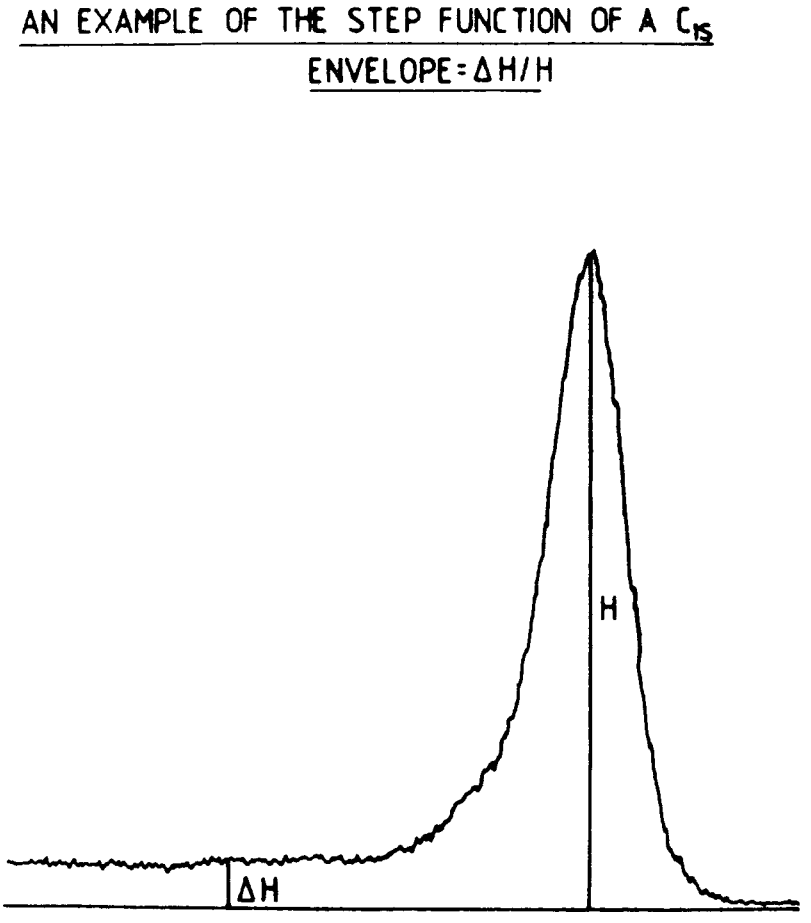

FIGURE 3.3 Step function as seen in the C_{1s} envelope - ΔH/H

to be directly related to the carbon to hydrogen ratio of the compound. Although the influence of the presence of heteroatoms on this relationship has not yet been investigated, a qualitative feel for carbon to hydrogen ratio in plasma polymerized fluoronaphthalene, with particular reference to the PPFN/H_2 polymer films can be felt. In this case it is to be expected that as the partial pressure of hydrogen is increased the extent of hydrogenation and loss of unsaturation will increase. This should be reflected by a decrease in the step ratio as is indicated by Figure 3.2.

In the work of Hutton,[19] the height of the background was measured directly after the main photoionisation peak before the $\pi \rightarrow \pi^*$ shake-up satellite. The C_{1s} core level displayed no shoulder to higher binding energies of the main peak but did have a distinct $\pi \rightarrow \pi^*$ shake-up satellite. In the present study, however, the presence of the peaks at the high binding energy side of the C-H peak made this impossible. Therefore the height of the background was measured 8eV to higher binding energies than the main peak at 285.0eV. This eliminated the possibility of including shake-up satellites in the ΔH measurement[19] due to unsaturated hydrocarbon which occur at 7eV up from the main photoionisation peak.[28]

It is interesting to note that as the extent of fluorine depletion in the plasma polymer begins to approach a $\sim$ constant value the decrease in the step ratio also levels out (Figure 3.2). This data tentatively suggest that the level of unsaturation in a deposited plasma polymer may be controlled by variation of the partial pressure of hydrogen in the starting mixture.[27]

The presence of a step function in a particular core level leads to errors in the calculation of its area. This arises because of the method of background subtraction used by the DS300. Other methods are not available on the system. The beginning and end of the spectral region is defined by two points on the background profile, a linear background subtraction is then performed between the two points - Figure 3.4. For peaks in which the background is essentially the same on each side, there is a minimum loss of significant peak intensity. But peaks which exhibit a large step in the background, due to extrinsic and intrinsic electron

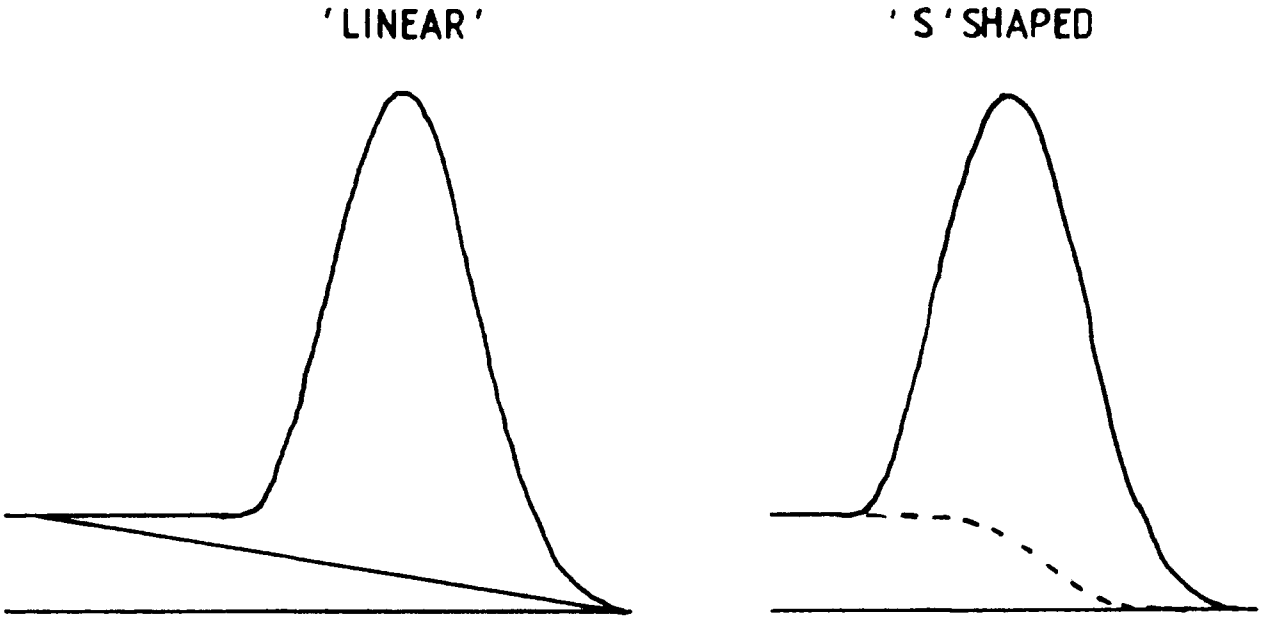

FIGURE 3.4 Linear and 'S' shaped background subtractions

energy loss mechanisms,[29] suffer a loss of peak height and thus peak area. There are no 'correct' solutions to the problem. If the asymmetry is a property of the core level, *i.e.* arises from inelastic tailing, then a non-linear 'S' shaped background subtraction - Fig.3.4 - can be performed.[30] However, if the step function is associated with the main photoionisation event arising from events which occur in the same time scale, *i.e.* shake-up transitions, then primary photoionisation peak becomes modified. The area under this step should then be taken with the area of the main peak to give the total area of the core level spectrum. In this instance, an S shaped background subtraction will take no account of the area under the step to the high binding energy side of the main peak. However, the use of a linear background subtraction in core levels which show a distinct asymmetry also leads to problems associated with peak synthesis. In most cases the actual discrepancy between the 'real' area and that calculated by a linear background subtraction is small in comparison to the total area of the envelope. This discrepancy only becomes important when accurate quantitative results are required, and in the present case may be neglected while looking at general trends.

This problem with peak synthesis will be discussed in Chapter Six, in the work on the copolymerization of aromatic fluorocarbons with their hydrocarbon analogues.

3.3.2 Valence Band Region of PPFN/H_2

Although the main information regarding structure and bonding from an ESCA experiment is derived from the core level spectra, from both the chemical shifts in core level

binding energies and also from the composition of a particular core level, the valence bands of polymers also contain much valuable information[31] especially for systems which display no chemical shifts. For example, high density and low density polyethylene and polypropylene[19] although identical in the C_{1s} region, they are clearly distinguishable from their valence band regions of the ESCA spectra. To be able to extract the maximum amount of information from this region however requires the additional support of quantum mechanical calculations and comparison with other experimental data. These regions can be readily used as 'fingerprinting' spectra.[31] The valence levels tend to reflect long range electronic effects and order whereas the core levels are essentially short range. The presence of asymmetry in the C_{1s} envelope of plasma polymerized fluoronaphthalene is thought to be a long range effect.

The valence band spectra for PPFN at 10w and PFFN at the same power but high pressure are displayed in Figure 3.5. In the valence band spectrum of plasma polymerized fluoronaphthalene the peaks at ∿35 and ∿27eV correspond to F_{2s} and O_{2s} levels.[19] On examining the same region in the valence band spectrum of PPFN/H_2 it is evident that the F_{2s} peak is essentially absent indicating that the low F:C stoichiometry ratio for PPFN/H_2 observed in the core level spectra (*i.e.* the surface) also extends into the bulk. Similarly, the presence of the O_{2s} band in both spectra indicates the oxidation present in the plasma polymer is also not necessarily confined to the very surface. This is not the result expected if the oxygen content of plasma polymers arises solely from the oxidation of the surface of the polymer

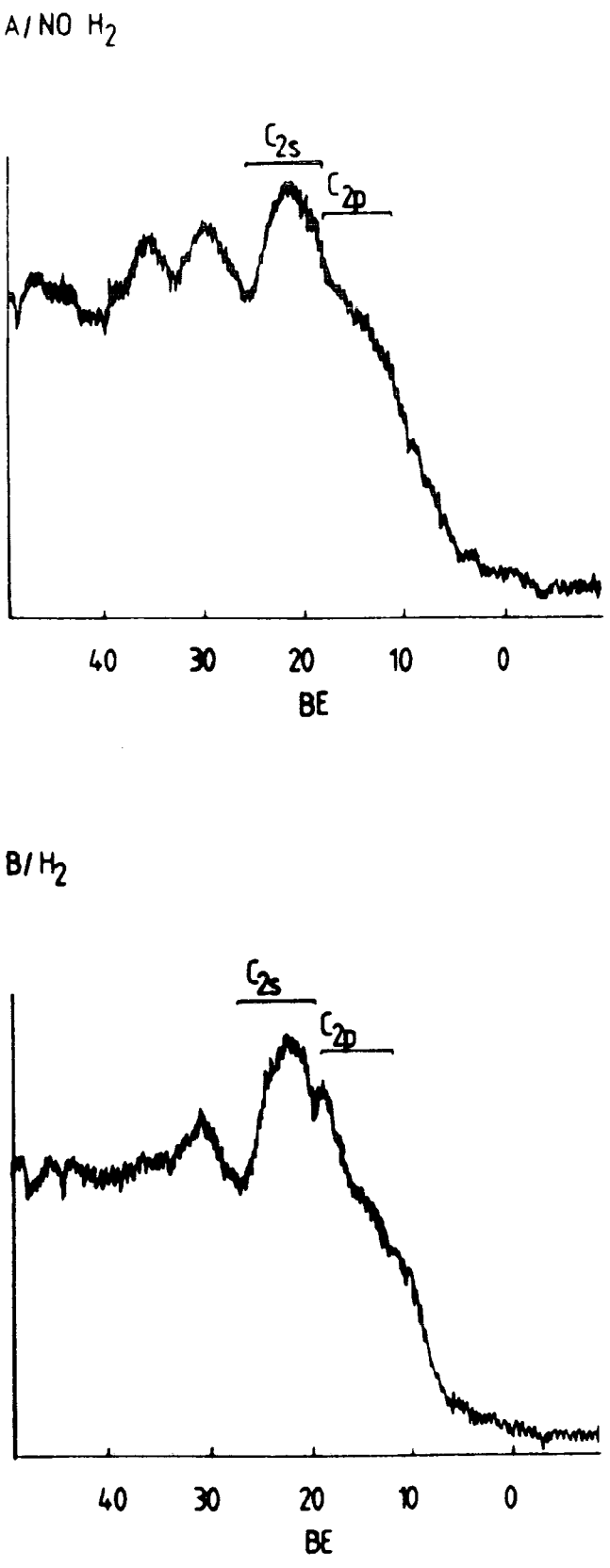

FIGURE 3.5 Valence band of plasma polymerized 1 fluoro-naphthalene (A), no hydrogen, (B) with hydrogen.

upon exposure to atmosphere, the oxygen would not be able to reach the subsurface of the plasma polymer. The rotation of oxidised groups turning into the polymer is also extremely limited due to the highly cross-linked rigid nature of the film.

This result therefore adds validity to the argument that some of the oxygen is incorporated during film formation and may arise from etching of the reactor walls by reactive F atoms, in the case of fluorocarbon plasmas, or through the presence of small leaks in the vacuum line. Under the present experimental configuration, the leak rate before each polymerization was tested to ensure that the rate was not below a 'satisfactory' level, which was personally determined. It is almost impossible to get a leak-free system, one of the biggest causes of leaks in this system is the use of Viton 'O' rings to seal the ground glass flanges of the reactor in the vacuum line, and in the Cajon 'ultra torr' couplings. An improved leak rate would result if the vacuum line were made in nearly one piece and the reactor had conflat flanges. But this, however, would make the vacuum system rigid and difficult to work with and the presence of the metal flanges in the plasma region may be undesirable, depending on the etching characteristics of the plasma under study.

Of most interest in the present valence band spectra are the C_{2s} and C_{2p} bands indicated in Figure 3.5. For plasma polymerized fluoronaphthalene the C_{2s} region consists of a broad structure. However, for PPFN/H_2 a band appears at $\sim$17eV which is distinguishable from the rest of the broad unresolved structure. Although it is of weak

intensity it is completely reproducible. Although it is dangerous to speculate on the origin of this additional peak without the aid of detailed model calculations it is clearly associated with the hydrogenation of the plasma polymer. Both spectra in Figure 3.5, in fact, resemble the valence regions of graphite and polyvinylnaphthalene respectively. It is possible that the observed peak at ∿17eV in PPFN/H_2 reflects a lower degree of cross-linking, chain branching and/or a decrease in unsaturation, *i.e.* some of the differences that exist between graphite and polyvinylnaphthalene.[19]

Thus, in conclusion, as with the study of the plasma polymerization of perfluorobenzene/hydrogen mixtures, the addition of hydrogen to the organic monomer feed to the reactor causes the increased elimination of fluorine and incorporation of hydrogen. This results in a decrease in the extent of unsaturation present which is evidenced by the loss of $\pi \rightarrow \pi^*$ shake-up satellites in the PPPFB/H_2 and from the decrease in step function together with the alteration of the valence band region in PPFN/H_2.

3.3.3 The Plasma Polymerization of Perfluorobenzene/Argon Mixes

(1) Introduction

There have been several studies on the copolymerization, or polymerization, of benzene in the presence of Ar.[15,32] Until now, however, there has been no comprehensive study in the composition of the resulting plasma polymer formed in the presence of varying amounts of the inert gas. The present study was made with the following facts in mind:

(i) The resonance emission lines of Argon, at around 100nm, have sufficient energy to cause the formation of the

radical cation of perfluorobenzene by photoionisation. Thus if the formation of the radical cation is important in the plasma polymerization of perfluorobenzene-the importance of the radical cation has been proposed in studies in the polymerization mechanism of 95% Ar/5% benzene - the presence of excess argon may reveal some interesting results.[32]

(ii) The presence of excess Ar will cause the frequency of electron-molecule collisions to increase, as will the sputtering of the depositing plasma polymer due to argon ions. The formation of Ar metastable states will also occur. These metastable particles cannot radiate and thus energy is stored in electronic excitation. This energy, 11.6eV for the first Ar metastable state,[33] is dissipated by collision with the surface or by energy transfer with another molecule. Thus the transfer of energy from these metastable to the organic molecules may play an important role in the plasma polymerization process.

(iii) The presence of argon will also cause a reduction in the number of bimolecular collisions between the perfluorobenzene molecules and can also deactivate reactive organic species by collision.

In the study on the plasma polymerization of 95% Ar/5% Benzene,[32] the polymeric deposit was said to increase with an increase in pressure. This effect could be simply accounted for by the statistical increase of organic bimolecular collisions necessary for gas phase polymerization. Also noted as products of this reaction, along with the polymeric layer, were biphenyl, methylbiphenyl, p terphenyl and quaterphenyl.[32]

The use of a non equilibrium plasma as a means of preparative organic chemistry has been well investigated,

especially by Suhr *et al.*[34] Plasma chemistry occasionally creates new compounds and more often leads in a simple step to substances which by classical methods can only be synthesised by a number of reaction steps. However, until very recently the results of such reactions were rather unspecific and the yields were much too small to prove plasmas as a viable synthetic route. This use of cold plasmas as a preparative method has been discussed in greater detail in Chapter One.

2. Results and Discussion

Initial experiments on the addition of Argon to perfluorobenzene vapour in a plasma were based on a constant partial pressure of perfluorobenzene (0.1mb) *i.e.* increasing the amount of argon caused an increase in the total pressure of the system.

3.3.4 Varying Ratios of PFB/Ar - Partial Pressure PFB Constant (0.1mb)

Typical core level spectra for plasma polymerized perfluorobenzene are shown in Figure 2.3, along with a discussion of the various features arising from the core levels and the reader is asked to refer back to this Section (2.3.1I) for a fuller account. For ease of comparison of the data presented there with the results given in this chapter, the essential features arising from the C_{1s} envelope are reiterated here. Namely, the presence of peaks at 285.0, 286.7, 288.3, 289.5, 291.2, 293.3 and 295.5eV arising from CH, $\underline{C}$-CF, CF, $\underline{C}F$-CF_n, CF_2, CF_3 and $\pi \rightarrow \pi^*$ shake-up satellite environments respectively. The latter, demonstrating the unsaturation present in the polymer film,[18] is also seen in the F_{1s} core

level spectrum and arises from fluorine bonded to unsaturated carbon. The $F_{1s}:C_{1s}$ stoichiometry of the plasma polymer reveals that the atomic ratio of the starting monomer has been retained, *i.e.* $C_1:F_1$ although extensive molecular rearrangement has taken place, as evidenced by the presence of C-CF, CF_2 and CF_3 functional groups in the C_{1s} envelope, in the processes leading to deposition. The polymer film was also found to contain a small amount of oxygen, $C_1:O_{0.03}$. Under the various conditions employed in the plasma polymerization of perfluorobenzene, the features described above were essentially constant although subtle changes in the composition of the C_{1s} envelope could be detected.

Typical values of the percentage composition of the various component peaks of the C_{1s} envelope of plasma polymerized PFB are shown in Figure 3.6. These data points all correspond to a sample position within the coil region. Also shown in Figure 3.6 are the corresponding values for the plasma polymer films formed in 'atmospheres' of 1:1, 1:2 and 1:3 ratios of PFB/Ar vapour respectively. It is very apparent that the excess argon mixtures have resulted in an increase in the amount of unsaturation present. In fact, from the 1:3 mixture the $\pi \rightarrow \pi^*$ shake-up satellite in the film has almost doubled compared with the percentage value of the satellite in the polymer from pure PFB. Concomitant with this change is a slight decrease in the amount of CF_2 functionalities together with a slight increase in the amount of total CF. The amount of CF_3 is essentially constant in all four polymer films, whilst the amount of C-CF also decreases. For unsaturation to increase, this would suggest, in view of the fact that most of the component peaks only show a slight change with

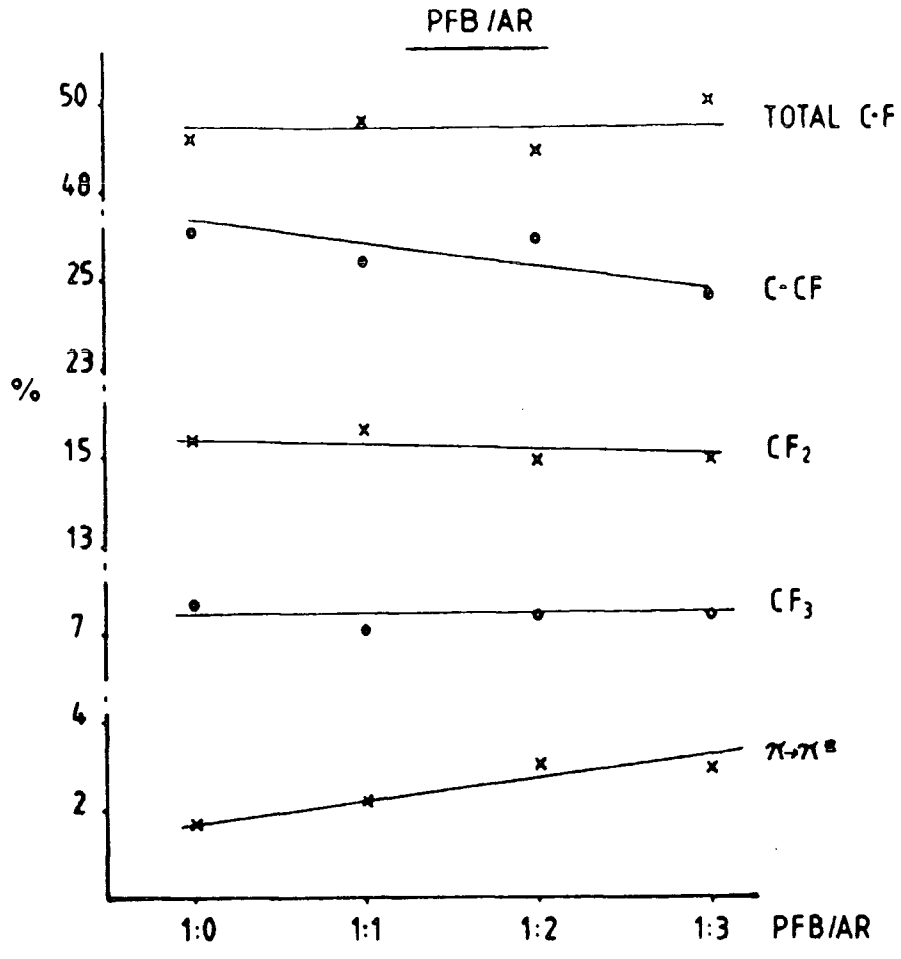

FIGURE 3.6 Percentage composition of the C_{1s} envelope as a function of increasing the total pressure (partial pressure of PFB is kept constant at 0.1mb).

increasing total pressure, that there is an overall loss of fluorine from the polymer film. This loss of fluorine would seem to be associated most with C-CF functionalities, to produce C=C groups to which no fluorine is directly attached. The binding energy of C=CF is expected to be in the same region as C-CF, but due to the decrease in this peak, it is suggestive of the fact that the increase in unsaturation is not associated mainly with an increase in C=CF in the plasma polymer as at first might be expected.

However, this is not in agreement with the information from the F_{1s} core level which shows a visible increase

in the amount of fluorine attached directly to unsaturated carbon, *i.e.* in the $\pi \rightarrow \pi^*$ shake-up satellite, and therefore suggests an increase of C=CF.

The loss of fluorine is borne out by a decrease in the F_{1s}/C_{1s} peak area ratios as shown in Figure 3.7. As the exciting vapour moves from pure perfluorobenzene to the 1:3 PFB/Ar ratio the C:F stoichiometry of the deposited film decreases from essentially unity to $C_1:F_{0.9}$. This is in contradiction with the F:C stoichiometry obtained by a carbon envelope calculation[35] which shows the C:F ratio to be essentially constant in all four polymer films. Possible reasons

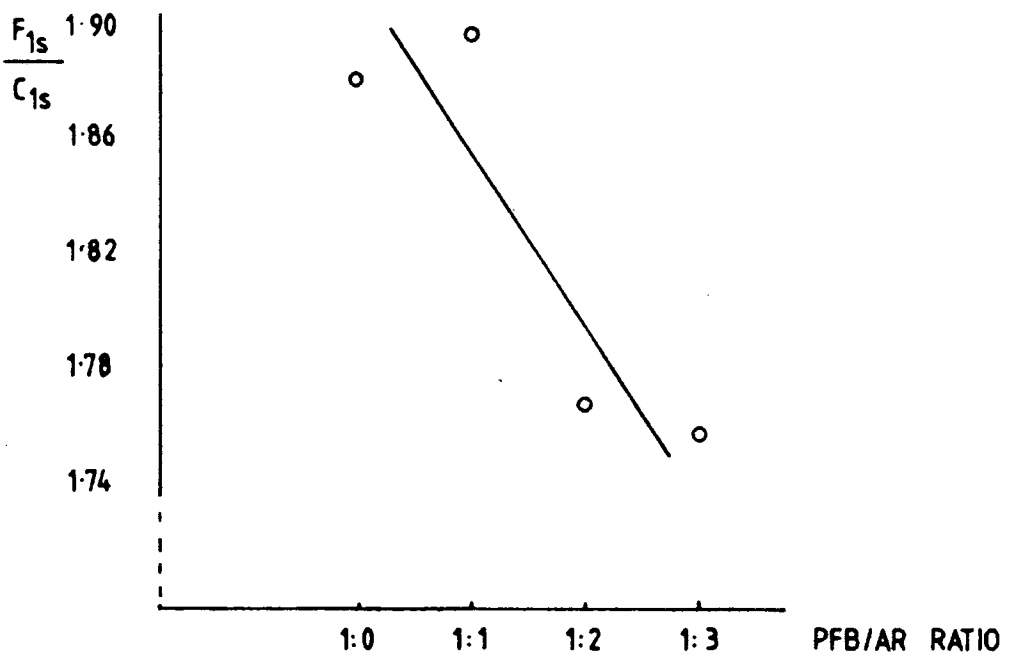

FIGURE 3.7 Peak area ratio of F_{1s} to C_{1s} envelopes as a function of increasing total pressure (partial pressure of PFB is kept constant at 0.1mb).

for this are:

1. An increase in the amount of oxygen incorporation into the polymer film which results in a 'false' component peak analysis of the C_{1s} envelope which assumes all the intensity is due to fluorine containing functionalities. In fact, as can be seen from Figure 3.7, the amount of total oxygen actually decreases to an almost negligible concentration of 1 in every 100 carbon atoms. This is itself an interesting phenomena and will be discussed later on.

2. Due to an increased amount of unsaturation associated with non-fluorine containing functionalities, there will be an increased amount of $\pi \rightarrow \pi^*$ shake-up satellite associated with the peaks formally assigned to CF_2 and CF_3 groups thus leading again to a 'high' apparent amount of fluorine.

3. An increased amount of hydrocarbon on the polymer surface, due to the different sampling depths for the F_{1s} and C_{1s} core levels,[36] would result in an apparent decrease in the total area associated with the F_{1s} core level spectrum. In fact, this again is not a valid argument since the amount of hydrocarbon associated with the PFB/Ar polymer films is less than that associated with the pure PFB polymer. (The percentage areas of the component peaks of the C_{1s} have been corrected for the amount of hydrocarbon in Figure 3.6).

4. The films might not be vertically homogeneous, and the surface is depleted in fluorine. This cannot be discounted with certainty since only one of the films were checked for vertical homogeneity by angular dependence when studies at 35° and 70° take-off angles were both in agreement.

Thus the anomaly between the two calculated F:C ratios cannot be resolved with certainty without further information about the depth profiles of all the polymer films.

The apparent reduction of the amount of oxygen by a factor of 2 would tend to suggest that the oxidation of the polymer film is increasingly inhibited by the presence of argon. This in itself suggests that there is some interaction between PFB and Ar resulting in a decrease in the number of reactive free radicals being trapped in the polymer matrix and/or an increase of free radicals, by argon ion bombardment, in the polymer film which then achieves a greater stabilization through an increased amount of cross-linking.

It should be added, though, that although the leak rate as measured in the absence of the organic vapour is approximately constant, the increased pressure in the vacuum system during the experiment will cause a reduction in the leak rate. However, it would not be expected to cause such a difference in the oxygen content of the plasma polymer.

Contact angles[37] of the various films as measured with distilled water were all constant at around 90^{o}, *i.e.* hydrophobic surfaces.

The above results may all be derived from the increased number of collisions within the reactor between the various species present, *i.e.* the argon is serving no other function than to cause an increase in the number of impacts with increasing total pressure. To examine this, a series of experiments were carried out where the total pressure of the system was kept constant but the partial pressure of PFB altered.

3.3.5 Varying Ratios of PFB/Ar - Total Pressure Constant (0.2mb)

Seven different ratios were examined ranging from a 1:1 to a 1:20 PFB/Ar mix. Figure 3.8 shows the change in the percentage composition of the C_{1s} envelope as the ratio decreases, *i.e.* the amount of Ar increases from a 1:1 to a 1:9 combination. The most noticeable change is an increasing amount of CF_2 and CF_3 as the PFB/Ar ratio decreases, this is accompanied by a decrease in C-CF and CF functionalities and an expected decrease in the amount of $\pi \rightarrow \pi^*$ shake-up satellites. Peak assignment has been on the basis that the component peaks are all due to F containing groups. The small contributions by oxygen and nitrogen functionalities has been ignored. This will be discussed later. This decrease in unsaturation is also seen in the F_{1s} core level spectrum. The shake-up satellite at ~696eV gradually decreases in intensity until the 1/9 ratio of PFB/Ar when it is no longer discernible above the background noise.

Also apparent, but not as noticeable, is the fact that the 1:1 mix produces a polymer whose C_{1s} envelope more closely resembles that of the polymer produced from 0.1mb pure perfluorobenzene, than it does the 0.2mb pure perfluorobenzene. The percentage components of the C_{1s} envelopes for these three plasma polymers are shown in Table 3.1, and would suggest that in a 1:1 ratio, the argon has had very little effect on the composition of the plasma polymer produced by a partial pressure of 0.1mb of PFB compared with a pure PFB polymer. Thus certainly in a 1:1 ratio there is no visible evidence for any effects of the rare gas on the plasma polymerization process

COMPONENT ANALYSIS OF THE C_{1S} ENVELOPE AS A FUNCTION OF PARTIAL PRESSURE OF PFB IN A PFB/Ar MIX

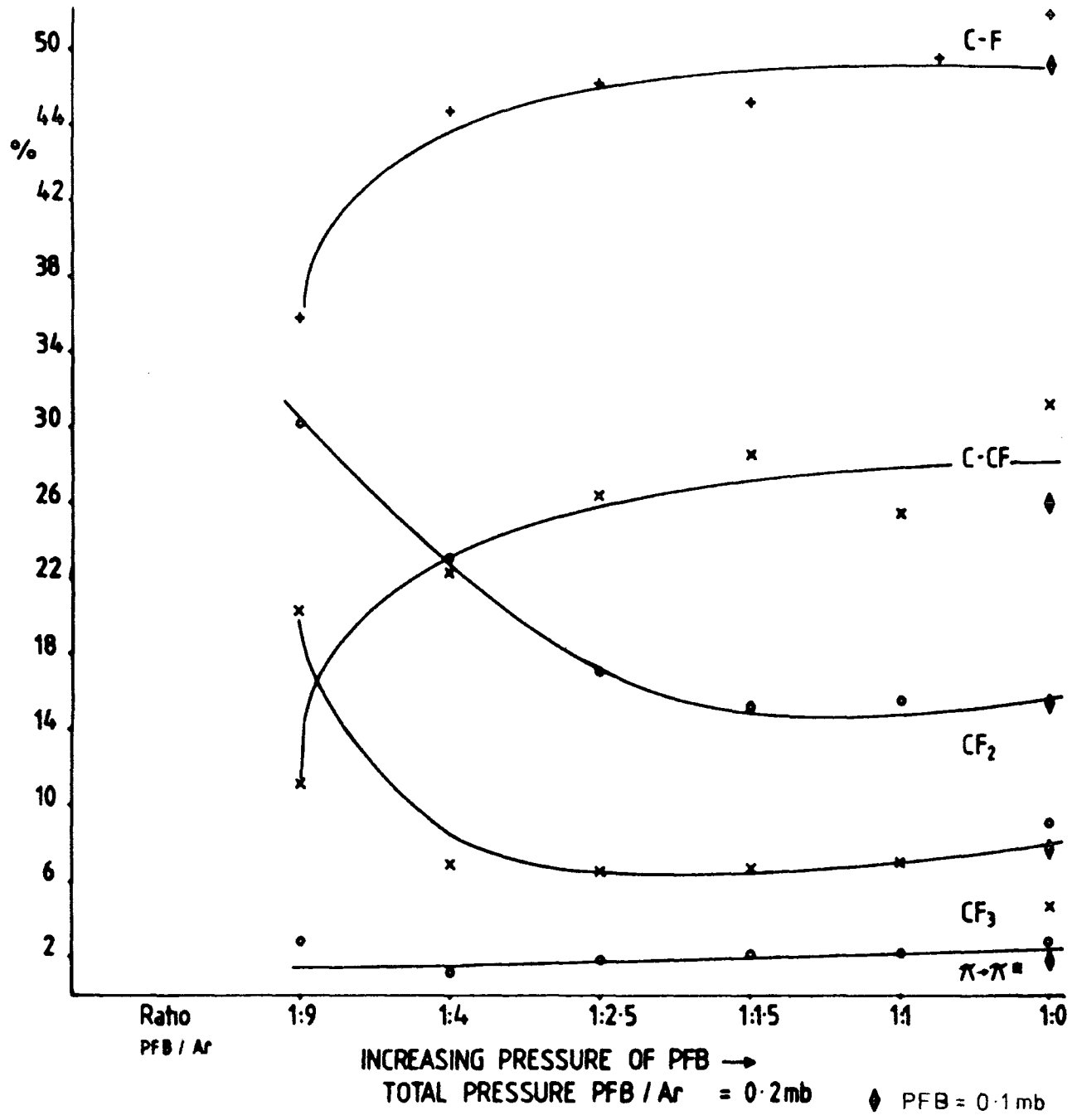

FIGURE 3.8 Percentage composition of the C_{1s} envelope as a function of increasing the partial pressure of PFB (Total pressure of PFB/Ar = 0.2mb).

TABLE 3.1 Percentage Areas of the Component Peaks of the C_{1s} Envelope for 0.1 and 0.2mb PFB and 0.1mb PFB/0.1mb Ar Plasma Polymers

Component peaks	C-CF	CF(total)	CF_2	CF_3	$\pi \rightarrow \pi^*$
0.2mb PFB	31	52	9	5	3
0.1mb PFB+0.1mb Ar	25	50	16	7	2
0.1mb PFB	26	49	15	8	2

of perfluorobenzene. It is possible that the increase in CF_2 and CF_3 component peaks arise from a combination of two processes:

1. A decrease in bimolecular organic collisions, accompanied by
2. An increase in fragmentation of the perfluorobenzene resulting from an increase in the number of the molecular collisions with Ar in the gas phase/surface interface.

Physical sputtering of the forming polymer by Ar^+ will also occur. The amount of C-CF might be expected to increase due to an increased amount of cross-linking if this process was important in determining the effects on the composition of the C_{1s} envelope.

The deposition rate was not monitored, but the films were sufficiently thick enough so that after a 10 minute deposition period, the aluminium substrate was not visible to ESCA. The deposition rate of styrene in excess argon has been examined in a d.c. discharge.[38] It was determined that the deposition rate was an additive of two factors: a deposition term and a sputtering term. The composition of the resultant polymer was not examined.

However, it should be remembered that in a d.c. discharge the ions themselves are also accelerated between the electrodes, which causes the ions to have a greater kinetic energy. The thermal energy of the system will then also increase. These two effects will also be expected to have some bearing on the polymer deposition rate/sputtering rate.

Over the range shown in Figure 3.8, the total F:C stoichiometry does not show any trend but appears to remain constant around $C_1:F_{1.02}$, *i.e.* there has been no fluorine elimination taking place. This is the reverse of the situation found in the plasma polymerization of a constant partial pressure of perfluorobenzene, with argon with an increasing total pressure, where fluorine elimination took place.

The total F:C ratio as calculated from the C_{1s} envelope is hampered by the increasing amount of nitrogen incorporation which takes place with excess argon. As was mentioned earlier, the numbers in Figure 3.8 represent the percentage area assuming that all contributions to the C_{1s} envelope arise solely from fluorine containing groups. In fact, the contribution to the C_{1s} core level envelope by nitrogen in the 1:4 to 1:1 mixtures is not very significant, the polymer films only contain less than 3 nitrogen atoms for every 100 carbon atoms. However, the amount of nitrogen in the 1:9 PFB/Ar combination can no longer be ignored, the polymer film has a C:N ratio of 1:0.14. Therefore the actual values quoted for the percentage composition of the C_{1s} envelope of the polymer derived from a 1:9 ratio of PFB/Ar may not be totally accurate due to the unknown contributions to the

various component peaks by nitrogen. Nitrogen incorporation was not seen in the plasma polymerization of 0.1mb PFB + Ar, where the partial pressure of argon was increased. Thus it would seem that when the partial pressure of the organic monomer is low, the excess argon present causes the incorporation of nitrogen into the polymer film. The presence of nitrogen is most likely to arise from a 'leaky' reactor/vacuum line, this leakage hampered the experimental study of very low pressures of argon/perfluorobenzene combinations due to the large amounts of nitrogen incorporation. In the 1:20 PFB/Ar plasma polymerization, discussed below, the nitrogen incorporation was, in fact, reduced but not eliminated, due to a better leak rate.

The amount of oxygen in all of the polymer films was not very great, the C:O stoichiometry was less than 1:0.08 and there was no particular variation with the partial pressure of perfluorobenzene.

In the presence of a great excess of argon, *i.e.* 1:20 PFB/Ar ratio, a combination of a reduction in the deposition rate and an increase in the sputtering rate resulted in the formation of only a thin polymeric film $\sim$35 Å. The C_{1s} consisted essentially of a main photoionisation peak at 285.0eV with a small shoulder to higher binding energies made up of peaks $\sim$1.6, 2.4 and 4.5eV shifted from the main peak, *i.e.* the C_{1s} envelope no longer consists of fluorine dominated environments. There was also a very healthy O_{1s} signal, but due to the visibility of the substrate it is not possible to determine the contributions from the oxide layer from the oxygen associated with the polymer film.

The F_{1s} signal consisted of two peaks: the main organic fluorine peak at ~688eV and a shoulder at 2.0eV lower binding energy. It is thought that this peak is due to an interaction between the perfluorobenzene and the aluminium oxide at the polymer/substrate interface and is another indication that the film thickness is not greater than 23 Å. This phenomenon has been noticed in the photopolymerization of perfluorobenzene and is discussed in greater detail in Chapter Seven.

3.3.6 1.9 Ratio of PFB/Ar - Total Pressure of 0.4mb

To check the effect of pressure in the 1:9 PFB/Ar ratio, the total pressure of the system was doubled to 0.4mb. During this experiment, the glow was only visible in the coil region, so the sample composition of the polymer deposited in the non-glow tail region was also examined. Considering the sample in the coil region first, the partial pressure of perfluorobenzene at this higher total pressure was equivalent to the partial pressure of PFB in the 1:2.5 PFB/Ar ratio and Table 3.2 shows a comparison between the percentage areas of the C_{1s} envelope component peaks from the two polymers deposited in the coil region.

TABLE 3.2 Percentage areas of the component peaks of the C_{1s} envelopes for polymers derived from 1:9 and 1:2.5 PFB/Ar ratios - Partial pressures of PFB identical

Component Peak	C-CF	CF(total)	CF_2	CF_3	$\pi \rightarrow \pi^*$
1:9 PFB/Ar	26	46	20	6	2
1:2.5 PFB/Ar	26	48	17	7	2

From the above comparison, it would seem that there is very little difference between the two polymers as far as the functional group composition of the C_{1s} envelope is concerned. This is reflected in the C:F stoichiometries which are both about 1:1. Thus it would seem that the composition of the plasma polymer from a perfluorobenzene/argon plasma depends almost entirely on the partial pressure of perfluorobenzene in the system. The excess argon in the 1:9 PFB/Ar ratio has caused a slight increase in the amount of CF_2 with a concomitant decrease in the amount of CF. This change in composition has most likely been caused by the increased amount of fragmentation due to the higher concentration of Ar. Considering that the total pressure between the two polymerizations has changed by a factor of 2, it would seem that argon does not have much of a role to play in the plasma polymerization of perfluorobenzene, or the composition of the deposited polymer film.

From the preceding discussion it could be inferred that the two polymers formed from 1:9 PFB/Ar plasmas, where the total pressure has been changed, are different. This is correct, the amount of CF_2 and CF_3 has decreased by 1/3 and 2/3rds respectively whilst the content of C-F has increased in the polymer film formed at the higher pressure. It is also interesting to note that at the higher pressure no nitrogen was incorporated into the polymer film. This may be a reflection of the smaller leak rate of the vacuum system with the higher pressure. As mentioned before, leak rates were measured by looking at an increase in the base vacuum pressure when the pumping was shut off from the vacuum line, and as such are not directly related to the leak rate in the

presence of a finite pressure of monomer vapour.

The C_{1s} envelopes from the polymer films deposited in the coil region and in the non-glow tail region from the 1:9 higher pressure ratio of PFB/Ar are displayed in Figure 3.9. These spectra emphasise the importance of specifying whether the sample was deposited in the glow or non-glow region. This change in composition of the C_{1s} envelope on moving from a glow region to a non-glow region has been noted before in the plasma polymerization of perfluorobenzene.[39] It was also reported that the total F:C stoichiometry of the film deposited in the non-glow region

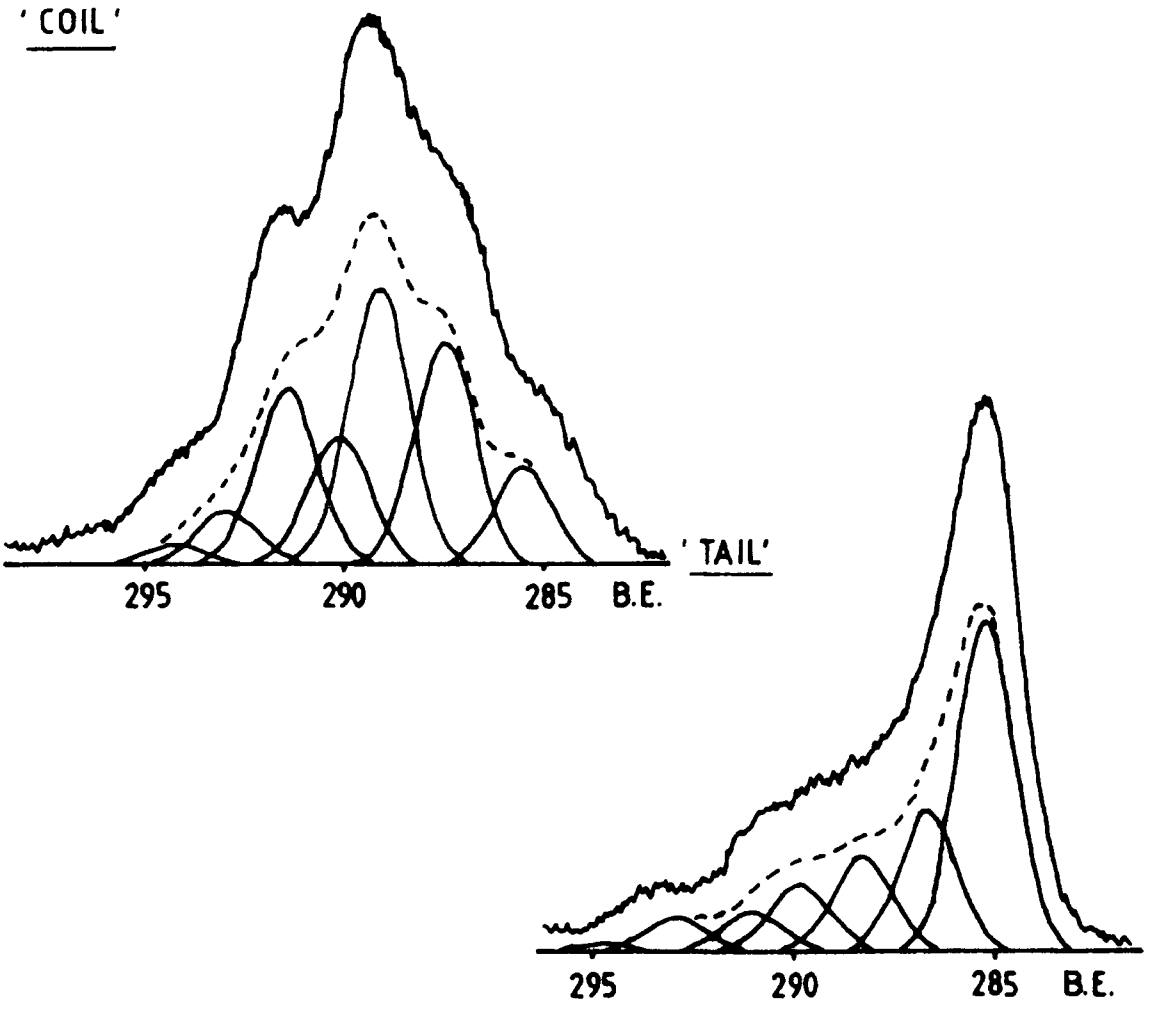

FIGURE 3.9 C_{1s} envelopes of polymers deposited in (a) coil region and (b) end of reactor (glow *versus* non-glow) 1:9 PFB/Ar, Total pressure = 0.4mb.

increased when compared with the stoichiometry of the polymer film deposited in the glow region in the same deposition experiment; this is in concordance with the present results. The C:F stoichiometry increases from an essentially 1:1 polymer in the coil region to 1:1.2 in the non-glow region. Unlike the results reported by Clark and Shuttleworth[39] however, the sample in the glow region is not rich in CF_2 functionalities. In fact, the percentage intensity of the CF_2 component peak is only half of the value of that in the C_{1s} envelope of the polymer deposited in the coil region. It should be noted that the conditions employed, power, pressure and time, for the present study are all different to those used in the previously mentioned[39] publication, so no direct correlation can be attempted.

The extent of extraneous hydrocarbon in the polymer formed in the non-glow region is much higher than that in the corresponding sample from the coil region. Due to the much thinner nature of the film formed at the end of the reactor, signals originating from the hydrocarbon on the surface of the substrate will also contribute to the C_{1s} envelope of the polymer film. Indications of the 'thin' nature of the film are also seen in the F_{1s} core level, where two fluorine environments are apparent. As it has been suggested before, the signal for the lower binding energy component peak arises from fluorine at the substrate/polymer interface and indicates an interaction of the adsorbed perfluorobenzene - see Chapter Seven. In the present sample 18% of the total F_{1s} signal is associated with the higher kinetic energy peak, indicating a film thickness of $\sim$12 Å.

As it has been previously reported,[39] the deposition rate in a plasma polymerization experiment is fastest in the coil region. This is borne out in the present study by the appearance of the Al_{2p} signal in an ESCA study of the plasma polymer deposited in the non-glow tail region - this signal is not visible in the sample deposited in the coil region.

3.3.7 1:1 Ratio of PFB/Ar - Total pressure of 0.4mb

The concluding experiment on the effects of argon on the plasma polymerization of perfluorobenzene involved a 1:1 PFB/Ar ratio using a total pressure of 0.4mb. The percentage composition of the component peaks of the C_{1s} envelope from the sample deposited in the coil region are shown in Table 3.3.

TABLE 3.3 Percentage areas of the component peaks of the C_{1s} envelopes for polymers derived from 1:1 PFB/Ar ratios and pure perfluorobenzene (Total pressure of the system is given in brackets)

Component Peak	C-CF	CF(total)	CF_2	CF_3	$\pi \rightarrow \pi^*$
1:1 PFB/Ar (0.4mb)	29	49	14	6	2
1:1 PFB/Ar (0.2mb)	25	50	16	7	2
PFB (0.2mb)	31	52	9	5	3

The major difference between the 1:1 PFB/Ar derived polymer and the polymer from pure perfluorobenzene where the pressures of PFB are the same in both experiments, is in the amount of CF_2. From Table 3.3, it can be seen that the amount of CF_2 in both of the 1:1 PFB/Ar derived polymers is high. In a comparison of the polymers derived

from differing PFB/Ar ratios and pure perfluorobenzene plasmas in the previous sections, the polymer films which bear the closest resemblance - as far as the percentage composition of the C_{1s} is concerned - are those films produced from the same total/partial pressure of PFB. In this instance, however, the amount of CF_2 formation is much greater in the 1:1 PFB/Ar plasma polymer formed with a total experimental pressure of 0.4mb than in the pure perfluorobenzene derived polymer using the same partial pressure, *i.e.* 0.2mb - see Table 3.3. Rather than being an effect arising solely from the argon, it is more likely that the total pressure of the system is too high and this increased pressure has resulted in much more fragmentation in the gas phase and collisions with the substrate surface, caused by both organic-organic and organic-inert gas collisions. This is echoed by the fact that the plasma was very difficult to sustain and balance. As an interesting feature the amount of CF_2 produced in perfluorobenzene derived plasma polymers actually decreases on going from 0.1mb to 0.2mb, from 15 to 9% . This suggests, tentatively, that the degree of fragmentation arises mainly from the presence of argon. In fact, the increased pressure of pure perfluorobenzene would seem to result in a polymer which contains more C-CF and CF groups than CF_2 and CF_3 functionalities, and has a greater degree of unsaturation, when compared with the polymer produced from the lower total pressure (0.1mb) of PFB. However, in the present case, the polymer was derived from a PFB/Ar ratio of 1:1 whose total pressure was 0.4mb, *i.e.* double that of the pure perfluorobenzene plasma. No conclusive statements about the presence of argon, when using a total pressure of 0.4mb can be made since

a polymer from 0.4mb pure perfluorobenzene was not examined.

The F_{1s} core level in the polymer derived from a 1:1 PFB/Ar ratio at a total pressure of 0.4mb also displays a $\pi \rightarrow \pi^*$ shake-up satellite, as does the corresponding polymer produced by reducing the total pressure to 0.2mb. The F:C stoichiometry of 0.92:1 indicates that a certain amount of fluorine elimination has taken place during polymerization, or in the formation of the precursors to polymerization. This is in agreement with the study carried out by increasing the total pressure of the PFB/Ar feed to the plasma where the partial pressure of PFB was kept constant (Section 3.3.4), *i.e.* an increased total pressure led to a plasma polymer whose fluorine content had decreased.

3.3.8 Plasma Polymerization of PFB/I_2

Following the report that iodonated polystyrene shows a greater resistance to an oxygen plasma due to the formation of iodine oxides in the surface of the polymer upon etching,[40] it was decided to investigate the behaviour of perfluorobenzene and iodine in a plasma. Iodine is also known to be a free radical 'scavenger'[41] and the presence of iodine in the PFB plasma may result in a polymer whose deposition rate and perhaps composition has been affected if free radicals are important in the processes leading to deposition.

The relevant C_{1s}, F_{1s} and $I_{3d_{5/2}}$ core level spectra from the resultant polymer formed in the coil region are shown in Figure 3.10. It is clear from the C_{1s} envelope that the extensive molecular rearrangement associated with a perfluoroaromatic plasma has still taken place to produce C-CF, CF,

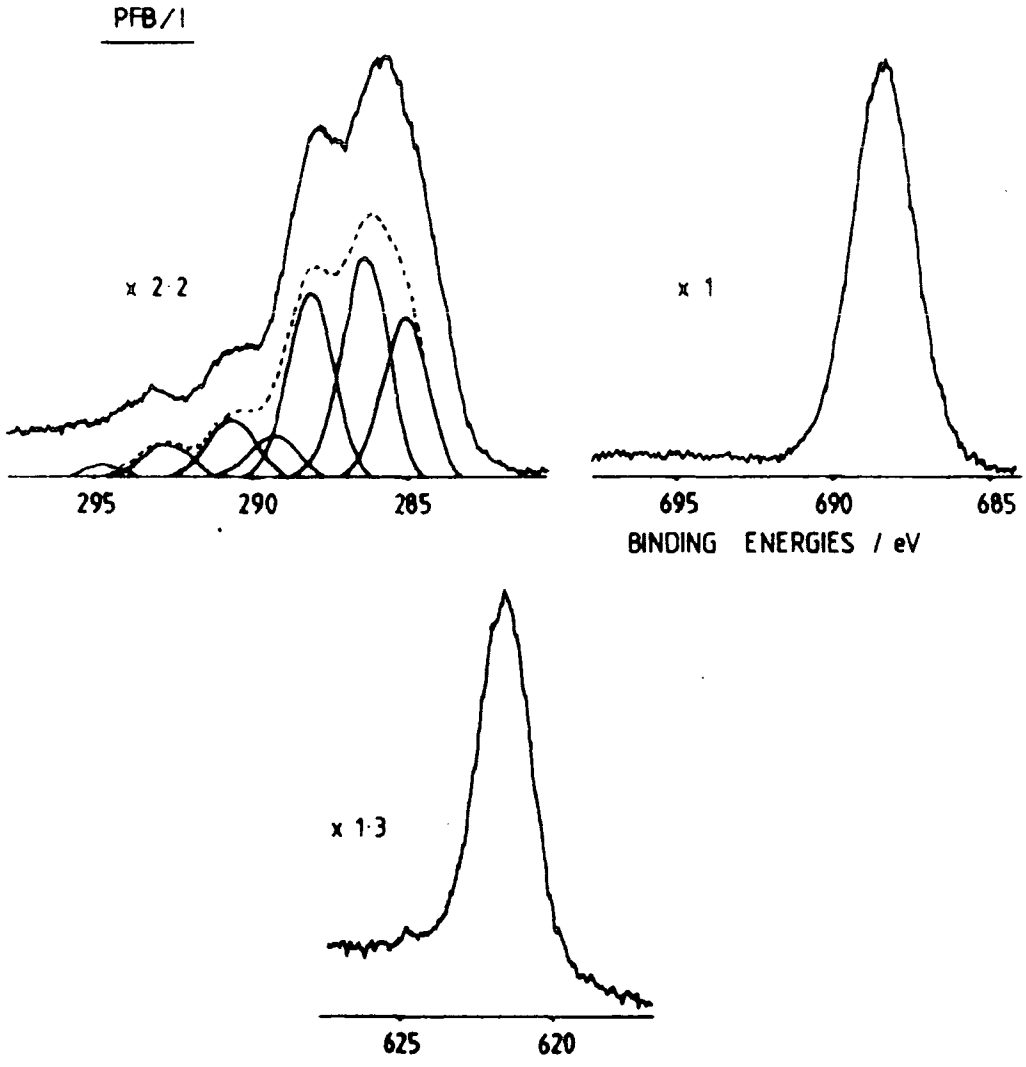

FIGURE 3.10 Typical core level spectra for plasma polymerized perfluorobenzene/iodine

$\underline{C}F\text{-}CF_n$, CF_2, CF_3 and $\pi \rightarrow \pi^*$ shake-up satellite environments at 286.6, 288.4, 289.7, 291.3, 293.7 and 295.7eV respectively. There is also a greater step function associated with the C_{1s} core level of the copolymer compared with that from a pure perfluorobenzene plasma polymer (Figure 2.3). This would tend to indicate a greater degree of long range unsaturation present in the copolymer. From a comparison of the percentage intensities of the component peaks† of the C_{1s} envelopes from

† The percentage intensities shown in Table 3.3 have been corrected for hydrocarbon contamination. A mention of the fact that the amount of CH in the copolymer is approximately twice that in the pure PFB polymer (23 of 12% in the raw data) is made.

the two polymers - Table 3.3 - it is apparent that the relative concentrations of the component peaks has changed.

TABLE 3.3 Percentage intensities of the component peaks of the C_{1s} envelopes from polymers derived from PFB/I_2 and PFB plasmas (6w 0.1mb 10 min)

	C-CF	CF	$CF-CF_n$	CF_2	CF_3	$\pi\rightarrow\pi^*$
PFB/I_2	40	34	8	11	6	1
PFB	28	32	17	16	6	1

The dominant peak in the PFB/I_2 copolymer is no longer that due to CF, as in the pure PFB polymer, but from the C-CF component functionality. The amount of $\underline{C}F-CF_n$ has also been decreased by a factor of 2. The reduction in the $\underline{C}F-CF_n$ component is noted in Chapters Four, Five and Six on the copolymerization of perfluorobenzene with various other monomers, as is the reduction in the amount of CF_2.

The amount of $\pi\rightarrow\pi^*$ shake-up would appear to be constant in both polymer films. However, there is no real evidence for a $\pi\rightarrow\pi^*$ shake-up satellite accompanying the main photoionisation peak of the F_{1s} core level in the copolymer unlike the situation in the pure polymer. The F:C stoichiometry of the copolymer reveals that a certain amount of fluorine elimination has taken place to produce a copolymer whose F:C ratio is 0.7:1. This is in contrast to the plasma polymer of pure perfluorobenzene which retains the stoichiometry of the starting monomer, *i.e.* 1:1. The loss of fluorine from the copolymer would seem to be associated with $\underline{C}F-CF_n$ and CF_2 functionalities.

Although deposition rates of either the copolymer or homopolymer were not monitored, there was a visible de-

decrease in the rate of polymer formation in the copolymerization experiment as determined by the visible amount of film formation on the reactor walls after exposure to a ten minute plasma, although the aluminium substrate was still not visible by ESCA.

The $I_{3d_{5/2}}$ core level at a binding energy of 622eV gives an $I_{3d_{5/2}}/C_{1s}$ peak area ratio of 1 (the iodine signal appears as a doublet due to spin-orbit coupling[42]). From the binding energy of this peak the presence of iodide rather than oxygenated species is suggested. This is collaborated by the amount of oxygen incorporation into the copolymer which is only very small giving a O:C stoichiometry of 0.02:1. This is equivalent to the amount of oxygen in the pure PFB plasma polymer.

The presence of iodine in an oxygen plasma has been found to inhibit the surface oxidation of polyethylene.[43] This seems to occur *via* the formation of loosely bound iodine oxides on the surface of the polymer which prevents the polyethylene being oxidized. This surface layer was readily removed by washing with solvent leaving behind a relatively unoxidized surface.[43]

Due to this protective effect of iodine in an oxygen plasma on the surface of polymers iodonated compounds have also been found to make a good bilayer photoresist developable by oxygen plasma etching.[40]

3.4 Conclusion

The plasma polymerization of 1 fluoronaphthalene in the presence of hydrogen resulted in an uptake of hydrogen into the plasma polymer. With an increasing amount of hydrogen uptake, the asymmetry associated with the C_{1s} envelope decreased demonstrating the decreasing amount of unsaturation present in the polymer film. The incorporation of hydrogen into the polymer was accompanied by an increasing amount of fluorine elimination, although even with a high incorporation of hydrogen not all of the fluorine was eliminated. These results tentatively suggest that the level of unsaturation in a plasma polymer may be controlled by variation of the partial pressure of hydrogen in the starting mixture. Associated with hydrogen incorporation, was the appearance of a new peak in the valence band spectrum of the 1 fluoronaphthalene/hydrogen copolymer.

Polymers produced by the plasma polymerization of perfluorobenzene in the presence of argon, under different conditions of partial pressures and total pressures, showed compositional resemblances to the polymers produced from pure perfluorobenzene, especially when the total pressure of the PFB/Ar system was not too high. This indicates that argon has very little effect on the surface composition of the perfluorobenzene derived plasma polymers formed in the presence of argon. The main effect would appear to be the amount of fragmentation, as seen in the increased amount of CF_2 and CF_3 functional groups, when the Ar:PFB ratio is in excess of 3:1. This may arise from an increased amount of collisions between PFB, and PFB derived species, with Ar in the gas phase and also physical sputtering of the growing polymer

film by argon/argon ion bombardment. The composition of 1:1 PFB/Ar derived polymer films - where the total system pressure $\leq$ 0.2mb - was identical to the polymer film produced from pure perfluorobenzene, where the pressure of PFB was identical to the partial pressure of PFB in the presence of argon.

The presence of iodine during the polymerization of perfluorobenzene resulted in the incorporation of a small amount of iodine into the polymer film. The fluorine to carbon stoichiometry of the copolymer film was no longer 1:1, as in a pure PFB film. Fluorine elimination had taken place to give an atomic ratio of $C_1:F_{0.7}$. The deposition rate of the copolymer visibly decreased although was still sufficiently fast enough to cover the aluminium such that the substrate was not detected by ESCA. The composition of the copolymer was also different from that of the homopolymer. The predominant peak in the C_{1s} envelope no longer arose from C-F functionalities as in the PFB homopolymer but was due to $\underline{C}$-CF functionalities. The amount of $\underline{CF}$-CF_n was halved in the copolymer.

REFERENCES - Chapter Three

1. U. Carmi, A. Inspektor and R. Avni, Plasma Chem.Plasma Process, 1(3), 233 (1981).

2. Japan.Synthetic Rubber Co. Ltd., Jpn. Patent 81 47,403 (1981).

3. M. Miinomi and K. Yanagihara, Brit.UK Pat.Appl. 2,023,152 (1979).

4. R.F. Wielonski and H.E. Beale, Eur.Pat.Appl. 25,772 (1981).

5a. E. Kay, A. Dilks and U. Metzler, Macromol.Sci.-Chem. A12(9), 1393 (1978).

5b. E. Kay, J. Coburn and A. Dilks, 'Topics in current Chem.', 94, S. Vepek, M. Venugo (Eds.), Springer-Verlag, Berlin,(1980)

6. E. Kay and A. Dilks, J.Vac.Sci,Technol. 18(1), 1 (1981).

7. E. Kay and A. Dilks, ACS Symp.Ser., 108 'Plasma Polymerization', M. Shen, A.T. Bell, Amer.Chem.Soc., (1979).

8. E. Kay, A. Dilks and D. Seybold, J.Appl.Phys. 51(11)5678(1980)

9a. H. Yasuda, J.Polym.Sci.Macromol.Revs., 16, 199 (1981).

9b. H. Yasuda, C.E. Lamaze, J.Appl.Polym.Sci., 17, 1519, (1973).

9c. H. Yasuda, C.E. Lamaze, J.Appl.Polym Sci., 17, 1533 (1973).

10. N. Inagaki, M. Matsunaga, Polymer Bulletin, 13, 349 (1985).

11. N. Inagaki, H. Kawai, Seni-i Gakkaishi, 40(9) 337 (1984).

12a. R. D'Agostino, F. Cramarossa, V. Colaprico, R. D'Ettole, J.Appl. Phys., 54(3), 1284 (1983).

12b. R. D'Agostino, F. Cramarossa, B. De Benedictis, G. Ferraro, J.Appl. Phys., 52(3), 1259 (1981).

13a. Y. Kasamo, T. Nakano, Y. Ohki, K. Yamagi, Jpn.J.Appl.Phys., Pt.1, 24(1), 83 (1985).

13b. H. Yasuda, T. Hascioka, H. Okihiko, Kenkyusho 132, 13 (1982).

14. T. Masuoka, H. Yasuda, J.Polym.Sci.,Polym.Chem.Ed., 20(9), 2633 (1982).

15. G. Smolinsky, M.J. Vasile, Int.J.Mass.Spec. and Ion Phy., 24, 311 (1977).

16a. B.V. Tkachuk, V.M. Kolotrykin, Vysolomol.Soedin.Ser., B10, 24 (1968).

16b. B.V. Tkachuk, V.M. Kolotrykin, Ukr,Khim.Zh, 35, 768 (1969).

17. M.Z. AbRahman, D.T. Clark, J.Polym.Sci.,Polym.Chem.Ed., 20, 1717, (1982).

18. D.T. Clark, Pure and Appl.Chem., 54, 415 (1982).

19. D.R. Hutton, Ph.D. Thesis, University of Durham, U.K. (1983).

20a. H.S. Munro and C. Till, J.Polym.Sci.,Polym.Chem.Ed., 22(12), 3933 (1984).

20b. H.S. Munro and C. Till, J.Polym.Sci.,Poly,.Chem.Ed., 24, 279 (1986).

20c. See Chapter Two, ref. 6c,e,g.

21. See Chapter Six, ref. 19.

22. H.S. Munro and H. Grunwald, J.Polym.Sci.,Polym.Chem.Ed., 23, 479 (1985).

23. H.S. Munro and J. Eaves, J.Polym.Sci.,Polym.Chem.Ed., 23, 507 (1985).

24. H.S. Munro and J. Eaves, unpublished data.

25. H.S. Munro and C. Till, J.Polym.Sci.,Polym.Chem.Ed., in press (1986).

26. D.T. Clark and A. Dilks, J.Polym.Sci.,Polym.Chem.Ed., 14, 533 (1976).

27. H.S. Munro and C. Till, J.Polym.Sci.,Polym.Chem,Ed., 23, 1621 (1985).

28. D.T. Clark in 'Polymer Surfaces', D.T.Clark, W.J.Feast (Eds.), Wiley, London, 1978.

29. J.C. Fuggle, J.Electron.Spec.Relat.Phenom. 9, 99 (1976).

30. P.M.A. Sherwood, in 'Practical Surface Analysis by Auger and X-ray Photoelectron Spectroscopy', D.Briggs, M.P.Seah (Eds.), John Wiley and Sons Ltd., (1983), Appendix 3.

31. D.T. Clark in 'Advances in Polymer Science', H.J. Cantow (Ed.), Springer-Verlag, Berlin, 24, 125 (1977).

32. E.W. Goerss, H. Deutsch and H. Sabaoil, Beitr.Plasma Phys. 15(4), 191 (1975).

33. 'Gaseous Electronics, Vol.1, Electrical Discharges', M.N.Hirsh, H.J. Oskam (Eds.), Academic Press, N.Y. (1978).

34. H. Suhr, Plasma Chem.Plasma Process. 3(1), 1 (1983).

35. See Chapter 2, Section 2.3.1I.

36a. D.T. Clark, and D. Shuttleworth, Eur.Poly.J., 15, 265 (1979).

36b. D.T. Clark and D. Shuttleworth, J.Polym.Sci.,Polym.Chem.Ed., 17, 1317 (1979).

36c. D.T. Clark and D. Shuttleworth, J.Polym.Sci.,Polym.Chem.Ed. 18, 407 (1980).

37a. P.J. Dynes and D.H. Kaelble, 'Plasma Chemistry of Polymers', M. Shen (Ed.), Marcel Dekker, Inc., N.U. (1976).

37b. D.H. Kaelble, 'Physical chemistry of Adhesion', Wiley, N.Y. (1971).

38. F.W. Breitbarth and H.J. Tiller, Proc.Int.Conf.Phenom.Ion. Gases, 13, 1, 385 (1977).

39. D.T. Clark and D. Shuttleworth, J.Polym.Sci., Polym.Chem.Ed. 18, 27 (1980).

40. T. Ueno, H. Shiraishi, T. Iwayanagi and S. Nonogaki, J.Electro.Soc., 132(5), 1168 (1985).

41. B. Ranby and J.F. Rabek, 'Photodegradation, Photooxidation and Photostabilisation of Polymers', Wiley-Interscience, London (1975).

42. See Chapter 5, Section 5.3.1.

43. H.S. Munro and H. Beer, Polymer Communications, 27,79 (1986).

CHAPTER FOUR

INCORPORATION OF A METAL INTO PLASMA POLYMERIZED PERFLUOROBENZENE

PART I: MERCURY INCORPORATION

4.1 Introduction

Metal Incorporation into Plasma Polymers

Various methods have been used for dispersing metals into conventional polymeric systems, such as coevaporative techniques,[1] solution growth techniques[2] and ion implantation.[3] The synthesis of organometallic films produced by plasma polymerization techniques is an attractive prospect. By a careful choice of the starting monomer/monomers and close control of the processing parameters and thus of the overall composition of the product, the scope of plasma polymerized films in electrical, magnetic and optical application can be extended. As examples, varying the metal content in the plasma polymer, substantial changes in conductivity were seen to occur in a tin containing film[4] whilst electrical resistivity has been changed by altering the amount of gold in a fluorocarbon plasma polymer.[5]

The introduction of metal into plasma polymers has been intensively studied over the last few years by numerous workers.[6] The mode of incorporation of the metal into the growing polymer film has been approached from several directions. These are (a) the plasma polymerization of an organometallic starting material on its own or copolymerized with a second (organic) compound,[7] (b) the etching of a metal substrate whilst polymerization incorporation occurs elsewhere in the reactor system[8], and (c) the simultaneous evaporation of a metal and polymerisation of an organic material.[9] A fourth method involves the ion implantation of metals[10] although this method differs from the other three since, in contrast, the metal is incorporated here into an already formed polymer

rather than into a growing film.

The evaporation of a metal into a growing polymer film has been attempted by Steve Johnson.[11] A molybdenum filament resistive heater was used as the metal evaporation unit in the hope of incorporating chromium into a PFB plasma polymer. This was unsuccessful, but ESCA did reveal the presence of molybdenum in the form of metal (V/VI) oxides in the polymer. The incorporation of Mo oxides proceeded independently of polymer deposition representing codeposition rather than copolymerization. The C_{1s} envelope of the PFB derived polymer was not perturbed nor were there any organo-metal bonds formed.

Further studies indicated that filament temperatures obtained were insufficient to cause significant evaporation of the filament. Thus the possibility of including Mo metal which was subsequently oxidized on exposure to air, was eliminated. Metal oxidation is reported to be a feature of tetramethylgermanium plasma polymers.[12] The incorporation of Mo was thought to be due to direct sublimation of MoO_3 from the filament.

Tin has been vaporised into a capacitively coupled benzene plasma[9a] to give spectra, using Mössbauer spectroscopy, very like those of organotin compounds. Both bismuth and tellurium have been evaporated into a carbon disulphide plasma, where it was suggested that IR measurements indicated some interaction between the carbon disulphide film and tellurium.[6d]

The use of simultaneous metal etching/sputtering and plasma polymerization has been extensively studied by Kay *et al*[8] as a means of incorporating metals into fluorocarbon polymers. The use of fluorocarbon plasmas is based here on

the two antoganistic processes, *i.e.* etching and polymerization which occur in the plasma and are in competition at the surfaces present. Gold, cobalt, aluminium, germanium, molybdenum and copper incorporation, into fluorocarbon polymers, either as elemental metal dispersed in the highly cross-linked network or as bound metal - either to carbon, fluorine or oxygen - have all been studied.[8]

The incorporation of tin *via* sputtering with an argon plasma whilst introducing an organic vapour elsewhere into the reactor has also been studied. With ethylene, the tin was present as metal oxide, no elemental metal being found, whilst in the presence of tetrafluoroethylene tin was present mainly as oxyfluoride species.[13]

An amorphous photosensitive device has been prepared in a capacitively coupled system by obtaining an alloy with the desirable electrical properties through the plasma polymerization of a fluorocarbon gas plasma and the simultaneous incorporation of Si, Ge, Sn or Pb from etching of the cathode into the growing polymer.[14]

Optical emission has also been used to monitor the deposition process of a metal into a fluorocarbon plasma polymer.[15] It was suggested that the extent of metal incorporation could be monitored by measuring the relative intensities of the Au^+ and CF_3^+ signals emitted by the plasma, a ratio of these two values giving a handle on the extent of metal incorporation into the plasma polymer film.[5]

For an initial investigation of structure and bonding in metal containing plasma polymers, by ESCA, a mercury

perfluorobenzene system was chosen for two main reasons. Firstly, mercury is a relatively volatile liquid and can be easily distilled through a low pressure system, thus presenting a facile method for the mixing of a metal and organic compound in the gas phase of a high frequency discharge. The extensive knowledge of perfluorobenzene plasma polymers already in the literature[16] is the second reason for choosing to study the above system. This chapter, therefore, presents the results of a study of the incorporation of mercury into plasma polymerised perfluorobenzene as functions of distillation temperature, power and substrate temperature.

4.2 Experimental

The experimental details are essentially those of Chapter Two, but with the following variation. Due to problems with retaining the integrity of the polymer films after preparation, samples were transported to the spectrometer under a blanket of nitrogen. As previously mentioned, all films were analysed almost immediately after preparation. Angular dependence studies, carried out by varying the electron take-off angle, revealed the films to be vertically homogeneous, so the results reported below are those obtained using an electron take-off angle of 35^{o}.

The mercury used had been purified by triple distillation, and perfluorobenzene was shown to be analytically pure by GLC.

The gold substrates were cleaned prior to deposition by a three-step procedure; firstly, polished using 'Brasso' then

flame heated until red hot and finally cleaned with AR hexane to remove any grease from the surface. Substrates, both gold and aluminium, were placed in the centre of the reactor in a glass slide in the coil region. The experimental configuration of the reactor and the position of mercury is shown in Figure 4.1

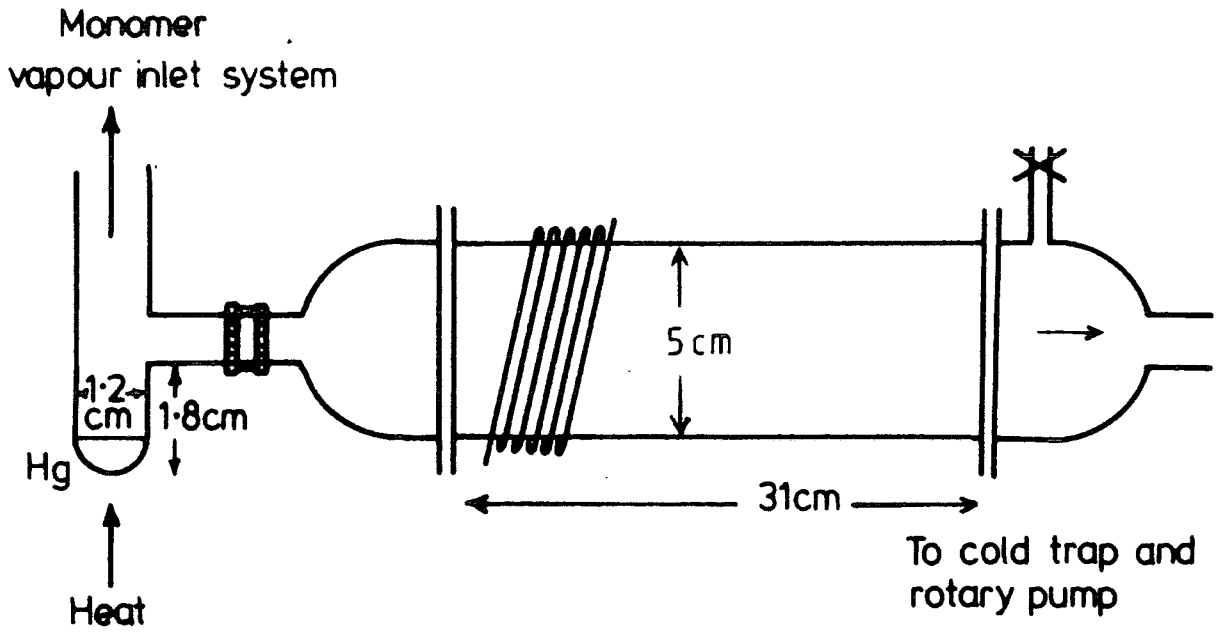

FIGURE 4.1 Experimental configuration of reactor and position of mercury

4.3 Results and Discussion

4.3.1 Metal incorporation as a function of distillation temperature

I. Full Glow

As a starting point to the discussion on mercury incorporation into plasma polymerised perfluorobenzene it is

convenient to describe the general features of the spectra obtained from a typical experiment.

The C_{1s}, F_{1s}, O_{1s} and Hg_{4f} core level spectra for a film obtained from a 0.1 mbar, 5W perfluorobenzene mercury plasma (distillation temperature 80°C) are displayed in Figure 4.2. The C_{1s} level consists of contributions arising from a variety of components. An example of the peak fit that is obtained from a knowledge of binding energies and the full width at half maximum is also shown in Figure 4.2. Peaks centred at 285, 286.6, 288.3, 289.5, 291.2, 293.3, 295.2 eV are due to $\underline{C}$-H, $\underline{C}$-CF_n, $\underline{C}$-F, $\underline{C}F$-CF_n, CF_2, CF_3 and $\pi \rightarrow \pi^*$ shake-up satellite environments respectively.[17] The presence of hydrocarbon is due to extraneous contamination as indicated by the increase in intensity on going to a higher electron take-off angle. The overall shape and contributions of the component peaks to the C_{1s} envelope are similar to those previously reported[16] and indicate that the presence of mercury in the plasma does not observably perturb the nature of the carbon components of the deposited film. The presence of CF_2 and CF_3 structural features in the plasma polymer is suggestive of extensive rearrangement.[16] Indeed comparison of the F:C stoichiometry in the starting "monomer" and in the plasma polymer reveals that the fluorine content of both is similar. As has been previously reported in the literature these data indicate that the polymerisation mechanisms involve mainly rearrangement processes[16] rather than elimination as is the case in the plasma polymerisation of the difluoroethylenes.[17]

The Hg_{4f} level reveals two peaks at 106.25 and

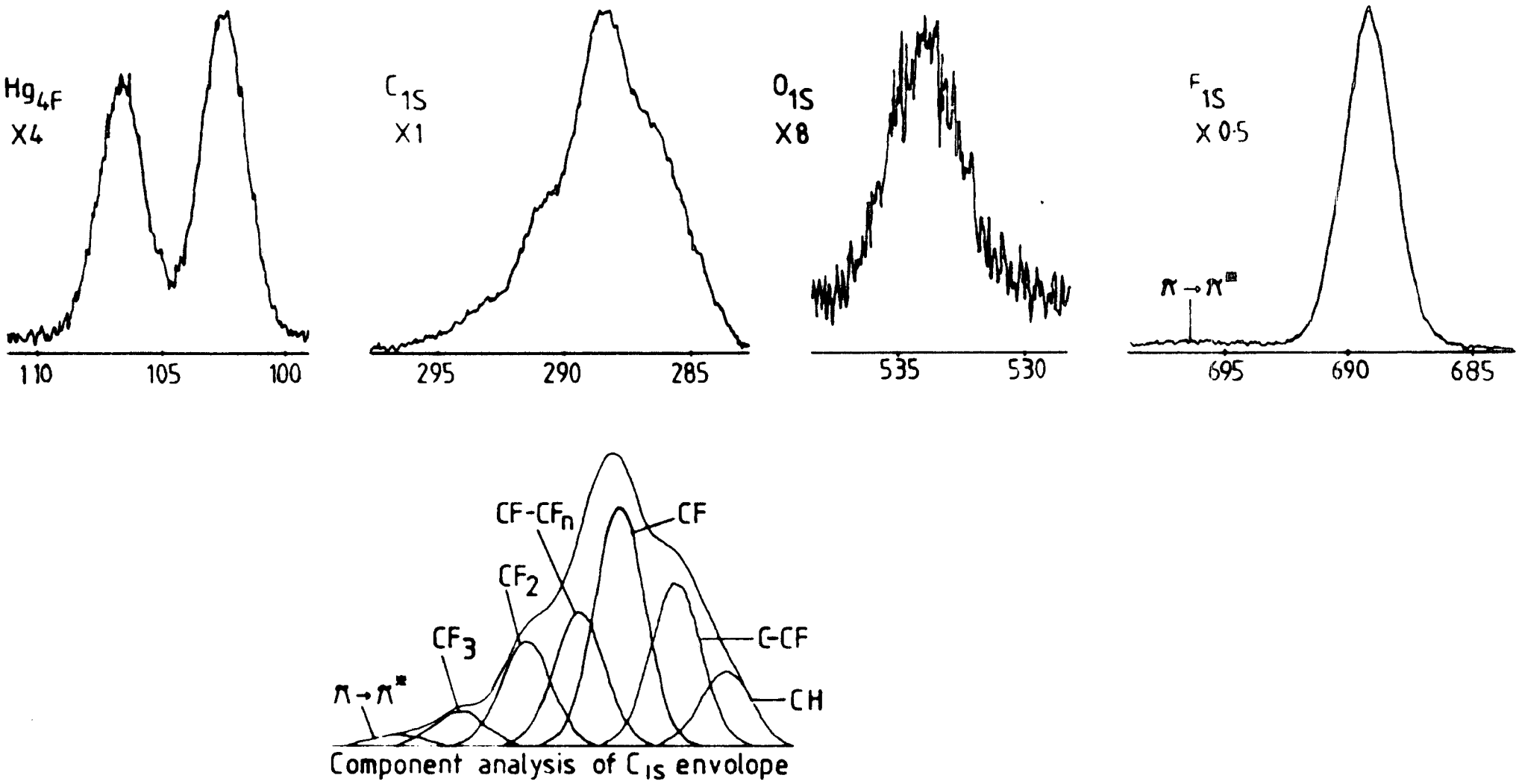

FIGURE 4.2 Typical core level spectra of plasma polymerized perfluorobenzene and mercury

102.25 eV. These correspond to the $Hg_{4f_{5/2}}$ and $Hg_{4f_{7/2}}$ due to the Hg_{4f} level undergoing spin orbit splitting, this is discussed in greater detail in Chapter Five. The binding energy of these levels is ∿3 eV higher than that expected for pure mercury.[18] It is unlikely that these peaks are due to an oxide as the oxygen content of the film is low ($C_1:O_{0.06}$) and coupled with this, a mass spectrometry study of the pyrolysis products of this film revealed peaks at 367, 534 and 701 mass units indicative of mercury bonded to (C_6F_5) groups. We feel that the data above suggest that the mercury is chemically bonded within the plasma polymer film as opposed to being a metal or metal oxide held within a polymer matrix. The latter appears to be a feature of the plasma polymerisation of tetramethyltin[19,20] and tetramethylgermanium.

The presence of a small oxygen peak in the ESCA spectra is normally observed in plasma polymers and may arise for instance from the etching of the glass walls of the reactor, or reaction of reactive species in the polymer matrix with oxygen after removal from the vacuum line.

Initial studies on the extent of mercury incorporation as a function of distillation temperature showed that a minimum temperature of 40°C was required for metal introduction and that a maximum was observed at 60°C and above, (Figure 4.6). This maximum corresponded to Hg:C stoichiometry of ∿0.04. However, on repeating the experiments it was observed that the extent of mercury incorporation was essentially constant at all temperatures between ambient and 190°C as indicated in Figure 4.3. Examination of the mercury distillation region of the reactor (Figure 4.1) revealed that mercury had deposited in the tube leading to the coil region

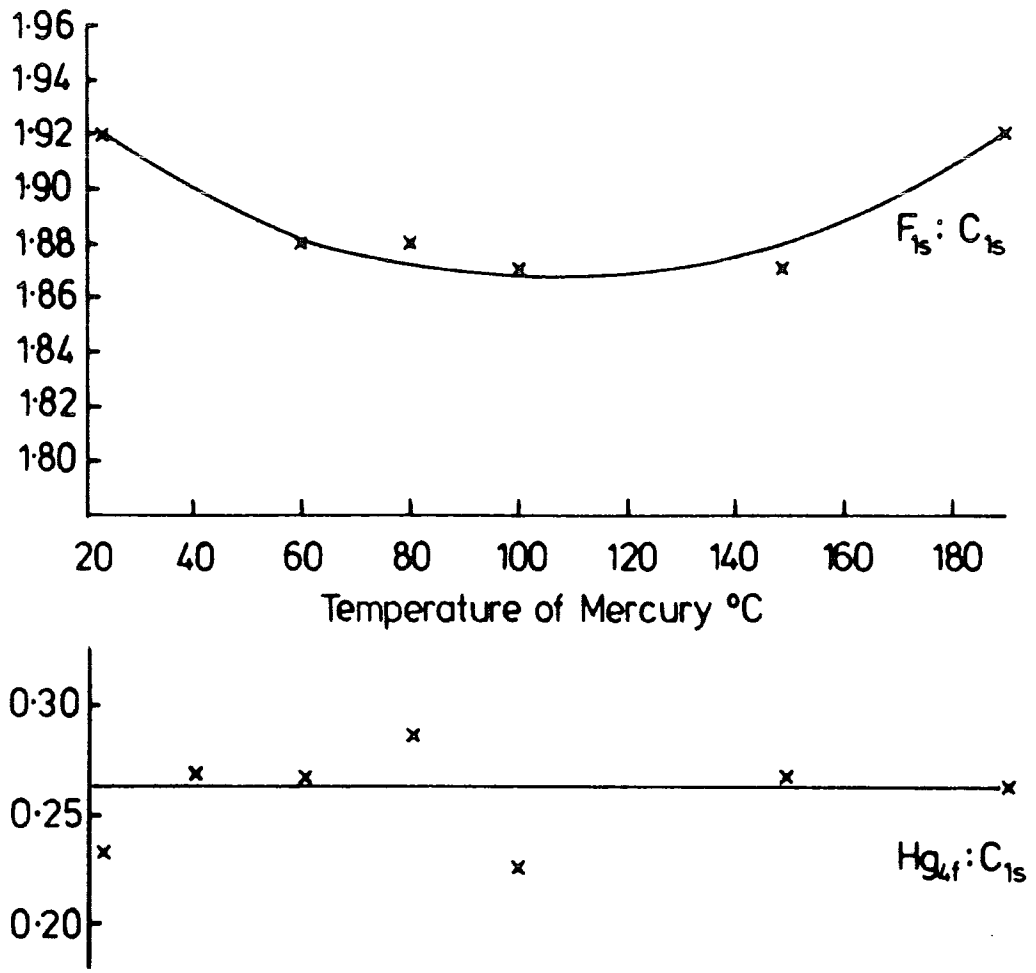

FIGURE 4.3 Peak areas F_{1s} and Hg_{4f} to C_{1s} envelope as a function of temperature

such that in these latter experiments the incoming perfluorobenzene vapour passed directly over a layer of mercury, *i.e.* the inlet system had undergone a preconditioning. In the initial studies this would not have occurred, and the extent of metal incorporation would, for lower distillation temperatures, be a direct function of the concentration of mercury in the gas phase. These results clearly indicate that the relationship between monomer flow and the position of the source of metal strongly influences the level of mercury incorporation.

However, even when the above considerations are taken into account within the experimental procedure, the

maximum Hg:C stoichiometry obtainable remains at ∿0.04.

The effect of increasing the distillation temperature for the preconditioned inlet system on the structural composition of the deposited plasma polymer is very small as is evidenced by the F_{1s}/C_{1s} area ratios in Figure 4.3 and the C_{1s} component analysis in Figure 4.4. The F:C stoichiometry remains close to that of the monomer reaffirming the dominance of rearrangement reactions in the polymerisation mechanism.[16b] The only changes in the component distributions are small tendencies for an increase in

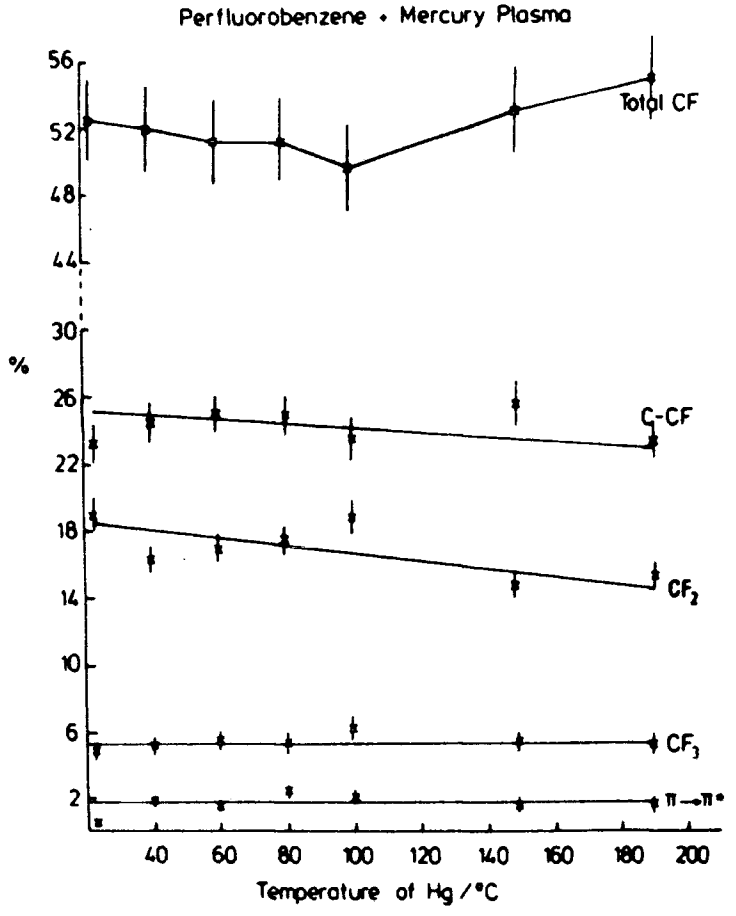

FIGURE 4.4 Percentage area of component peaks from C_{1s} envelope as a function of temperature of mercury

total C-F and a decrease in CF_2 with increasing distillation temperature.

There also appears to be an effect in the amount of oxygen incorporation into the polymer film as a function of increasing distillation temperature. Even though in the 'conditioned' system the amount of mercury incorporation is constant, the amount of oxygen decreases. This may be due to the excess mercury vapour quenching reactive oxygen species present in the plasma and thus preventing reaction with the growing organometallic polymer film. As there are previous reports in the literature on the use of mercury in removing atomic oxygen and ozone from microwave discharges in oxygen,[21] the above suggestion is not unreasonable.

II. Partial Glow

The volume of the visible glow in a discharge - glow characteristic - has been reported as being an important definable parameter of the plasma polymerization experiment. In their study on the plasma polymerization of acrylonitrile, Yasuda and Hirotsu[22] found that the polymer deposited in the tail flame portion of a fully developed plasma (filled the entire reactor) was different in nature to that deposited in the same position from a partial plasma (where the visible glow filled only part of the reactor). The polymer deposited from a full plasma was brown and insoluble in any solvent whilst the polymer formed in the weak glow was light yellow and soluble in polar solvents. The difference in properties of the two polymers was directly attributed to the character of the glow since other variables, *i.e.* flow rate, power, pressure and reactor configuration, were all kept constant.

It was suggested that this difference in properties reflected the difference in polymerization mechanisms between a full and partial glow discharge; that the chemistry involved in the incomplete glow region was different.[22]

In the present study, the results reported are those obtained whilst using a fully developed glow discharge, *i.e.* the whole of the reactor volume was emitting visible light. However, in this section the effect of a partial glow - visible in and around the coil region only - on the composition of the plasma polymer and the difference in metal incorporation as a function of distillation temperature is examined. Polymer samples were analysed from the coil region, *i.e.* both samples were in the glow region. This is in contrast to the study by Yasuda[22] where samples were collected from the end of the reactor only.

The component peak analyses of the C_{1s} envelopes from polymers derived from both full and partial glow discharge conditions as a function of mercury distillation temperature are displayed in Figure 4.5. There are several noticeable variations between the compositions of the two different polymers, the most prominent perhaps being the level of unsaturation present in the polymer sample deposited in the partial glow. Under both glow discharge conditions the intensity of the $\pi \rightarrow \pi^*$ shake-up satellite is roughly constant, but is 2% greater in the 'partial glow' polymer. This increased unsaturation is also reflected in the increased intensity of the $\pi \rightarrow \pi^*$ shake-up satellite present in the F_{1s} core level spectra.

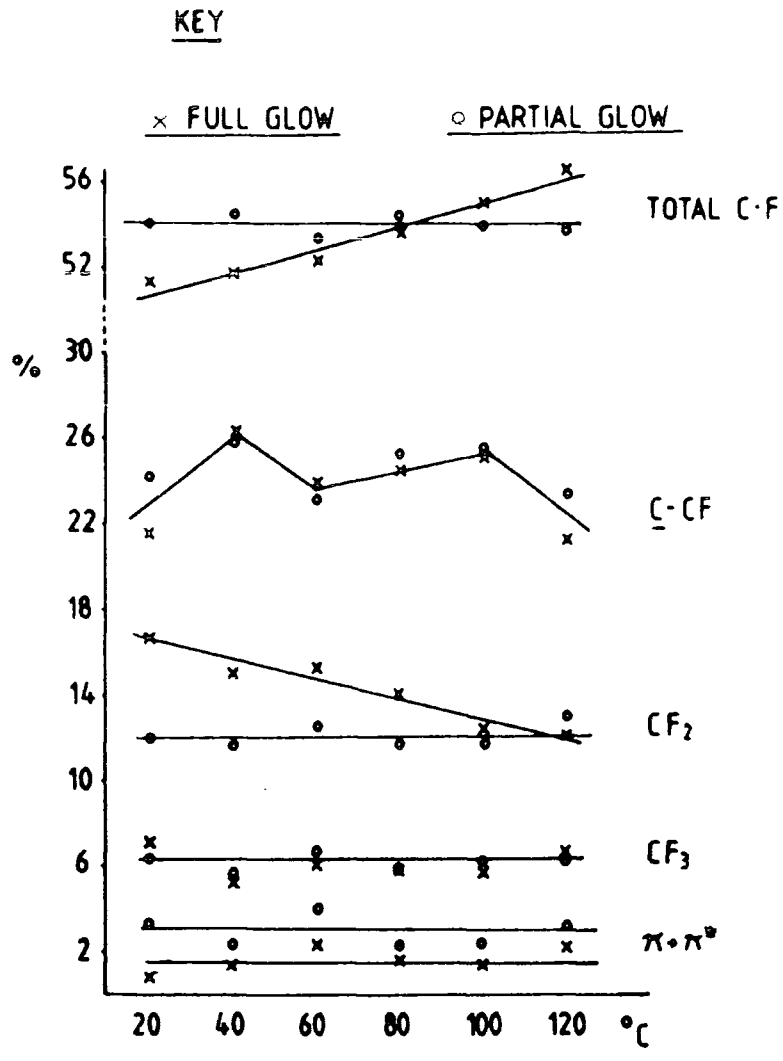

FIGURE 4.5 Percentage area of component peaks from C_{1s} envelope for two different glow discharge conditions as a function of mercury distillation temperature

The amount of CF_3 and C-CF would appear to be very similar and approximately constant in both polymer types as a function of distillation temperature of the mercury: as would the amount of CF_T * in the polymer formed in a partial glow. However, this apparently 'static' situation masks the changes in intensity of the two component peaks due to CF and CF-CF, which balance out to make an overall constant amount of CF_T. Due to the difficulties in peak fitting of these two component peaks no absolute values are assigned to them

---

* $[CF_T] = [CF] + [CF\text{-}CF]$ - Chapter Two.

but it is noticeable that the CF component peak increases whilst the CF-CF peak decreases in intensity with increasing distillation temperature. A similar situation arises in the amount of CF in the polymer formed in a full glow discharge which appears to increase as a function of the temperature of the mercury, both the CF and CF-CF component peaks show an increase. It should be pointed out here that the amount of CF in the 'partial glow' polymer is some 3-4% greater than in the corresponding 'full glow' polymer, whilst the amount of CF-CF is between 2-6% greater in the 'full glow' polymer.

With an increasing distillation temperature, the amount of CF_2 present in the 'full glow' polymer shows a decreasing trend from nearly 17% at 20°C to 12% at 120°C. This is in contrast to the 'partial glow' polymer which retains a more or less constant amount of CF_2 of around 12%.

Thus from the preceding discussion and a knowledge of the effects of a partial or full glow on the composition of the deposited polymer film, a limited amount of polymer 'tailoring' would seem possible upon the suitable choice of type of glow discharge.

The glow characteristic also affected the amount of metal incorporation into the polymer film. Initial metal incorporation into the 'partial glow' polymer did not proceed until a minimum mercury distillation temperature of 60°C was utilized. An increasing concentration of metal incorporation was then observed up to a 100°C when the level of mercury became constant, at the same level as in the 'full glow' polymer, at a C:Hg stoichiometry of 1:0.04 (Figure 4.6).

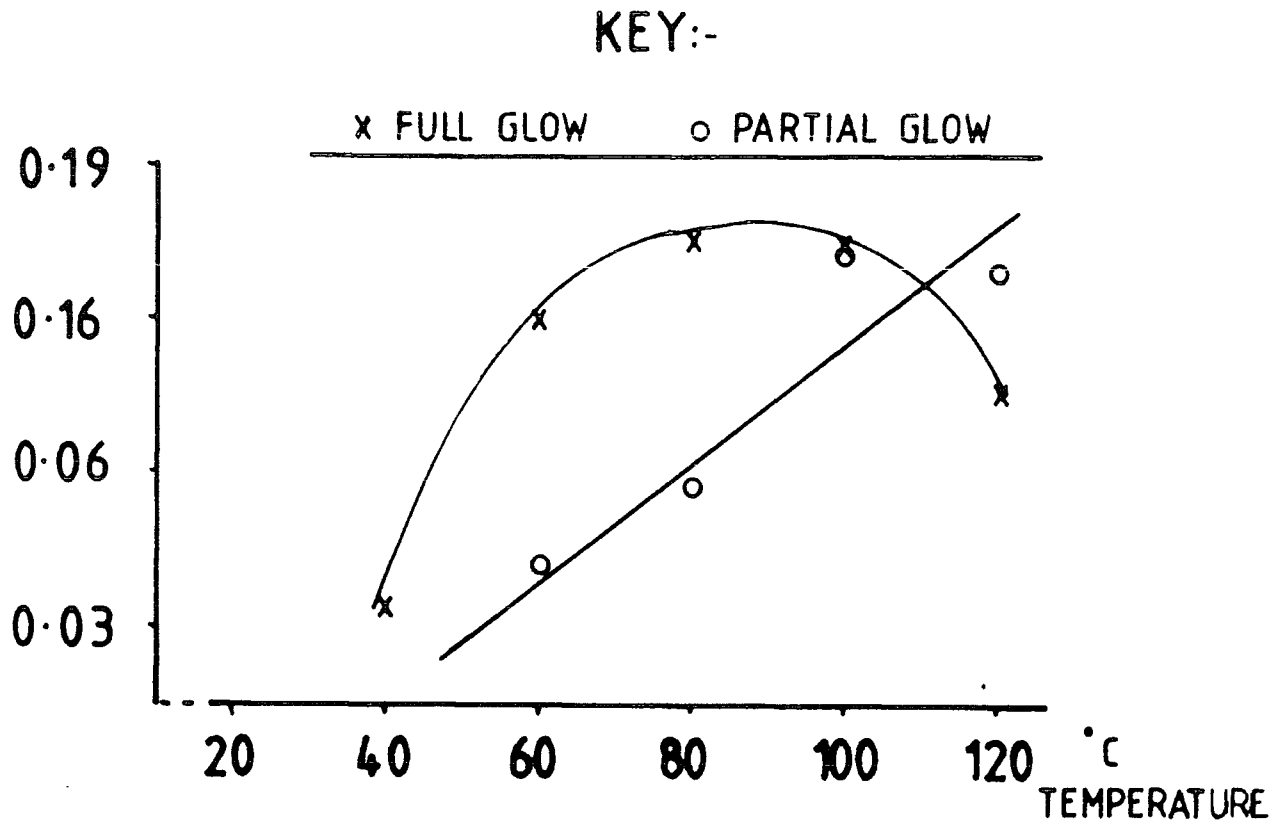

FIGURE 4.6 Mercury incorporation into the polymer film as a function of the distillation temperature for both partial and full glow polymers

In contrast initial metal incorporation into the 'full glow' polymer proceeded at a lower minimum temperature and also reached the maximum concentration at a lower distillation temperature of 80°C. Thus, in agreement with Yasuda[22], the plasma polymerization - and hence composition of the deposited polymer - depends strongly on the nature of the glow.

4.3.2 Metal Incorporation as a function of power

As a preliminary to the study of mercury incorporation, at a fixed distillation temperature (*i.e.* 80°C), as a function of power a detailed investigation of the effect of this parameter on perfluorobenzene was undertaken due to

to the paucity of data on component distribution in the literature.

The relevant C_{1s} component analysis is displayed in Figure 4.7. From these data it is clear that changes occur in total C-F, C-CF and CF_2 over the range 5 to 15 W and thereafter the levels remain constant. With the decrease in total CF there are concomitant increases in C-CF and CF_2. It is interesting to note that an increase in the F_{1s} to C_{1s} area ratio occurs not in 5 to 15 W range, as would be predicted from the C_{1s} component analysis, but in

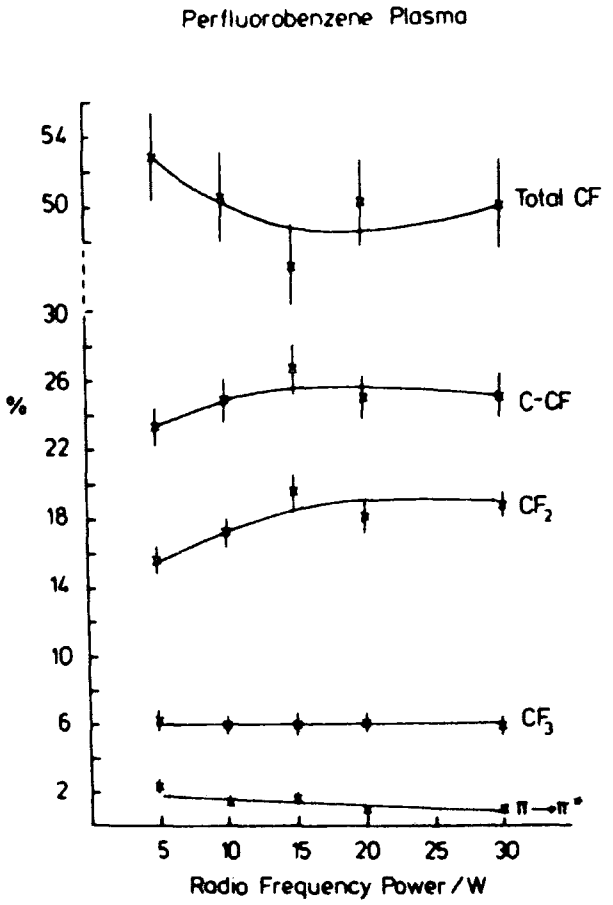

FIGURE 4.7 Percentage area of component peaks from C_{1s} envelope as a function of radiofrequency discharge power of perfluorobenzene plasma

the 15 to 30 W region. The present available data does not allow for a reasonable explanation for this phenomena to be undertaken.

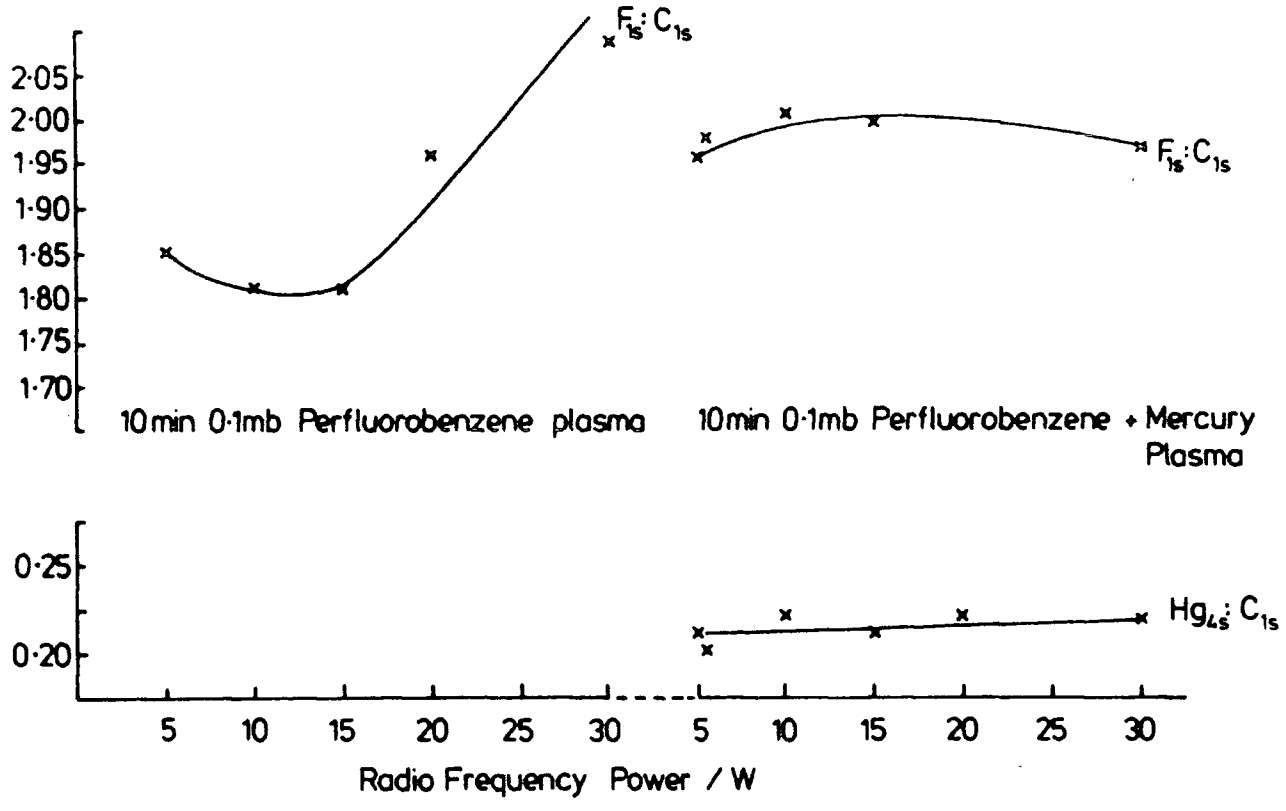

FIGURE 4.8 Peak areas of F_{1s} and Hg_{4f} to C_{1s} envelope as a function of radiofrequency discharge power for the perfluorobenzene and perfluorobenzene plus mercury plasmas

In contrast to the above data the fluorine content for mercury incorporated films (Figure 4.8) shows very little variation as a function of power. Similarly the mercury level is constant over the range of powers investigated. The main effect of increasing power on the composition of the mercury-

perfluorobenzene plasma polymer is observed in the component distribution as displayed in Figure 4.9.

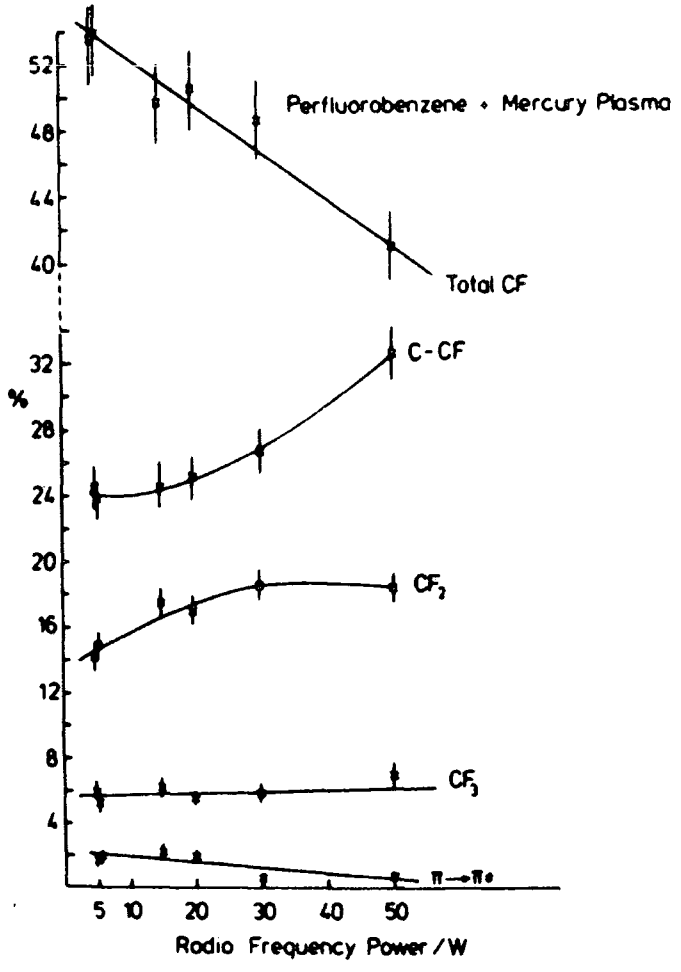

FIGURE 4.9 Percentage area of component peaks from C_{1s} envelope as a function of radiofrequency discharge power of perfluorobenzene and mercury plasma

An essentially linear decrease in the total C-F contribution of the order of 10% is observed on going from 5 to 30 W. Whereas in the "pure" perfluorobenzene system C-CF and CF_2 components showed initial increases only CF_2 reveals this behaviour in the range 5 to 15 W. C-CF increases at powers greater than 20 W. These data reveal that

mercury has a definite influence on the organofluorine content of the plasma polymer dependent on the power used.

The nature of the role of mercury in the plasma polymerisation mechanism is by no means straightforward. As observed in the data in Figure 4.3 the mercury content remains constant over the power range studied. Thus the variations in structure as a function of power cannot be directly due to the level of mercury incorporated. Likewise from the study of perfluorobenzene alone the behaviour cannot be explained only in terms of the reactions of the monomer as a function of power. Therefore the data strongly suggest that there is a complex interaction between the mercury and perfluorobenzene in the gas phase of the plasma.

Mercury is well known for its sensitisation of photochemical reactions[23] and the observed trends in this film's structure may well arise from the sensitisation of reactions involving perfluorobenzene and/or its rearrangement products. As power is increased the energy absorption of the mercury will be increased with the effect of enhancing or changing the nature of reactions in the gas phase possibly by sensitisation. The interrogation of the species present in the gas phase *via* optical techniques that do not perturb the plasma presents the best approach to investigate variations in plasma reactions as functions of the operating conditions. The use of optical emission analysis as a means of correlating the gas phase chemistry and the composition of the plasma polymer is demonstrated, in Chapters Five and Six, in the co-polymerization of perfluorobenzene with other organic/ organometallic monomers.

4.3.3 Substrate temperature

The influence of substrate temperature on the structure and bonding in plasma polymers is an area of investigation that has received little attention in the literature. In a recent study on the plasma polymerisation of acrylonitrile distinct differences in the nitrogen content of the deposited films dependent on power and substrate temperature[24] were found. A study was therefore conducted on the composition of plasma polymerised perfluorobenzene and mercury/perfluorobenzene at a substrate temperature of 150°C in order to compare the results with those obtained at ambient temperature.

At the higher temperature, which for acrylonitrile was sufficient to induce marked differences when compared with ambient, no detectable deviations from the data obtained at 20°C were observed in plasma polymerised perfluorobenzenes over a 5-30 W power range. A comparison of the component peak analysis of plasma polymerized PFB at the two substrate temperatures is shown in Chapter Two. This may well arise from the good thermal stability imparted to the system by the high fluorine content and for which fluoropolymers are well known.[25]

The mercury/perfluorobenzene system, although at the power studied (5 W) showed the same C_{1s} and F_{1s} spectra as at 20°C, revealed a factor of ∿4 decrease in mercury content. This tends to confirm the conclusion, alluded to earlier, that the nature of the mercury incorporation into the plasma polymer does not induce observable perturbations to the C_{1s} and F_{1s} core levels and indicates that the bonding to the system is considerably weaker than the C-C or C-F bonds.

4.3.4 Internal Stress in the Plasma Polymers

All films were deposited onto gold and aluminium foil and transported from the reactor to the spectrometer under a blanket of nitrogen. This was particularly important when using aluminium foil as the substrate for "pure" perfluorobenzene plasma polymers. When the films were exposed to air, cracking was observed which was accelerated by moisture. A similar phenomena has been noted in plasma polymerised 1-fluoronaphthalene[26] and is dependent on the nature of the substrate material used as evidenced by the absence of cracks when gold is used. The mercury containing plasma polymerised perfluorobenzene is stable with respect to this feature and seems to indicate that mercury improves the internal stress of the films on aluminium foil. The mechanism for this is at present unknown.

This phenomenon of cracking of the polymer film was thought to be associated with the absorption of moisture from the atmosphere and consequent swelling of the film. Water vapour would appear to 'help' the process as seen by the increased rate of cracking of these films in the presence of H_2O. However, it has been shown that a thin layer plasma polymer deposited onto a flexible polymeric substrate often shows a strong tendency to bend and curl.[27] This curling took place during the process of plasma polymerization in which no swelling due to the absorption of moisture could occur, and was therefore attributed to internal stresses arising during the polymer deposition.

Further, it was noticed that the slower the deposition rate, the larger was the internal stress.[27] The thickness of the deposited polymer layer was also found to be

related to the stress in the film, as polymer thickness increased above approximately 500 nm the stress decreased, although up to this thickness stress had been constant in three different plasma polymer films. The internal stresses of plasma polymers prepared from perfluorobenzene, tetrafluorobenzene and difluorobenzene have been measured[28] and found to be essentially the same, *i.e.* at 400 nm film thickness to have a stress of $\sim 3.7 \times 10^{8}$ dyne cm^{-2} * which is very similar to that of plasma polymerized acetylene.[29]

If the internal stress of the polymer substrate interface is greater than the adhesive forces in this region, then poor adhesion - as evidenced by buckling of the polymer - will result. Cracking results when the internal stress is greater than the cohesive force of the plasma polymer.[27]

In the present study, the lack of cracking of the metal containing films may result, in view of the above facts, from a faster deposition rate. Indeed the percentage weight increase of the substrate was greater in the deposition of the metal containing film. However, the density of the metal containing film can no longer be assumed to be the same as that of the organic film, and would, in fact, be expected to be greater. Visibly, the deposition rate did not appear to

---

* Stress in the film was calculated using the empirical equation below[29] which holds when the plasma polymer thickness is much less than that of the substrate:

$$\sigma_{s.d} = ED^2/6R$$

where σ_s = stress in the plasma polymer
d = film thickness
E = Young's modulus of the substrate
D = thickness of the substrate
R = radius of the curling substrate

differ in the two experiments and the increased weight gain may be due solely to the increased density of the film when it contains mercury. Therefore, it may be the increased density of the mercury containing film which is responsible for the elimination of cracking within the plasma polymerized film. The density of SiN films,[30] prepared by plasma chemical vapour deposition, has also been noted as being an important parameter in the determination of the resistance of such films to cracking. The lower the density of the film, the greater was the amount of crack generation.

4.4 Conclusion

The incorporation of mercury into a plasma polymer of perfluorobenzene is facile in an inductively coupled radio-frequency discharge. A maximum Hg:C stoichiometry of 0.04 is observed over a range of distillation temperatures and powers. The contrast in C_{1s} component distribution when polymerisation is studied as a function of power is not a direct function of the level of mercury incorporated but is probably due to energy transfer processes between the mercury and perfluorobenzene in the gas phase of the plasma. It is also evident from examination of the C_{1s} core levels and the appropriate F_{1s}/C_{1s} area ratios that the polymerisation mechanisms involve rearrangement of the perfluorobenzene as opposed to elimination reactions.

The influence of substrate temperature on the structure and bonding of the organofluorine component of the deposited films is negligible under the conditions used but significantly

decreases the mercury content. The inclusion of mercury into perfluorobenzene plasma polymers improves the stability of the polymer film on aluminium foil substrates.

REFERENCES - Chapter Four

1. N. Boonthanom and M. White, Thin Solid Films, 24, 295 (1974).

2. R.V. Rao and K.L. Chopra, J.Chem.Phys., 68, 1484 (1978).

3. S. Osaki and T. Ishida, J.Polym.Sci.,Polym.Phys.Ed., 11, 801 (1973).

4. H.A. Beale, Ind.Res.Dev., 23, 135 (1981).

5. E. Kay and M. Hecq, J.Appl.Phys., 55(2), 370 (1984).

6a. E. Kay, L.L. Levenson and W.J. James, J.Phys.Chem., 84, 1635 (1980).

6b. R.F. Wielonski and H.A. Beale, Thin Solid Films, 84, 825 (1981).

6c. Y. Asano, Thin Solid Films, 105, 1 (1983).

7a. D. Carlson, J.Electro.Soc., 122, 1334 (1975).

7b. E. Kny *et al*, Thin Solid Films, 64, 395 (1979).

7c. E. Kay *et al*, Thin Solid Films, 84, 1635 (1980).

8a. E. Kay, A. Dilks and U. Hetzler, J.Macromol.Sci.Chem., A12, 1393 (1978).

8b. E. Kay and A. Dilks, J.Vac.Sci.Technol.16, 428 (1979).

8c. E. Kay, A. Dilks and D. Seybold, J.Appl.Phys. 51, 5678 (1980).

8d. E. Kay and M. Hecq., J.Vac.Sci.Technol. A2(2), 401, (1984).

9a. H. Holzinger, K. Meyer and H. Tiller, Z.Chem., 13, 32 (1973).

9b. H.S. Munro and C. Till, J.Polym.Sci.,Polym.Chem.Ed., 22, 3933 (1984).

10. Venkatesan *et al*, J.Vac.Sci.Technol. 19, 1379 (1981).

11. S. Johnson, Ph.D. Thesis, Durham University, U.K. (1985).

12. N. Inagaki and M. Mitsuuchi, J.Polym.Sci.,Polym.Chem.Ed., 21, 2887 (1983).

13. D. Shuttleworth, J.Phys.Chem., 84, 1629 (1980).

14. N. Inagaki and M. Mitsuuchi, J.Polym.Sci.,Polym.Lett.Ed., 22, 301 (1984).

15. L. Martinu and H. Biederman, Plasma Chem.Plasma Processing 5(1), 81 (1985).

16a. D.T. Clark and D. Shuttleworth, J.Polym.Sci.,Polym.Chem.Ed., 18, 27 (1980).

16b. D.T. Clark and N.Z. AbRahman, J.PolymSci.,Polym.Chem.Ed., 20, 1717 (1982).

16c. D.T. Clark, M.Z. AbRahman, J.Polym.Sci.,Polym.Chem,Ed., 20, 1729 (1982).

17. D.T. Dlark in 'Photon, Electron and Ion Probes of Polymer Structure and Properties', T.J. Fabish, D. Dwight, H.R.Thomas, (Eds.), ACS Symp.Ser. 162, Am.Chem.Soc., Washington,D.C.(1977)

18. C.D. Wagner, L.E. Davis, J.F. Moulder, W.M. Riggs and G.E. Muilenberg, (Eds.), 'Handbook of X-Ray Photoelectron Spectroscopy, Perkin-Elmer, Eden Praire, MN (1979).

19. N. Inagaki, T. Yagi and K. Katsuura, Eur.Polym.J., 18, 621 (1982).

20. H.S. Munro and C. Till, Thin Solid Films, 131, 255 (1985).

21. D.T. Clark and H.S. Munro, Polymer, 25, 826 (1984).

22. H. Yasuda and T. Hirotsu, J.Appl.Polym.Sci., 21, 3139 (1972).

23. P. Borrell, 'Photochemistry: A Primer', Arnold Press (1973).

24. H.S. Munro and H. Grunwald, J.Polym.Sci.,Polym.Chem.Ed., 23, 479 (1985).

25. W.E. Gibbs and T. Helminiak, 'Polymers for use at high and low temperatures', in Polymer Science 2, Jenkins (Ed.), North-Holland, Amsterdam (1972).

26. H.S. Munro and C. Till, J.Polym.Sci.,Polym.Chem.Ed., 24, 279 (1986).

27. H. Yasuda, 'Plasma Polymerization', Academic Press, London. (1985).

28. D.T. Clark and M.Z. AbRahman, J.Polym.Sci., Polym.Chem.Ed., 20, 1729 (1982).

29. H. Yasuda, T. Hirotsu and H.G. Olf, J.Appl.Polym.Sci., 21, 3179 (1977).

30. R. Gereth and W. Scherper, J.Electrochem.Soc., 119(9), 1248 (1972).

CHAPTER FIVE

INCORPORATION OF A METAL INTO PLASMA POLYMERIZED PERFLUOROBENZENE

PART II: COPOLYMERIZATION OF AN ORGANOMETALLIC WITH PERFLUOROBENZENE

5.1 Introduction

The incorporation of metals into polymeric materials is an active area of interest.[1] Applications range from polymer-supported catalysts[2] to the use of these films as photoconductors.[3] One particularly active area of research is in the use of metallated plasma polymers as electron beam resists[4] following the development of the use of plasma polymers as photoresists.[5]

5.1.1 Plasma Polymers as Resists

The use of plasma polymer films as electron beam resists is attractive for several reasons. The practical optical limit of photoresists is around 2μm,[6] due to diffraction patterns caused by radiation projected through mask lines narrower than 1μm which result in a blurring effect of the pattern. However, the use of electrons results in a higher potential resolution (∿0.05μm) since this is not limited by diffraction considerations, and the electron beam can be focussed to a spot diameter two or three orders of magnitude less than the wavelength of light.[6] The use of an electron beam whose intensity and energy can easily be controlled leads to the capability of writing directly on the substrate at final image size.

Other advantages associated with the use of electron beams to delineate the circuit pattern in a substrate include a faster turn around time, better line width control and smaller features. Electron beam lithography also offers the possibility of a one-step fabrication of high quality photolithographic master masks with overall lower

defect densities than conventional methods.[7] All these advantages result primarily from a reduction in the number of lithographic steps needed as well as the inherently higher resolution capabilities of electron lithography.

The resolution of an electron beam is a direct function of film thickness. Plasma polymerization can give rise to the controlled deposition of thin organic films of known thickness. These ultra-thin, highly cross-linked films exhibit two inherent properties which makes their use as resists very attractive:

1. the deposition of a uniformly thick thin film minimises line width variations stemming from resist thickness variations which occur when the lines traverse a step in the wafer.[8] The thin nature of the film minimises the amount of electron scattering which occurs within the resist.

2. The excellent adhesive properties demonstrated by a plasma polymer limit the undercutting of the patterns which would result in a loss of resolution. Poor adhesion, in the limit, can cause complete destruction of the pattern.

One of the basic problems in the use of any organic film as an electron beam resist arises from the energy dissipated by the incident electron beam. Organic materials do not absorb all the energy of a high energy electron beam. Electron scattering in the resist, arising from the thickness of the resist, sets the practical limit to the minimum feature size that can be resolved. However, if too thin a film is used in order to minimise scattering within the resist, then backscattering from the substrate will become a problem affecting the practical resolution of the resist.[9] This may be

overcome to some extent by the incorporation of metal into the plasma polymer resist. Due to the higher absorption cross section of these atoms, absorption of the energy of the incident electron beam may be increased. This has been considered to some extent by previous workers.[10]

In a positive electron resist,[9] the pattern is produced by development in a suitable solvent in which the degraded polymer dissolves much faster than the unexposed areas. The sensitivity of the resist is determined by the scission probability and the solubility rate ratio for the degraded polymers.[11] Methacrylic polymers have been extensively studied,[12] because these polymers are readily degraded by high energy beam exposure. Polymethyl methacrylate was the first material reported as an electron beam resist.[13] This material has a rather poor sensitivity, but is still believed to show the highest resolution.[14]

The sensitivity of a methacrylate resist has been improved by the incorporation of fluorine atoms into the molecule.[15] The authors reported that this increased sensitivity was due to the excellent development characteristics of the resultant film.[15]

Paralleling the popularity of the use of conventional methacrylate polymers, is the development of the use of methacrylate plasma polymers as electron beam resists. Here, hopefully, the advantages of the conventional polymer are combined with the advantages gained from plasma polymerization. There have been many studies reported in the literature in this area.[16] One such study involved the incorporation of tin into a plasma polymer of methylmethacrylate by introducing

a small amount of tetramethyl tin into the plasma.[17] The resultant plasma polymer was incompletely analysed, no mention was made of the composition of the plasma polymer. However the authors did find that as the amount of tin incorporated into the polymer increased the sensitivity of the film improved due to an increased absorption energy.

The actual amount of metal incorporation into the polymer was not measured. The authors assumed that by increasing the weight percent of TMT from 1-5 in the starting monomer, the metal content of the polymer film reflected the concentration of tin in the starting monomer.

One of the problems which was associated with the incorporation of a high content of tin into resists was the formation of unwanted SnO_2 in the surface of the substrate[18] after dry lithographic techniques have been used to remove the resist. This could only be removed by wet treatment,[19] hence negating the benefits obtained by having totally dry processing methods. The problem was solved by the development of new purer forms of photoresist, in which the tin catalyst had been removed. However, with the intentional incorporation of tin into a polymer to improve energy absorption by the resist, the above may once again become a problem.

With the increasing sophistication in device fabrication a greater demand on resist technology is being made. The continued push to higher resolution has led to the development of other emerging lithographic techniques such as X-ray lithography, where resists specifically designed for interaction with X-rays are being studied.[20] One such system is based on the incorporation of gold into a plasma polymerised

styrene film based on the knowledge that gold is an X-ray absorbing material over a wide range of X-ray wavelengths.[20] For a fuller discussion of the use of plasma polymers/metallated plasma polymers as resist materials, the interested reader is referred to comprehensive reviews on this topic.[8,10]

5.1.2 Other uses of Metallated Plasma Polymers

On a totally different line of research, there has been a considerable interest in the synthesis of organotin polymers:[21] the extensive investigations in this area being stimulated by the unique physical, chemical and biological properties of organotin compounds.[22] Of particular importance is the versatile biocidic activity of organotin compounds which may be used as fungicides, insecticides, bactericides, rodenticides, mollusicides and antifoulants.[22] They also possess stabilizing activities[23] against thermal, oxidative and light induced destructive processes of polymers, and are widely used as stabilizers of plastics used for food packaging.[22]

Organotin stabilizers and biocides have been usually used as low molecular weight additives to polymeric materials. As examples, tributyl tin compounds are added to paints to form antifouling coatings for the protection of ships hulls and sea water cooling pipes from the attachment of barnacles and other marine organisms.[25] Mono- and dialkyltin compounds are added to polyvinyl chloride for stabilisation against the loss of chlorine.[23] However, being bonded to the polymer only by physical forces, they show serious deficiencies connected with a tendency to escape from the

material by leaching, *etc*. This causes the material to display a short lifetime of biocidic or stabilizing activity.[22] Another problem associated with tin, when it is present as an environmental contaminant, is in the large toxicology of low molecular weight compounds to mammals where it can concentrate[26] and become toxic. Both of the above problems can be minimised by incorporating the organotin group into the polymer by chemical bonds.[27]

Other properties of tin containing polymers are a reduced flammability, corona resistance and a hydrophobic surface.[28]

Similarly, the incorporation of silicon into a polymer is attractive. This results from the distinctive properties exhibited by silicon containing polymers. Those include water repellency, surface hardness, thermal stability, gas permeability and high dielectric constant. Such films have found use as dielectrics for microelectronics, and in optical and biomedical applications.[29]

Inagaki *et al*[30] have studied the plasma polymerization of the tetramethyl compounds of group IV whilst W.J. James *et al* have conducted an extensive investigation into the properties exhibited by organotin plasma polymer films.[31]

From the foregoing discussion it can be seen that there is a great technological importance on the incorporation of metals into polymers. For this reason a study of the plasma polymerization behaviour of the tetramethyl compounds of group IV was re-examined. It should be stressed here that the high sensitivity of the plasma polymerization process to

the experimental conditions means that the plasma polymer deposited under two non-identical conditions could be completely different; hence validating the present comparison of the behaviour of the tetramethyl group IV compounds in a plasma for a direct comparison of the behaviour of the same compounds when copolymerized with perfluorobenzene under identical experimental considerations. The first half of this chapter describes the results obtained from a study of a composition of the polymers produced by the plasma polymerization of the single monomers. The second half investigates the behaviour of these monomers when polymerized in a 1:1 ratio with perfluorobenzene and examines in some detail the influence of metal incorporation into plasma polymers on the structure and bonding of the polymer as revealed by ESCA.

5.2 Experimental

5.2.1 Single Polymerization

The reactor used for this study was the short reactor shown in Chapter Two, Figure 2.1. Aluminium substrates were placed along a glass slide, which was inserted into the reactor, such that polymer samples were collected from before the coil (0-1cm), in the coil region, (6-7cm from the inlet of the reactor) and at the end of the reactor (19-20cm).

All samples were placed in position and then exposed to a 50w 0.2mb Argon plasma for 15 minutes to help 'clean' the reactor and substrates prior to deposition. The organometallic monomer vapour was then leaked into the reactor and its flow rate adjusted such that when using a plasma of

low, the W/FM parameter for all plasma polymerizations was identical as far as was experimentally possible. The W/FM value was approximately 4.4×10^7 J/Kg

After a deposition time of ten minutes, the reactor was let up to atmosphere with Ar and the samples analused by ESCA. Angular dependent studies, *i.e.* using a variable electron take-off angle were carried out on the first polymer sample (0-1cm) to check vertical homogeneity.

The monomers were supplied by the following commercial sources:

Aldrich - Tetramethyl Tin (99% purity), Tetramethyl Silane (99.9%)

Venton - Tetramethyl Germanium (99.5%)

BDH - 2,2-Dimethylpropane (99%)

Bristol Organics Ltd. - Perfluorobenzene (99.5%)

All were checked for purity by GLC and used without further purification. The flow rates used for each of the organometallic monomers were such that the W/FM parameter was constant throughout. For a fuller description of the experimental procedure, the reader is referred back to the experimental section in Chapter Two.

5.2.2 Copolymerization

Each monomer was leaked independently into the reactor, mixing of the two vapours occurred through a 'Y' piece just before the reactor end cap. The flow rate of the tetramethyl compound was first set so that it matched the corresponding flow rate in the single polymerisation. Perfluorobenzene vapour was then let into the system such that the flow rate was doubled, *i.e.* there was a 1:1 ratio of the

two vapours. All other experimental details were as before.

5.2.3 Optical Emission

The optical emission analysis were performed using the equipment described in Chapter Two. However, the total acquisition time used was cut down from 100 sec. to 15 sec. - each individual scan still being 20 msec. - for tetramethyltin and tetramethyltin/perfluorobenzene plasmas.

5.3 Results and Discussion

5.3.1 Tetramethyl Tin (TMT)

Typical core level (C_{1s}, O_{1s} and $Sn_{3d_{5/2}}$) spectra obtained from a plasma polymer derived from TMT are shown in Figure 5.1. Although the absolute stoichiometries depended on sample position, the peak shapes are all very similar in profile so only 1 set are depicted.

The C_{1s} envelope consists of the one main photoionisation peak at 285.0eV due to C-H, with a small shoulder to higher binding energy containing components arising from C-O and C=O moieties which together contribute less than 4% of the total C_{1s} area.

The O_{1s} level, at $\sim$532eV, is a broad peak and contains peaks arising from C-O and C=O. Peak analysis of the component peaks of the O_{1s} envelope have been attempted in the past, but due to the small chemical shifts involved and the fact that the overall O_{1s} peak shape is more or less

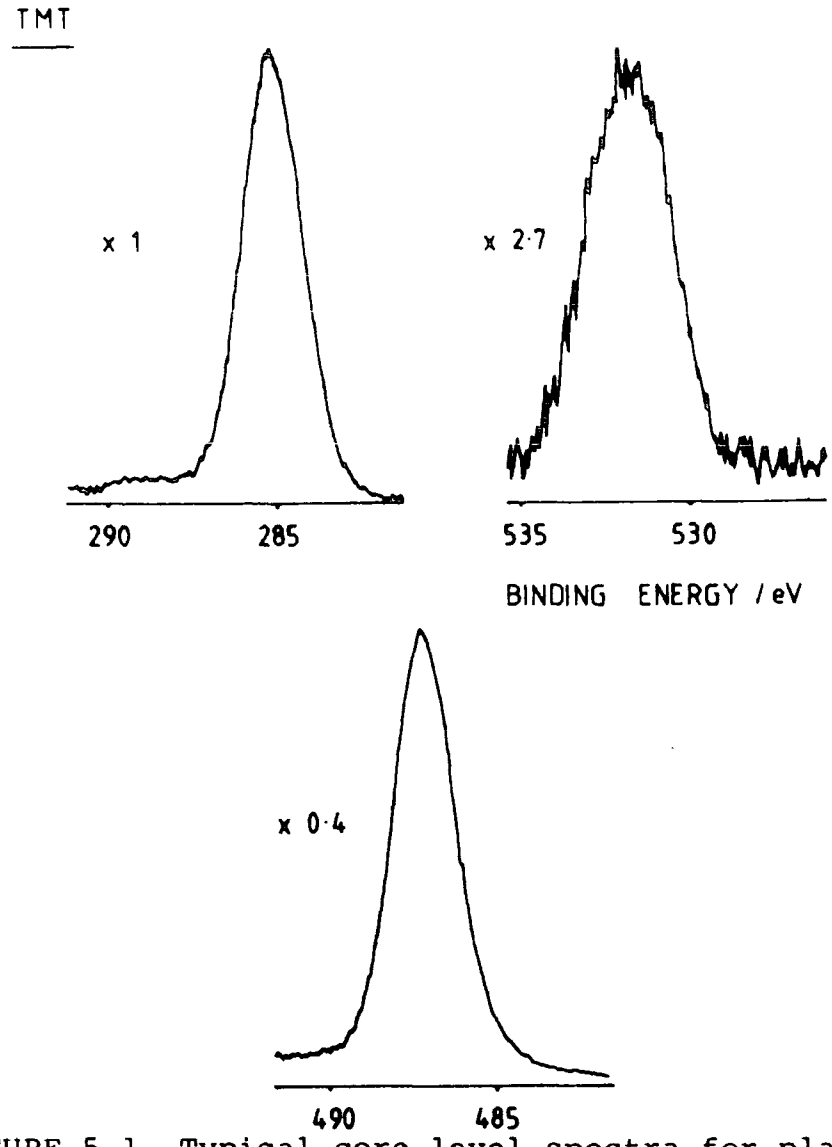

FIGURE 5.1 Typical core level spectra for plasma polymerized tetramethyltin

gaussian in shape makes peak assignment ambiguous. The level of oxygen incorporation is high as can be seen from the intensity of the core level in Figure 5.1 and Table 5.1.

This is in agreement with the work carried out by Inagaki *et al.*[32] The level of oxygen incorporation is much greater than that found in the plasma polymerization of organic systems, which generally yield films containing around 3 oxygen atoms for every 100 carbon atoms.[33] Unlike the previous study,[32] however, there is no detectable nitrogen present in the plasma polymer.

The presence of oxygen in the surface of plasma polymers goes hand in hand with plasma polymerization. The reactive surface present after termination of the plasma, due

to trapped reactive species in the cross-linked network [34] results in an uptake of O_2 by the sample as it is transferred to the spectrometer. There may also be contributions due to the presence of small leaks and the desorption of oxygen species from the reactor walls during polymerization.

The high level of oxygen in the film indicates TMT is more readily oxidized than the aromatic perfluorocarbons (whose plasma polymers contain around $C_1:O_{0.03}$). This could be explained by the extremely low energy of the Sn-C bond (272 kJ mol^{-1}) [35] and its high susceptibility towards homolytic scission. TMT under plasma conditions may therefore, be able to produce many more radical sites resulting in a much higher oxygen incorporation.

The oxygen to carbon ratio seems to follow the tin to carbon ratio, *i.e.* at the inlet of the reactor the film is particularly rich in tin, it is from this area that the highest oxygen content is also found. The sample taken from the end of the reactor has the lowest level of oxygen incorporation, and also has the lowest level of tin. Thus the Sn/C ratio is not constant throughout the reactor. Films high in tin content are deposited at the front end of the reactor whereas carbon enriched films are deposited at the other end. The stoichiometry of the starting material ($C_1:Sn_{0.25}$) is retained in the sample taken from the coil region, whereas the minimum and maximum observed values for Sn/C are found to be lower and higher respectively than the Sn/C value of the starting monomer, tetramethyltin, see Table 5.1.

TABLE 5.1 Tin to carbon and oxygen to carbon area ratios as a function of distance in the reactor

	Position			TOA
	0-1cm	(coil region) 6-7 cm	19-20 cm	
$Sn_{3d_{5/2}}/C_{1s}$	3.87	2.42	1.88	35°
$Sn_{3d_{5/2}}/C_{1s}$		1.90		70°
O_{1s}/C_{1s}	0.63	0.48	0.39	35°

The plasma polymerization of tetramethyltin has been found to produce semi-conducting polymer samples. The tin content of the polymer film can be increased, with a resultant increase in conductivity, by having a steady, but small flow of oxygen with the TMT vapour. In the plasma the oxygen oxidises the carbon fragments to CO_2 and CO which are then lost as exhaust gases.[29e]

The Sn signal consists of a doublet at 487.1 and 495.5eV corresponding to the signals from the $Sn_{3d_{5/2}}$ and $Sn_{3d_{3/2}}$ levels respectively. This doublet arises from spin-orbit coupling.

In the photoionisation from an orbital of orbital quantum number (l) greater than 0 (*i.e.* not from an S orbital) coupling occurs between the spin (S) and orbital angular momentum (L) to yield total momenta (J) resulting in the peak appearing as a doublet in the ESCA spectrum. Up to the lanthanides the Russell-Saunders coupling scheme is applicable (L+S=J); this is valid when spin-orbit coupling is weak compared with electrostatic interactions. The ratio of intensities of the components of the doublet obtained in the ESCA spectrum are

proportional to the ratio of the degeneracies (2J+1) of the states. Thus the relative intensities of the states arising from a d level (orbital quantum number = 1) gives a total quantum number of $^{1}/_{2}$ and $^{3}/_{2}$ giving rise to an intensity ratio of 2:3.

All calculations are based on the area of the $Sn_{3d_{5/2}}$ peak. Owing to the small differences in binding energy between Sn-C and Sn-O environments it is not possible to distinguish between them to provide an unambiguous assignment of the amount of tin oxide present from the Sn_{3d} level. Although some of the oxygen may be attributed to the C_{1s} envelope, the intensity of the core level is such that tin oxide is also present. However there is not enough oxygen present in the polymer film to account for all of the tin being present as tin oxide. This implies that the rest of the tin is either present as elemental metal or that Sn-C bonds have been retained in the plasma polymer. It is unlikely that elemental tin is present from the binding energy of the Sn core level, this would occur at ~484.5eV.[36] The fact that the binding energy is some 3eV higher suggests that there are some organic-tin bonds in the polymer.

It is tempting to assign the lower binding energy peak in the Sn_{3d} core level as arising from the metal. In fact, the binding energy of this peak is still too high to be due to the metal. By doing a cold probe experiment, *i.e.* cooling the probe in the spectrometer down to -130°C and then condensing out the tetramethyltin monomer before recording the relevant core levels, it is apparent that this smaller peak is an integral part of the spectrum of the Sn_{3d} core level. The

Sn_{3d} core level cannot be fitted with one gaussian peak. As further evidence that the plasma polymer film contains Sn-C bands, the binding energy of the Sn core level in the condensed organometallic monomer occurs at 487.5eV.

Inagaki *et al* has looked at the infrared spectrum of plasma polymerized tetramethyltin[32] by depositing the polymer into KBr powder sprinkled thinly on a plate placed inside the reactor. This polymer coated KBr was then used to prepare a KBr disc. Absorbtions due to CH_3, CH_2, CH, Sn-O-Sn and Sn-C groups were found.[32] The possibility of Sn-Sn bands was not eliminated since the spectrum in the range ($\sim$200 cm^{-1}) was not examined.

Kny *et al* have looked at the interface composition and adhesion[31a] of glow discharge formed organotin polymers using polymer samples from a monobutyltrivinyl tin plasma deposited onto aluminium and stainless steel. A 3eV splitting and shift of the $Sn_{3d_{5/2}}$ ESCA peak was noticed. This implied a changing chemical environment for Sn and the authors concluded that a strongly electronegative element was attached to Sn in the interface region between aluminium and plasma polymer. From the high amount of oxygen observed at this interface region they suggested that the bonding of Sn-oxygen was very likely. The composition at this interface was shown to be dependent on sample position within the reactor during deposition. These results, however, were reached by examination of the substrate-plasma polymer composite <u>after</u> carrying out a pull test. The cohesive failure mode created a thin residual film left on top of the substrate. It was this thin film that was subject to an ESCA depth profile using Ar ion etching. Two important points are raised concerning this approach:

Firstly, the freshly revealed surface is not the interface. Only an accurate analysis of the interface can be achieved when a very thin film is deposited onto the substrate such that the substrate is still 'visible' to ESCA. This has been examined in Chapter Seven during the photopolymerization of perfluorobenzene onto Al foil substrates.

Secondly, due to the differential sputtering yields and possible damage to the plasma polymer caused by the Ar ions, great care has to be taken in interpreting data which involves depth profiling by this method. From Knys' results[31a] the amount of oxygen increased dramatically as etching proceeded towards the interface, as did the amount of aluminium. Prior to deposition the aluminium samples were precleaned with a low power argon plasma which hinders the interpretation of these results. The problem arises from the lack of reported knowledge concerning the state of the surface of the substrate, *i.e.* whether the argon plasma had removed all the oxide layer. If the argon plasma did not remove the oxide layer, then the observation of an increased amount of oxygen at the interface is not unexpected. The signal from tin decreased rapidly with time.

As has been pointed out in Chapter Two, the composition of the deposited films depends greatly on its position in the reactor and whether deposition occurred in the glow or non glow region. All samples examined here were deposited in the 'glow region', as the visible glow from the plasma filled the whole of the reactor. Further, after a 10 minute deposition period all film thicknesses were such that the aluminium substrate was not 'visible'. Qualitatively, the rate of deposition also varied with distance from the inlet, the

greatest rate of film formation being found in the coil region as seen by the thicker film on the reactor walls in this region. This is in agreement with other investigations studying the plasma polymer of tetramethyltin.[31]

By varying the electron take-off angle to 70°, surface features of the plasma polymer are enhanced. Such a study on the sample taken from the coil region revealed that there was a 'decreased' amount of tin present in the surface ($C_1:Sn_{0.20}$ *c.f.* $C_1:Sn_{0.27}$) A decrease in the tin signal on going to higher electron take-off angles could be the result of the presence of a hydrocarbon overlayer contaminant. The signal derived from the substrate through an overlayer will be attenuated. [The attenuation experienced depends strongly on the kinetic energy of the photoemitted electron; as a result of the different sampling depths for the various core levels, a larger mean free path and hence ESCA sampling depth - related to kinetic energy - will result in a smaller attenuation due to an overlayer.[37]] This decrease in the total amount of metal present when using a 70° Take-off angle compared with 35° has also been observed in the plasma polymerizations of tetramethyl germanium, and tetramethyl silane.

5.3.2 Tetramethyl Germanium (TMG)

Typical C_{1s}, O_{1s} and Ge_{3d} core level spectra from plasma polymerized tetramethyl germanium are shown in Figure 5.2. As with the plasma polymerization of tetramethyltin, absolute stoichiometries depend on sample position in the reactor. Since peak profiles remain constant, with only the relative intensities changing only the one set of core level spectra are shown.

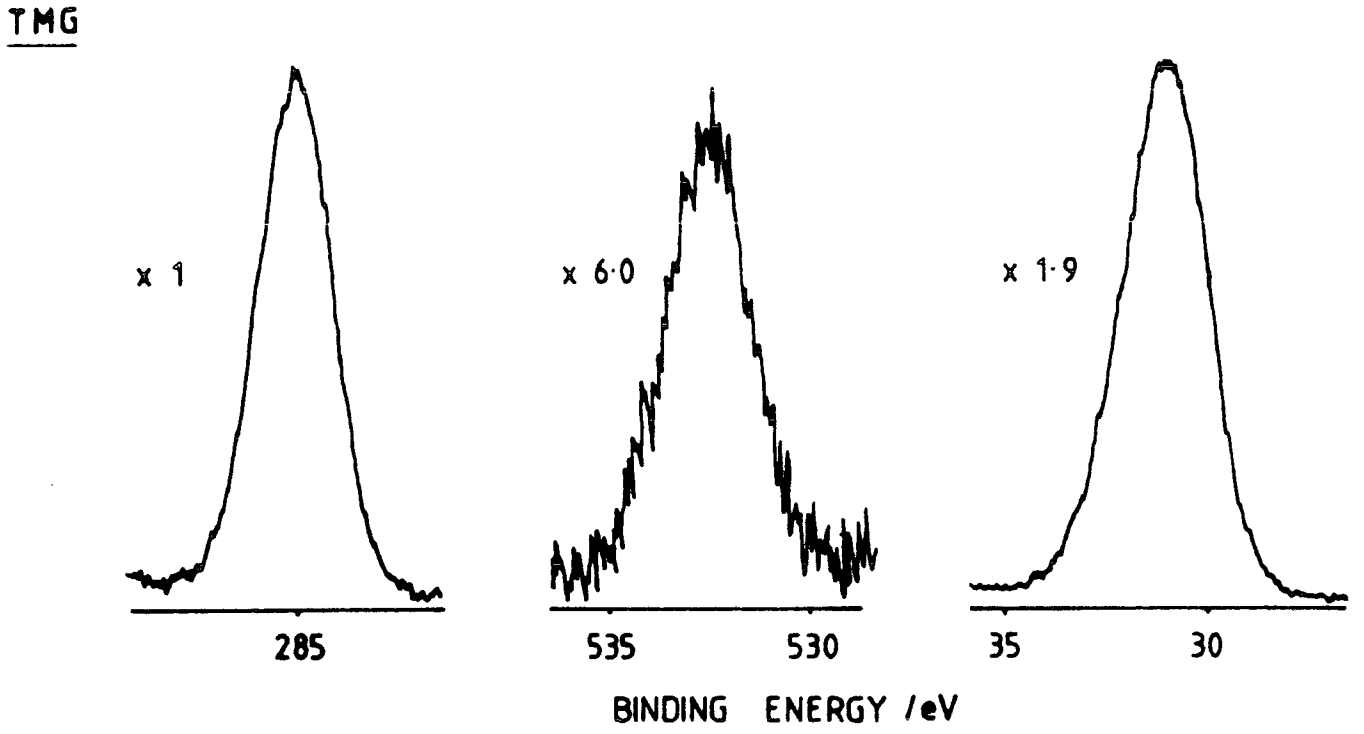

FIGURE 5.2 Typical core level spectra for plasma polymerized tetramethyl tin germanium

The C_{1s} core level consists of the one main photoionisation peak at 285.0eV due to carbon not bonded to oxygen or nitrogen, *i.e.* C-H. The sample taken from the coil region displayed a very small amount of C-O, shifted 1.8eV to higher binding energies, about 3% of the total area of the C_{1s}. This small shoulder was not visible to the eye and was only apparent on peak fitting.

The O_{1s} signal is present at a binding energy of ∿533eV. This contamination, most likely to arise from oxidation of the sample on being transferred to the spectrometer, has been discussed in greater detail in the section on tetramethyltin. The binding energy of the Ge-C bond, however, is slightly stronger than the Sn-C band by ∿40kJ mol^{-1} which gives the

Ge-C bond an energy of 318kJ mol^{-1}.[38] This difference in bond strength may be related to the amount of fragmentation of the two compounds in a plasma resulting in a greater amount of fragmented, oxidisable metal species in a TMT plasma, which would then be reflected in the oxygen content of the deposited polymer film. In fact, the O:C ratio in the TMT plasma polymer is more than a factor of two greater than that in the TMG derived polymer. However, the difference in bond energy is small and would not be expected to account for the differences observed. This would tend to suggest that there are other factors controlling the behaviour of a compound in a plasma.

As was the case with the plasma polymer from TMT, the amount of oxygen present in the film derived from TMG varied with position. Unlike the former material, the amount of oxygen incorporation was greatest in the sample taken from the coil region and showed the least amount of oxygen in the sample from the O-1cm position, see Tables 5.2 and 5.3.

The germanium to carbon stoichiometry in the plasma polymer (Ge_{3d}=30.8eV binding energy) shows the same trend as that exhibited by the organotin polymer. Namely on progressing down the length of the reactor there is a decreasing amount of metal present in the polymer film.

TABLE 5.2 Germanium to carbon and oxygen to carbon area ratios of the polymer as a function of distance in the reactor

	Position			
	O-1 cm	coil region 6-7 cm	19-20 cm	TOA
Ge_{3d}/C_{1s}	0.65	0.64	0.43	35^{o}
Ge_{3d}/C_{1s}		0.43		70^{o}
O_{1s}/C_{1s}	0.13	0.18	0.18	35^{o}

The observed germanium 3d signal actually arises from the photoionisation from two different states - $Ge_{3d_{5/2}}$ and $Ge_{3d_{3/2}}$. However, the energy separation between these two states (which arises from spin-orbit coupling) is small resulting in the appearance of an unresolved single peak.

From an analysis of the Ge_{3d} core level, Figure 5.2, two component peaks are present. The first at 30.8eV is due to metal to carbon bonds and accounts for 85.5% of the total Ge_{3d} signal. As with the tetramethyltin polymer, it is very unlikely that this peak is due to elemental metal. Although in this instance, the energy shift between metal and metal-carbon peaks is much smaller ($\sim$1.0eV), it should still be large enough to detect the presence of any germanium metal.

The higher binding energy peak, at 32.2eV, accounts for <20% of the total area. This peak is likely to be due to some form of germanium oxide (which are shifted about 1.5eV to higher binding energies from the organogermanium peak). The percentage area of this peak (of total Ge_{3d} area) shows a correlation with the amount of oxygen incorporation, *i.e.* in the coil region where maximum oxygen incorporation takes place, this higher binding energy peak is also at its greatest intensity. These values are shown in Table 5.3.

TABLE 5.3 Percentage area of high binding energy Ge_{3d} peak and metal to carbon peak area ratios as a function of distance compared with O_{1s} to C_{1s} area ratios

	Position			TOA
	0-1 cm	coil region 6-7 cm	19-20 cm	
High B.E. Ge_{3d}	17.3%	17.3%	14.5%	35°
		18.5%		70°
O_{1s}/C_{1s}	0.13	0.18	0.15	35°
Ge_{3d}/C_{1s}	0.10	0.11	0.08	35°

It is also apparent from the ratio of this high binding energy metal peak to oxygen (roughly a 1:1 ratio of metal to oxygen - Table 5.3) that there is not enough oxygen present to account for GeO_2 if the film is vertically homogeneous within the sampling depth of the metal.

It has been reported that the plasma polymerization of TMG[39] resulted in a release of germanium metal such that metal was incorporated into the growing polymer film through purely physical forces, *i.e.* the metal was held in the highly cross linked metwork. Upon exposure to atmosphere, the germanium metal present in the topmost layers of the polymer film was oxidised to germanium dioxide. The metal present in the 'bulk' of the polymer film was unaffected and remained as germanium metal.[39]

This result is not in agreement with the present data, as previously pointed out there is not enough oxygen present in the polymer film to account for metal dioxide formation. However, oxygen incorporation does seem to be associated with the amount of metal present in the polymer - Table 5.2. As already discussed with the TMT plasma polymer, the variation in metal content with distance is reflected in the change in oxygen content of the polymer, *i.e.* the film with greatest metal content also shows the greatest amount of oxygen incorporation.

From IR studies carried out on polymers derived from TMG, Inagaki *et al*[39] postulated the presence of Ge-O-Ge and Ge-O-C bonds as well as $Ge-CH_3$, Ge-H and Ge-C functionalities. (The existence of Ge-Ge groups in the polymer film could not be determined due to the limitations of the spectrometer used).

This is inconsistent with the conclusion put forward by the same author that the germanium was present as Ge in the bulk and GeO_2 at the surface. Since IR studies are not surface feature orientated, the presence of Ge-O-C bands in the IR spectrum indicates the presence of Ge-O-C groups in the bulk of the polymer film. This feature seems to have been ignored, or forgotten, by the authors when they arrived at their conclusion as to the state of the metal in the polymer film.

Since the presence of GeO_2 is ruled out by the insufficient concentration of oxygen in the film, the peak at 32.2eV cannot be due to the air oxidation of trapped elemental metal in the polymer matrix. The vertical homogeneity of the polymer sample is demonstrated to a large extent by the lack of change of intensity of the high binding energy Ge peak on going to a higher electron take-off angle - Table 5.3. However, the large sampling depth of the Ge_{3d} core level means that ESCA analysis at a 70^{o} take-off angle is not as surface sensitive as for C_{1s} and O_{1s} core level analysis.

The above data may tend to suggest that the higher binding energy peak arises from metal-oxygen-carbon functionalities present throughout the sampling depth. The present data from the C_{1s} core level does not really support this. The peak at 286.6eV is only a very small proportion of the total area of the C_{1s} spectrum ($\sim$3%). Therefore if this peak arises from Ge-O-C, this grouping cannot be a very significant feature within the plasma polymer. However, the chemical shift of the Ge-O-<u>C</u> carbon in the C_{1s} envelope may be such that it is indistinguishable from the hydrocarbon component peak. In view of the limited amount of data available, conclusive evidence about the existence of this functionality derived from

the available ESCA data, can not be put forward. From the significant contribution of the high binding energy Ge_{3d} peak to the overall intensity of the metal core level in comparison with the very low concentration of the high binding energy C_{1s} peak it is unlikely that the two are directly related.

From Table 5.2 it is apparent that the metal to carbon stoichiometry of the starting material has not been retained in all of the polymer samples. In the coil region, the amount of metal in the polymer is 30% greater than that expected from the stoichiometry of the parent monomer, and is similar to the sample taken from the 0-1 cm position. However the sample taken from the tail region of the reactor does appear to have the expected metal constant, *i.e.* 1 germanium atom for every 4 carbon atoms. Thus it can be seen that there has been carbon depletion in the plasma polymerization process resulting in the deposition of films which are mostly rich in metal compared to tetramethyl germanium. Angular dependent studies reveal that, as with the polymer from TMT, on increasing the take-off angle, the total amount of germanium present has decreased. This reduction is probably associated with the presence of a hydrocarbon overlayer which has caused an attenuation of the germanium signal.

In the ESCA studies on the plasma polymerization of TMT by Inagaki *et al*,[39] a small amount of nitrogen was found to be present in the polymer. This is not the case in the present study, as with aluminium, there were no detectable signals present in scans of the relevant core level binding energies.

The calibration method used by Inagaki *et al*[39] in their

ESCA studies is by reference to the gold 4f core level at 84.0eV. This was achieved by vacuum deposition of trace amounts of gold on to the surface of the polymer sample before analysis. However, this method of energy calibration is not to be recommended. The presence of the metal can cause differential charging of the sample surface which can lead to a broadening of the peaks and in its extreme cause two separate peaks to appear. There is also the very real fear of damage to the polymer surface when it is hit by the gold atoms, either through chemical reactions or physical sputtering.

5.3.3 Tetramethyl Silane (TMS)

Typical peak profiles of the C_{1s}, O_{1s} and Si_{2p} core levels obtained from plasma polymerized TMS are shown in Figure 5.3.

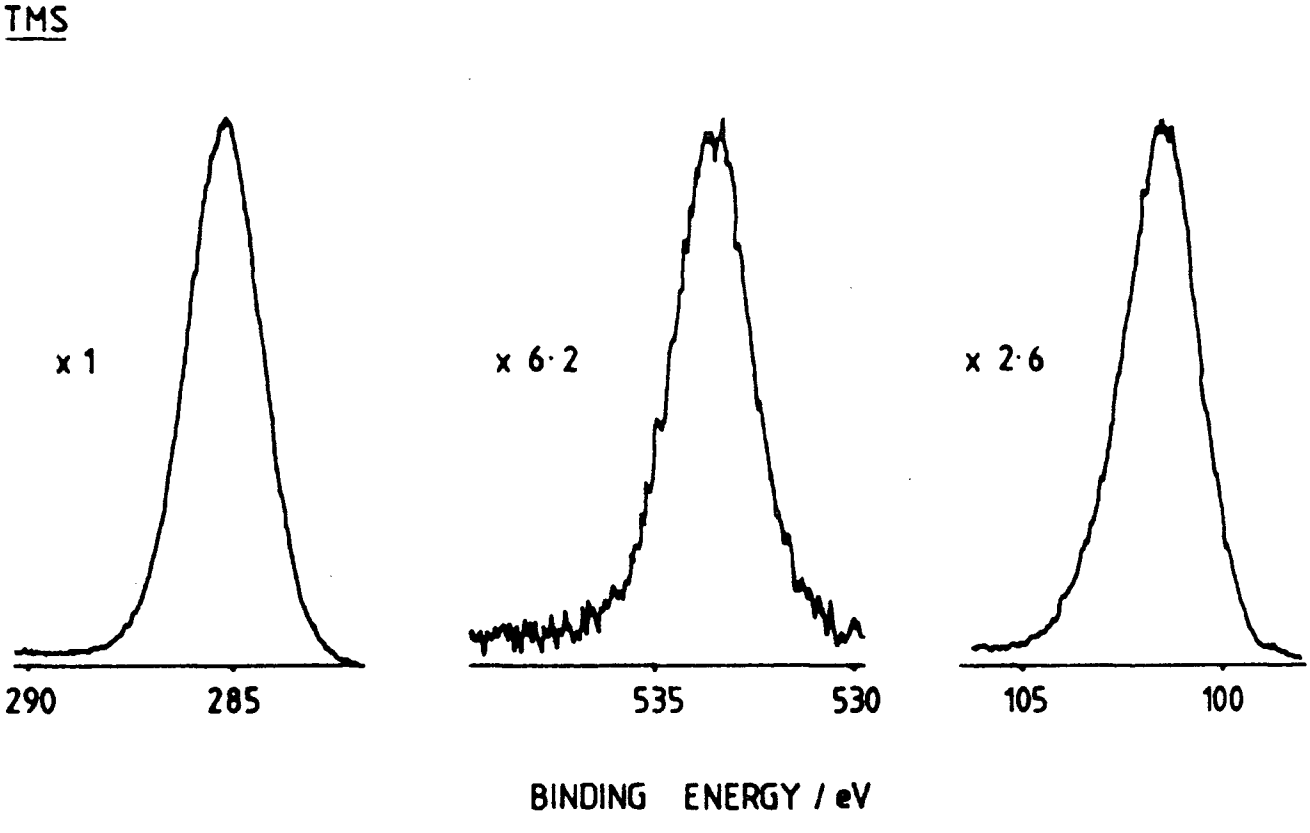

FIGURE 5.3 Typical core level spectra for plasma polymerized tetramethyl silane

As might be expected, the C_{1s} envelope consists mainly of the photoionisation peak at 285.0eV due to carbon bonded to hydrogen. There is a very small peak (∿4% of the total area of the C_{1s} envelope) at higher binding energies (∿1.8eV shifted). From a comparison of the amount of covalent silicon with the intensity of the higher binding energy C_{1s} peak it is apparent that the latter does not arise from C-Si. In fact experimental data has shown that due to the low electronegativity of silicon the chemical shift induced in the signal arising from C-Si is such that it is shifted by <1 eV from CH in the C_{1s} envelope.[40] The high binding energy C_{1s} peak can therefore be assigned to the presence of C-O functionalities.

The O_{1s} core level is at a binding energy of 533.3eV. As with the two previous compounds, TMT and TMG, the plasma polymerization of TMS results in a polymer which has slight variations in the oxygen content depending on the position of the sample. The highest oxygen content is seen in the sample taken from the coil region (Table 5.4). As with the polymer from TMG, however, oxygen incorporation is below 1 oxygen for every 10 carbons. This is not the case for the material derived from TMT, in this polymer oxygen varies between 2 to 3.5 for every 10 carbons.

As with the germanium core level, the silicon core level (at a binding energy of 101.05eV) consists of two peaks arising from the $Si_{2p_{3/2}}$ and $Si_{2p_{1/2}}$ states - whose energy separation is such that only one apparent peak appears in the spectra. The main photoionisation peak, due to Si-C (elemental silicon has a binding energy of ∿99eV), accounts

TABLE 5.4 O_{1s} to C_{1s} and Si_{2p} to C_{1s} area ratios of the polymer as a function of distance in the reactor

	Position			TOA
	coil region			
	0-1 cm	6-7 cm	19-20 cm	
O_{1s}/C_{1s}	0.13	0.17	0.15	35°
Si_{2p}/C_{1s}		0.36		70°
Si_{2p}/C_{1s}	0.43	0.40	0.39	35°

---

for 85+% of the total Si_{2p} area and a small shoulder shifted 1.5eV to higher binding energies, to 103.55eV. This corresponds to oxidised silicon. Once again, if the intensity of the higher binding energy silicon peak is compared with the amount of oxygen incorporation into the polymer, as with the polymer from TMG, there is a direct correlation between the two : An increased intensity of the Si_{2p} peak indicated an increased amount of oxygen in the plasma film. On going to a 70° Take-off angle, the intensity of the peak increases slightly (from 12-13%) demonstrating the fact that there is a greater amount of oxidation of silicon in the surface of the plasma polymer than in the bulk. The silicon to carbon stoichiometry at this higher take-off angle indicates that there is a reduced amount of silicon in the surface, see Table 5.4, this is probably due to hydrocarbon on the surface of the plasma polymer.

From Table 5.4 it is clear that the atomic ratio of the starting monomer is not retained in the plasma polymer, and that the amount of silicon varies as a function of distance in the reactor. This is in agreement with the studies carried

out on the plasma polymerization of TMT and TMG.

Deposition of the polymer from TMS, which is reported to be similar in deposition rate to that of TMT,[32] is such that after the ten minute plasma, signals from the aluminium core levels could not be detected by ESCA. Unlike the previous studies of the plasma polymer of tetramethyl silane, no nitrogen was detected in the film.

Inagaki *et al*[39] have also looked at the infrared spectrum of tetramethyl silane plasma polymer. They detected absorbtions due to $Si-CH_3$, $Si-CH_2$, Si-H, Si-O-C and Si-O-Si groups. From a comparison of this spectrum with the spectra obtained from the plasma polymers of TMT and TMG, they concluded that from the functional groups present, little major difference exists between the polymers as far as infra red can determine.[39]

5.3.4 2,2-Dimethyl Propane (DMP)

The C_{1s} and O_{1s} core levels for plasma polymerized 2,2-dimethyl propane are shown in Figure 5.4.

The C_{1s} core level is dominated by the peak due to C-H environments at 285.0eV. As with the polymer from TMS, there is a small peak (<4% total area) shifted $\sim$1.8eV to higher binding energies. This peak arises from C-O functionalities. The O_{1s} core level (533.0eV) is very small in intensity and gives a C:O stoichiometry of 1:0.03 independent of position of the sample in the reactor. This degree of oxidation is consistent with the amount of oxygen incorporation into the plasma polymers from perfluoroaromatic compounds (see Chapter Two).

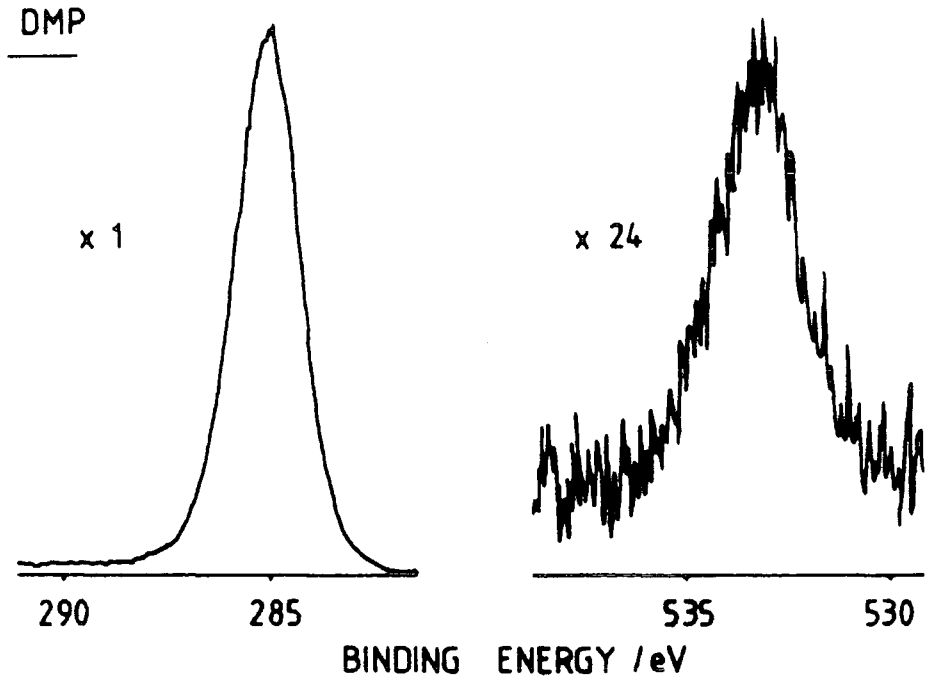

FIGURE 5.4 Typical core level spectra for plasma polymerized dimethylpropane.

Inagaki *et al*[32] has studied the photoconductivity for the polymeric films prepared from the plasma polymerization of the group IV tetramethyl compounds in a capacitively coupled 20kHz plasma. Films from DMP were not photoconductive whilst TMS, TMT and TMG all showed some photoconductivity. All four films were good insulators, the surface electrical resistance measuring 10^{14}-10^{15} Ω/cm^2 at 10^{-4} Pa.

5.3.5 Summary of the Plasma Polymerizations of the Group IV Compounds

Trends in, and similarities between, these plasma polymers are as follows:

1. Deposition rates for all four compounds was such that after a 10 minute period, the aluminium substrate was not visible to ESCA.
2. The three different sampling positions were all within the glow region.
3. The amount of Sn, Ge and Si present in the polymer varied as a function of distance in the reactor: the maximum amount was found in sample position 1, at the inlet to the reactor, whilst the minimum amount was present in the sample taken from the end of the reactor.
4. The degree of incorporation of the group IV element into its plasma polymer varied with the monomer used, and the order varied with sample position, *e.g.* in the coil region, the concentration of the group IV element in the polymer followed the trend Si>Ge>Sn.
5. Using a 70^{o} TOA, the concentration of Sn, Ge and Si present decreased compared with that revealed by a 35^{o} TOA, *i.e.* there was less of the element apparently present in the surface of the polymer film. However, this could be due to a hydrocarbon overlayer effect.
6. The amount of oxygen incorporation varied both with sample position in the reactor and also the group IV compound used. The greatest amount of oxygen incorporation was seen with TMT, TMS and TMG showed comparable amounts of oxidation whilst DMP showed only a very slight amount of oxygen contamination.

5.3.6 Copolymerization of the 'Organometallic' with Perfluorobenzene

There have already been some reports on plasma

copolymerisation[40] but as yet the characterization of the resulting materials has not received much attention. It is tempting to consider a plasma copolymer in terms of the known products arising from the individual monomers. This might certainly be the case in the plasma polymerization of more than one organic monomer when each can be polymerized independently in a plasma. If this were so, plasma co-deposition as opposed to plasma copolymerization would describe the processes occurring. Each monomer could then deposit in the plasma independently of the other, resulting in a film which was a mixture of the two products of deposition. Another example of codeposition is the simultaneous deposition of a plasma polymer and an evaporated metal. Each component can be deposited regardless of whether or not the other component is deposited. This can only be truly applied to systems where the presence of another monomer does not alter, or interfere with, the chemistry occurring which leads to the production of the polymer film.

The results in the second half of this chapter highlight the differences, which can occur when more than one organic monomer is present in the vapour phase, between the plasma copolymer and the single plasma polymer: cases of copolymerization rather than codeposition.

5.3.7 (I) Tetramethyl Tin and Perfluorobenzene

For ease of comparison, the C_{1s}, F_{1s}, O_{1s} and Sn_{3d} core level spectra of the polymer resulting from a 1:1 vapour phase mixture of TMT and PFB are shown in Figure 5.5 along with the relevant spectra for the plasma polymers from TMT and PFB respectively.

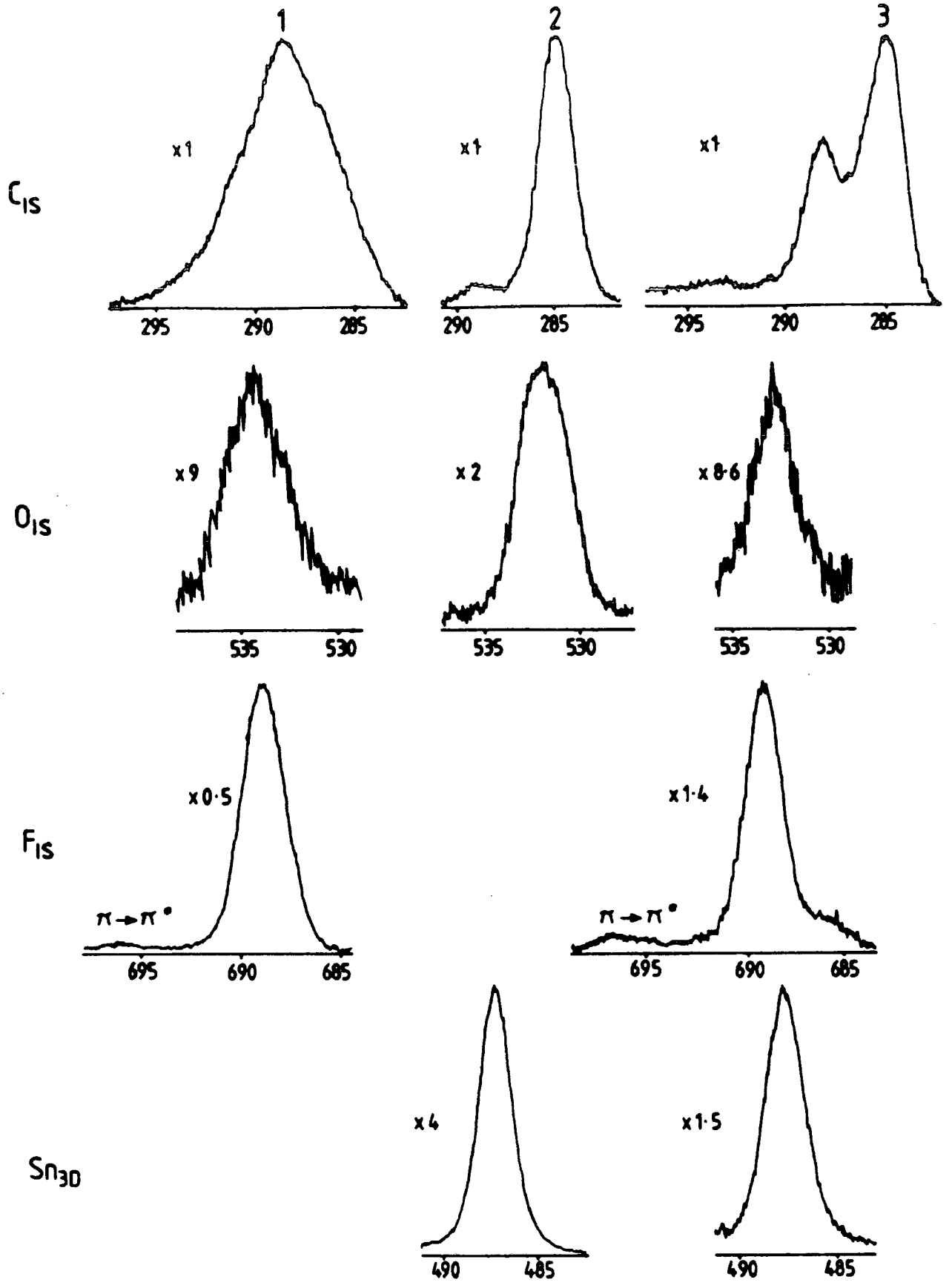

FIGURE 5.5 Core level spectra of plasma polymerized perfluorobenzene (1) tetramethyltin (2) and perfluorobenzene/tetramethyltin (3)

Considering PFB first it is evident that the broad C_{1s} envelope arises from carbon in a number of different electronic environments. Using standard peak fitting techniques a component analysis may be derived as shown in Figure 5.6.

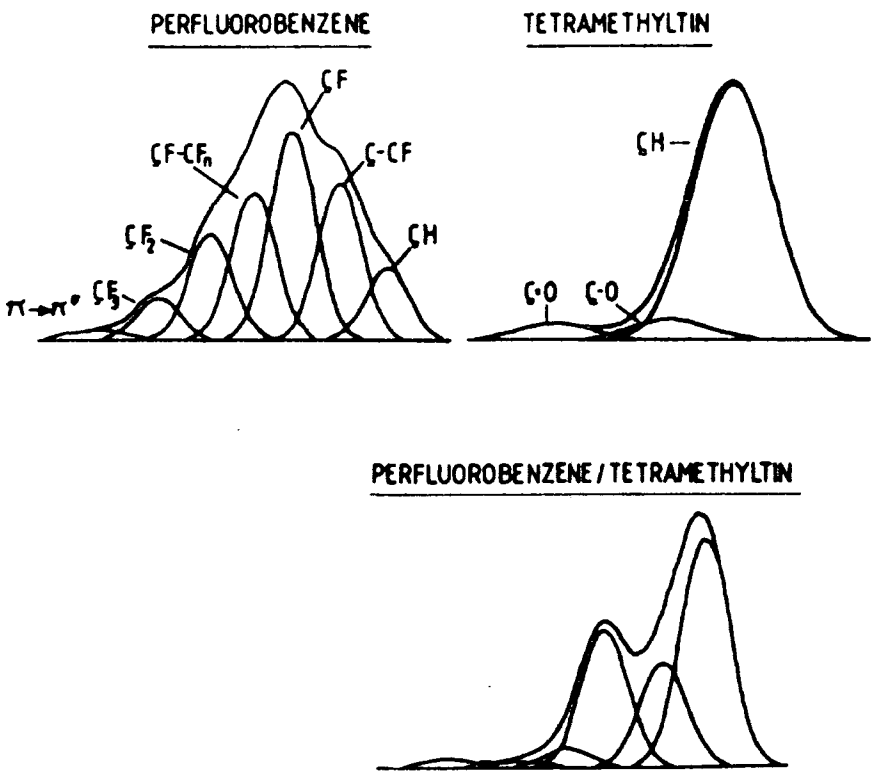

FIGURE 5.6 Component analysis of the C_{1s} core level envelopes for plasma polymerized films of perfluorobenzene, tetramethyltin and perfluorobenzene/tetramethyltin polymers

This gives rise to peaks at 285.0, 286.7, 288.5, 289.3, 291.0, 293.2 and 295.2eV due to C-H, C-CF, C-F, CF-CF_n, C-F_2, C-F_3 and $\pi \rightarrow \pi^*$ shake-up satellite environments. The hydrocarbon is in fact extraneous, as by employing variable electron take-off angle experiments it can be shown to be present only on

the surface. The cause of this hydrocarbon contamination has been discussed in greater detail in Chapter Two. The presence of C-CF, $C-F_2$ and $C-F_3$ components is indicative of extensive molecular rearrangement of the monomer in the formation of the precursors to polymerization. The $\pi \rightarrow \pi^*$ shake-up satellite is a diagnostic of the unsaturation present in the film and arises some 8eV from the component peak due to C-F, *i.e.* the unsaturation is present as =C-F. Any unsaturation present involving the hydrocarbon, which is not very likely considering the intensity and nature of the hydrocarbon, would be shifted some 7eV up from the peak at 285.0eV.[42] This would place it at around 293eV which is the peak assigned to CF_3 structural features. Thus there might be some ambiguity in the amount of CF_3 present. This situation arises in the copolymerization of an aromatic fluorine compound with its hydrocarbon analogue - see Chapter Six. It may also apply to the results discussed in the following pages but is unlikely for two reasons: firstly, the hydrocarbon in the monomer mix is not unsaturated and an appreciable quantity of unsaturation in the polymer film is therefore not expected. Secondly, the hydrocarbon associated with the perfluorobenzene homopolymer is due to overlayer contamination following deposition. From the preceding discussion it is therefore extremely unlikely that there will be unsaturation present involving hydrocarbon in the present experiments.

The presence of unsaturation is also visible in the F_{1s} core level spectrum, giving rise to a $\pi \rightarrow \pi^*$ shake-up satellite some 7-8eV removed from the main photoionisation peak at 689.3eV.[42] The C:F stoichiometry of the film is 1:1 and reveals that rearrangement and not elimination - as found in

the mono- and difluorobenzenes - reactions are important in the plasma polymerization of this compound. A low level of oxygen, evidenced by the peak at 534eV, is also present in the film. This is generally thought to be due to the reaction of any trapped free radicals in the polymer matrix reacting with oxygen upon exposure to atmosphere.[34] This has been considered in greater detail in Chapter Two. The C:O stoichiometry is such that it gives rise to a film typically with about 8 oxygens for every 100 carbons.

The C_{1s} core level of the plasma copolymer reveals some interesting differences from the corresponding envelopes for the individual films.[43] From Figure 5.6 and Table 5.6 it can be seen that the C_{1s} spectrum is dominated by two peaks at about 285.0eV and 288.3eV due to CH and CF environments respectively. The intensity of components at higher binding energy to CF arising from CF_2 and CF_3 functionalities is very low in comparison with those for perfluorobenzene, suggesting that the extent of molecular rearrangement of PFB is not as great during plasma copolymerization. This change in the C_{1s} envelope is the first indication that there has been some kind of interaction between the two vapours in the plasma, *i.e.* that this is not just plasma codeposition.

The $\pi \rightarrow \pi^*$ shake-up satellite is more intense revealing perhaps a greater retention of the PFB monomer structure in this film. This is consistent with the shake-up satellite present in the F_{1s} core level of the copolymer. However, for the copolymer the peak is more intense and more clearly defined than for PFB reflecting the greater number of C-F bonds in an unsaturated environment.[43]

Further evidence for the retention of the aromatic nature of perfluorobenzene is shown in the binding energy of the peak assigned to C-F. This has been shown to be the same binding energy as the component arising from CF-CF groups in one of the aromatic monomers - see Chapter Six.

The O_{1s} core level from the copolymer is present at 532.6eV. This is much smaller in intensity than the oxygen signal from the TMT plasma polymer. As all three films were subject to the same experimental conditions, it is evident that TMT is not readily oxidized with PFB in a 1:1 mixture of PFB+TMT. It appears that in a 1:1 mixture the TMT structure is stabilized resulting in a much lower degree of radical formation and hence a greatly reduced oxygen content similar to that of PFB.[43] As the oxygen content is so low, the contribution of C-O functionalities to the C_{1s} envelope will be negligible.

The F_{1s} core level, at 688eV, is composed of two component peaks. The lower binding energy peak shifted 2eV to lower energies is about 15% of the total intensity of the F_{1s} signal. This peak arises from a small amount of tin fluoride and is constant in all three sample positions. The main peak is due to organic fluoride. Assuming that all the $\underline{C}H$ arises from the tetramethyltin and the rest of the components arise from PFB then the C_{1s} envelopes indicate that on the whole a 1:1 incorporation of species derived from PFB and TMT into the plasma copolymer occurs. As with the single monomer of TMT, however, there is a slight dependence of position in the reactor (Table 5.5). The Sn:C stoichiometries vary from 0.12 at the inlet, 0.09 in the coil region and 0.07 at the end of the reactor, *i.e.* the starting ratio of tin to carbon in the

plasma is retained in the coil region only. Assuming that the sample is vertically homogeneous, *i.e.* the number density of tin atoms is constant throughout the sampling depth, then angular dependent studies show that there has been an accumulation of hydrocarbon on top of the polymer film during analysis.

TABLE 5.5 Tin, fluorine and oxygen to carbon area ratios as a function of distance in the reactor

	Position			TOA
	coil region			
	0-1 cm	6-7 cm	19-20 cm	
$Sn_{3d_{5/2}}/C_{1s}$	1.08	0.81	0.63	35°
$Sn_{3d_{5/2}}/C_{1s}$	0.81			70°
F_{1s}/C_{1s}	0.77	0.69	0.69	35°
F_{1s}/C_{1s}	0.52			70°
O_{1s}/C_{1s}	0.15	0.15	0.15	35°

At the higher take-off angle, the level of oxygen appears to be constant. However due to the attenuation of the oxygen signal, and O_{1s}/C_{1s} area ratio, by the hydrocarbon layer, this in reality indicates that there is a higher amount of oxygen at the surface.

The F to C stoichiometry of the copolymer indicates that some elimination of fluorine has taken place ($\sim C_1:F_{0.4}$ *c.f.* $C_1:F_{0.6}$ of the starting monomers). If the aromatic nature of the perfluorobenzene monomer is to be retained, and due to the retention, by tin, of the majority of its Sn-C bonds then the elimination of a small amount of fluorine would not be unexpected if both 'monomers' are joined together in the polymer with covalent bonds. The amount of elimination of fluorine shows a slight increase, giving a stoichiometry of

$C_1:F_{0.36}$, in the coil region and at the end of the reactor in comparison to the inlet region (Table 5.5).

The component analysis of the C_{1s} envelope of the copolymer shows little effect due to the variation of position in the reactor and a typical component peak area analysis gives rise to the following:

TABLE 5.6 Percentage area of the component peaks of the C_{1s} envelopes of the copolymer of the PFB plasma polymer

Peak Position/eV	285.0	286.5	288.2	290.0	291.5	292.5	294.0
C_{1s} TMT/PFB % area	63	12	19	3	1	1	1
C_{1s} PFB % area	-	26	29	21	17	6	1

As might be expected from the reduction in the metal signal at the higher take-off angle, there is a much greater contribution to the 285.0eV component peak at 70° consistent with the accumulation of hydrocarbon on the surface of the TMT/PFB copolymer.

It is clear from the above ESCA results that the nature of the plasma polymer derived from the 1:1 mixture of PFB and TMT cannot be straightforwardly predicted by a detailed knowledge of the structure and composition of plasma polymerized PFB and TMT respectively. Plasma copolymerization decreases the extent of molecular rearrangement of PFB and stabilizes the oxidation tendencies of TMT. Copolymerization rather than codeposition has occurred. It is also expected that the properties of the copolymer will also differ from those of the simple systems. In fact, the copolymer has already been found to have some biocidic activity.[44]

5.3.7 (II) Optical Emission from a TMT:PFB Plasma

Further evidence that there is a chemical interaction between the two monomers in the plasma is clearly demonstrated by the gas phase emission from the copolymer when it is compared with the emission from TMT and PFB plasmas respectively. Figure 5.7 gives the wide scan spectrum of the optical emission from the coplasma covering the 270-650nm region. For ease of comparison, this spectrum is then repeated in Figure 5.8 along with the emission from a TMT and a PFB plasma respectively.

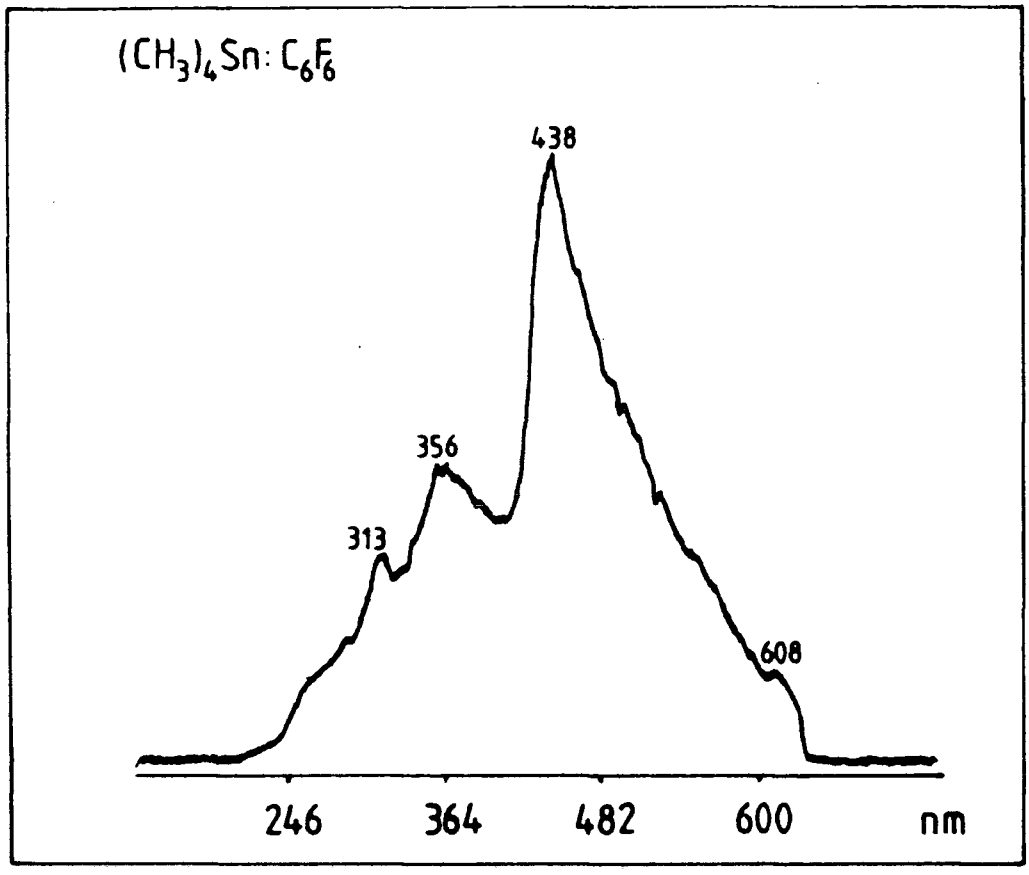

FIGURE 5.7 A wide scan of the optical emission from ~245-600nm for a perfluorobenzene/tetramethyltin plasma

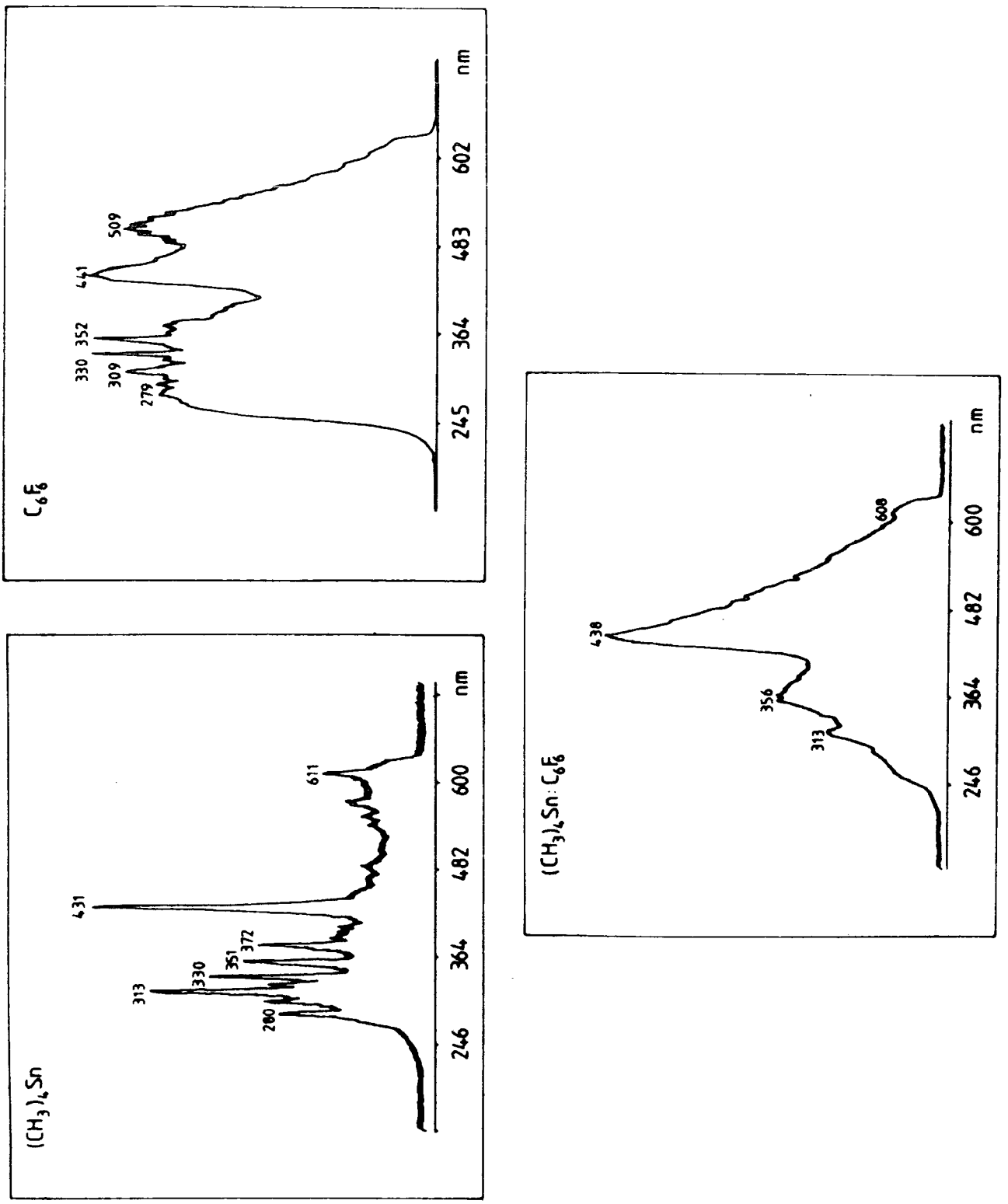

FIGURE 5.8 A comparison of the optical emission spectra from ~245-600nm for perfluorobenzene, tetramethyltin, and perfluorobenzene/tetramethyltin plasmas

Before going on to discuss the optical emission spectra, it is pertinent to draw the reader's attention to yet another fact which indicates that this deposition is a result of an interaction of the two monomers. The deposition rates of the individual monomers should, in a codeposition situation, result in a deposition rate of the coplasma which is a summation of the individual rates and the composition of the co-deposited film would reflect this. However, the deposition rate of TMT is much more rapid than PFB, as evidenced by the much shorter acquisition time allowed whilst acquiring the emission data. The time of acquisition of emission data is much less than that for the perfluorobenzene plasma due to the rapid deposition of a polymer film on the window - an equivalent acquisition time resulted in a negative spectra after background subtraction due to this film. Yet the composition of the copolymer is roughly 1:1, and thus the deposition rates of TMT and PFB have been altered during their combined polymerization.

The emission spectrum from the TMT plasma shows several dominant peaks in the 300-450nm region. The most dominant peak in the spectra occurs in the 430nm region also in this area is the emission from a radical cation of perfluorobenzene. Although peak assignment is not unambiguous it is likely that the peak arising at ∿440nm in the TMT:PFB plasma is contributed to by both a PFB radical cation and the emitting species in the TMT plasma. However this is based on assumption rather than fact. As with the most dominant peak in the 1:1 plasma, the other main peaks at ∿313 and ∿356nm correspond to emission bands in the emission spectra of both individual plasmas. Thus both of these bands could also arise from a

contribution by both of the individual emissions. However, it is also possible that although they correspond in position, these peaks in the coplasma may arise from some totally new species formed by the interaction of perfluorobenzene with tetramethyltin.

The peak at ∿280nm due to the difluorocarbene emission which is very prominent in the perfluorobenzene plasma (this is discussed more in Chapter Two) and the associated peak at 510nm, have been 'lost' in the spectrum from the 1:1 plasma

It should be pointed out here that the emission spectra are intensified over the main scan region only. The emission from the various plasmas in all three spectra is therefore likely to be present above ∿650nm, and may be present below ∿260nm.

5.3.8 Tetramethyl Germanium and Perfluorobenzene

The typical C_{1s}, F_{1s}, O_{1s} and Ge_{3d} core level spectra for a 1:1 copolymer are shown in Figure 5.9. Most evident from the C_{1s} is the fact that, as with the tetramethyl tin perfluorobenzene copolymer, the extensive rearrangement of the perfluorobenzene monomer has not taken place. This is evidence of another situation where copolymerization rather than codeposition has occurred. A component peak analysis of the C_{1s} has also been included in Figure 5.9 and the percentage area of each peak - where the sample is from the coil region - is given in Table 5.7.

From Table 5.7 it is clearly apparent that the most noticeable difference between the C_{1s} envelopes of the two polymers is the drastic reduction in the areas of the peaks

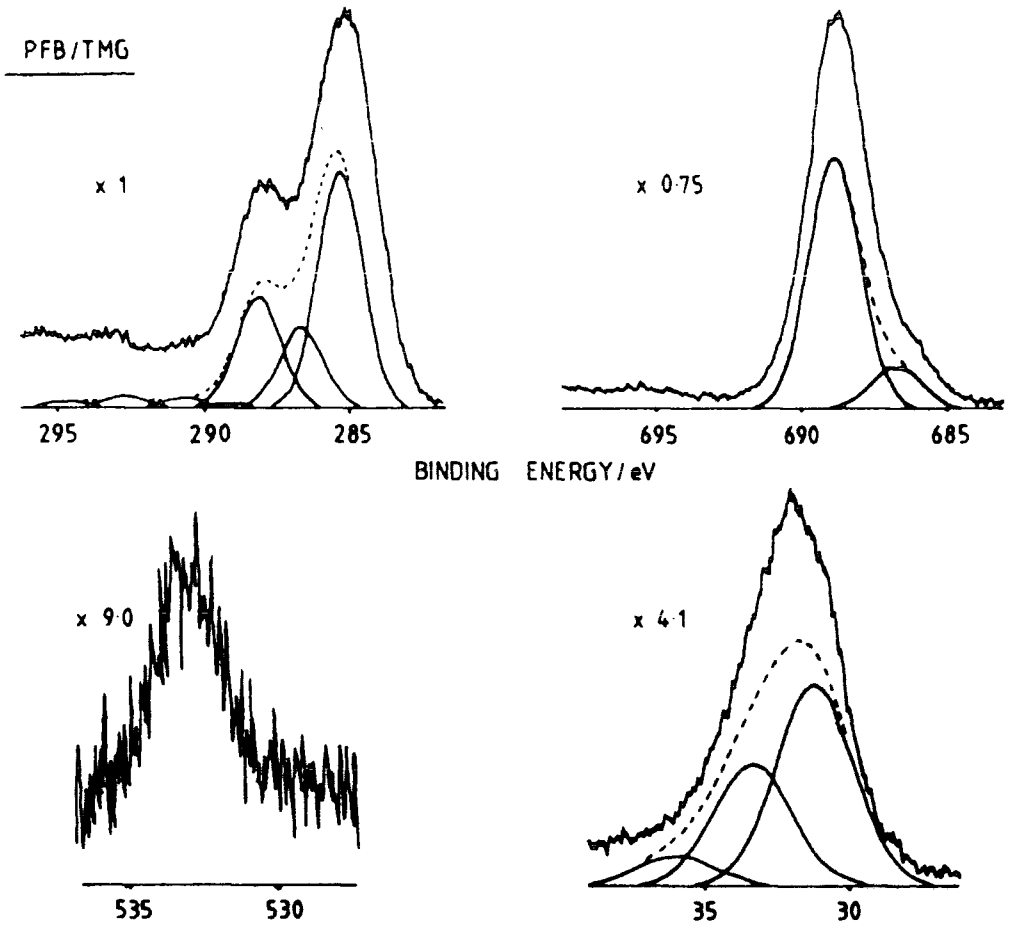

FIGURE 5.9 Core level spectra from plasma polymerized tetramethyl germanium/perfluorobenzene

TABLE 5.7 Percentage area of the component peaks of the C_{1s} of the copolymer of perfluorobenzene homopolymer

Peak position eV	285.0	286.3	288.1	289.8	291.0	293.0	295.5
C_{1s} TMG/PFB % area	48	18	24	1	3	4	2
C_{1s} PFB % area	-	25	30	21	17	6	1

---

which occur at ∿289.8eV upwards. Peak assignment of these compounds is hindered by the asymmetry of the C_{1s} envelope, *i.e.* the step in the background on going from low binding energies to the high binding energy side of the envelope,

which is very apparent. This is thought to be due to long range unsaturation present in the polymer film. The asymmetry, and the problems associated with component peak analysis are discussed in Chapters Three and Six respectively. It is unlikely that the intensities of the peaks at 291.0eV and 293.0eV arises solely from CF_2 and CF_3 functionalities - there are no resolved peaks visible in the spectrum in this energy region, just a very large step function. However, to obtain the C:F stoichiometry of 1:0.37 (from peak area ratios) some of these functionalities must exist if peak assignment is correct.

The F_{1s} core level is composed of two peaks. The main peak at 689eV is due to covalent C-F, the shoulder at lower binding energies is due to F-Ge. The area of this peak is about 14% of the total F_{1s} area and shows little variation with position. This is consistent with the behaviour shown in the F_{1s} core level from the TMT/PFB copolymer. Unlike the previous polymer, the F_{1s} does not exhibit a clearly defined $\pi \rightarrow \pi^*$ shake-up satellite in the TMG/PFB copolymer but a distinct asymmetry of the F_{1s} peak does exist. This is the first real example of an asymmetry appearing in the F_{1s} core level from all the plasma polymers described in this thesis.

Elimination of fluorine has taken place during copolymerization ($C_1:F_{0.37}$ *c.f.* $C_1:F_{0.5}$ monomer mix), the extent of elimination increasing with distance along the reactor. This mirrors the situation in the copolymerization of TMT and PFB.[43]

The Ge_{3d} is made up of three component peaks, Figure 5.9. These appear at 31.4, 33.25, and 35.2eV binding energies respectively. The first peak coincides with the position due to Ge-C bonds whilst the second is likely to be due to

germanium oxide. As with the homopolymer there is not enough oxygen present for the metal to be present as GeO_2. The stoichiometry of this middle peak in the germanium envelope gives rise to $O_{0.4}:Ge_{0.6}$. However, the existence of Ge-O-C bonds has previously been noted and the formation of GeO is possible. On going to a higher take-off angle the intensity of the 33.25eV peak shows a small increase as does the amount of oxygen, thus indicating that the surface is slightly more oxidised than the bulk. The third peak in the germanium envelope, which accounts for about 9% of the total area is due to germanium fluoride. The ratio of the high binding energy peak to the high binding energy peak of the F_{1s} core level gives rise to a stoichiometry of $Ge_1:F_4$.

The O_{1s} core level appears at 533.1eV, and constitutes a very broad gaussian peak, due to the numerous slightly different electronic environments. However, the chemical shifts are such that individual peaks cannot be picked out. The $C_1:O_{0.04}$ stoichiometry is halved from that in the homopolymer ($C_1:O_{0.01}$), and thus it appears that the 1:1 copolymerization of TMG and PFB has caused a reduction in the amount of oxidation of the polymer film which is comparable with the behaviour of the TMT/PFB copolymer.[43]

As with the TMT/PFB copolymer, the amount of metal deposited depends on the position of the substrate in the reactor. The greatest amount of metal is seen in the sample from the 0-1cm position, giving rise to a stoichiometry of $C_1:Ge_{0.14}$, assuming the sample to be vertically homogeneous, whilst the smallest amount of germanium $C_1:Ge_{0.07}$ is seen in the sample position furthest from the coil. The vertical

homogeneity is suggested by the close comparison of the Ge:C stoichiometries obtained by using both a 35 and 70° take-off angle. The elemental peak area ratios are shown in Table 5.8.

TABLE 5.8 Germanium, fluorine and oxygen to carbon area ratios as a function of distance in the reactor

	Position			TOA
	coil region			
	0-1 cm	6-7 cm	19-20 cm	
Ge_{3d}/C_{1s}	0.26	0.19	0.14	35°
Ge_{3d}/C_{1s}	0.21			70°
F_{1s}/C_{1s}	1.02	0.69	0.58	35°
G_{1s}/C_{1s}	0.79			70°
O_{1s}/C_{1s}	0.07	0.13*	0.13*	35°

* NOTE: These two samples were not analysed until two weeks after deposition. Although they were kept under an inert atmosphere, the amount of oxidation may be a reflection on the length of time before analysis rather than of the sample position in the reactor.

From Table 5.8, two main facts are evident:

1. On the whole the starting ratio of the monomer mix, as determined by the metal content, has been retained in the polymer films deposited in all three sample positions, *i.e.* the germanium content is close to 1 atom of metal for every 10 carbon atoms. (The concentration of metal in the polymer film deposited at the inlet is slightly higher and the film deposited at the end of the reactor is slightly lower, the actual stoichiometries have been previously given). From this it would seem that as with the TMT/PFB copolymer, the metal composition of the TMG/PFB copolymer is a reflection of the

gas phase composition, *i.e.* a 1:1 incorporation of the two comonomers has taken place.

2. The fluorine to carbon ratio also seems to show positional variation. There has been some elimination of fluorine, this is more marked in the coil and tail glow regions, than at the inlet of the reactor where the C:F stoichiometry is 1:0.53 which is close to the F:C stoichiometry of the starting vapour phase. The elimination of a small amount of fluorine may be expected if the aromatic structure of the monomer is to be retained and covalently bonded within the polymer structure.

As with the TMT/PFB copolymer, the rate of deposition is such that there is no Al_{2p} signal visible in the ESCA core level scan after the 10 minute deposition period. There is also no signal due to nitrogen.

5.3.9 Tetramethyl Silane/Perfluorobenzene and 2,2-Dimethyl Propane/Perfluorobenzene

Both of these copolymers do not show evidence for the inhibition of the rearrangement of the perfluorobenzene nucleus and as such will be discussed together.

Typical core level scans for the two copolymers are shown in Figure 5.10. Both C_{1s} core level spectra look similar to an 'expected' envelope shape, *i.e.* the addition of more C-H intensity to the C_{1s} envelope of perfluorobenzene (Table 5.9). As such both of these copolymers could be examples of codeposition rather than copolymerization.

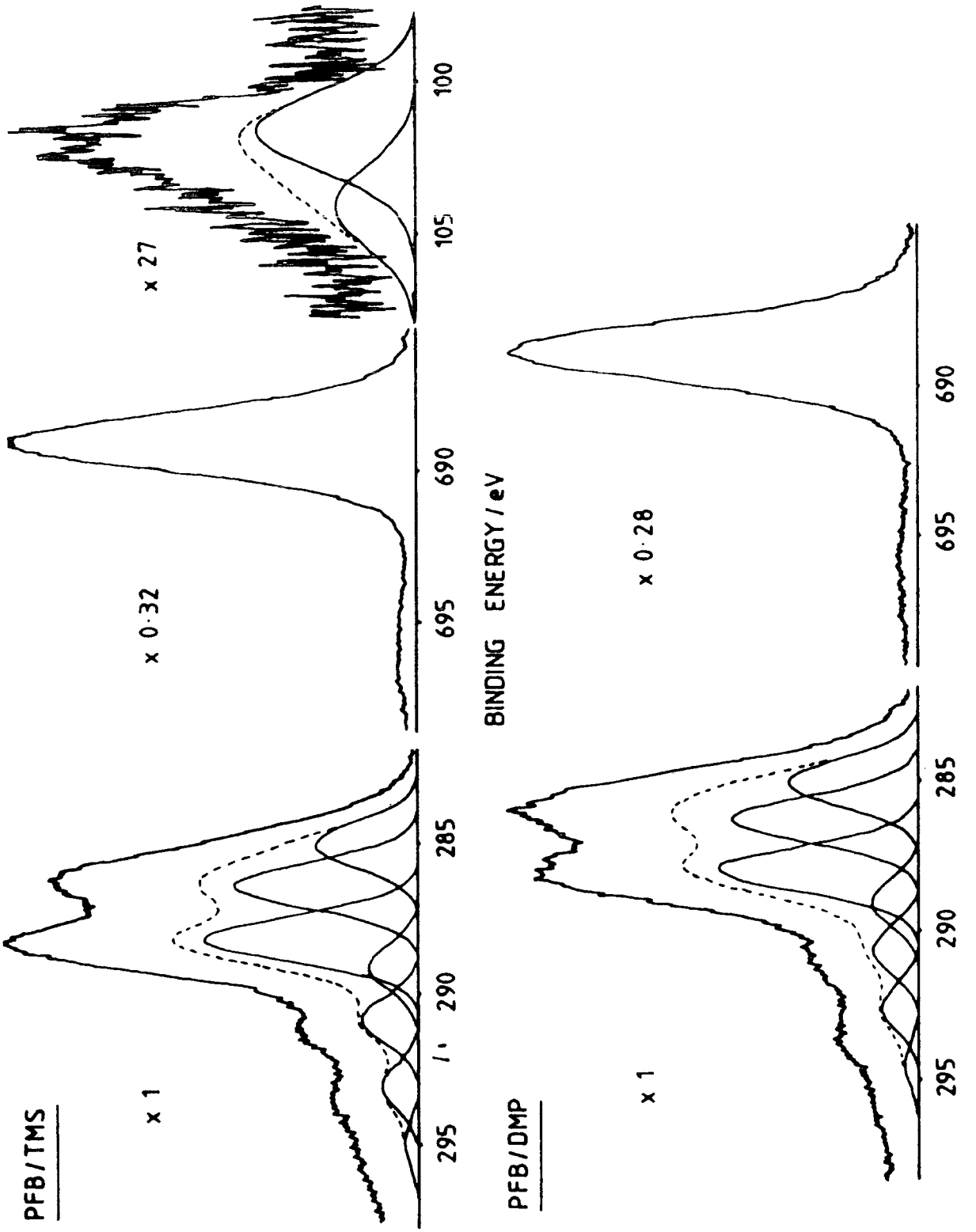

FIGURE 5.10 Core level spectra from plasma polymerized tetramethyl silane/perfluorobenzene and dimethylpropane/perfluorobenzene

TABLE 5.9 Percentage composition of the components of the C_{1s} envelopes of TMS/PFB and DMP/PFB copolymers and PFB homopolymer

Peak position eV	285.0	286.4	288.2	289.2	291.1	293.4	295.6
C_{1s} TMS/PFB	25	25	29	7	8	5	1
C_{1s} DMP/PFB	23	26	30	6	7	6	2
C_{1s} PFB (uncorrected for C-H)	10	23	29	15	14	7	2

A closer look at the percentage areas of the component peaks in Table 5.9 show, however, that there has been some effect on the contribution to the C_{1s} envelope from perfluorobenzene in both copolymer films. The amount of $CF\text{-}CF_n$ and CF_2 component peaks are reduced to less than half their original value in the PFB homopolymer. This is in contrast to the amount of CF_3 and $\pi \rightarrow \pi^*$ shake-up intensity which appears to be more or less constant in all three of the polymer films.

The amount of oxygen present (BE=533eV) in both films is very low and the $C_1:O_{0.03}$ stoichiometry is that expected in the plasma polymerization of perfluorocarbons.[33] There is very little variation in the amount of oxygen incorporation as a function of distance. In fact, all of the group IV compounds when copolymerized with PFB in a 1:1 mix show very little variation in the amount of oxidation with position.

The F_{1s} signals (BE=689eV) are very intense and both show a $\pi \rightarrow \pi^*$ shake-up satellite. The typical stoichiometry of $C_1:F_{0.7}$ shows that far from elimination of fluorine, there is in fact, an enhancement of the amount of fluorine present.

Unlike the TMT/PFB and TMG/PFB copolymers, the amount of fluorine increases as a function of distance in the reactor in the TMS/PFB and DMP/PFB copolymers (Table 5.10). This increase in fluorine as a function of distance has been shown to occur in the plasma polymerization of perfluorobenzene.

TABLE 5.10 Silicon, fluorine and oxygen to carbon peak area ratios as a function of position in the reactor for TMS/PFB and DMP/PFB copolymers

		Position			
Copolymer	Area Ratios	0-1cm	6-7 cm	19-20 cm	TOA
TMS/PFB	Si_{2p}/C_{1s}	0.017	0.019	0.015	35°
	Si_{2p}/C_{1s}	0.018			70°
	F_{1s}/C_{1s}	1.42	1.40	1.46	35°
	F_{1s}/C_{1s}	1.26			70°
	O_{1s}/C_{1s}	0.05			35°
DMP/PFB	F_{1s}/C_{1s}	1.25	1.31	1.38	35°
	F_{1s}/C_{1s}	1.27			70°
	O_{1s}/C_{1s}	0.036	0.036	0.05	35°

The amount of silicon in the copolymer is almost non-existent giving a $C_1:Si_{0.017}$ stoichiometry compared with $C_1:Si_{0.42}$ in the homopolymer. At first sight this might appear to be due to the formation of SiF_4, a volatile compound which is lost in the exhaust gases of the reactor. This reaction of fluorine radicals with silicon

$$4F\cdot + Si \longrightarrow SiF_4$$

is a well known reaction[45] and used in the plasma etching of silicon in the microelectronics industry.[46] The selective

attack of Si by fluorine atoms is shown by the retardation of the etching of SiO_2 in the presence of exposed silicon, whilst the silicon etches faster than normal.[45]

However the 'greater than expected' fluorine to carbon ratio in the polymer film does not tend to back up this supposition. This indicates two possibilities -

(a) The starting ratio of the plasma feed was not 1:1 but rich in perfluorobenzene. This is possible but in view of the excess perfluorobenzene needed to account for the loss of all the silicon is exceedingly unlikely.

2. The second, and most probable cause of the lack of silicon in the plasma polymer is the inhibition of the deposition of the tetramethyl silane by the presence of perfluorobenzene. There has been some exchange in the plasma as evidenced by the slightly increased amount of hydrocarbon in the C_{1s} core level spectra and a decreased amount of fluorine as evidenced by the reduction in the CF_2 and CF-CF component peaks. The F:C ratios can be viewed as resulting from the elimination of fluorine from the perfluorobenzene monomer to give a stoichiometry of $C_1:F_{0.7}$ (*c.f.* a theoretical value of 1:1), with most of the tetramethyl silane being lost as volatile 'products' along with a certain amount of SiF_4 accounting for some of the eliminated fluorine.

The composition of the DMP/PFB copolymer may be similarly explained by the behaviour of the dimethyl propane monomer in the plasma, *i.e.* as with the TMS/PFB plasma copolymerization, the extent of incorporation of the DMP monomer into the copolymer could be limited due to the inhibition of the fragmentation of the DMP by the presence of PFB in the plasma.

This is based solely on the very small increase in the hydrocarbon component of the C_{1s} envelope. It is extremely unlikely that the fragments from DMP have become completely fluorinated in the plasma leading to the incorporation of mainly fluorinated species into the polymer which would account for the low level of hydrocarbon. This argument also applies to the copolymerization of TMS/PFB.

Due to the lack of independent information derived from the core level of the group IV element in the DMP/PFB copolymer - the group IV element is carbon which is present in all organic polymer films - the fate of the central carbon atom in the dimethyl propane monomer cannot be determined. From the carbon to fluorine stoichiometry, (which apart from the O:C stoichiometry is the only information available from which to derive knowledge of the behaviour of the two comonomers in the plasma leading to polymer deposition), if both monomers are incorporated, then the amount of fluorine in the polymer films is greater than would be expected, *i.e.* $C_1:F_{0.65}$-$C_1:F_{0.72}$ compared with a theoretical value of $C_1:F_{0.55}$ However, if mainly only perfluorobenzene has been incorporated into the polymer films, then the C:F stoichiometries reveal that compared with the theoretical value of 1:1 fluorine elimination has taken place from the perfluorobenzene monomer. This is in agreement with the evidence presented in the C_{1s} envelope, *i.e.* there is a reduction in the amount of CF-CF and CF_2 functionalities compared with the polymer derived from pure perfluorobenzene.

5.4 Summary of the Plasma Copolymerization of the Group IV Compounds with Perfluorobenzene

1. The copolymerization of TMT and TMG with PFB, results in a large stabilisation of the oxidation tendency of the metal and a decrease in the extent of molecular rearrangement of PFB.

2. The copolymerization of TMS and DMP with PFB, although not inhibiting the rearrangement of PFB result in polymer films which have only $\sim^{1}/_{3}$ of the amount of $CF\text{-}CF_n$ and CF_2.

3. The amount of the group IV element deposited in the copolymer depends on the nature of the element:

(a) Both TMT/PFB and TMG/PFB plasma copolymerizations result in films which show essentially retention of the atomic ratio of the feed vapour as demonstrated by the amount of metal incorporation into the polymer film to give films with approximately 1 metal atom to every 10 carbon atoms.

(b) TMS/PFB results in virtually no incorporation of silicon into the polymer film.

(c) DMP/PFB gives rise to films whose composition, as determined from the C_{1s} envelope, is different from that produced by pure perfluorobenzene.

4. The amount of the group IV element in the plasma polymer also shows a variation with the position of the substrate in the reactor. Generally, the most amount of incorporation found at the inlet whilst the least incorporation takes place at the end of the reactor.

5. The amount of fluorine in the copolymer films depends both on the nature of the group IV compound, *i.e.* metal or

non metal and the position of deposition:

(a) In both TMT/PFB and TMG/PFB copolymerizations, there has been a certain amount of fluorine elimination occurring in the deposition processes such that the copolymer has a reduced amount of fluorine (*c.f.* the gas phase composition). The amount of fluorine incorporation also shows a decrease on going down the reactor, *i.e.* the highest amount of fluorine is seen in the sample deposited in position 1.

(b) As a contrast to the above behaviour, the copolymerization of TMS/PFB and DMP/PFB results in a higher than expected fluorine content of the copolymer which increases with distance along the reactor.

6. The amount of oxygen in the copolymers derived from TMT/PFB, TMG/PFB and TMS/PFB mixes is greatly reduced compared with that in the TMT, TMG and TMS homopolymers.

7. As far as the composition of the fluorinated C_{1s} envelope is concerned, the major indication of copolymerization of PFB with one of the group IV tetramethyl compounds is in the greatly reduced amount of $CF\text{-}CF_n$ and CF_2 functional groups.

REFERENCES - Chapter Five

1. See Chapter 4, refs. 5-8.

1b. A. Bradley and J.P. Hammes, J.Electrochem.Soc., 110, 15 (1963).

2. A. Akelah and D.C. Sherrington, Polymer, 24, 1369 (1983).

3. A. Bradley, Trans. Faraday Soc. 773 (1965).

4. S. Morita *et al*, Symp.Proc.Int.Symp.Plasma Chem. 5th, 259 (1981).

5. Hitachi Ltd., Jpn. Patent 58 66,938 (1983).

6. G. Brewer, Proc. 4th Int.Conf. on E and Ion Beam Sci. Technol., R. Bakish (Ed.), Electrochem.Soc., Princeton, N.J. (1970).

7. J.P. Ballantyne, J.Vac.Sci.Technol. 12(6), 1257 (1975).

8. M.J. Bowden, Solid State Technol., 24(6), 73 (1981).

9. M.J. Bowden, CRC Critical Reviews in Solid State and Materials Sciences, 8(3), 223 (1979).

10. S. Morita *et al*, Proc.Int.Conf.Vac.Metall. 7th, 1, 262 (1982).

11. T. Tamamura, S. Imamura and S. Sugarwara, J.Electrochem. Soc., 131(5), 1122 (1985).

12. L. Martinu and H. Biederman, Vacuum, 33(5) , 253 (1983).

13. M. Hatzakis, J. Electrochem.Soc., 116, 1033 (1969).

14. A.N. Broers, J.Electrochem.Soc., 128, 166 (1981).

15. T. Tamamura and S. Sugawara, 'Semiconductor Technology', J. Nishizawa (Ed.), OHM-North-Holland, Tokyo, (1982),Chap.10.

16. L. Martinu and H. Biederman, Vacuum, 33(5), 253 (1983).

17. M. Yamada, J. Tamano, K. Yoneda, S. Morita and S. Hatton, Jpn.J.Appl.Phys., 1, 21(5), 768 (1982).

18. S.M. Irving, Kodak Photoresist Seminar, 2, 26 (1968).

19. H. Hughes, W.L. Hunter and K. Ritchie, J.Electrochem.Soc., 120, 99 (1973).

20. D.J. Webb and M. Hatzakis, J.Vac.Sci.Technol. 16(16), 2,008 (1979).

21. R.H.Chandler; J.Chandler, 'Fungicides, Preservatives and Antifouling Agents for Paints', Bibliog.Paint Technol.No.29, R.G. Chandler Ltd., Braintree (1977).

21b. D. Lanigan, in 'Proc.Int.Conf. on PVC Process', Plastics and Rubber Institute, London (1978).

22. Comprehensive Organometallic Chem., Vol.2, G. Wilkinson; F.G.A. Stone (Eds.), Pergamon Press, Oxford (1982), p.519.

23. G. Ayrey, B.C. Head and R.C. Poller, Macromol.Rev.8,1 (1974).

24. C.J. Evans and P.J. Smith, J.Oil Col.Chem.Assoc., 58, 160 (1975).

25. S. King, Tin its uses, 1217 (1979).

26. H.J.M. Bowen, Trace Elements in Biochem., Academic Press, N.Y. (1966).

27. R.V. Subramanian and B.K. Garg, Polym.-Plast.Technol. 11, 81 (1978).

28. J. Kowalaski, W. Stanczyk and J. Chojnowski, Rev.Silicon, Germanium, Tin and Lead Compds., 6(4), 225 (1982).

29. See ref. 22 p.333-359.

30. N. Inagaki and M. Mitsuuchi, J.Polym.Sci.,Polym.Lett.Ed., 22, 301(1984).

31a. E. Kny, L.L. Levenson and W.J. James, J.Vac.Sci.Technol., 16(2), 359 (1979).

31b. E. Kny, L.L. Levenson, W.J. James and R.A. Auerbach, Thin Solid Films, 85, 23 (1981).

31c. E. Kny, L.L. Levenson, W.J. James, R.A. Auerbach, *ibid*, 64(3), 395, (1979).

31d. R.K. Sadhir, W.J. James and R.A. Auerbach, Thin Solid Films, 97(1), 17 (1982).

31e. R.K. Sadhir and W.J. James, ACS Symp.Ser., 242, 533 (1984).

31f. E. Kny, L.L. Levenson, W.J. James and R.A. Auerbach, J.Phys.Chem., 84, 1635, (1980).

31g. R.K. Sadhir, H.E. Saunders, and W.J. James, Org.Coat.Appl. Polym.Sci.Proc., 48, 673 (1983).

32. N. Inagaki, T. Yagi and K. Katsuura, Eur.Polym.J., 18, 621 (1982).

33a. D.T.Clark,and D. Shuttleworth, J.Polym.Sci.,Polym.Chem.Ed., 18, 27 (1980).

33b. H.S. Munro and C. Till, J.Polym.Sci.,Polym.Chem.Ed., 23(6), 1621 (1985).

33c. H.S. Munro and C. Till, J.Polym.Sci., Polym.Chem.Ed., 24,179 (1986).

34. H.K. Yasuda, 'Plasma Polymerization', Academic Press, London, (1985).

35. A.K. Sawyer, Organotin Compounds, Vol.3, Dekker,N.Y.(1972).

36. C.D. Wagner, L.E. Davis, J.F. Moulder, W.M. Riggs and G.E. Muilenberg (Eds.), Handbook of X-ray Photoelectron Spectroscopy, Perkin-Elmer, Eden Praire, MN. (1979).

37. See Chapter 2, Section 2.3.1.

38. R.A. Jackson, J. Organomet.Chem., 166, 17 (1979).

39. N. Inagaki and M. Mitsuuchi, J.Polym.Sci.,Polym.Chem.Ed., 21, 2887 (1983).

40. H.R. Thomas, Ph.D. Thesis, Durham University, U.K. (1977).

41a. A.M. Wrobel and M. Kryszewski, J. Macromol.Sci.,Chem. A12(7), 1041 (1978).

41b. H. Yasuda, H.C. Marsh and J. Tsai, J.Appl.Polym.Sci., 19(8), 2157 (1975).

41c. A.B. Gilman and V.M. Kolotrykin, Khin Vys,Energ. 12(5), 456 (1978).

42. D.T. Clark and D.B. Adams, Theoret.Chim.Acta (Berl.), 39, 321 (1975).

43. H.S. Munro and C. Till, Thin Solid Films, 131, 255 (1985).

44. H. Grunwald, H.S. Munro, H. Suhr and C. Till, Ger.Patent Appl. 35, 22, 718.2.

45. R.W. Kirk in 'Techniques and Applications of Plasma Chemistry', J.R. Hollahan, A.T. Bell (Eds.), Wiley -Inter-Science, N.Y. (1974).

46. H. Abe, Y. Sonobe and T. Enomote, Jpn.J.Appl.Phys. 12, 154 (1973).

CHAPTER SIX

THE PLASMA COPOLYMERIZATION OF A FLUOROCARBON WITH A HYDROCARBON

6.1 Introduction

There have been no ESCA studies, to date, reported in the literature on the composition of plasma polymers derived from mixtures of fluorocarbons and hydrocarbons. If each monomer is polymerizable in its own right then either co-deposition or copolymerization may result depending on whether there is an interaction between the two systems during polymer formation. As an example, the polymer produced from a 1:1 tetramethyltin/perfluorobenzene[1] combination is a true co-polymer. The tetramethyltin inhibited the extensive molecular rearrangement of the perfluorobenzene nucleus whilst the oxidative tendencies of the tin in the homo plasma polymer were greatly reduced by the presence of the perfluoro-aromatic in the copolymer.

To gain an understanding of the different behaviours shown by fluorocarbon and hydrocarbon based plasmas, Yasuda *et al*[2] has conducted a study on a comparison of the plasma polymerization behaviour of hydrocarbons with their analogous perfluorocarbons under closed system conditions. Each monomer was polymerized independently, although subject to the same experimental conditions of position, length of deposition, *etc.*, and in almost all cases polymer formation was slower in the perfluorocarbon plasmas. However, a knowledge of the independent behaviour of the two monomers in a plasma cannot be used necessarily to predict the behaviour of each in a situation where both monomers are present. In the case of the material derived from tetramethyltin and perfluorobenzene,[1] the structure and composition of the copolymer could not have been determined by a prior knowledge of the composition of each of the individually plasma polymerized monomers.

Although the literature contains very few reports on copolymer composition, several authors have examined the deposition rate of copolymer systems. Bell *et al*[3] studied the deposition rate of tetrafluoroethylene/ethylene polymers produced by varying the composition of each monomer in the plasma. They reported that the deposition rate of the copolymer could not be explained by simply summing the separate deposition rates obtained for each monomer. It was suggested that a synergistic effect, on deposition rate, existed between the two compounds.

Similarly, Inagaki *et al*[4] noted that the rate of copolymer formation reached a maximum at a 1:1 molar ratio of methane and tetrafluoromethane. As an indication that the fluorocarbon component was being incorporated into the growing plasma polymer, the surface energy of the copolymer film was reported to decrease as the fluoromethane content in the gas phase increased. This increase in deposition rate has also been noticed in the 1:1 plasma polymerization of cyclohexane and perfluorodimethylcyclohexane,[5] in the production of dielectric layers.

Copolymerization can be used to form polymeric films containing systems which independently would not deposit; such an example is seen in the plasma copolymerization of methane and tetrafluoromethane.[4] CF_4 in a pure gas plasma does not give rise to a plasma polymer, but is in fact a very good etchant due to the large amount of reactive fluorine produced in the plasma.[6] However, in the presence of the hydrocarbon polymer formation occurs.[4] This etching behaviour of fluorine can be used to advantage in the incorporation of metals into the plasma polymer.[7] In the presence

of a perfluoropropane plasma and molybdenum metal volatile fluorides are formed by chemical etching of the metal which are then incorporated into the growing polymer film. Kay[8] has demonstrated that the main effect of CF_4 plasmas can also be shifted from etching to polymer forming by the addition of hydrogen into the plasma: the balance between these two processes being controlled by the amount of hydrogen added to the perfluoromethane. This change of character of the coplasma from ablative to non-ablative is achieved by the scavenging action of hydrogen which reacts with the ablative fluorine to form hydrogen fluoride.

There are several examples to be found in the patent literature on copolymerization.[9,a-d] An organic photo-conductor film with increased sensitivity in the near IR region was obtained by mixing a halogen containing compound with an organic hydrocarbon.[9a] A laser beam recording material has been produced by the copolymerization of carbon disulphide with an organic monomer such as styrene, with the simultaneous evaporation of a metal, onto a glass or polyester support.[9b] Similarly, polymer membranes were formed by the plasma copolymerization of an arene monomer vapour and carbon disulphide.[9c]

The copolymerization of hydrocarbons and halogenated hydrocarbons has resulted in the production of a positive radiation resist coating.[9d] This polymerization was carried out in the presence of a non polymerizable gas such as ammonia, carbon dioxide or sulphur dioxide which was said to improve the adhesion of the resist layers to the support. A positive resist for vacuum lithography has also been formed

by the copolymerization of methyl methacrylate and hexafluorobutyl styrene to form an electron beam resist with increased sensitivity.[10]

As a novel application of plasma polymerized films, acrylonitrile, styrene, polymethylmethacrylate or combinations of 1:1 mixtures have been polymerized onto packing used for gas-liquid chromatography columns.[11] The effectiveness of these polymer coated supports was increased in comparison with the same packing material before coating.

Like the general scientific literature, the patent literature also suffers from an almost complete lack of plasma copolymer characterization as evidenced by the lack of information given on the products in all of the previously cited examples.

Following the results on the copolymerization of perfluorobenzene and the group IV tetramethyl compounds,[12] the behaviour of mixtures of fluorocarbon compounds with hydrocarbons was investigated. The first half of this chapter discusses the results of an investigation into copolymerization of a perfluoroaromatic with the analogous hydrocarbon and reports the structure and bonding in the resultant films as determined by ESCA; of benzene/perfluorobenzene, naphthalene/octafluoronaphthalene, and biphenyl/decafluorobiphenyl under a variety of conditions. The structural composition of a polymer produced by the copolymerization of two perfluoroaromatic monomers, perfluorobenzene and octafluoronaphthalene, is also examined. The behaviour on copolymerizing an aromatic fluorocarbon or hydrocarbon with a series of six-membered ring compounds (hydrocarbon or fluorocarbon respectively)

containing an increasing amount of unsaturation is discussed in the latter part of this chapter.

6.2 Experimental

These preliminary studies on plasma copolymerization of mixed fluorocarbon/hydrocarbon systems were carried out in the hope of gaining a qualitative feel for the effect on, and any trends in, polymer composition. Due to practical difficulties encountered the parameters governing plasma deposition were not stringently controlled. The lower overall vapour pressure of some of the combined systems seemed to require a higher power to sustain a stable plasma, hence the naphthalenes and biphenyls were polymerized using powers of 30 and 50W respectively, whilst the others were polymerized using 10W plasmas. All depositions were carried out over a six minute period and samples collected from the coil region unless specified otherwise.

A fuller account of experimental details is given in Chapter Two.

6.3 Results and Discussion

6.3.1 Plasma Polymerization of Perfluorobenzene (PFB) and Benzene (B) - 1:1 Ratio

Typical C_{1s}, F_{1s} and O_{1s} core level spectra obtained from the polymer produced by the plasma polymerization of a 1:1 gas phase ratio of B/PFB are displayed in Figure 6.1. Also shown in Figure 6.1 is a peak fit of the

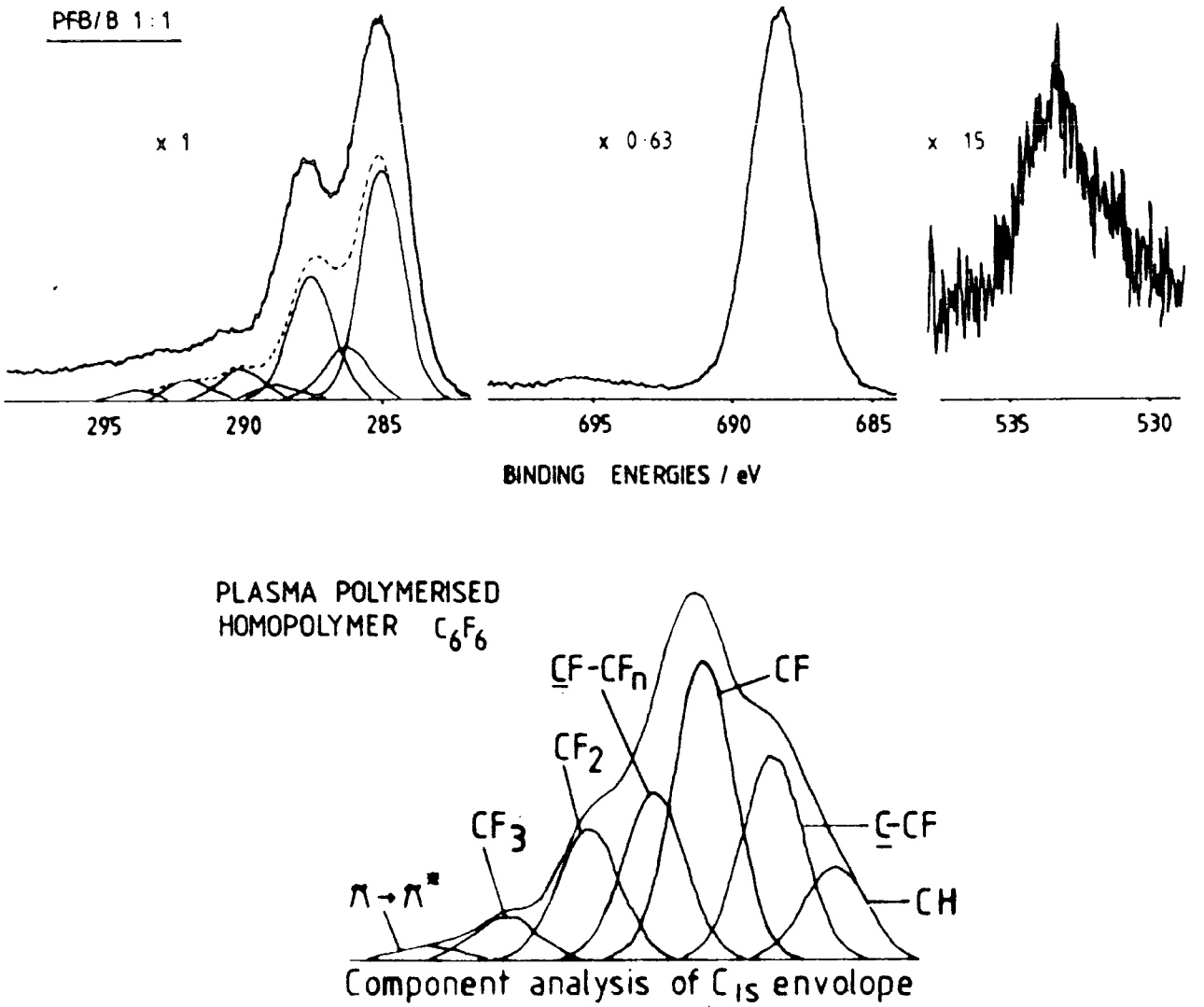

FIGURE 6.1 Core level spectra from PFB/B derived plasma copolymer and a component peak fit of the C_{1s} envelopes for PFB and PFB/B plasma polymers

---

C_{1s} envelope of the copolymer and for comparison, a peak fit of a typical C_{1s} envelope from a pure PFB plasma polymer. The most striking feature of the copolymer is in the shape of the C_{1s} envelope. As with the TMT/PFB and TMG/PFB co-polymers, the polymerization of PFB in the presence of benzene has resulted in an inhibition of the extensive rearrangement of the perfluorobenzene nucleus.

The C_{1s} core level spectrum shows a main photoionisation peak at 285.0eV due to carbon-carbon and carbon-hydrogen environments. Peaks at 286.5, 287.9, 289.3, 290.9, 293.0 and 295.2eV form the shoulder to higher binding energies of the main peak. The functionalities which give rise to these component peaks are $\underline{C}$-CF, CF, $\underline{C}$F-CF_n, CF_2, CF_3 and $\pi \rightarrow \pi^*$ shake-up environments respectively. These same functionalities are present in a plasma polymer of pure perfluorobenzene. Although the same functionalities are present in the copolymer the distribution of the component peaks arising from these groups, however, is noticeably different at the higher binding energy part of the spectrum. Of the peaks arising from carbon in a fluorinated environment, the dominating functionality is still C-F. The major difference between pure plasma polymerized PFB and a copolymer of PFB/B is in the amount of $\underline{C}$F-CF_n and CF_2 functionalities which are greatly reduced in the copolymer.

To emphasise the difference in relative peak contributions arising from the various C-F environments in the homo- and coplasma polymers, the peak intensities of both C_{1s} envelopes - corrected for hydrocarbon - are shown in Table 6.1. Uncorrected values for the PFB/B copolymer are given in brackets underneath.

TABLE 6.1 Percentage intensities of the component peaks of the C_{1s} envelopes from plasma polymers produced by PFB and PFB/B in a 1:1 ratio corrected for hydrocarbon - Uncorrected values for PFB/B in brackets

Peak Assignment	CH	C-CF	CF	CF-CF	CF_2	CF_3	$\pi \rightarrow \pi^*$
PFB	-	26	33	16	15	8	2
PFB/B	1	21	50	6	12	7	4
	(48)	(11)	(26)	(3)	(6)	(4)	(2)

This peak assignment was based on the component peak analysis of plasma polymers derived from perfluorobenzene. Two factors, however, suggest that peak assignment is not as straightforward as it might at first appear:

1. The chemical shifts of the component peaks of the C_{1s} envelope, especially those formally assigned to C-CF, CF and CF-CF_n are different, being shifted to lower binding energies in the copolymer, (Table 6.2).
2. The binding energy of the peak assigned to C-F groups is, in fact, at the same binding energy as the aromatic C-F peak in the ESCA C_{1s} spectrum of the condensed monomer,[13] *i.e.* equates to CF-CF aromatic. Similarly, the aromatic CF-CF binding energy shift in the spectrum of condensed octafluoronaphthalene corresponds to that observed in the C_{1s} envelope from the octafluoronaphthalene/naphthalene copolymer. Further, where copolymerization of perfluorobenzene with another monomer has resulted in an inhibition of rearrangement of the PFB nucleus, the shift exhibited by the CF assigned component peak is always reduced from that exhibited in the C_{1s} spectrum of pure perfluorobenzene. This suggests that the peak arising at ∿287.9eV is in fact from aromatic C-F derived in this instance from the perfluorobenzene monomer.

TABLE 6.2 Chemical shifts - eV from 285.0 - in the C_{1s} envelopes of plasma polymerized perfluorobenzene and perfluorobenzene/benzene polymers.

Peak Assignment	C-CF	CF	CF-CF_n	CF_2	CF_3	$\pi \rightarrow \pi^*$
PFB	1.7	3.3	4.5	6.2	8.3	10.2
PFB/B	1.5	2.9	4.3	5.9	8.1	10.2

This evidence, together with the step function in the C_{1s} envelope and the pronounced shake-up satellites in both the F_{1s} and C_{1s} core level spectra attests to the more pronounced aromatic nature of the deposited polymer film, *i.e.* the presence of aromatic CF indicates that a greater degree of the unsaturated PFB monomer structure is retained in the plasma copolymer. The aromatic nature of benzene may also be retained upon copolymerization, however the resolution of the ESCA spectrometer, together with the very small chemical shifts induced in the various hydrocarbon functionalities, leads to the production of only 1 peak in the C_{1s} envelope: that is, the component peak at 285.0eV assigned to hydrocarbon. Thus no information can be derived from ESCA about the state of the benzene nucleus in the copolymer.

For the sake of completeness it should be mentioned here that in a study on the plasma polymers derived from the series of fluorinated benzenes,[14] as the degree of fluorination decreased, the binding energy of the F_{1s} core level in particular was also found to decrease. Although a similar effect may be taking place on the binding energy shifts seen in the C_{1s} envelope due to the presence of hydrogen, the polymer is no longer perfluorinated - the other evidence, noted above, suggests that this is not the whole answer.

Further complications arise in the intensity of the component peaks of the C_{1s} envelope due to the presence of a step function. This step function is thought to be due to the presence of long range unsaturation in the polymer[13] and is discussed in more detail in Chapter Three. As has already been pointed out the method of linear background sub-

traction used by the DS300 can cause problems in peak synthesis especially where there is a large asymmetry of the C_{1s} photoionisation peak as in the tetramethylgermanium/perfluorobenzene copolymer.[15] If the step function is very pronounced as in the latter copolymer, then the peak synthesis routine can cause the appearance of peaks at higher binding energies, especially those associated with CF_3 and $\pi \rightarrow \pi^*$ shake-up environments, which are not at all apparent in the C_{1s} core level. In this instance, the C_{1s} envelope of the PFB/B derived material suggests 'at a glance' the presence of CF_2, CF_3 and $\pi \rightarrow \pi^*$ shake-up environments, and the fact that the peak asymmetry is not large means that there is little uncertainty over peak intensities. To check the peak assignment, and their intensities, the values of the F:C stoichiometry obtained by both methods (F_{1s}/C_{1s} area ratio and from the C_{1s} envelope) were compared. There was very good agreement (0.49 cf. 0.53) indicating that peak assignment was correct. It should be borne in mind, however, throughout the following chapter that the presence of a step function in the C_{1s} envelope, depending on its magnitude, could lead to errors in the intensity of functional group component peaks at higher binding energies.

It should also be noted that there will be some contributions to the CF_2 and CF_3 intensities arising from shake-up satellites due to unsaturated hydrocarbon, if as expected the benzene nucleus also retains much of its aromatic nature, since the $\pi \rightarrow \pi^*$ shake-up satellite due to unsaturated hydrocarbon occurs some 7eV to higher binding energies from 285.0eV.[16] In the polymer derived from pure perfluorobenzene

the probability of shake-up arising from hydrocarbon is extremely small and can be effectively ignored as the only source of hydrocarbon is from contamination. In a copolymer, the probability of unsaturated hydrocarbon being present is real and can no longer be assumed to be negligible. This may also account for the slightly greater F:C stoichiometry calculated by using the intensities of the component peaks of the C_{1s} envelope.

The F_{1s} core level, present at a binding energy of 688.0eV is very intense and consists of one main photoionisation peak due to C-F environments. The binding energy of fluorine has decreased from that in pure PFB plasma polymer by about 1.0eV. This shift is similar in magnitude to that observed by Clark and AbRahman[14] on going to plasma polymerized monofluorobenzene from perfluorobenzene. The presence of the very pronounced $\pi \rightarrow \pi^*$ shake-up environment some 8eV to higher binding energies,[17] which has already been mentioned, is due to fluorine which is attached to unsaturated carbon, *i.e.* C=C-F groups.[17] Peak area ratios of the F_{1s}/C_{1s} core levels indicate a stoichiometry of $C_1:F_{0.49}$ for the polymer film.

Assuming that all the hydrocarbon is derived from the benzene monomer, this would indicate that there has been a 1:1 incorporation of benzene and perfluorobenzene into the plasma polymer if, as in the pure PFB plasma polymer, fluorine elimination does not play a dominant role in polymer formation. The inhibition of the rearrangement of the perfluorobenzene monomer indicating that as with TMT, copolymerization and not codeposition has taken place. Studies using a 70^{o} take-off angle reveal that the polymer is vertically homo-

geneous, with respect to the C:F stoichiometry, throughout the sampling depth of the C_{1s} core level, and that of the amount of oxygen revealed at a 35^{o} take-off angle - $C_1:O_{0.02}$ - a large proportion of that is present at the surface. That is, as in the plasma polymer derived from pure PFB, surface oxidation of the copolymer takes place on exposure to the atmosphere subsequent to preparation.[18] The extent of oxidation is not very great, but indicates that there are still present in the polymer matrix reactive sites which react with oxygen, *i.e.* unpaired electrons are trapped in the polymer matrix during plasma polymerization.

The O_{1s} core level, at 533.2eV binding energy, is broad and arises from the various oxygen containing functionalities, namely C-O and C=O groups, as in the pure plasma polymer, component peaks cannot be resolved. The deposition rate - not measured - was such that the aluminium substrate was not visible after a 5 minute deposition period.

The above discussion relates to a polymer sample deposited in the coil region at ambient substrate temperatures. The next few paragraphs discuss the effects of deposition, with respect to sample position within the reactor, $150^{o}C$ substrate temperature and using a higher flow rate, on the composition of a nominally 1:1 PFB/B plasma copolymer.

The composition of the C_{1s} envelope from the polymer deposited at the end of the reactor - although still in the visible glow discharge region - is slightly different from the composition of the sample in the coil region - Table 6.3.

TABLE 6.3 Percentage Composition of the C_{1s} envelopes of the PFB/B derived Polymers deposited in the coil region and at the end of the reactor

Binding Energies/eV	285.0	286.45	287.9	289.25	290.8	293.05	295.15
coil region	48	11	26	3	6	4	2
end of reactor	47	13	24	5	6	4	1

The sample deposited in the coil region would appear to be richer in the component peak of 287.9eV with an associated greater intensity of the $\pi \rightarrow \pi^*$ shake-up satellite, and have a smaller contribution from the peak at 286.5eV assigned to C-CF structural features. These three differences would tentatively suggest that a greater degree of retention of the monomer configurations in the copolymer is associated with deposition in the coil region. This is not the expected result since the area of greatest power density is in the coil region[19] and therefore the greatest amount of fragmentation might be expected to occur in this zone. In the absence of more detailed studies in the copolymerization of 1:1 mixes of PFB/B, it is difficult to determine whether these results are real or just apparent. The F_{1s}:C_{1s} stoichiometry of the deposited copolymer is 1:0.49, *i.e.* as in the sample deposited in the coil region, there is a 1:1 composition of the deposited copolymer film. This is in contrast to the results obtained for plasma polymerized PFB[18] where the F:C stoichiometry of the deposited film has been reported as being richer in fluorine in the tail region of the reactor in comparison to the coil region. The F:C stoichiometry also indicates that, as in the plasma polymerization of pure perfluorobenzene,[18] fluorine elimination is not important in the processes leading up to deposition.

The $O_{1s}:C_{1s}$ stoichiometry of the polymer deposited at the end of the reactor shows a slight increase in oxygen content (0.03 *c.f.* 0.02). However this may just be a reflection on the increased time of exposure of the polymer film to atmosphere, as the sample deposited in the coil region was analysed first.

The 1:1 copolymer deposited at a substrate temperature of 150°C would appear from the C_{1s} and F_{1s} peak areas to be, in fact, richer in the hydrocarbon component ($C_1:F_{0.33}$) and this is backed up by the composition of the C_{1s} envelope which is dominated by the peak at 285.0eV. However, this result may not be an indication of the selective incorporation of benzene into the copolymer at higher substrate temperatures but rather a reflection of the gas phase composition in the reactor during polymerization. The results obtained for copolymer composition by varying the gas phase mixture of $C_{10}F_8/C_{10}H_8$[20] suggest that the gas phase composition is reflected in the polymer film. Further, the plasma polymerization of perfluorobenzene at a substrate temperature of 150°C results in a polymer whose composition is virtually identical to that deposited at room temperature (Chapter Two), so it is difficult to see why in the present case, a high substrate temperature should lead to a polymeric deposit which is richer in benzene, if the gas phase is a 1:1 ratio of the two monomers. To add further doubt on the selective incorporation of benzene, hydrocarbons are usually less thermally stable than fluorocarbons,[21] but without a detailed study on the deposition rate of benzene at the two different temperatures this cannot be used as a conclusive argument.

Accepting that there has been less incorporation of perfluorobenzene into the plasma copolymer, the relative intensities of the component peaks of the C_{1s} envelope still reflect the lack of extensive rearrangement of the perfluorobenzene nucleus, *i.e.* the excess hydrocarbon has not disturbed the component distribution due to fluorine containing functionalities. This in turn suggests that if a 1:1 reaction is needed in the gas phase to result in stabilization of the parent monomers in the copolymer, then a reduction of perfluorobenzene will result in a lack of retention of configuration of the excess benzene molecules. Unfortunately, any effect on benzene is not visible in an ESCA spectrum, unless there is a direct effect on the composition of the fluorinated part of the C_{1s} envelope.

As with the sample deposited at ambient temperatures, the deposition time of 5 minutes was sufficient to deposit a film at least 70Å thick, *i.e.* the Al_{2p} core level spectrum revealed no aluminium present. There was also no evidence for nitrogen incorporation.

Like the PFB/B polymer deposited at the end of the reactor at ambient temperatures, the amount of $\underline{C}$-CF in the C_{1s} envelope of the polymer deposited in the same region at 150°C substrate temperature was also increased compared to that in the sample deposited in the coil region, as was the component peak at 289.3eV assigned to $\underline{C}F\text{-}CF_n$ structural features. Unlike the previous polymerization, though, the amount of CF appeared to be constant and this was reflected in the intensity of the shake-up satellite on the C_{1s} envelope. The F:C stoichiometry of the copolymer deposited in the end of the

reactor was the same as that of the sample deposited in the coil region, *i.e.* $C_1:F_{0.33}$.

As with the polymer samples deposited at a substrate temperature of 150°, the copolymer deposited at a higher flow rate was also deficient in perfluorobenzene as evidenced by the F:C stoichiometry. No comment will be made on the relative intensities of the component peaks of the C_{1s} envelopes† (Figure 6.2) other than the sample deposited at the end of the reactor was very similar in composition to the polymer deposited in the coil region. The F:C stoichiometry of both copolymers was $C_1:F_{0.29}$.

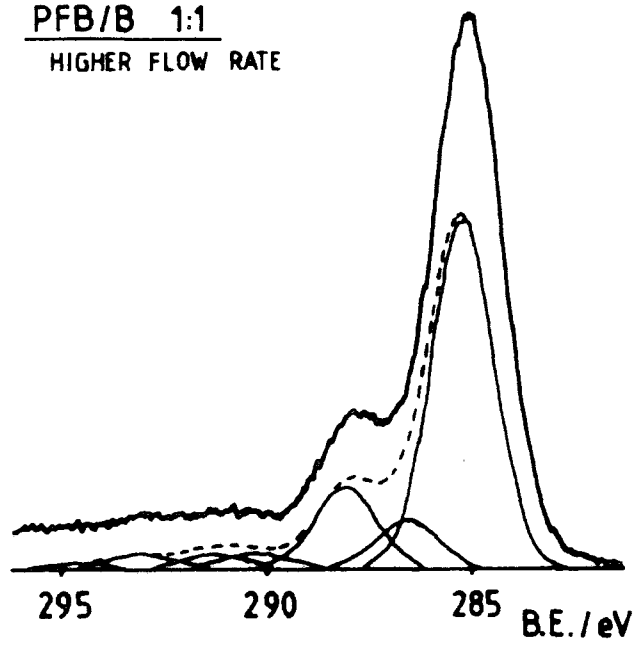

FIGURE 6.2 Component peak fit of C_{1s} envelope for PFB/B copolymer - higher flow rate

† As the amount of perfluorobenzene in the copolymer drops, the intensity of the high binding energy peaks decreases - in the present example to below 5% for CF-CF, CF_2, CF_3 and $\pi\rightarrow\pi^*$ shake-up environments. Thus peak assignment becomes ambiguous.

However, unlike previous depositions, the F_{1s} core level revealed an unsymmetrical photoionisation peak due to the presence of a very small (∿5%) peak to lower binding energies. This was at first thought to arise from an interaction of adsorbed perfluorobenzene with the aluminium oxide which is discussed in more detail in Chapter Seven. This would have been an indication that the deposition rate of the copolymer had decreased at the higher flow rate. However, in the present case this may not be the answer. The Al_{2p} core level region indicates the absence of any signal originating from aluminium, and as the sampling depth of Al is greater than for F (∿70 *c.f.* 24Å), the origin of the low binding energy F_{1s} peak is unlikely to be due to an interaction of perfluorobenzene with the substrate. Also the intensity of the smaller peak in the F_{1s} core level spectrum increases on going to a higher take-off angle, suggesting that the peak arises from some interaction near the surface. As this was the only time a small binding energy peak was seen in the F_{1s} spectrum, it may, in fact, be an artifact of this particular deposition or ESCA experiment rather than a true result.

6.3.2 Plasma Polymerization of Octafluoronaphthalene (OFN) and Naphthalene (N) - Varying Ratios

(I) ESCA Studies

Following the detailed discussion on the plasma copolymerization of perfluorobenzene and benzene in a 1:1 ratio, as most of the discussion is applicable in the present case, discussion of the appearance of the core levels will be brief. The typical C_{1s} envelope for a copolymer derived from a 1:1 ratio of $C_{10}F_8$:$C_{10}H_8$ in the gas phase at 150°C is

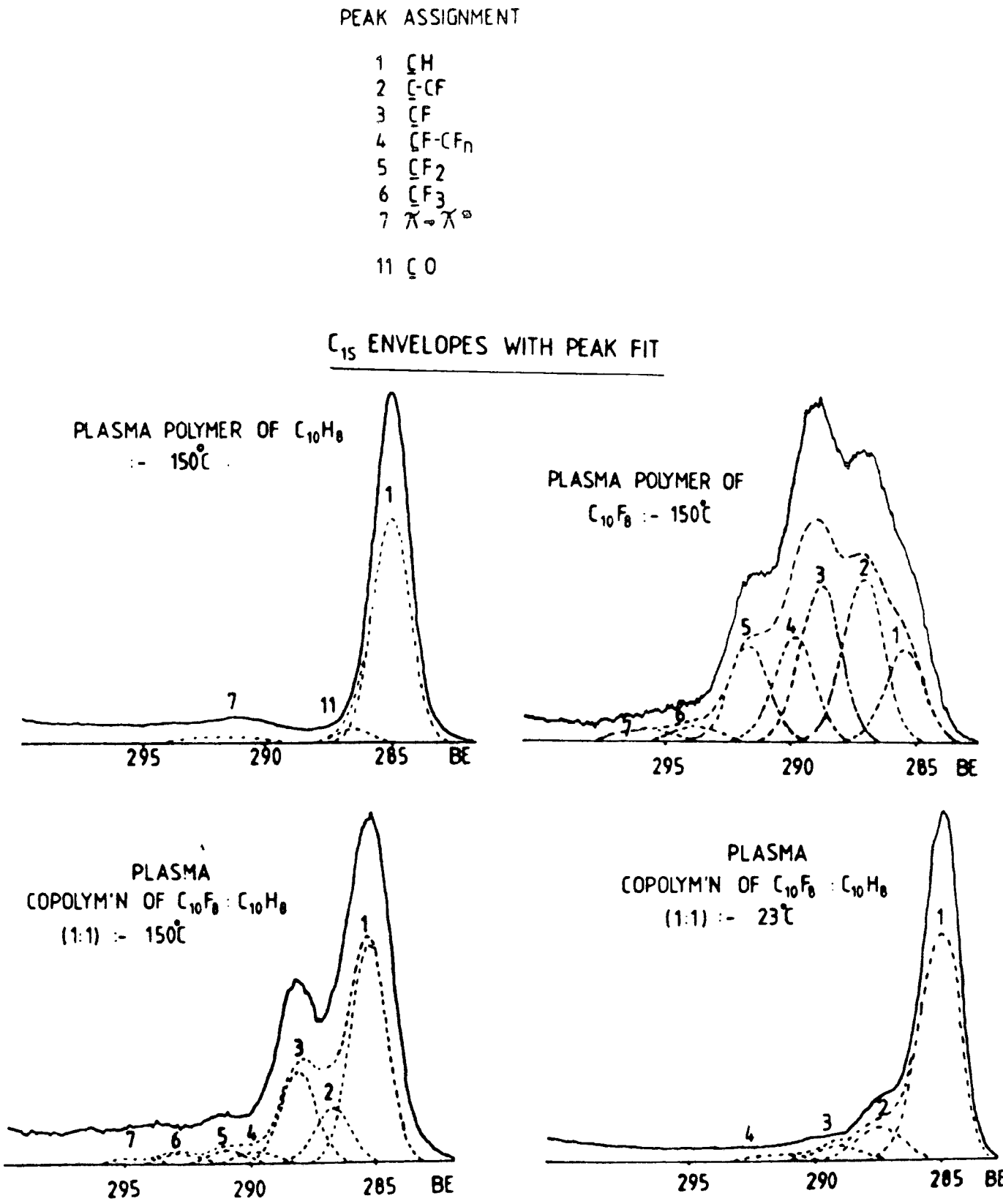

FIGURE 6.3 Component peak fit of C_{1s} envelopes for OFN, N and 1:1 ratio OFN/N at 23°C and 150°C

shown in Figure 6.3. As with the PFB/B copolymer, the C-F peak is dominant in the material derived from OFN/N. For comparison, in the C_{1s} envelope for octafluoronaphthalene also shown in Figure 6.3 the C-CF and C-F intensities are comparable. This suggests that the plasma polymer derived from a 1:1 mixture of OFN/N is not a straightforward codeposition of building blocks similar in nature to those of the single monomer. There has been some interaction/reaction in the plasma altering the composition of these building blocks, *i.e.* copolymerization of 1 mole of OFN and 1 mole of N has taken place, resulting in a polymer film whose F:C stoichiometry is 0.41:1. This F:C ratio is only indicative of a 1:1 incorporation, though, if it is assumed that as in the simple monomer, very little fluorine has been eliminated from the octafluoronaphthalene.[22] In view of the very pronounced $\pi \rightarrow \pi^*$ shake-up satellite accompanying the F_{1s} photoionisation peak (not shown) indicative of the unsaturated nature of the fluorine environments[17] and the step function present in the C_{1s} envelope,[13] this is not an unreasonable assumption. A small amount of fluorine elimination is to be expected, however, if the deposited polymer contains both monomer/monomer fragments covalently bonded together.

Further, as it has already been stated, the binding energy of peak 3 at 287.9eV (assigned to C-F in the plasma polymers of the single perfluorinated monomers) is in fact the same as that observed for $CF\text{-}CF_n$ in the ESCA analysis of condensed octafluoronaphthalene. The C_{1s} envelope for condensed OFN and its component peak fit, is shown in Figure 6.4.

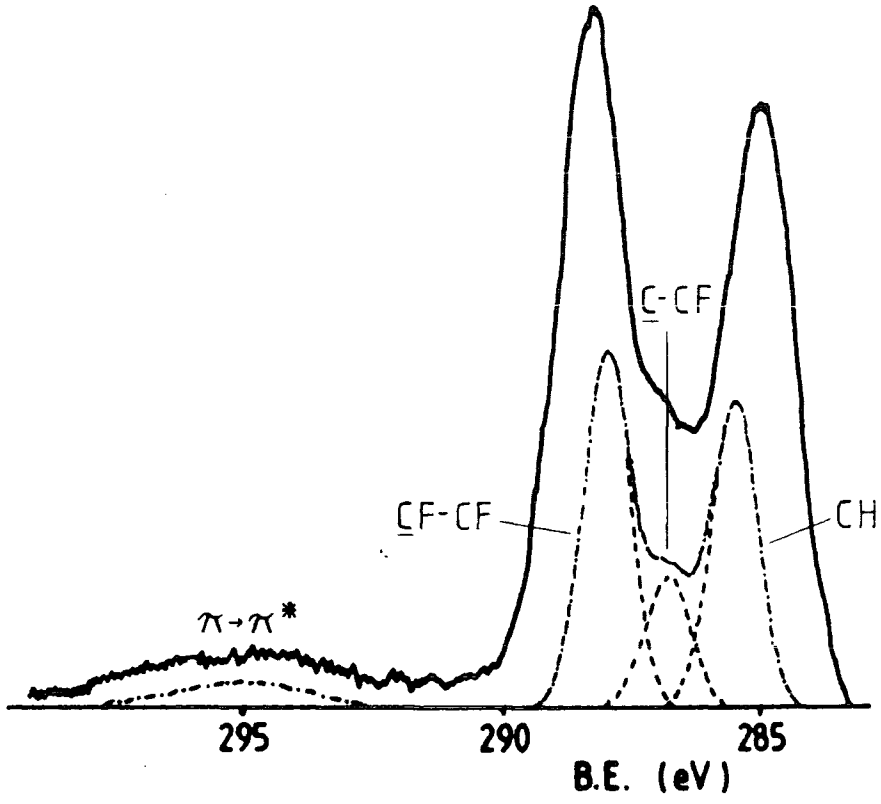

FIGURE 6.4 C_{1s} envelope of condensed OFN

The peak at 285.0eV in Figure 6.4 is due to condensed extraneous hydrocarbon. This contamination arises mainly from the X-ray window[23] which heats up during analysis, thus any hydrocarbon deposit is 'boiled off', only to be condensed in the present experiment onto the probe which was cooled down to -130°C. The ratio of the areas of the other two peaks at 287.9 and 289.2eV due to C-CF and CF-CF aromatic, is not the expected value for a similar reason, *i.e.* extraneous contamination.

The C_{1s} envelope from the 1:1 OFN/N copolymer shown in Figure 6.3 is, in fact, from the film deposited at a substrate temperature of 150°C. In contrast, the C_{1s} spectrum for the copolymer film deposited at 23°C is very different.

As can be seen from Figure 6.3 the hydrocarbon component dominates the envelope. The low level of higher binding energy components indicates that very little fluorine is present in the film as is evident by a F:C stoichiometry of 0.15:1. Assuming that plasma copolymerization results in the deposition of a material that reflects the molar ratio of the two monomers present in the gas phase then this latter result indicates that a ∿4:1 naphthalene to octafluoronaphthalene ratio has undergone plasma copolymerization. Although a 1:1 molar ratio of powder was used the difference in vapour pressure and flow rate of the two compounds is readily apparent at 23°C. Consequently, an investigation of the composition of films deposited during the plasma copolymerization of varying the starting ratios of monomer at the two temperatures was undertaken.[20]

The ESCA determined fluorine content *versus* the octafluoronaphthalene/naphthalene ratio of the initial powder is displayed in Figure 6.5. At 150°C the composition lies close to the theoretical value, and, as with the films deposited at 23°C, when the fluorocarbon monomer is in excess the content of fluorine in the copolymer is greater than expected and *vice versa*. However, for the films deposited at 23°C, the negative deviation from the theoretical value of percentage F content was much greater in the copolymers derived from nominal 1:1, 1:2 and 1:4 OFN/N ratios. The control of the gas phase composition is difficult using solids as the starting material and the above data directly reflects this and shows the need for this control in plasma copolymerization especially if the desired material is to have the same F:C ratio

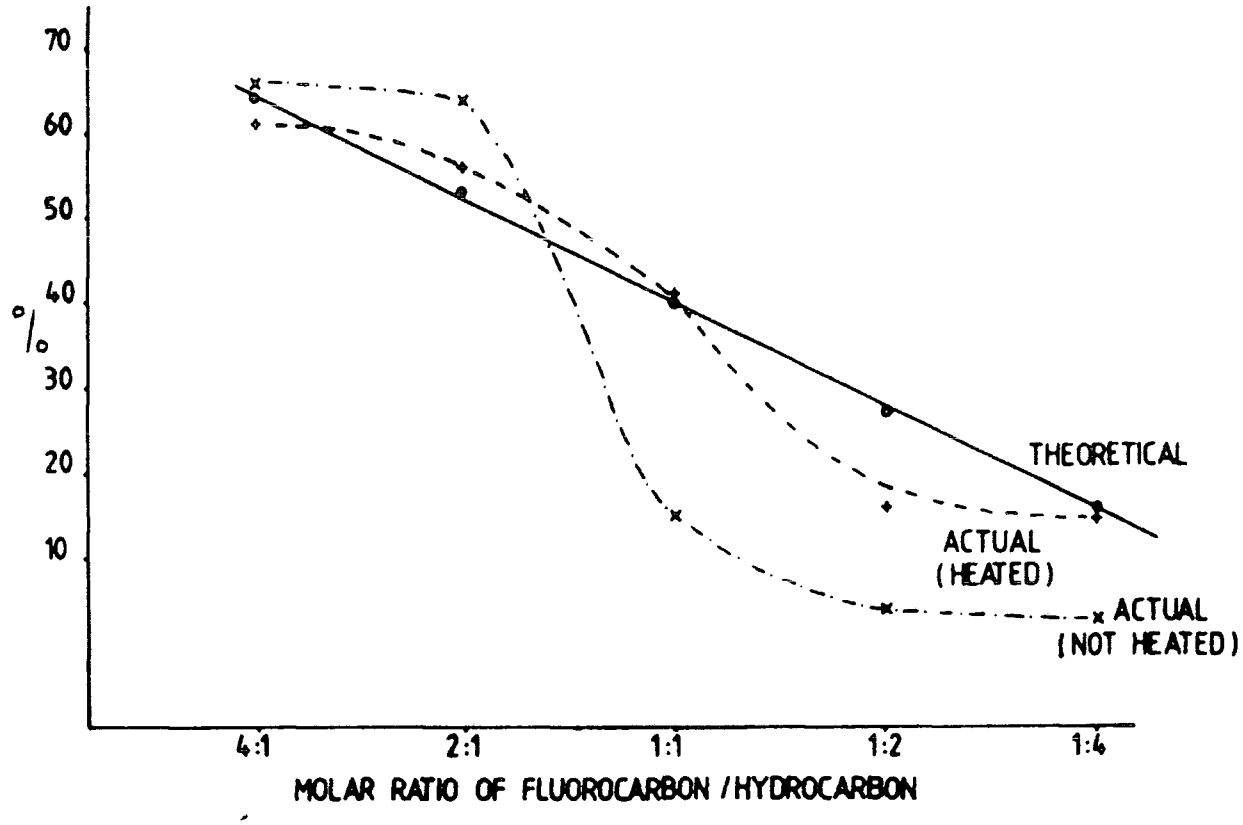

FIGURE 6.5 Percentage composition of F in plasma copolymer from OFN/N *versus* molar ratio of feed to the plasma

---

as the starting monomer composition. Similar problems were seen in the plasma copolymerization of a 1:1 biphenyl/decabiphenyl ratio discussed in the next section.

At high octafluoronaphthalene/naphthalene ratios, *e.g.* 4:1 the plasma polymer produced becomes much more like plasma polymerized octafluoronaphthalene in its composition (*e.g.* contributions of $\underline{C}F\text{-}CF_n$, CF_2 and CF_3 to the C_{1s} envelope become very significant) whereas when naphthalene is in excess the fluorocarbon part of the copolymer is similar to that of the 1:1 copolymer deposited at 23°C. This suggests that in order to perturb the nature of the plasma reactions of 1

molecule of octafluoronaphthalene or derived species, then 1 molecule of naphthalene or some other compound (compared with perfluorobenzene and tetramethyltin or benzene) must be present.

The composition of a polymer sample from a 1:1 nominal gas phase composition of OFN/N deposited in the end of the reactor at a substrate temperature of 150°C was also examined - Table 6.4.

TABLE 6.4 Percentage Composition of the C_{1s} envelopes for 1:1 copolymers of OFN/N deposited in the coil region at the end of the reactor

Peak Assignment	CH	C-CF	CF	CF-CF	CF_2	CF_3	$\pi \rightarrow \pi^*$
Coil Region	54	14	23	3	3	2	1
Reactor End	48	17	25	3	4	2	1

It would appear from Table 6.4 that the sample deposited in the coil region has a higher amount of hydrocarbon with a resultant decrease in the intensities of the C-CF and CF component peaks. This is not reflected in the F:C stoichiometry of the copolymer, which indicates that the sample deposited in the coil region has a greater amount of fluorine (0.34:1 *cf.* 0.31:1) than the sample deposited at the end of the reactor. Both were in the visible glow region. This slight decrease may not be a real trend however since the difference is not that great. As with the copolymer produced from a 1:1 ratio of perfluorobenzene/benzene, the copolymers deposited in the coil region and at the end of the reactor both tend to show the same C:F stoichiometry. This is unlike the results from plasma polymers of pure perfluoronaphthalene or perfluorobenzene which show a greater amount of

fluorine in the sample deposited at the end of the reactor.[24]

The visible colour of a naphthalene plasma is bright purple, whilst the glow from an octafluoronaphthalene plasma is pale pink. In the coplasma, there was a gradual change in colour from purple at the inlet (due to naphthalene) to pink at the outlet. This might tend to suggest that the film deposited in the coil region would be richer in hydrocarbon, since the plasma emission was dominated by N in this region. The C_{1s} envelope of the copolymer deposited in the coil region tended to support this (Table 6.4). The O:C stoichiometry of samples deposited, by various N/OFN ratios, in the coil and end zones were always below 0.04:1.

(II) Optical Emission

Examination of the nature of the emission arising from a plasma can give some valuable insights into the nature of the excited species being formed. However, it should be remembered that caution must be used in interpreting such data when looking for polymer forming precursors, the species responsible for the emission may not be involved in the polymerization process or could be a by-product of it. Bearing this in mind, the plasma emissions from the pure octafluoronaphthalene and the octafluoronaphthalene/naphthalene plasmas were compared to see if the inclusion of naphthalene into the plasma had perturbed the gas phase chemistry (as determined by the emitting species), as might be suggested by the ESCA analysis of the composition of the two plasma polymers.

The relevant spectra for the optical emissions arising during the plasma polymerization of naphthalene, octafluoro-

naphthalene and the copolymerization of a 1:1 mixture of these two compounds are shown in Figures 6.6 and 6.7. The plasma emissions from OFN and N plasmas have been discussed in Chapter Two and the reader is asked to read the relevant section therein (2.3.2). The essential features of interest in the emission from the OFN plasma is the emission at ∿280nm which is characteristic of CF_2, a high resolution scan of this region has been displayed in Figure 2.7 in Chapter Two, and the prominent emission at ∿510nm - origin unknown - whose intensity is equal to that of the peak at ∿280nm.

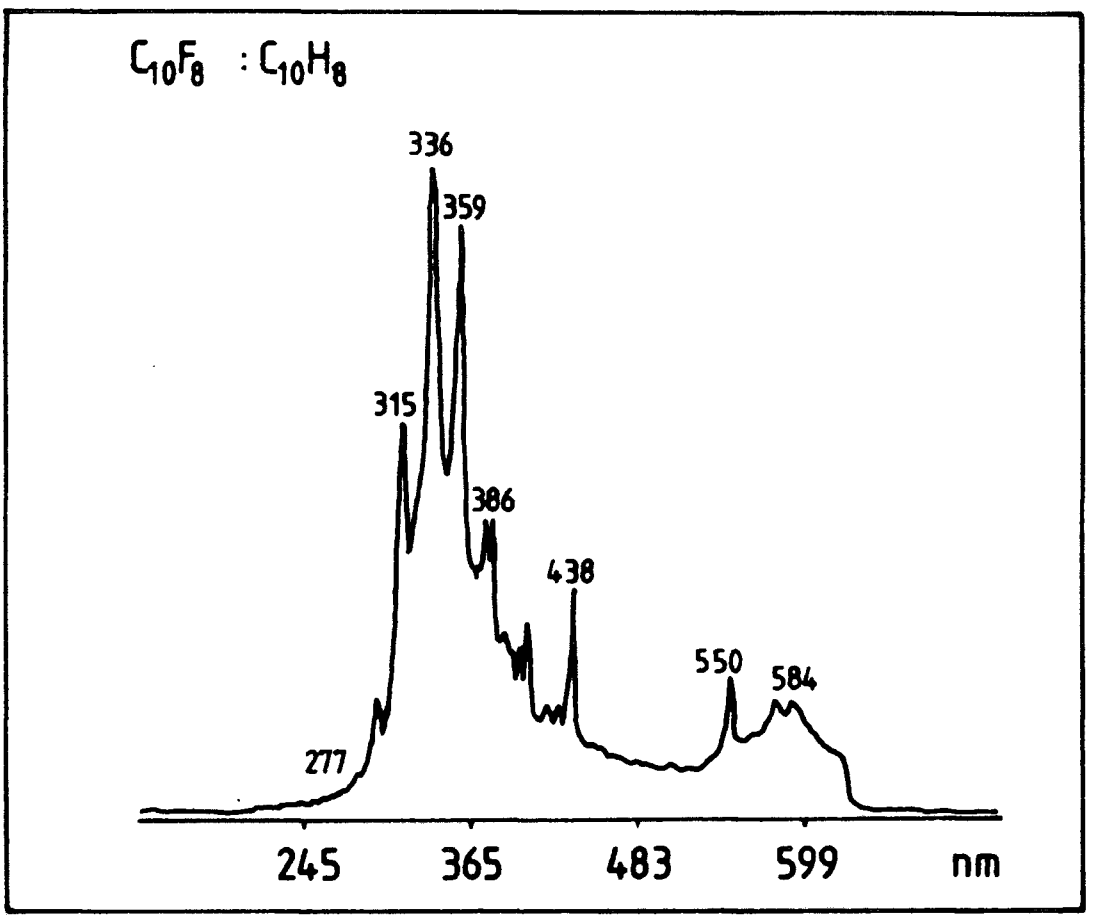

FIGURE 6.6 Optical Emission spectrum from a 1:1 OFN/N plasma, ∿250-650nm.

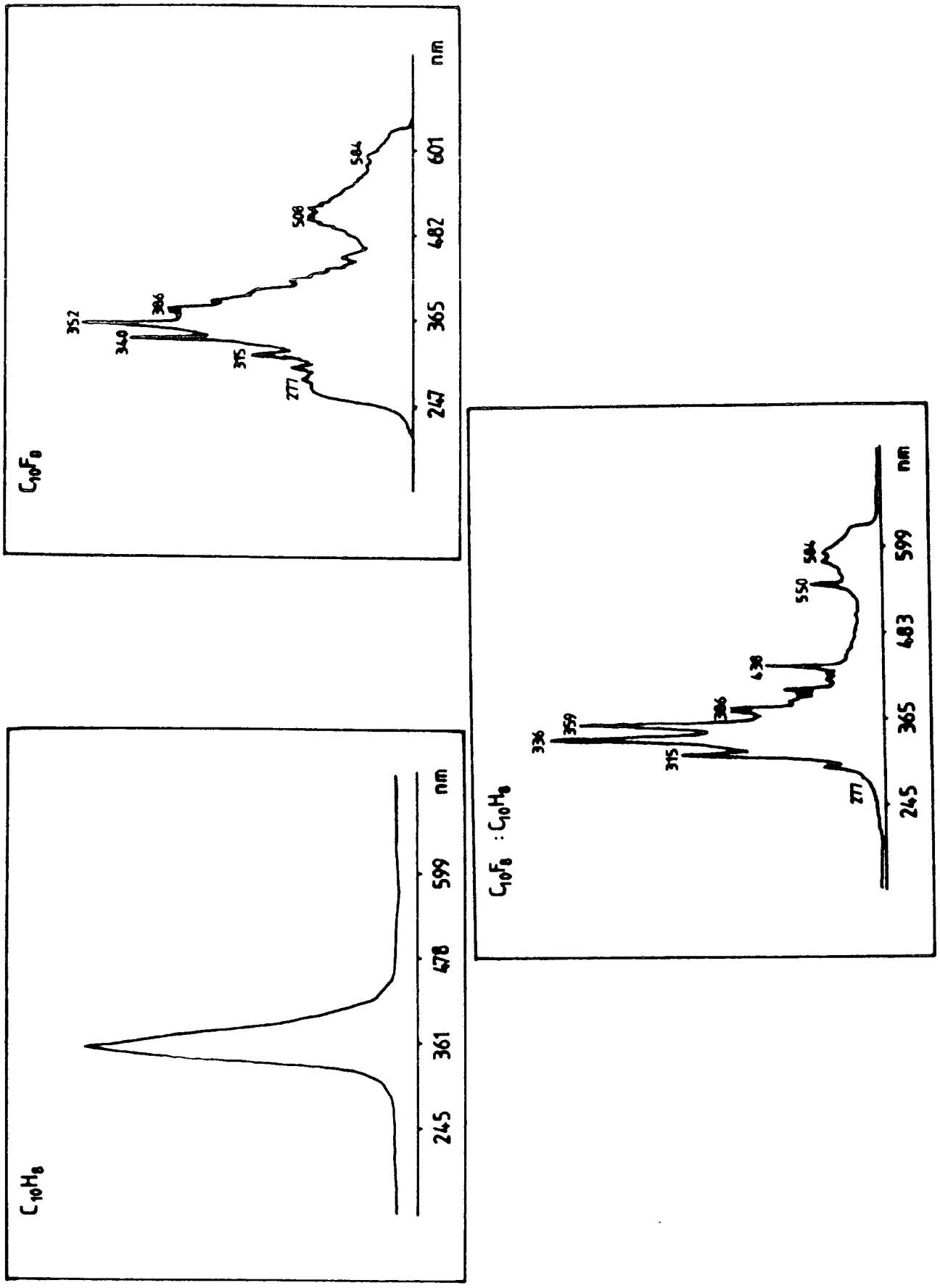

FIGURE 6.7 Comparison of optical emission spectra from OFN, N and 1:1 OFN/N plasmas

That the nature of the excited states emitting in the gas phase has been altered during the copolymerization of OFN and N can clearly be seen from Figures 6.6 and 6.7. There is no longer any significant amount of emission at ∿280nm. Similarly, the peak at 510nm has disappeared. In the plasma polymerization of the single fluorinated monomer this band is thought to arise from a rearrangement or fragmentation product of octafluoronaphthalene. There would appear to be a relationship between these two peaks, *i.e.* when there is a strong emission at ∿280nm due to CF_2 there is also a band present at ∿510nm. Conversely, when the emission due to CF_2 is greatly reduced the 510nm line is either reduced in intensity such that it is lost in the background, or else it no longer exists. This partnership has been observed in other aromatic systems, *e.g.* the biphenyls, benzenes and benzene/TMT.[1]

From both the ESCA data and plasma emission data a correlation would appear to exist between the reduced CF_2, CF_3 contribution to the functional group composition of the plasma polymer and the decrease in emission arising from difluorocarbene and the unidentified species emitting at ∿510nm in the gas phase. Assuming that the excited states of, for example, CF_2 arise predominantly from electron impact of the ground state and that the radiative decay is more rapid than collisional quenching then the intensity of emission will be proportional to the concentration of CF_2 in the ground state. Consequently the reduced emission during copolymerization would be a direct indication of a smaller number of CF_2 ground species being present. This latter decrease could be accounted for by -

(a) CF_2 formation in the ground state is rapidly followed by reaction with another species before excitation can occur.

(b) The reaction pathways for perfluoronaphthalene that normally give rise to CF_2 formation no longer occur to the same extent in the presence of naphthalene.

The ESCA data for the ~1:1 copolymer of OFN and N reveals that the C-F environment is similar to that of the OFN monomer. This indicates that the fluoro aromatic content of the copolymer is much greater than in the OFN plasma polymer. This suggests that the extent of rearrangement and fragmentation of OFN during the plasma copolymerization is greatly reduced. Thus assuming that CF_2 formation is the result of extensive reaction than (b) above would be the more probable cause for the reduction in the CF_2 concentration.

The above discussion does not imply that CF_2 is necessarily a precursor for a building block in the plasma polymerization of OFN and hence responsible for the CF_2 functional group in the deposited material. It is the nature of the rearrangement and fragmentation reactions that influences the composition of the building blocks and hence the plasma polymer. The detection of CF_2 emission might only be an indication of the extent of these reactions rather than the identification of a genuine precursor.

Deposition of a plasma polymer is highly dependent on the discharge conditions and hence the relative balance of polymerization and ablation. Although the reactive nature of CF_2 makes it an appealing precursor/building block its presence does not necessarily mean that deposition will occur.

In perfluoroaliphatic plasmas[25] emission from CF_2,CF and F excited states has been reported. It is thought that the F atom density is the parameter controlling etching. Thus in, for example, a CF_4 plasma, although CF_2 is formed the concentration of fluorine atoms is such that etching and not deposition is observed as the overall process.[6] When CF and CF_2 concentrations (as determined from the intensity of their emission) exceed that of the F atom by 10^3 - 10^5, as in C_2F_4, deposition occurs.

The above discussion should indicate that the interpretation of the plasma emission diagnostic data is not trivial.

Although the present analysis of the emission spectra does not permit the unambiguous identification of the polymer forming species it does give some interesting insights into the nature of some of the excited species present in the gas phase during plasma polymerization.

6.3.3 Plasma Polymerization of Decafluorobiphenyl (DFB) and Biphenyl (B) - 1:1 Ratio

The C_{1s} spectrum of a copolymer derived from a nominal 1:1 ratio of DFB/B deposited at 150°C in the coil region is shown in Figure 6.8.

The corresponding C_{1s} from the polymer deposited at ambient temperatures is also displayed in Figure 6.8. As with the copolymerization of the naphthalenes, control of the gas phase composition is essential in producing a 1:1 copolymer. At room temperature, the gas phase is dominated by decafluorobiphenyl and hence the composition of the deposited film

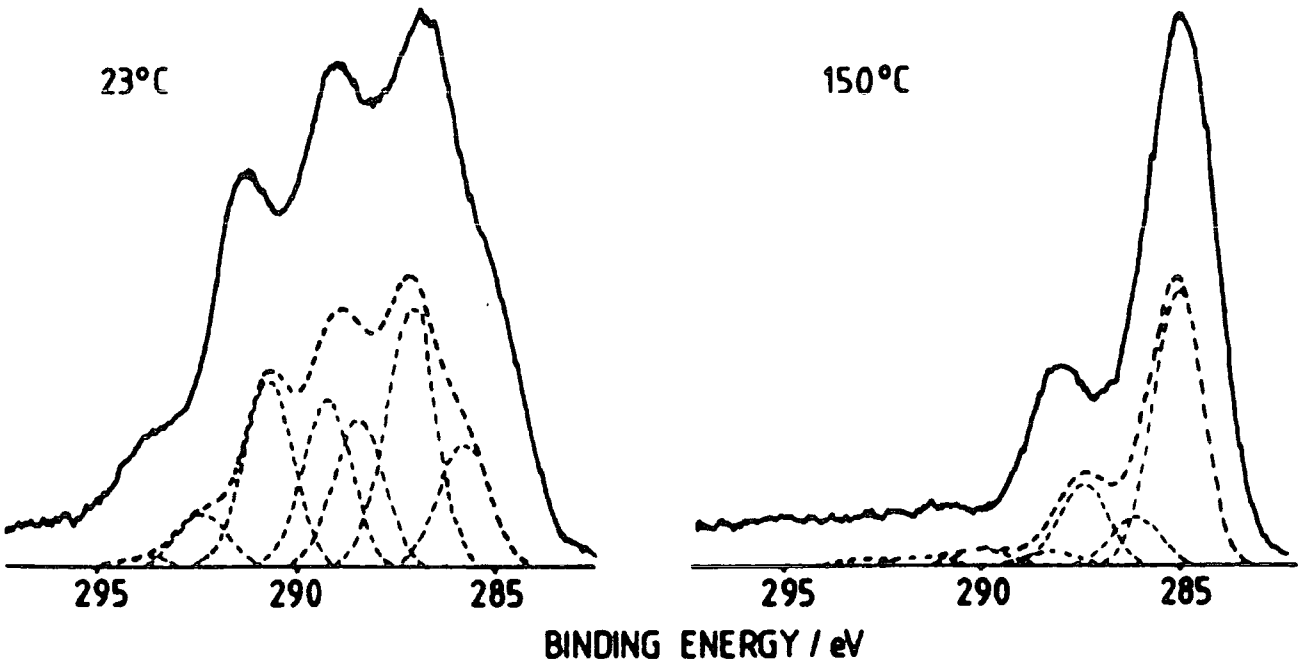

FIGURE 6.8 Component peak fit of the C_{1s} envelope for DFB/B at 23°C and 150°C

---

reflects this - the C_{1s} envelope is essentially that of decafluorobiphenyl. This is supported by the optical emission spectrum obtained from the coplasma (shown in Appendix One) which showed all of the characteristic features of a DFB plasma, namely, a strong emission at ∿280nm due to the fluoresence from difluorocarbene radicals and an associated peak of equal intensity at 510nm. In comparison with the optical emission from a pure decafluorobiphenyl plasma shown in Figure 2.16, the main emissions from a plasma containing a mix of these two compounds at room temperature are very similar. As such this indicates the small amount of biphenyl emission and hence the reduced amount of biphenyl present in the plasma. As further confirmation, elemental analysis of the solid mixture after the plasma polymerization

experiment revealed it to be strongly deficient in fluorine in comparison to the initial value of the 1:1 DFB/B mix, *i.e.* the gas phase in the reactor was rich in DFB.

At the higher substrate temperature, more biphenyl is present in the gas phase. This means that as the number of molecules begins to equalise, stabilisation of the perfluoroaromatic becomes a dominant feature of the C_{1s} envelope. Excess DFB may fragment/rearrange in the plasma in the normal manner, and will contribute as such to the C_{1s} core level. However, when the majority of the fluoromonomer is stabilised, the visible effect in the C_{1s} envelope from unstabilised DFB will be negligible, and will produce the C_{1s} spectrum shown in Figure 6.8.

6.3.4 Plasma Polymerization of Perfluorobenzene and Octafluoronaphthalene

So far, two plasma environments have resulted in stabilisation of the perfluoroaromatic:copolymerization of

(1) Perfluorobenzene and a tetramethyl metal, *i.e.* Sn or Ge, or

(2) Perfluoroaromatic and a hydrocarbon analogue.

To investigate this area further, perfluorobenzene and octafluoronaphthalene were copolymerized using a nominal gas phase composition of 1:1. The C_{1s} envelope of the deposited polymer is shown in Figure 6.9, and the percentage composition of the component peak fit is shown in Table 6.5.

TABLE 6.5 Percentage Compositions of the C_{1s} envelopes for PFB, OFN and 1:1 PFB/OFN plasma polymers

Peak Assignment	CH	C-CF	CF_{Total}	CF_2	CF_3	$\pi\rightarrow\pi^*$
PFB	-	26	50	16	7	1
PFB/OFN	-	33	50	10	4	3
OFN	-	27	52	15	4	2

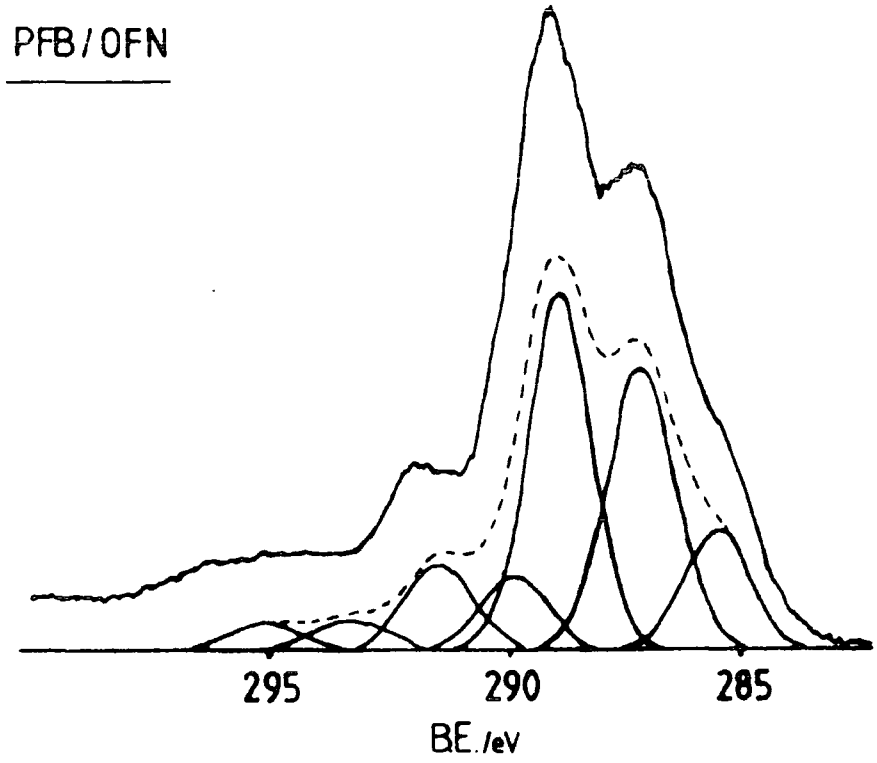

FIGURE 6.9 Component peak fit of the C_{1s} envelope for PFB/OFN copolymer

---

As with the polymerization of 1 fluoronaphthalene and, to a lesser extent, octafluoronaphthalene,[22] there is an asymmetry associated with the C_{1s} envelope of the copolymer thought to be due to long range unsaturation present in the film. The F_{1s} photoionisation peak is also accompanied by a $\pi \rightarrow \pi^*$ shake-up satellite. The F:C stoichiometry of the resultant polymer (0.75:1) indicates that there has been an essentially 1:1 incorporation of the two monomers to produce a film which is virtually homogeneous throughout the ESCA sampling depth, determined by using two electron take-off angles.

Although the amount of C-CF in the copolymer is still high (Table 6.5 and Figure 6.7) in comparison to the stabilised copolymers (Table 6.1 and Figure 6.3) the copolymerization of the two fluoroaromatic compounds has resulted in a large decrease in the amount of CF-CF although this is masked in Table 6.5 by the large increase in the amount of CF and CF_2. In fact, the amount of $CF-CF_n$ has been reduced by a factor of two. This situation is analogous to that in the copolymerizations of perfluorobenzene/2,2-Dimethyl propane and perfluorobenzene/tetramethyl silane (Chapter Five). As in the previous two examples, copolymerization did not produce the C_{1s} envelope associated with the 'true' copolymer. However, the distribution of the component peaks of the C_{1s} core level was affected such that only half of the amount of $CF-CF_n$ and one third of the amount of CF_2 were produced. Thus although copolymerization has taken place, the effect on the composition of the deposited film has been to alter the percentage intensity of the component peaks, rather than alter the nature of the plasma polymer as evidenced by the lack of rearrangement of the perfluoroaromatic nucleus in the stabilised copolymer.

This tentatively suggests that the gas phase chemistry occurring in the PFB/OFN coplasma has been affected by the presence of the second monomer, but in such a manner that the reaction pathway leading to deposition has been perturbed rather than changed. Thus the copolymer, as determined by the compositional analysis of the C_{1s} envelope, is similar, although not the same as, the plasma polymers produced from the single perfluoroaromatic monomers. Unfortunately, the

optical emission from this plasma was not recorded but the emission due to CF_2, and the associated peak at 510nm, is implied by the presence of CF_2 and CF_3 groups in the ESCA analysis of the deposited copolymer.

6.3.5 Plasma Polymerization of an Aromatic with a non aromatic 6-membered ring system

In the light of the results obtained above by the copolymerization of an aromatic fluoro-carbon with its analogous hydrocarbon, and as an extension to this study, the behaviour of an aromatic fluorocarbon with non aromatic six-membered ring hydrocarbons, and *vice versa*, in a plasma were examined.

This formed two series: the copolymerization of perfluorobenzene with a non aromatic hydrocarbon, *i.e.*

Series 1 - 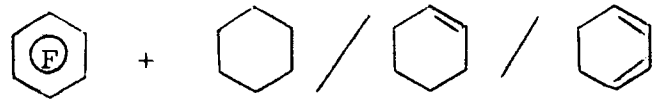

and the copolymerization of benzene with a non aromatic fluorocarbon, *i.e.*

Series 2 - 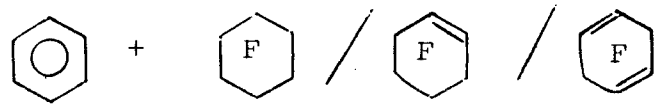

In a previous study on the composition of the plasma polymers derived from the isomeric tetrafluorobenzenes,[26] no differences were found between the 1,2,4,5 and 1,2,3,5 isomers. Similarly, polymers synthesised by excitation of inductively coupled plasmas in the perfluorohexadiene[27] isomers have been shown to be structurally very similar as far as ESCA can determine. Both retain the F:C stoichiometry of the parent monomer. For the former reason, and due to the availability of each monomer, 1,4-fluorocyclohexadiene and 1,3-cyclohexadiene were used.

The polymers derived from the perfluoro non aromatic six-membered ring systems, *i.e.* C_6F_{12}, C_6F_{10} and C_6F_8 have been studied previously by an earlier member of this laboratory.[18,27] It is pertinent here to give a brief review of the results, as determined by ESCA.

As the amount of unsaturation decreased in the monomer, there was an increasing amount of CF_3 and CF_2 structural features although all polymers exhibited extensive rearrangement giving rise to component structural features of the C_{1s} envelope not present in the parent monomer,[27] Table 6.6.

TABLE 6.6 Percentage intensity of the component peaks of the C_{1s} envelopes for plasma polymers derived from C_6F_8, C_6F_{10} and C_6F_{12}

	C-CF	CF	$CF-CF_n$	CF_2	CF_3	$\pi\rightarrow\pi^*$
1,3 C_6F_8	21	25	18	27	8	1
1,4 C_6F_8	23	24	13	29	10	1
C_6F_{10}	18	12	15	38	17	-
C_6F_{12}	12	8	17	39	24	-

There were low intensity $\pi\rightarrow\pi^*$ shake-up satellites in the C_{1s} envelopes of the polymers derived from the unsaturated C_6F_8 systems only, these two polymers were also the only ones to retain the F:C stoichiometry of the parent monomer. Plasma polymerization of both C_6F_{10} and C_6F_{12} resulted in an elimination of fluorine in the processes leading to deposition to produce polymers whose F:C stoichiometries were $\sim$1.58:1 and 1.68:1 respectively, compared with 1.7:1 and 2:1 of the parent monomers. The rate of deposition of these monomers was found to be in the order 1,3 and 1,4 $C_6F_8 > C_6F_{10} \sim C_6F_{12}$,[27] and as such the ease of polymerization seems to be associated with the

degree of unsaturation in the fluoro monomer. This association has been noted previously.[27]

As the deposition rate dropped, the substrate Au_{4f} level became visible and a two-component F_{1s} signal was observed - the normal high binding energy component characteristic of covalent C-F bands and a low intensity component some 2eV shifted to lower binding energies. This phenomena was noted in the deposition of perfluorobenzene onto Al substrates when irradiated by vacuum UV and will be discussed in Chapter Seven.

Using the shape of the C_{1s} envelope as a marker to whether stabilization had occurred or not, the copolymers were examined by ESCA and the resultant C_{1s} core levels for series 1 are shown in Figure 6.10 whilst those for series 2 are shown in Figure 6.11.

It is very apparent from Figure 6.10, that the copolymerization of perfluorobenzene with the cyclohexane, cyclohexene or cyclohexadiene hydrocarbons have all resulted in a polymer whose C_{1s} envelope shows the now classic lack of rearrangement of the perfluoroaromatic monomer, *i.e.* there are two main peaks in the C_{1s} spectrum which are due to hydrocarbon at 285.0eV and to $CF_{aromatic}$ at 287.9eV. There is no longer a large contribution of CF_3, CF_2 or $\underline{C}F\text{-}CF_n$ component peaks to the C_{1s} envelope.

The deposition rates of all three copolymers in both series were such that after a 10 minute exposure to the plasma, the aluminium substrates were completely covered, *i.e.* the films were at least 70Å thick.

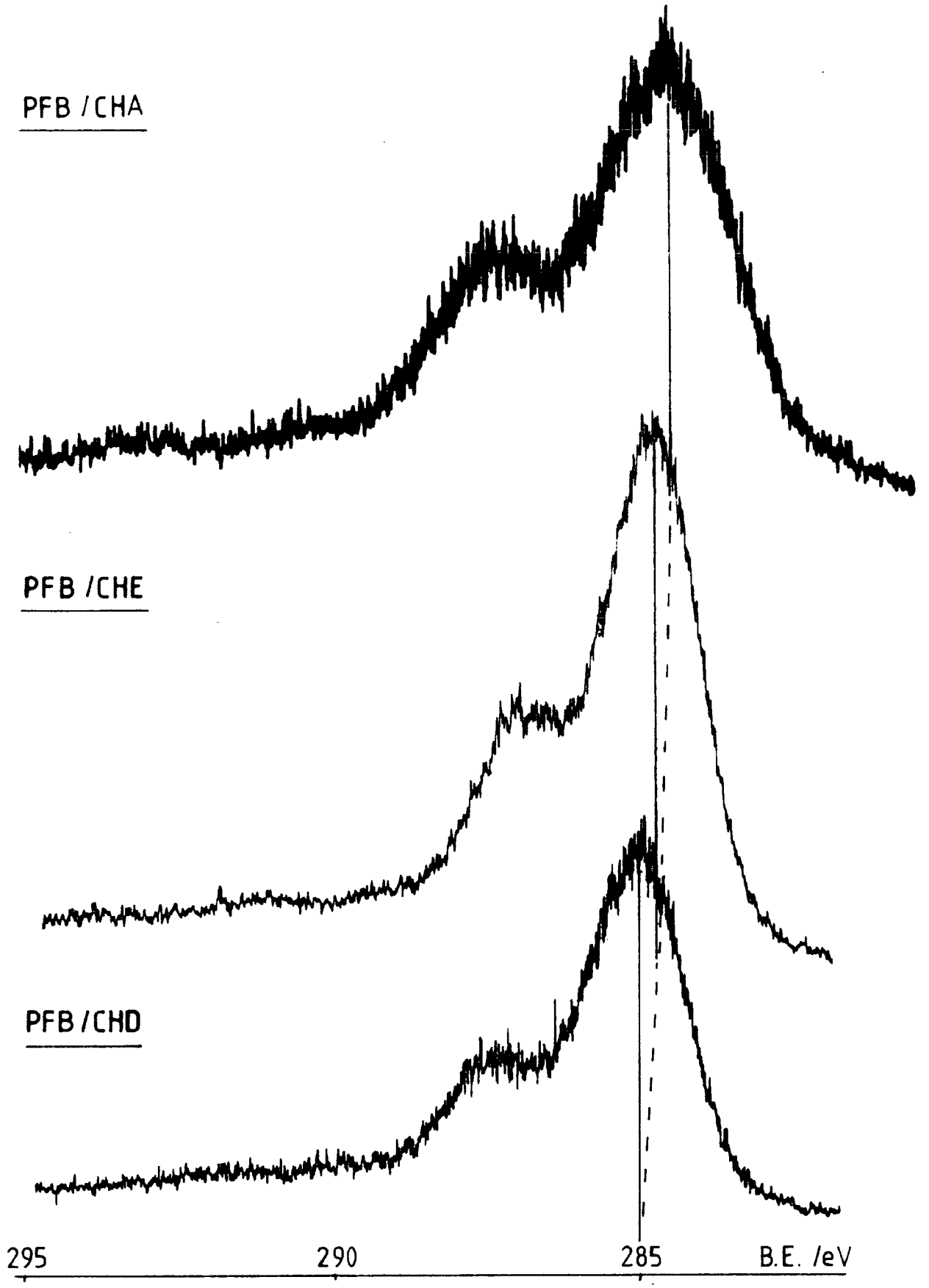

FIGURE 6.10 C_{1s} envelopes from PFB non aromatic hydrocarbon copolymers

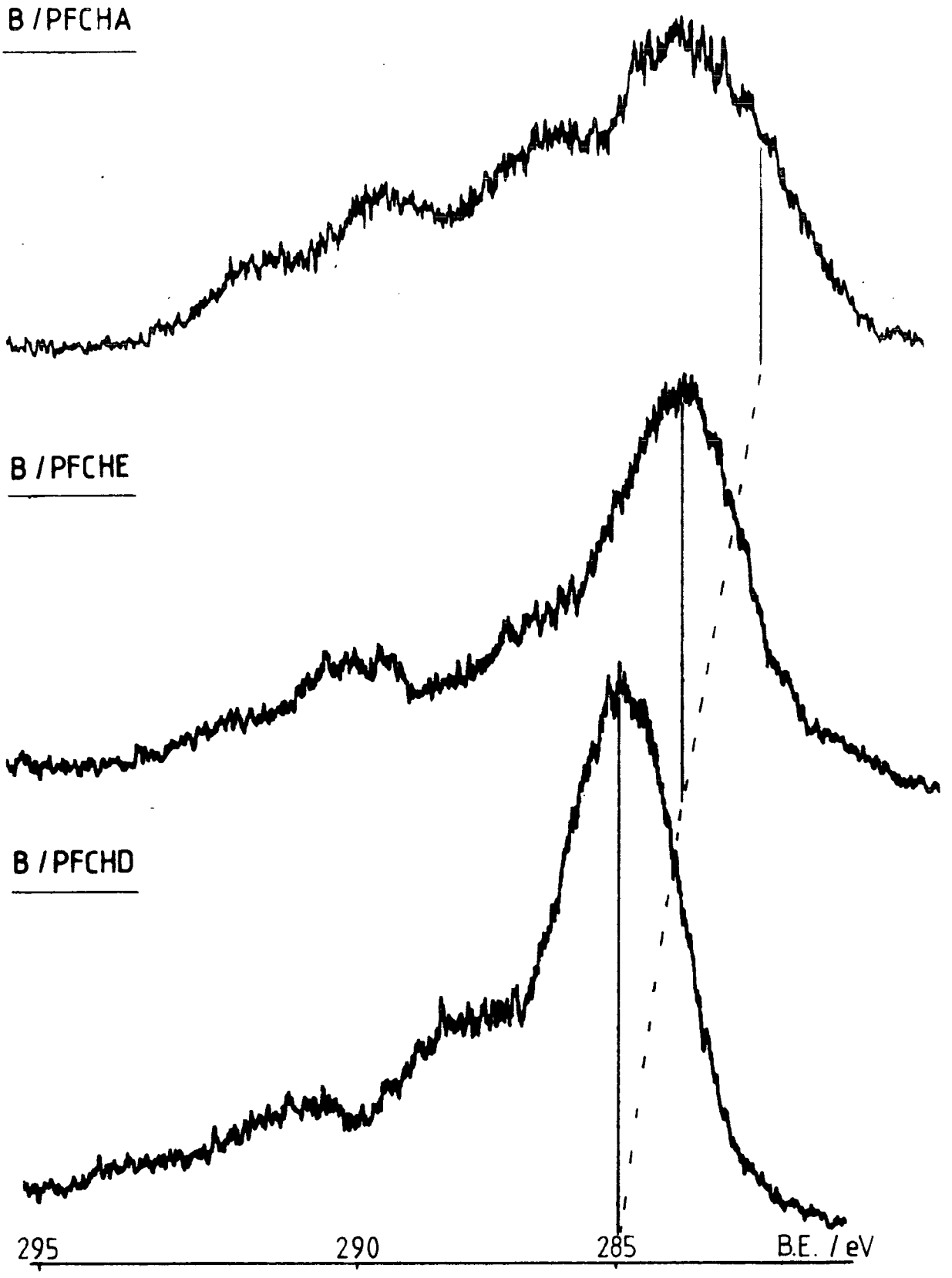

FIGURE 6.11 C_{1s} envelopes from B non aromatic fluorocarbon copolymers

From Figure 6.11 it is also apparent that the copolymerization of benzene with the cyclohexane, cyclohexene and cyclohexadiene fluorocarbons have all resulted in a polymer whose fluorocarbon component has not been stabilised. The C_{1s} envelope shows evidence for the two different components: the classic rearrangement of the fluoro compound,[1,13,22] producing $\underline{C}$-CF, $\underline{C}F$-CF_n, CF_2 and CF_3 component peaks, which forms the shoulder to higher binding energies of the main photoionisation peak at 285.0eV due to the hydrocarbon component. On this evidence alone, it might appear that codeposition rather than copolymerization has occurred in series 2. However, in series 1 the aromatic compound was stabilized, whilst all that can be said about stabilization in series 2 is that the non-aromatic ring system was not. What perhaps would be of more interest in the present experiment is a knowledge of what has happened to the aromatic hydrocarbon. Unfortunately, the use of ESCA does not allow for the interrogation of different hydrocarbon environments, therefore the fate of the non-aromatic hydrocarbons, and of the aromatic hydrocarbon, upon copolymerization with a fluorocarbon, is undetermined.

The use of another surface sensitive technique such as SIMS may prove to be beneficial, and complimentary to the information derived from ESCA. The fragmentation pattern of the copolymers may give an insight into the nature of the hydrocarbon component, after copolymerization, in the polymer film.

One interesting feature of the C_{1s} envelopes shown in Figure 6.11, *i.e.* those produced by copolymerizing benzene with a non aromatic fluorocarbon, is in the percentage intensities

of the fluorocarbon component peaks. Visually these differ from the distributions in the plasma polymers derived from pure C_6F_{12}, and to a lesser extent from C_6F_{10} and C_6F_8 - see Table 6.6.

Copolymerization has resulted in an increased intensity of the component peaks associated with C-CF and CF functional groups with a concomitant decrease in the amount of CF_2 and CF_3. This has resulted in a change in the relative intensities of each component peak which for benzene/perfluorocyclohexane means that the dominant peak in the spectrum arises from C-F and not CF_2 as in the pure C_6F_{12} plasma polymer. Thus although copolymerization has not resulted in stabilization of the fluorocarbon component, it has caused the distribution of the component peaks to be affected indicating that an interaction of the two compounds has taken place within the plasma.

From Figures 6.10, 6.11 and Table 6.7 it is also evident that the F:C stoichiometries are not exactly 1:1. If, as expected from the data to date, the composition of the deposited film is a reflection of the gas phase composition, then to obtain a stoichiometric film monitoring of the gas phase composition during polymerization is essential to ensure the required film composition. In the present case, for both series 1 and series 2 it would appear that the gas phase composition is not exactly 1:1 assuming that elimination of fluorine has not occurred in the deposition processes leading to formation of the copolymer. That it is not sufficient to know the composition of the starting mixture is clearly demonstrated in the copolymerization of the naphthalenes and the biphenyls

where the copolymers, under certain conditions, did not have the expected F:C stoichiometry. This, in turn, points to the need for an ESCA analysis of the plasma polymer. Without ESCA, the lack of rearrangement of the perfluoroaromatic component in the polymer - which is suggestive of an alternative reaction pathway occurring in the plasma on copolymerization - would not have been noted.

TABLE 6.7 Fluorine to carbon and oxygen to carbon peak area ratios for the copolymers produced from series 1 and 2

	Series 1		Series 2	
	F_{1s}/C_{1s}	O_{1s}/C_{1s}	F_{1s}/C_{1s}	O_{1s}/C_{1s}
A + CHA	1.08	0.05	1.73	0.03
CHE	1.12	0.03	1.05	0.05
CHD	0.80	0.04	0.85	0.04

where A = aromatic, CHA = cyclohexane, CHE = cyclohexene, CHD = cyclohexadiene.

The concentration of oxygen, between 2 and 4 per cent is not unexpected in view of the O_2 level seen in other copolymers. Increasing the electron take-off angle to 70° indicates a higher proportion of oxygen containing species at the surface, indicating the surface oxidation of the plasma on exposure to the atmosphere. The homogeneous nature of these films within the ESCA sampling depth is also revealed by the analysis at a 70° take-off angle.

6.4 Conclusion

The plasma copolymerization of benzene, naphthalene and biphenyl with their respective analogous perfluorocarbons all result in polymers whose compositions show similar trends, *i.e.* the C_{1s} envelope no longer shows the extensive rearrangement of the simple perfluorocarbon plasma polymer. This results in a large decrease in the amount of $CF\text{-}CF_n$, CF_2 and CF_3 functional groups in the polymer film. The fluorine to carbon stoichiometry of the deposited film reflects the gas phase composition in the plasma, *i.e.* a 1:1 copolymer will result if the gas phase has a 1:1 composition. The ratio of fluorocarbon to hydrocarbon in the gas phase is difficult to predict when using a 1:1 molar ratio of mixed sublimable solids. More success is achieved by using needlevalves and monitoring the flow rates of the simple and combined monomer vapours.

There appears to be a greater retention of the aromatic nature of the fluorocarbon monomer as evidenced by the increased $\pi \rightarrow \pi^*$ shake-up satellites in both the C_{1s} and F_{1s} core level spectra and the position of the peak formally assigned to CF. The position of this peak is very similar to the binding energy of the CF-CF peak in the spectrum of condensed octafluoronaphthalene, which is some 0.4eV less than the binding energy of CF in the pure perfluoroplasma polymer, *i.e.* the peak in the copolymer arises from $CF\text{-}CF_{aromatic}$ groups. Unfortunately, no information regarding the state of the aromatic hydrocarbon in the plasma copolymer can be derived from ESCA.

Optical emission from the OFN/N coplasma show that, on copolymerization, there is a great reduction in the amount of CF_2 emitting in the gas phase. An unknown peak at 510nm,

which seems to be associated with the difluorocarbene peak, also shows a reduction in the intensity such that it is no longer visible above the background.

From the composition of the deposited copolymer and the emission given off by the coplasma, the reaction pathway leading to the deposition of a film seems to have altered from that in the pure perfluorocarbon plasmas.

The copolymerization of perfluorobenzene and perfluoronaphthalene results in a copolymer whose composition is similar to that which results from each single perfluorocarbon plasma. However there is a difference, this is shown in a factor of two reduction in the amount of $\underline{C}F\text{-}CF_n$ and a reduction in the amount of CF_2 functionalities apparent in the C_{1s} envelope. This reduction in the amount of fluorine is reflected in the C:F stoichiometry of the copolymer which indicates that there has been an elimination of fluorine in the processes leading to deposition. This elimination of fluorine is not seen in the polymers resulting from the pure perfluoroaromatic compounds. As such, this is an indication that the behaviour of each monomer in the plasma has been altered by the presence of the other. Thus although the perfluoroaromatic compounds have not been stabilized, the polymer produced by a mixture of perfluorobenzene and perfluoronaphthalene in a plasma is not due to the independent codeposition of each individual monomer.

From the plasma polymerization of an aromatic with a non aromatic 6-membered ring system, using a combination of hydrocarbon and fluorocarbon, the copolymers produced by perfluorobenzene (plus hydrocarbon) all show stabilization of the

perfluorobenzene monomer. This is seen in the inhibition of rearrangement of the fluorocarbon component of the C_{1s} envelope compared with the single pure perfluoro plasma polymer. The compositional properties exhibited by these copolymers are analogous to those produced by the copolymerization of an aromatic fluorocarbon with its analogous hydrocarbon. The copolymerization of benzene (plus fluorocarbon) results in a copolymer whose fluorocarbon component, as seen in the C_{1s} envelope, is essentially the same as in the pure perfluoro plasma polymers, *i.e.* the fluorocarbon component has not been altered by the presence of the aromatic hydrocarbon in the plasma.

REFERENCES - Chapter Six

1. H.S. Munro, C.Till, Thin Solid Films, 131, 255, 1985.

2. H. Yasuda, T. Hsu, Surface Science, 76, 232 (1978).

3. K. Nakajima, S. Bourguard, A.T. Bell and M. Shen, Commun. - Table Ronde Int. Trait.Surf.Polym. Plasma, RT 15 8pp. 1977.

4. N. Inagaki, K. Nakazawa and K. Katsuura, J.Polym.Sci., Polym.Lett.Ed., 19(7), 335, 1981.

5. H. Pachonik, Ger.Patent 2,557,899, (1977).

6. E. Kay, A. Dilks, U. Hetzler, J. Macromol.Sci., Chem., A12 (9), 1393 (1978).

7. E. Kay and A. Dilks, J.Vac.Sci.Technol. 16(2), 428, (1979).

8. E. Kay, A. Dilks and J. Coburn, Topics in Current Chem., No. 94, S. Vepêk, M. Venugoplan, (Eds.), Springer-Verlag, Berlin Heidelberg (1980).

9a. Tokyo Shibaura Electric Co. Ltd., Japan Patent 81 60,447 (1981)

9b. Nippon Telegraph and Telephone Public Corp., Neth.Patent 80 04,541 (1981).

9c. Kazuo Horiguchi, Japan Patent 75 52,198 (1975).

9d. M. Miyamura, Jpn. Patent 78 120,527 (1978).

10. S. Morita, K. Yoneda, S. Ishibashi, J. Tamano, Y. Yamada, S. Hattori and M. Ieda, Symp.Proc. - Int.Symp. Plasma Chem. 5th, 1 259 (1981).

11. N. Petsev, M. Gigova, S. Ivanov, and C. Dimitrov, God. Sofii,Univ., Khim.Fak., 72(1), 73, (1977).

12. See Chapter Five.

13. D.R. Hutton, Ph.D. Thesis, Durham, U.K. (1983).

14. D.T. Clark and M.Z. AbRahman, J.Polym.Sci., Polym.Chem. Ed., 20, 1729 (1982).

15. See Chapter Five, Section 5.3.8.

16. P.W. Atkins, 'Physical Chemistry', Oxford University Press (1978).

17. D.T. Clark and D.B. Adams, Theor.Chim.Acta, 39, 321 (1975).

18. D.T. Clark and D. Shuttleworth, J.Polym.Sci., Polym.Chem. Ed., 18, 27 (1980).

19. J.R. Hollahan and R.P. McKeever, in 'Chemical Reactions in Electrical Discharges', Advances in Chemistry, Series 80, Am.Chem.Soc., Washington, D.C. (1969).

20. H.S. Munro and C. Till, J.Polym.Sci., Polym.Chem.Ed. in Press.

21. S.L. Madorsky, 'Thermal Degradation of Organic Polymers', Interscience, N.Y., Chapter 5 (1964).

22. H.S. Munro and C. Till, J.Polym.Sci., Polym.Chem. Ed., 24, 279 (1986).

23. D.T. Clark, H.R. Thomas, A. Dilks and D. Shuttleworth, J.Electron Spectrosc. Relat.Phenom., 10, 455 (1977).

24. See Chapter Two, Sections 2.3.1/2.

25. R. D'Agostino, F. Gramarossa, V. Colaprico and R. D'Ettole, J.App.Phys., 54(3), 1284 (1983).

26. D.T. Clark and M.Z. AbRahman, J.Polym.Sci., Polym.Chem.Ed., 19, 2689 (1981).

27. D.T. Clark, M.Z. AbRahman, J.Polym.Sci., Polym.Chem.Ed., 18, 407 (1980).

CHAPTER SEVEN

PHOTOPOLYMERIZATION

7.1 Introduction

Absorption of radiation, by molecules, plays an important role in organic chemistry. This energy input may have varying effects on a chemical reaction, from subtle changes in reaction rate to drastic alteration of reaction pathway.[1]

The absorption of a photon promotes a molecule from its ground state to an excited state, the level of excitation being dependent on the wavelength of radiation and hence the energy available:

where $E = h\nu = \frac{hc}{\lambda}$

h = Plancks constant, ν = frequency,

λ = wavelength and c = speed of light.

As the incident radiation energy increases from the microwave to the UV, excitation moves from rotational to vibrational and finally electronically excited states. At very high energies an absorption continuum is reached where the quantum of radiation absorbed results in ionization or dissociation of the molecule[1]:

$$M \xrightarrow{h\nu} M^{+} + \bar{e} \text{ or } X + Y$$

Before the ionization level is reached, however, the excited molecule, which is a new distinct chemical species with its own chemical and physical properties, may well react to stabilise the molecule. Excess energy is lost by a variety of radiative and non radiative processes (which includes both photophysical and photochemical reactions) to produce a more stable ground state molecule.

In an attempt to understand such processes numerous photochemical experiments have been carried out in different organic monomers. It was whilst carrying out such studies, limited to 200nm and above by experimental considerations, that the formation of a polymeric deposit which often accompanied a UV irradiation experiment, was noticed.[2]

This deposition of thin polymeric films by irradiating organic vapours with UV light has been termed 'Surface Photopolymerization'.[3] Polymers produced by this method possess some of the properties exhibited by the analogous plasma polymer, not least the integrity and strongly adherent nature associated with plasma polymers, but also possess many of the characteristics of the polymer prepared from the same starting monomer by conventional synthetic techniques. As an example, tetrafluoroethylene has been surface photopolymerized to give a very thin coating of high integrity which can be deposited directly onto substrates[4] to give a highly hydrophobic surface.[5] Similar polymer films of C_2F_4 have been prepared by plasma polymerization,[6] and like these films, surface photopolymerization produces a film which has structural differences from PTFE as shown by the presence of CF_3 groups.[4]

To some extent, therefore, surface photopolymerization ($200<\lambda<300$nm) could be considered as an intermediate between plasma and conventional polymerization, where starting materials range from conventional monomers such as ethylene[7] and butadiene[8] to materials not subject to conventional forms of polymerization such as benzene.[9] Although some organic compounds not conventionally polymerizable have been demonstrated

to undergo surface photopolymerization, the range, unlike plasma polymerization may be severely restricted by the lower wavelength limit of 200nm.

With the development of the rare gas low pressure resonance lamp in the 1950s,[10] the available photon energy was extended to the vacuum-UV and numerous workers studied the photolysis of organic compounds below this wavelength in the 1960s.[11]

Vapour	Wavelength/nm	Energy/eV
Xenon	147	8.4
Krypton	123.6	10.0
Argon	104.8-106.7	11.81-11.60
Helium	58.4	21.21

Benzene, in particular, has been the subject of extensive photochemical studies by several workers using photon energies below 200nm.[12a-d] Hentz and Rzad reported that the major photolysis product was a polymer.[12a] With 147nm radiation this polymer formation showed a pressure dependence similar to that at 184.9nm, namely that as the pressure increased polymer formation decreased.[12b] Jackson, Faris and Donn reported the major products of photolysis of benzene at 147nm were acetylene and fulvene along with polymeric material.[12c] Ward *et al* reported on the formation of two novel compounds, *cis* and *trans* hexa 1,3-diene-5-yne in the vacuum UV photolysis of benzene in the vapour phase, along with polymer:[12d]

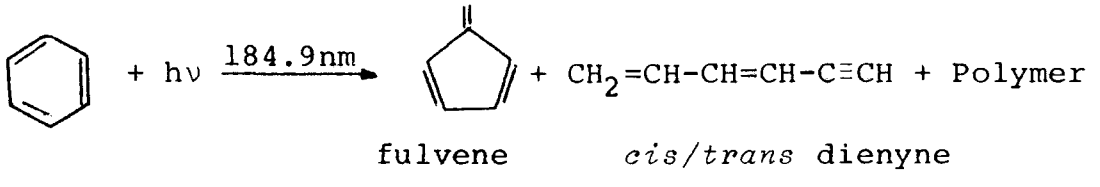

fulvene *cis/trans* dienyne

In all of these examples the polymer formed was not analysed but it has been reported that 'the general behaviour of this material was similar to that of cuprene'.[13]

Non aromatic molecules have also been photolysed by wavelengths below 200nm.[14] Scala and Ausloos studied the gas phase photolysis of cyclopropane with photon energies above and below the ionisation energy of c-C_3H_6 [15] (I.E. = 10.06eV≡122.9nm). The products formed in both experiments, at 104.8nm and 123.6nm, indicated that the major primary act is the formation of highly excited neutral cyclopropane molecules which may then relax by either rearrangement or by elimination of hydrogen or methylene. Interestingly, photolysis of the pure compound at both energies resulted in the formation of polymer on the window of the resonance lamp, whose growth rate in the presence of 5% oxygen or nitrogen oxide was inhibited.[15] This is in agreement with the work reported by Kozak *et al.*[16]

It has long been known that excitation of a plasma in the appropriate gas can provide a rich source of vacuum UV light.[17] Corbin, Cohen and Baddour studied the surface fluorination of various polymers using plasma discharges as the source of electromagnetic radiation.[18] They concluded that the radiation from this source, especially in the vacuum UV, was capable of enhancing the reactivity of the polymer surface toward fluorine gas.

This chapter presents the results of an investigation into the photopolymerization of N vinyl pyrrolidone (NVP) and perfluorobenzene using the output from an Argon plasma as the source of vacuum-UV. The structure and bonding in

the resultant polymers as determined by ESCA is reported, and a comparison made with the plasma polymer prepared from the same starting material.

7.2 Experimental

N-vinyl pyrrolidone was supplied by Aldrich and vacuum distilled prior to being degassed by freeze thaw cycles. Argon was supplied by B.O.C. and used as bought.

I. Photopolymerization

A calcium fluoride window, of 50mmx5mm dimensions (Specac) was mounted into an aluminium holder using viton 'O' rings - this is shown diagrammatically in Figure 7.1I. This assembly was then held in between two FG50 flanges as shown in a schematic of the experimental configuration in Figure 7.1II.

Each side of the window was pumped by an Edwards ED2M2 $21s^{-1}$ pump, a typical base pressure of 0.02mbar being achieved. For vacuum UV irradiations an Argon plasma was initiated on the right hand side of the window whilst the monomer vapour of interest was let into the left hand side of the window both flows being dynamic. The 50W Ar plasma with a pressure of 0.1mb, was sustained for one hour periods by a Tegal Corporation 13.56 MHz RF generator and LC matching network (as in Chapter Two). The photon output from the plasma irradiating a vertically positioned aluminium foil substrate in the presence of the organic vapour, placed 3cm behind the window. The substrate was held in place by Scotch double sided tape and removed after exposure for an ESCA analysis of any polymeric deposit.

I

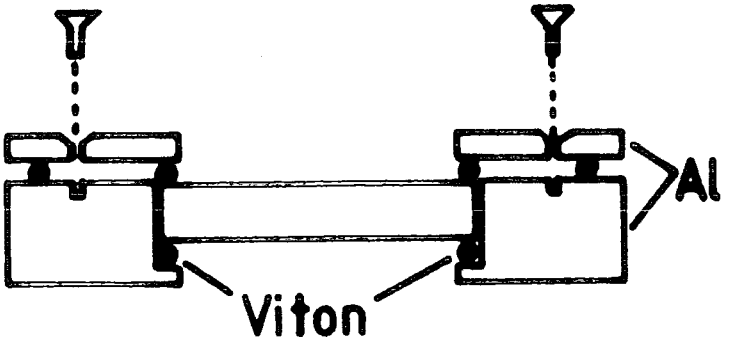

II

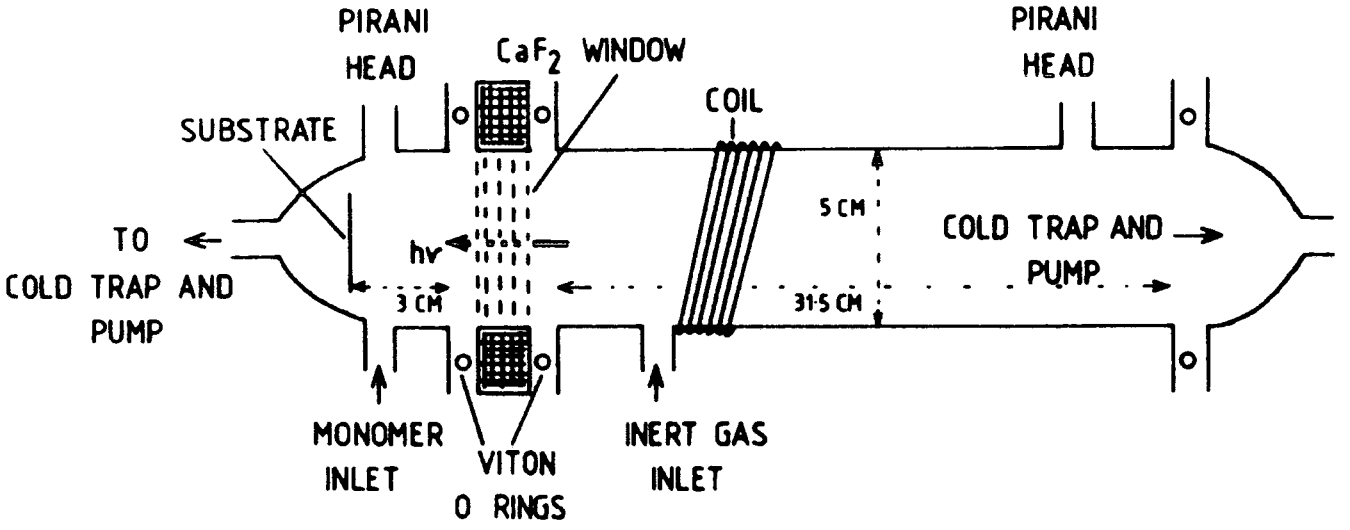

FIGURE 7.1 I and II Schematic of calcium fluoride window assembly (I) mounted as shown in (II)

Typical flow rates for the monomers were:

Monomer	Pressure/mb	Flow rate/cm^3STP min^{-1}
Perfluorobenzene	0.1	2.3×10^{-4}
NVP	0.095	1.3×10^{-4}
NVP	0.06	6.9×10^{-5}

For irradiation with wavelengths larger than 200nm, *i.e.* to eliminate wavelengths below 200nm, the output from an

Oriel Scientific Ltd. 200W medium pressure Hg/Xe arc lamp was used in place of the argon plasma.

After the deposition period, the sample chamber was let up to atmospheric pressure with nitrogen to limit the initial reaction of any reactive sites in the polymer matrix with oxygen. The aluminium foil substrate was then transferred and mounted onto a probe tip in air prior to ESCA analysis. For a fuller discussion of the ESCA and plasma experimental procedures the reader is referred back to the experimental section in Chapter Two.

FAB/SIMS spectra were recorded on a Kratos SIMS 800 system, and analysed using the Kratos SIMSCAN software package employing a DEC PDP-11 minicomputer. Samples were introduced into the SIMS spectrometer *via* a fast insertion lock. The base pressure of the system was $\sim 5 \times 10^{-10}$ torr. Argon gas was introduced into the ion gun to a pressure of 1×10^{-6} torr, and there subsequently to the neutralisation chamber of the FAB gun to a pressure of 3×10^{-6} torr.

The 3kV beam gave a secondary electron emission current of $\sim 5 \times 10^{-6}$A. Positive ion spectra were acquired using an 85 second acquisition period.

7.3 Results and Discussion

(I) N Vinyl Pyrrolidone (NVP)

NVP has previously been plasma polymerized[19] and its polymer shown to have the potential of forming a semi-permeable membrane when deposited onto a porous substrate.

This property is associated mainly with the hydrophilic nature of the plasma polymer derived from the oxygen and nitrogen containing functionalities in the surface. Yasuda[19] did not, however, attempt to characterize the surface composition of the plasma polymer.

The presence of the pendant vinyl group in the N vinyl pyrrolidone molecule indicates the possibility for conventional polymerization mechanisms to occur, both by photon irradiation[20] and/or electron impact,[21] within a plasma environment. This could produce a linear polymer with pendant pyrrolidone groups. Since both radical and cationic species exist in a plasma it is not unreasonable to postulate reaction pathways based on these processes. The mechanism whereby NVP polymerizes within a plasma has not yet, however, been determined. The amorphous and highly cross-linked film contains functional groups not originally present in the starting material indicating that monomer structure is not retained in the polymer. This would tend to indicate that conventional polymerization processes are not dominant.

NVP was chosen for photopolymerization studies since the presence of functional groups within the molecule could allow polymerization to occur by photochemical pathways. By comparison with the structure of the plasma polymer, the photo polymer would then highlight the importance, or absence of, photochemical reactions occurring in plasma polymerization.

(a) Mercury/Xenon Photopolymerization

Due to the extremely low vapour pressure of NVP, when using a needlevalve fully open the pressure was still only 0.06mb and hence experiments were carried out at this pressure and the full vapour pressure only.

Both high and low flow rates of NVP produced a polymer when the monomer vapour was irradiated with a mercury arc lamp. Although the cut-off† wavelength of the calcium fluoride window is at ∿130nm and the light output from the mercury arc lamp goes down to ∿180nm with fused silica lenses, air starts to absorb below 200nm. This means that the maximum effective energy available for the polymerization of NVP is up to ∿6.2eV. As the surface composition of each, as revealed by ESCA, are identical only the core level spectra for the polymer produced by the low flow rate of monomer are displayed in Figure 7.2.

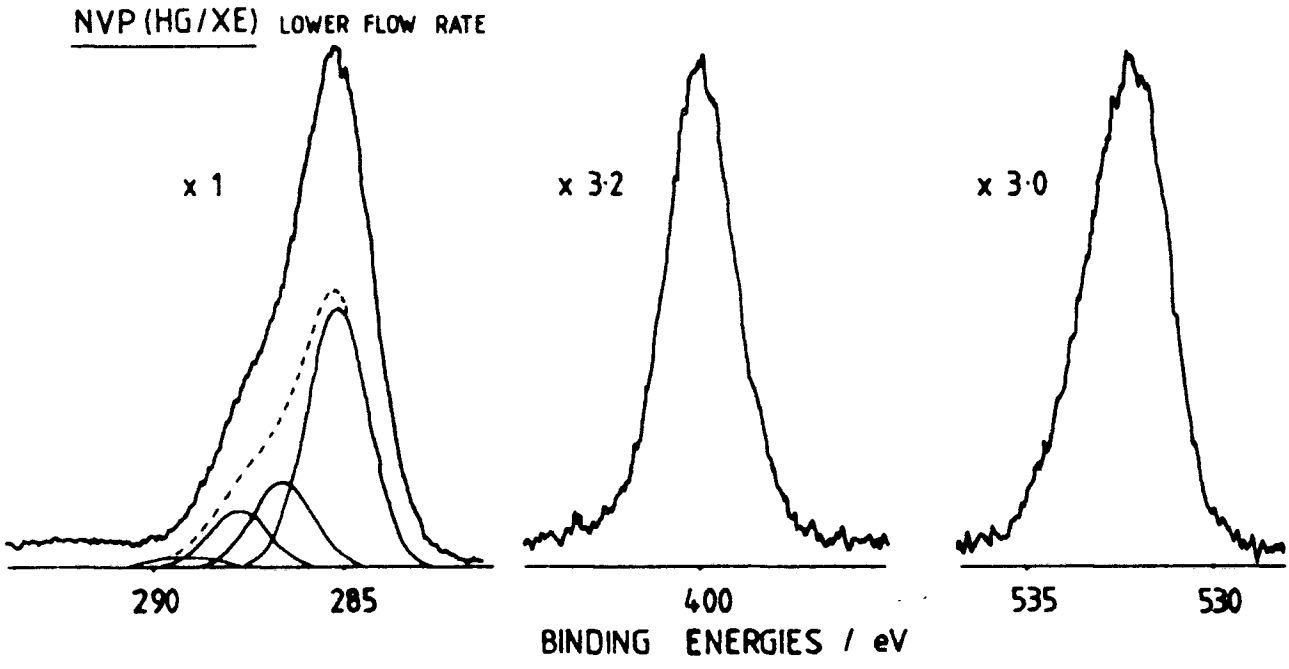

FIGURE 7.2 Core level spectra for UV photopolymerized NVP

†The cut-off point of an optical filter is defined as the wavelength below which there is less than 50% transmission.

The N_{1s} signal is present at a binding energy of 399.4eV (corrected for charging) and consists of essentially the one main photoionisation peak. This is in contrast to the O_{1s} core level which is composed of at least two different environments at binding energies of 531.8 and 533.8eV. In some of the N_{1s} core level spectra, acquired using analogue mode, however, there is evidence for a very small peak to lower binding energies of the main photoionisation peak. The main drawback to using an XY plotter is the inability to acquire and average several scans to improve the signal to noise ratio, thus any peaks of very low intensity may get 'lost' in the background. Thus the nature, either real or apparent, of the low binding energy peak was not ascertained.

The C_{1s} envelope consists of the main photoionisation peak at 285eV, due to carbons not attached to nitrogen or oxygen, with a sloping shoulder to higher binding energies. Peak fitting of the core level, using standard peak fitting techniques developed by Clark *et al*[22] gives rise to peaks at 286.6, 288.1 and 289.1eV. These have tentatively been assigned to C-N or C-O, O=C-N and O=C-O functional groups respectively. However as the chemical shifts demosntrated by oxygen and nitrogen containing functionalities are very similar a definitive assignment is not possible.

The C:N:O ratio calculated using the appropriate peak areas gives rise to a stoichiometry of $C_1:N_{0.13}:O_{0.14}$ for the polymer film. This is very close to the atomic ratio of the monomer, whose stoichiometry is $C_1N_{0.16}O_{0.16}$, indicating that there has been very little elimination of nitrogen and oxygen taking place in the processes leading up to polymer formation.

Studies of the polymer films using a 70° electron take-off angle reveal the films to be vertically homogeneous throughout the ESCA sampling depth, and also shows the presence of extraneous hydrocarbon contamination. This hydrocarbon overlayer will cause the signals from oxygen and nitrogen to appear artificially low due to the smaller sampling depths of the N_{1s} and O_{1s} core levels, thus giving a possible explanation for the apparently low content of these two elements. However, it has been previously noted in other oxygen containing systems that UV irradiation can be accompanied by elimination of the carbonyl group[1,2] and thus a small amount of oxygen elimination cannot be ruled out.

Over the 1 hour period, the rate of deposition of the two polymer films varied. Using the higher flow rate of NVP a thicker film was produced which completely suppressed the Al_{2p} core level signal whilst at the lower flow rate the film thickness, produced from the higher flow rate, is greater than 70Å. The film produced by the low flow rate is about 60Å thick.

In plasma polymerization, the rate of deposition falls into two regions.[23] The first region is monomer deficient; here there is sufficient power within the system but the amount of monomer available is limited. The second region is power deficient, there is sufficient monomer within the system but energy availability is limited.[23] Thus if a graph is plotted of deposition rate against the $^{W}/_{FM}$ parameter, an increase in monomer availability will increase the deposition rate up to a point where the amount of power available becomes the limiting factor when a further increase in monomer will reduce the deposition rate:

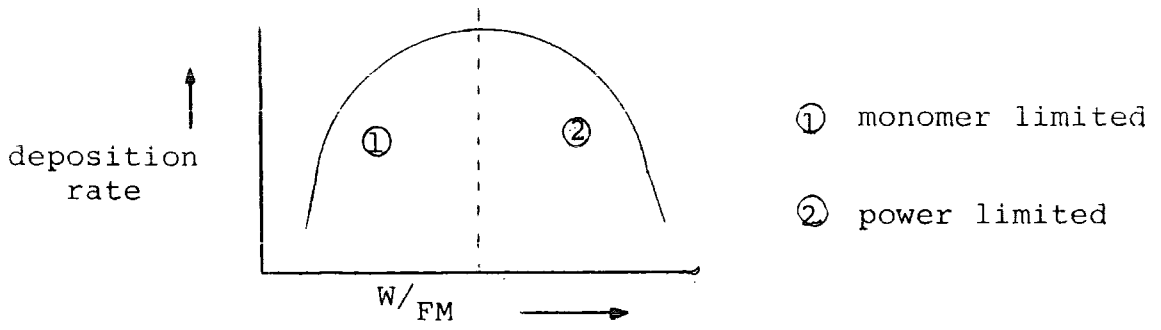

An analogous situation may exist in the deposition rate during photopolymerization of NVP, where W now refers to the photon flux from either the mercury arc lamp or the argon plasma. Both flow rate values are still in the area of the curve which is monomer deficient and thus an increase in the amount of monomer available at the higher flow rate has the effect of increasing the deposition rate.

That there has been no contamination from the silicon tape used to hold the substrate in position during irradiation is evidenced by the lack of a signal from the Si_{2p} core level in both deposition experiments.

(b) Vacuum UV Photopolymerization

Both high and low flow rates of NVP gave rise to a polymer when the vapour was irradiated by the output from an argon plasma. Unlike the polymers produced by $\lambda \geq$ 200nm radiation, however, the two polymers produced by $\lambda \geq$130nm radiation are different in composition. The spectra recorded from the polymer deposited at the lower flow rate are identical to those produced by mercury arc lamp irradiation and are therefore not repeated here.

The C_{1s}, N_{1s} and O_{1s} core level spectra for the polymer produced at the higher flow rate are displayed in Figure 7.3.

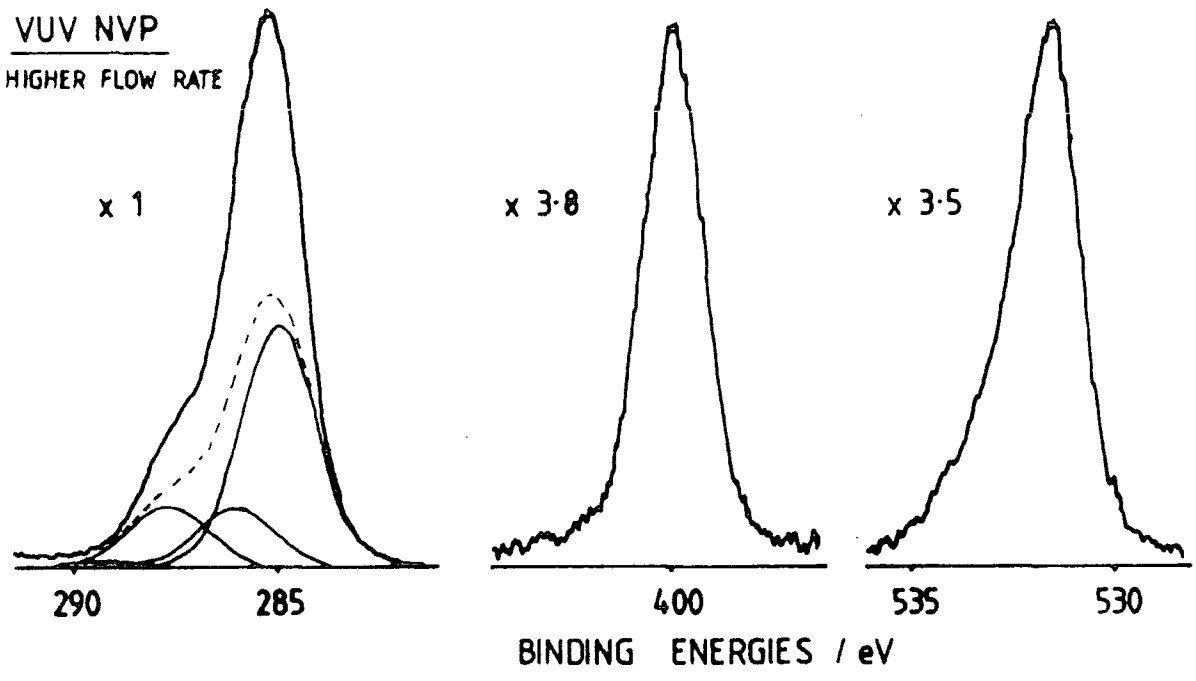

FIGURE 7.3 Core level spectra for VUV photopolymerized NVP using a higher flow rate

The two sets of spectra, *i.e.* from both high and low flow rate polymers, are remarkably similar. Both give rise to a film with the same stoichiometric composition of $C_1N_{0.13}O_{0.14}$ and the C_{1s} envelopes of both are visibly very similar although not identical.

The main difference, as far as ESCA is concerned, is in the peak fitting of the C_{1s} envelope. The component peaks in the C_{1s} envelope of the film formed at a higher flow rate are shifted closer into the main photoionisation peak, and the peak at 288.7eV is reduced in intensity and in some instances lies only just above the detection limit. The ex-

ception to this is the polymer formed by $\lambda \geq 200$nm radiation at high flow rates which is much closer in composition to the polymers produced by a low flow rate of NVP.

Peak	Binding Energy/eV	
	Low	High
CH	285.0	285.0
C-N/C-O	286.6	286.0
O=C-N	288.1	286.4
O=C-O	289.1	288.7

TABLE 7.1 Binding energies of component peaks in the C_{1s} envelope as a function of flow rate

This situation is identical to that which occurs in the plasma polymers derived from NVP under the two different flow rate conditions using a lower power (see Chapter One), *i.e.* two different polymers are produced whose dissimilarity is apparent on peak fitting the C_{1s} envelopes. Since the binding energies of the component peaks are now different, peak assignment is made even more difficult. The same functionalities, but in different environments, may be responsible for the component peaks in the C_{1s} envelope of the high flow rate polymer. But equally well these could be derived from different functional groups.

The ESCA evidence therefore points to the fact that polymerizing N vinyl pyrrolidone will result in one of two different polymers generally dependent upon the flow rate condition used for the polymerization.

(1) Low flow rate conditions - plasma polymerization and photo irradiation, by both mercury arc lamp and plasma emission, produce identical polymer films.

(2) High flow rate conditions - plasma polymerization and irradiation by the plasma output will produce identical polymers but different to those above.

The exception to this is the polymer formed under high flow rate conditions by mercury arc lamp irradiation whose composition falls into group 1. This phenomena could be associated with a W/F parameter. As with deposition rate, the composition of the polymer could also be affected by altering the value of this parameter. Those in group 1 would appear to be mainly limited by the amount of monomer flowing through the reactor whilst those in group 2 are energy sufficient. The exception, the polymer composition formed at high flow rates, would appear to be due to insufficient energy input into the system which causes a group 1 type polymer to be formed.

It should be stated here that the same phenomena could apply to plasma polymerization, that is, as the $^{W}/_{FM}$ parameter changes, the composition, as well as deposition rate, is affected. No one to date has made a systematic study of the composition of a plasma polymer as a function of its $^{W}/_{FM}$ value, it has previously been tacitly assumed that the polymer composition at one end of the curve is identical to that at the other end.

This similarity/dissimilarity between the two types of polymer composition evidenced by the chemical shifts in the C_{1s} envelopes, is reflected by the surface energies of the two different groups. Those polymer films formed primarily under low flow rate conditions have a measurable contact angle with distilled water of around 50^{o}. This is in contrast to those

films formed by plasma polymerization and vacuum UV irradiation under high flow rate conditions which have a very hydrophilic surface, *i.e.* the contact angle $<5^{o}$.

Unfortunately, the percentage intensity of component peaks of the C_{1s} envelope of each group do not fall neatly into any real trends. Plasma polymerization using a high flow rate - group 2 polymer - produces a film whose composition is much richer in the component at ∿288eV with a reduced amount of the component at ∿289eV. On the other hand, the composition of the polymer formed by UV irradiation - group 1 polymer - appears to be closer, in percentage intensity of the component peaks, to the plasma polymer produced at high flow rates.

However, it should be added that discrepancies might arise in peak intensities due to the fact that some of the peaks were digitally fitted using the DS300 whilst others were fitted using a curve resolver which produces errors of consistency, especially in maintenance of the FWHH.

To examine these films further, SIMS spectra were recorded on a Kratos SIMS 800 spectrometer. The conditions were not optimized but all spectra were recorded under identical conditions. The SIMS spectra shown in Figures 7.4I and II are for the vacuum UV photopolymerized NVP under low and high flow rate conditions respectively. Spectra from the plasma polymers are shown in Chapter One, whilst those from the UV irradiated NVP are in Appendix One.

The positive ion spectra of both NVP polymer films are quite complex and the present aim is not to undertake a comprehensive analysis of the fragment peaks but to highlight any

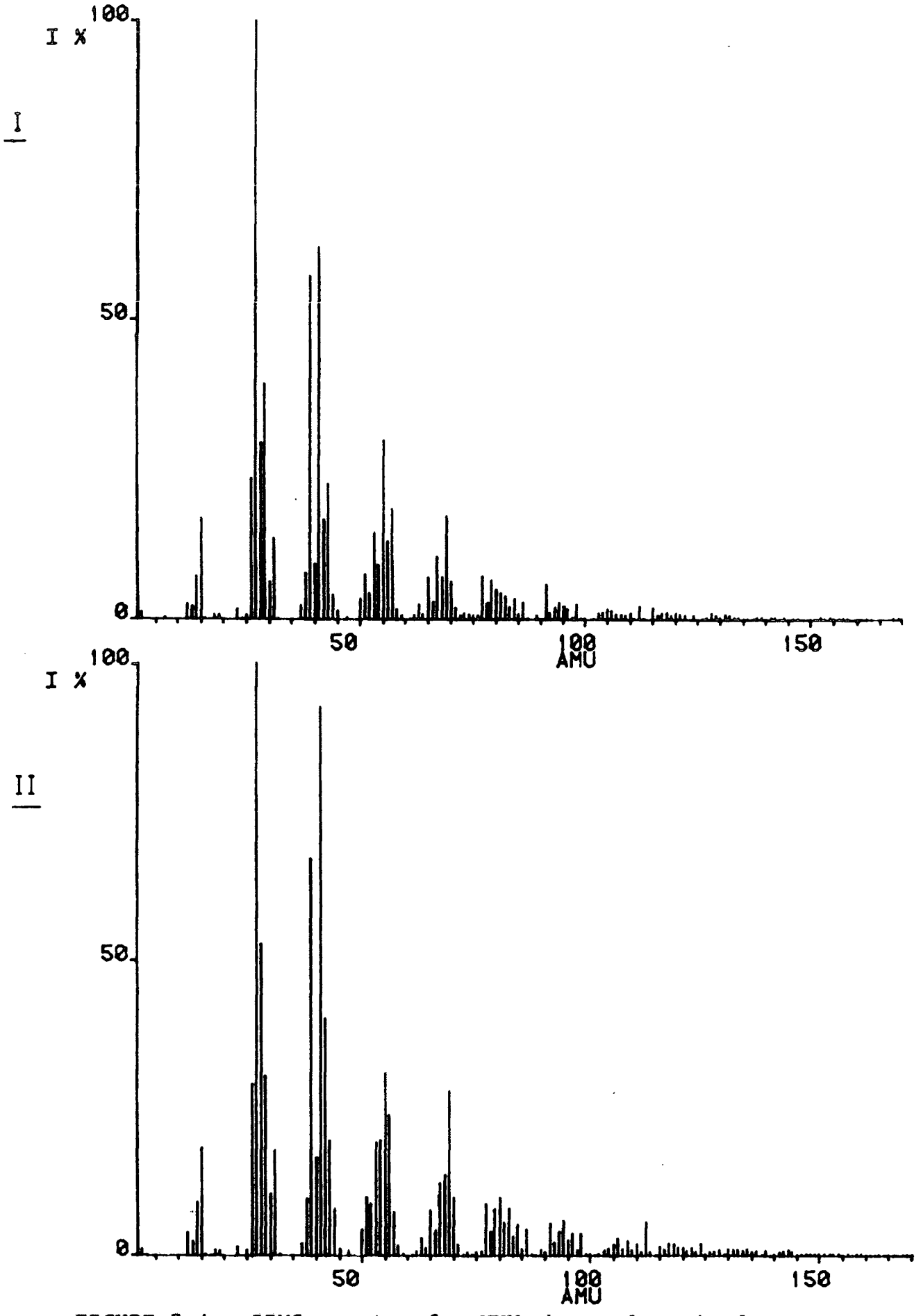

FIGURE 7.4 SIMS spectra for VUV photopolymerized NVP
I. low flow rate, II. high flow rate

features which may be used as a monitor for the differences in each sample.

Like the ESCA spectra, the SIMS spectra in Figures 7.4I and 7.4II are remarkably similar to each other, but there are slight differences in the fragmentation patterns. This is particularly noticeable in the relative intensities of each peak within the groups at 28, 29, 30; 46, 47, 48; 55, 56 and 57 AMU. This difference is reproducible between the other NVP derived films (see Chapter One and Appendix One). For the film formed under high flow rate conditions, the intensity of each fragment peak decreases from one peak to the next within each group of three. However, for the low flow rate polymer, the middle peak of each group has the smallest intensity. Possible fragments giving rise to each of these peaks are given in Chapter One.

ESCA, SIMS and contact angle measurements, therefore, all indicate that although N vinyl pyrrolidone can be polymerized under different flow rate conditions by three different 'sources', only two distinct polymer types are produced.

Work on chloroacrylonitrile, which is in progress, has also shown that there are similarities between the polymers produced by plasma polymerization, vacuum UV and UV irradiations[24].

Whilst carrying out these photopolymerization studies, two problems associated with the use of an optical filter quickly became apparent. The first, and more important, was the gradual build up of polymer on the window during deposition. This caused not only a gradual decrease in the light intensity irradiating the vapour/substrate over the hour long exposure , but also problems associated with film removal from the window

after each experiment. Chemical etching of the surface with dilute hydrogen fluoride has been reported as one method for polymer removal,[12d] whilst washing with solvent is another.[12a] Throughout these experiments the window was placed in a very high power (∿80-100W) oxygen plasma after each irradiation to oxidise the polymer film to simple gases which could then be pumped away. The removal of this 'unwanted' film is very important, especially for the vacuum UV polymerizations since the films absorb radiation below 200nm and hence can cause problems with polymer formation, in the case of PFB - see next section - or with polymer type in the case of NVP.

The second problem is associated with the irradiation of the window itself. This caused the formation of absorption bands in the visible and ultraviolet regions.[25] The colour in the visible region being dependent on the nature of the crystal, for CaF_2 a purple/blue colouration was produced. The defects in the crystal giving rise to this colouration are called F or V centers depending upon the defect.

These centers are believed to be formed as shown by the schematic representation below:

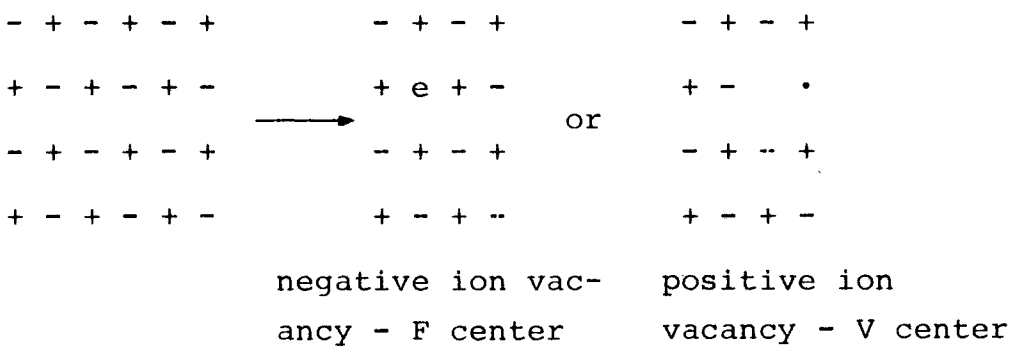

FIGURE 7.5 Formation of F and V Centres in CaF_2

Irradiation of the regular three-dimensional array of positive and negative ions causes electrons to be ejected from some of the atoms in the crystal lattice. Whilst most of these electrons return to the relevant atoms, some are trapped and held in a negative-ion vacancy to form F centers. The formation of a V center is by the loss of an electron from one of the negative ions surrounding a positive ion vacancy, to form an atom.[25]

These absorption bands can be bleached by heating or by irradiation of the window with the mercury arc lamp, the electrons being released from their traps to combine with electron deficient centers. Therefore after cleaning the window with an oxygen plasma, it was placed in front of the mercury arc lamp for thirty minutes.

(II) Absorption of Fluorocarbons

The UV absorption spectrum of a given molecule is due to electronic transitions from the molecular ground state to one or more of its excited electronic states; the energy of the absorbed photon being equal to the energy difference between the excited and ground states.[1] These excited states are either Rydberg or valence shell[26] in nature although mixing between them is possible.

Rydberg states can be thought of as states in which the excited electron 'occupies' a molecular orbital of large size. The excited electron is therefore far from the 'core' which is nearly pointlike compared to the size of the orbital.[26] Molecular Rydberg transitions yield a series of bands whose wave numbers can be expressed by Rydberg formulas:

$$\frac{1}{\lambda} = I - \frac{R}{(n-\Delta)^2}$$

where λ = wavelength in cm^{-1}; I = ionization potential;

n = principal quantum number;

R = Rydberg constant = 109737.3 cm^{-1};

and Δ = 'quantum defect' which takes into account the fact that energy also depends on the azimuthal quantum number, l.

$\frac{R}{(n-\Delta)^2}$ = Rydberg 'term' and has determined values.

In all aromatic molecules the valence shell $\pi \rightarrow \pi^*$ bands are the bands of lowest energy and at least two or three of these are encountered before reaching the lowest Rydberg band.[26]

For benzene, the lowest energy $\pi \rightarrow \pi^*$ transitions have been determined and are centred at 254, 204 and 184nm respectively.[27] The first two bands are formally symmetry forbidden although vibronic mixing does occur to give weak bands in the absorption spectrum. The third band, however, is allowed.

Vibronic mixing occurs when vibrations of the molecule destroy its symmetry and therefore removes the constraints of the formally symmetry forbidden transition which can then occur.

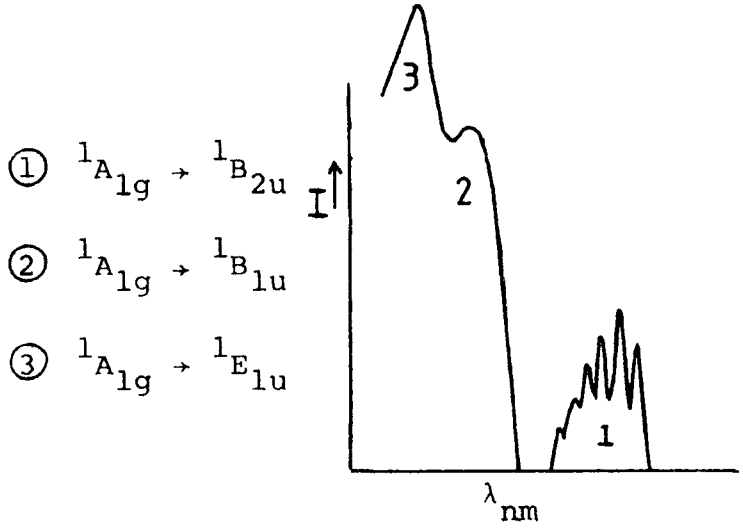

FIGURE 7.6 UV absorption spectrum of benzene

The effects on the absorption spectrum resulting from the substitution of hydrogen for fluorine has been labelled as the 'Perfluoro Effect'.[28] Its effects on the photoelectron spectroscopy of PFB in comparison to benzene has been studied by Brundle, Robin and Kuebler.[28] They found that the fluorination of benzene results in a shift of around 0.5eV to higher energies in the first two ionisation potentials.

The substitution of hydrogen for fluorine atoms should influence the absorption spectrum mainly by the inductive effect of fluorine which is expected to affect the σ orbitals much more than the π orbitals.

The UV and vacuum UV absorption spectra of fluorocarbons has been examined by Sandorfy *et al.*[29,30] The substitution for fluorine in methane and ethane causes a shift in absorption bands to higher frequencies.[29] In perfluorobenzene, the $\tilde{X}^1A_{1g} \rightarrow \tilde{B}^1B_{1u}$ $\pi \rightarrow \pi^*$ transition of benzene is shifted slightly to higher frequencies whilst the $\tilde{X}^1A_{1g} \rightarrow \tilde{C}^1E_{1u}$ transition is shifted to lower frequencies.[30] The influence on the $\sigma \rightarrow \sigma^*$ transition upon perfluorination of benzene is stronger, as with the paraffins,[31] fluorine substitution stabilises the σ levels and shifts the $\sigma \rightarrow \sigma^*$ bands to higher frequencies in PFB.[30]

The first Rydberg bands of perfluorobenzene possibly begin to appear in the high energy region of around 140nm.[30]

The lone pair of electrons in the fluorine atoms have ionization potentials of $\sim$16-17eV and their electronic transitions are expected to appear at wavelengths shorter than

120nm[30] and would thus not be expected to contribute to the photochemistry of a fluorocarbon when irradiated with wavelengths longer than 130nm.

III. Perfluorobenzene (PFB)

(a) Mercury/Xenon Photopolymerization

A one hour irradiation of PFB vapour was not successful in producing a polymer, so the exposure time was lengthened to six hours which still did not cause polymer formation to occur on the aluminium substrate. As the maximum energy available from irradiating PFB with the mercury arc lamp is ∿6.2eV, *i.e.* wavelengths greater than 200nm, the importance of the transitions at ∿254 and ∿204nm can be discounted as being of any real relevance in the photopolymerization of perfluorobenzene.

(b) Vacuum UV Photopolymerization

Perfluorobenzene vapour was then irradiated with the electromagnetic output from an Argon plasma. In this instance photopolymer formation was observed indicating that photopolymerization of PFB had occurred using wavelengths between ∿130 to ∿200 nm, *i.e.* ∿8.3 to ∿6.2eV.

Photopolymerization of PFB using vacuum UV irradiation was not unexpected. The photolysis of hexafluorobenzene at 185nm has been previously examined and polymer formation reported as one of the products.[32]

The vacuum UV emission from an inductively coupled RF plasma in Argon has been previously reported.[33] The most intense portion of the observed output is associated predomin-

antly with the Ar(I)† resonance lines at 104.8 and 106.7nm respectively being some two orders of magnitude more intense than the Ar(II) lines at 93.2 and 92.0nm. Although there is still a significant output in the UV/visible from the plasma, the intensity is generally two orders of magnitude or so lower than for the vacuum-UV components[33] and since the calcium fluoride window employed in these experiments has a wavelength cut-off at 130nm, the resonance emission lines will not contribute to surface photopolymerization. However, emission lines from argon also occur between 150 and 200nm which, as previously stated, gives the maximum energy available of 8.3eV. This is not enough energy to form a perfluorobenzene radical cation, the first ionization potential of PFB is at 9.97eV.[34] Therefore the ionized state of PFB cannot play an important role in vacuum UV photopolymerization.

ESCA Analysis

The C_{1s}, F_{1s} and O_{1s} core level spectra of the films derived from PFB irradiated with wavelengths below 200nm are shown in Figure 7.7. The absence of a signal from aluminium indicates that the film thickness is greater than 70Å. These core level spectra are not unlike those produced by the plasma polymerization of perfluorobenzene. The F_{1s} core level has a main photoionization peak at 689.5eV and is accompanied by a small shake-up satellite to higher binding energies. This peak at 697.5eV is diagnostic of the presence of unsaturation in the polymer network[35] and is due to fluorines which are bound to unsaturated carbons. This unsaturation is also shown in the C_{1s} core level.

---

† Ar(I) lines result from transitions of the neutral atoms.
Ar(II) lines result from transitions of the singly ionized state.

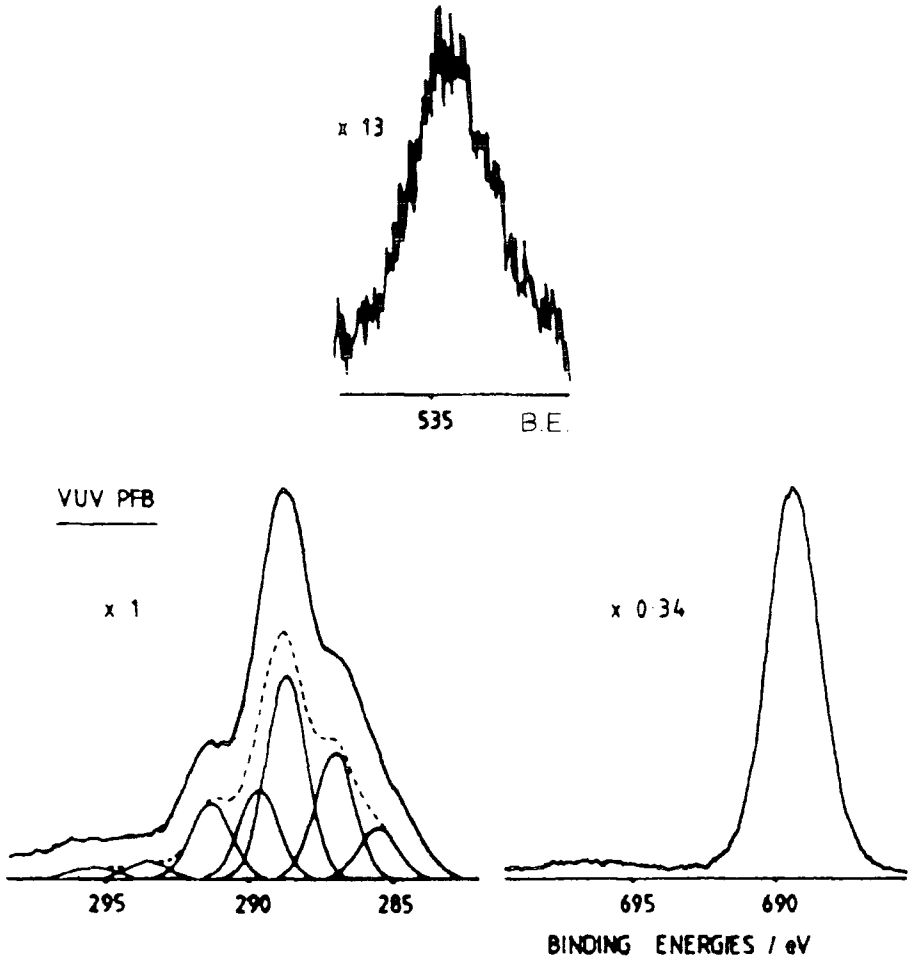

FIGURE 7.7 Core level spectra for Vacuum UV photo-polymerized PFB

As with the plasma polymer, there is a small signal from the O_{1s} core level, indicating the presence of approximately three oxygen atoms to every 100 carbon atoms. This 'contamination' is most likely to arise from small leaks within the vacuum line, and by subsequent exposure of the polymer film to the atmosphere after formation.

Peak fitting of the C_{1s} envelope indicates contributions arising from C-H, C-CF, C-F, CF-CF_n, CF_2, CF_3 and $\pi \rightarrow \pi^*$ shake-up satellites. The hydrocarbon results from extraneous contamination as shown by the C_{1s} level using a 70° electron take-off angle, allowing for this the F:C atomic ratio is 0.91:1, *i.e.* very close to that of the starting material.

It is also very similar to the atomic ratio produced by the plasma polymerization of perfluorobenzene. Figure 7.8 gives the component peak fits of the C_{1s} envelopes produced by plasma polymerization and by vacuum UV irradiation. Table 7.2 indicates the percentage contributions arising from each of these peaks (corrected for the hydrocarbon contamination), and their binding energies.

TABLE 7.2 A comparison of the component analysis of the C_{1s} envelope: Plasma polymerization *versus* vacuum UV polymerization

Peak	Percentage Contribution		Binding Energy Shifts (eV) from the hydrocarbon at 285.0eV
	Plasma Polymer	Vacuum UV Polymer	
C-CF	26	24	1.7
CF	49	56	3.63 + 4.7
CF_2	15	15	6.6
CF_3	8	3	8.2
$\pi \rightarrow \pi^*$	2	2	11.0

It can be seen from comparison of the ESCA data in Figure 7.8 and Table 7.2 that the polymers derived from perfluorobenzene, by irradiation with vacuum UV and by plasma, reveal some remarkable similarities. Although there are very slight differences in the intensities of the C_{1s} component peaks - the most noticeable is a reduction in the number of CF_3 functionalities in the vacuum UV photo-polymer - the type of environments as detected by ESCA is the same. So too, are, within experimental error, the binding energy shifts within the carbon 1s core level.

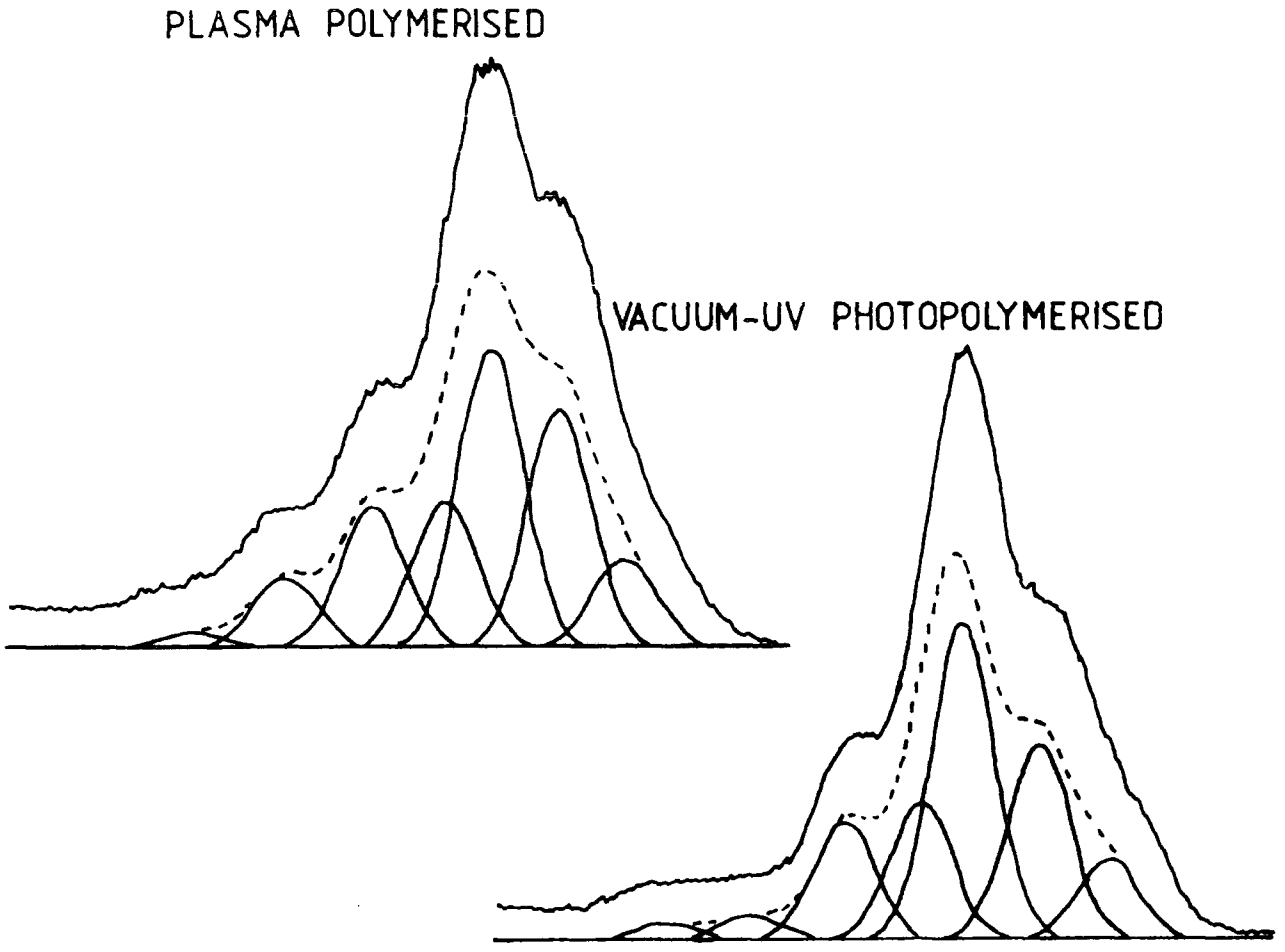

FIGURE 7.8 Component peak fit of the C_{1s} envelope for plasma polymerized and VUV photopolymerized PFB

Further, since the fluorine to carbon stoichiometry in both of these polymer films is close to unity, the mechanistic pathway which results in polymer formation in both cases involves the retention of the monomer atomic ratio, *i.e.* elimination of fluorine which is observed in the plasma polymerization of the lower fluorinated aromatic molecules does not occur.[36]

The similarity of the C_{1s} envelopes for the photopolymer and plasma polymer, *e.g.* the presence of CF_2 and CF_3 environments strongly suggests that the reactions of perfluorobenzene in both cases follow similar pathways. As already mentioned

earlier, the energy available for photopolymerization is less than that required for photoionisation.[34] Consequently this material must be derived from reactions initially involving electronically excited states of perfluorobenzene. Electron impact excitation of perfluorobenzene in the plasma to the same excited states could lead to a similar material being deposited. The observed differences in the C_{1s} envelope of the two materials might arise from variations in the flux and distribution of the excitation energy.

This similarity between the products of a reaction which is initiated by different means has been documented. Aliphatic hydrocarbons, for example, are transformed into mixtures of paraffins, olefins and acetylenes. These products are the same whether formed by plasma reactions or by pyrolysis.[37] Similarities are also observed between plasma reactions and photochemical reactions in, for example, the isomerization of olefins,[38] and between the behaviour of a substance in plasma reactions and in mass spectroscopy.[38] In the latter case this is not totally unexpected since both involve the collision of an electron as the initial step. The one big difference between the two collisional processes is in the energy of the electron, which is about 70eV in a mass spectrometer but only a few electron volts in a glow discharge.

Since the products of both plasma polymerization and vacuum UV irradiation show strong similarities, the mechanism in the plasma leading to polymer formation may be understood by considering the vacuum UV photopolymerization. Simplistically, since the products are almost identical, it is reasonable to assume the existence of similar mechanisms. If this is so,

reactions involving the radical cation, although essential for the maintenance of the plasma do not need to be involved in the pathway for polymer building block formation.

This point emphasises a fact which has been discussed in the introductory chapter in plasma diagnostics. Namely, that the presence of an emission from a certain species does not identify it as being involved in polymer forming reactions. In a perfluorobenzene plasma the peak due to emission from a radical cation is very prominent in the gas phase emission spectrum (see Figure 2.6) but the radical cation has now been ruled out as being directly important in any deposition mechanisms which occur in the plasma.

To check whether the appellation of Surface Photopolymerization[3] could be applied to the processes occurring when PFB vapour was irradiated with vacuum UV light, half of the calcium fluoride window was masked with paper. Upon examination of the substrate by ESCA, the irradiated portion of aluminium showed the normal core level spectra associated with a PFB polymer. However, the non irradiated sample of aluminium showed only the characteristic spectra of adsorbed perfluorobenzene. Deposition had therefore only occurred on the irradiated aluminium.

The C_{1s} and F_{1s} core level spectra for adsorbed perfluorobenzene on aluminium are shown in Figure 7.9. The oxygen signal in this instance is very large and is dominated by the signal due to oxide on the substrate surface. The C_{1s} signal is very intense and is due mainly to the hydrocarbon contamination on the substrate surface. The signal due to the adsorbed fluorocarbon is, in relative terms, much

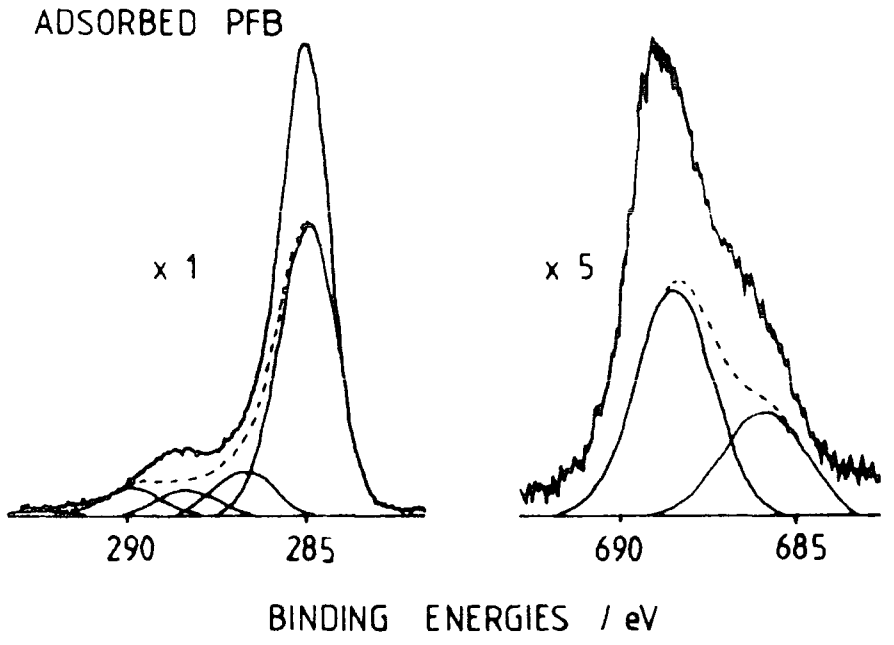

FIGURE 7.9 C_{1s} and F_{1s} core level spectra for adsorbed PFB

---

less intense and is 'buried' in the shoulder to higher binding energies of the main photoionisation peak amongst the oxidised hydrocarbon. It is the fluorine F_{1s} core level which is of most interest.

Analysis of the broad envelope of the F_{1s} envelope allows the identification of two different types of fluorine environment. The main peak, centered at 686.6eV, is due to fluorine covalently bonded to carbon. The shoulder to this peak shifted approximately 2eV to lower binding energies is thought to be due to the interaction of adsorbed perfluorobenzene with the substrate surface. It is definitely not due to metal fluoride formation as this would be shifted some 2eV lower still. This has been shown in the work of Goosedge and Cadman[39] who studied the interaction of PTFE with various metals and found the peak due to metal fluoride was shifted so much to lower binding energies that the F_{1s} spectrum consisted of two essentially independent peaks - organic fluoride and metal fluoride.

If the amount of perfluorobenzene adsorption forms only a monolayer coverage, as indicated by the thickness of the adsorbed layer which is $\sim$5Å, then the intensity of the peak at lower binding energies in relation to that at higher binding energies should give, perhaps, some indication of the orientation of the adsorbed molecule.

Adsorption studies of benzene in graphitized carbon black and boron nitride have been previously reported[40]. There the benzene molecule is considered to lie flat with the substrate. If this was the case for perfluorobenzene adsorbed into aluminium, all six fluorine atoms would be equally affected by the interaction and there would only be a simple environment present in the F_{1s} spectrum. This is not the case, however, since the peak at lower binding energies has only a third of the total area. This is suggestive of the molecule adopting a vertical orientation, perpendicular to the surface. In this model, only two out of the six fluorines will interact with the substrate causing the electronic environment of just two fluorines to be affected; thus giving rise to two environments with peak area ratios of 2:1 in the F_{1s} core level.

Studies on the rate of polymer deposition by vacuum UV irradiation were hampered by two problems. Firstly, information available from the C_{1s} spectrum about the amount of polymer formed at low irradiation times is very limited. This is due to the intense signal from the underlaying hydrocarbon layer when the polymer film is less than $\sim$40A thick. The greater thickness of polymer coating with longer irradiation times causes this to be less of a problem, since the signal

from the fluorocarbon will be much more intense in relation to that from the hydrocarbon underneath.

Although studies of deposition kinetics were concentrated mainly over the first 15 minutes of irradiation, when the aluminium signal was still intense, it is noticeable that the amount of CF_3 and $\pi \rightarrow \pi^*$ shake-up satellite component peaks increased linearly over the 60-minute irradiation period from 1-2 and 2-3% respectively. Other trends are not at all apparent, the C-F component seems to increase and then decrease whilst the CF_2 and CF-CF components seem to decrease and then increase.

The second problem is associated with the calcium fluoride window. After a series of exposures it was seen that the 'polymer' film deposited was no longer characteristic of perfluorobenzene. The C_{1s} core level was dominated by a peak due to hydrocarbon contamination with a small shoulder to higher binding energies - Figure 7.10. This is thought to

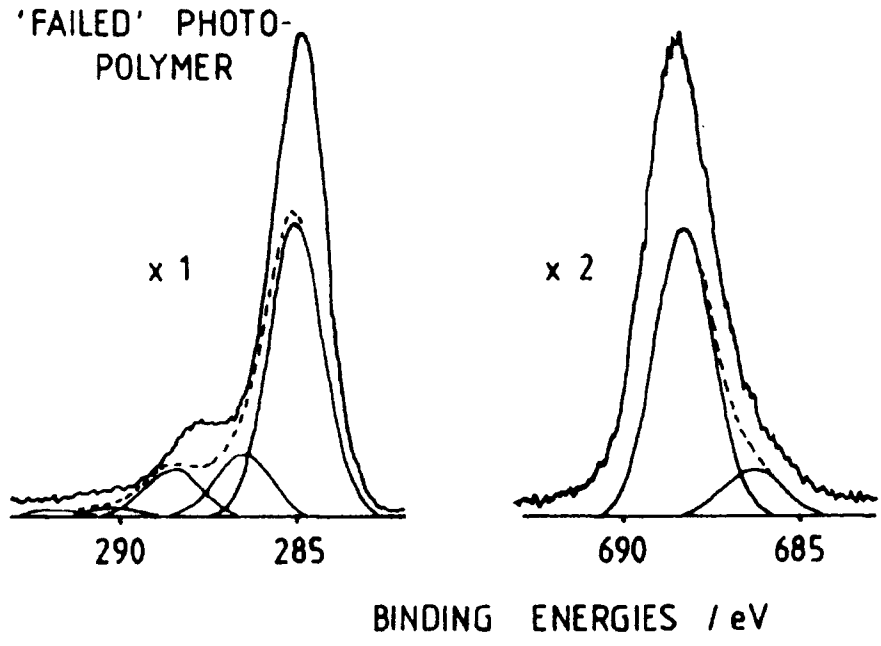

FIGURE 7.10 C_{1s} and F_{1s} core level spectra for VUV irradiated PFB in the presence of polymer film on the window

be associated with a reduction in the transmission efficiency of the window caused by a build up of polymer on the calcium fluoride surface. From the signal intensity of the fluorine, it is apparent that there is more than a monolayer coverage of fluorocarbon, but the peak to lower binding energies is still present at around 10% intensity. Hence there has been some reaction of the perfluorobenzene. This result could be explained in terms of the effective quanta of light per second reaching the organic vapour and/or the maximum energy available. When the surface of the window is covered by a deposit the amount of light being absorbed by the window is greatly increased, and initial reactions will be slowed down. It is more likely that the shorter wavelengths will be absorbed by the film on the window. These facts indicate that the C_{1s} spectrum seen in Figure 7.10 is either the result of the very initial stages of polymer formation or else the effective energy required for photopolymerization/plasma polymerization is not present, but that there is sufficient energy to initiate some other reaction pathway of PFB. This problem is not resolved by increasing the irradiation exposure time; while wavelengths sufficient to cause polymerization are being transmitted to the organic vapour, polymer film will be continuously deposited on the window throughout the length of the experiment until this deposit absorbs all the effective wavelengths and polymerization stops.

However, the intensity of the lower binding energy fluorine peak was found to give some indication of film coverage, as can be seen from the graph of the intensity of this peak time (Figure 7.11). The graph forms an exponential decay curve with the intensity of this peak at 60 mins being just visible above the background.

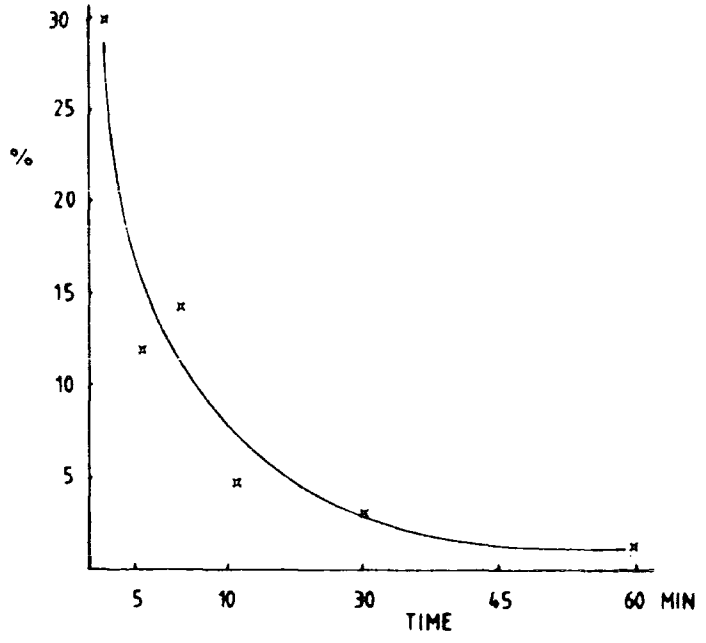

FIGURE 7.11 Intensity of the lower binding energy F_{1s} peak with time

---

In the work by D.T. Clark and M.Z. AbRaham[41] on the plasma polymerization of perfluorocarbons, especially of perfluorobenze, deposited onto gold an asymmetry of the F_{1s} photoionisation peak was noticed due to the presence of a low binding energy peak. An explanation for the origin of this peak was not, however, given. It could, perhaps, in view of the results just discussed be due to an interfacial interaction of the perfluorobenzene with the gold substrate.

(c) Vacuum UV irradiation of perfluorobenzene/benzene

Figure 7.12 displays the relevant C_{1s} core level spectra for the surface photo- and plasma polymers derived from a 1:1 gas phase composition of perfluorobenzene and benzene. The C:F atomic ratios of the copolymers correspond to a 1:1 contribution from benzene and perfluorobenzene. Similar results have also been observed in the plasma copolymerization of C_6H_6/C_6F_6, $C_{10}H_8/C_{10}F_8$, $C_{10}H_{12}/C_{10}F_{12}$ and $C_6F_6/(CH_3)_4Sn$.[42]

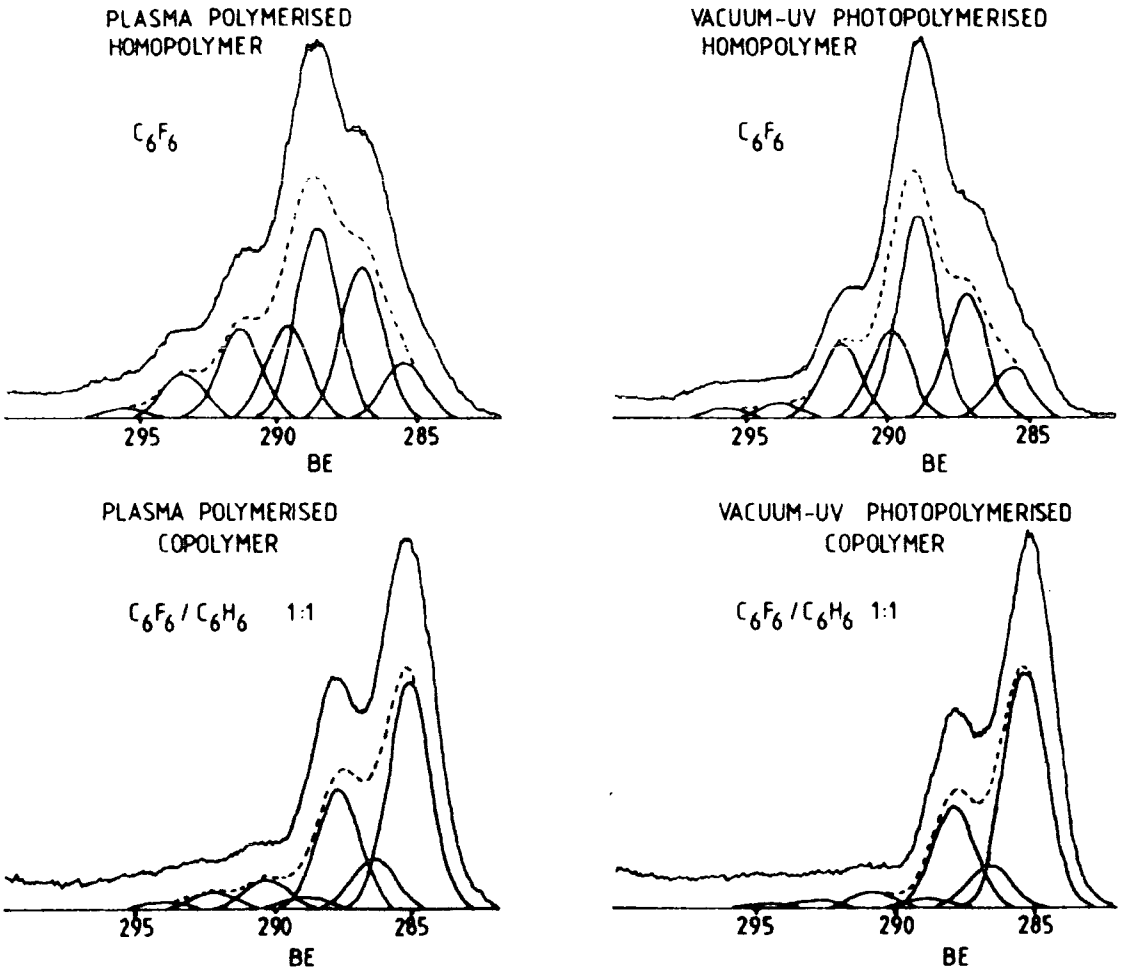

FIGURE 7.12 C_{1s} core level spectra for plasma polymers and VUV photopolymers derived from PFB and a 1:1 PFB/B mixture

---

A fuller discussion is given in Chapters Five/Six which are based on the copolymerization in their own right. It is sufficient and pertinent to point out here, that as in plasma copolymerization, the perfluoroaromatic does not exhibit the same degree of fragmentation and rearrangement in the C_{1s} envelope. The deposited film also appears to retain to a greater extent the aromatic features of the starting 'monomer', as evidenced by the greater intensity of the shake-up satellites in both the F_{1s} and C_{1s} core level spectrum.

The main feature to be gained from these results is that the copolymers obtained by vacuum UV and plasma techniques are

essentially the same. Thus as in the case for the 'homo-polymers', the reactions involved in the formation of building blocks for polymer deposition in the two methods could be derived from the same excited states. In one case these are formed by the absorption of vacuum UV and in the other by electron impact excitation.

It has been suggested that the valence isomers and polymer formation observed in the vacuum UV photolysis of benzene arises from the decay of third excited singlet state of benzene into a super vibrationally excited ground state singlet. It is from this latter state that the photolysis products are formed.[12d] Vibrationally excited ground electronic states have also been proposed in connection with the vacuum UV photolysis of o-xylene.[43]

Similarly, evidence has been presented which has been interpreted as indicative of an intermediate vibrationally excited ground state of 1,4,5-cycloheptatriene[44] in the gas phase photoinduced rearrangement to toluene. It was seen that as the pressure is increased the quantum yield of toluene, from near unity at very low pressures decreased very rapidly to 0.081 at 2.6mm.Hg.

Ward and Wishnok observed in their studies of the gas phase photolysis of benzene[12d] that the major photoproducts at low pressure were fulvene, 1,3-hexadiene-5-yne and polymer (uncharacterised). They proposed that although the initial excitation was to high electronically excited states (*e.g.* S_3) these did not go directly to photoproducts. The quantum yields of product formation exhibited a pressure dependence which would not be expected if these states were directly

involved, due to their lifetimes being too short to be affected by collisions. Further, due to the very low emission arising from S_1 to S_o transitions, the decay of the higher S_n states did not follow the pathway $S_3 \rightarrow S_2 \rightarrow S_1$, but crossed over to a vibrationally excited ground electronic state of benzene (S_o^v). It is from this state that the pathways for the photoproducts are thought to occur.[12d] The fluorescent yield of hexafluorobenzene is also very small[45] and therefore a similar situation may also be valid for perfluorobenzene.

Figure 7.13 displays a generalised scheme for the electron impact excitation of benzene or perfluorobenzene, and incor-

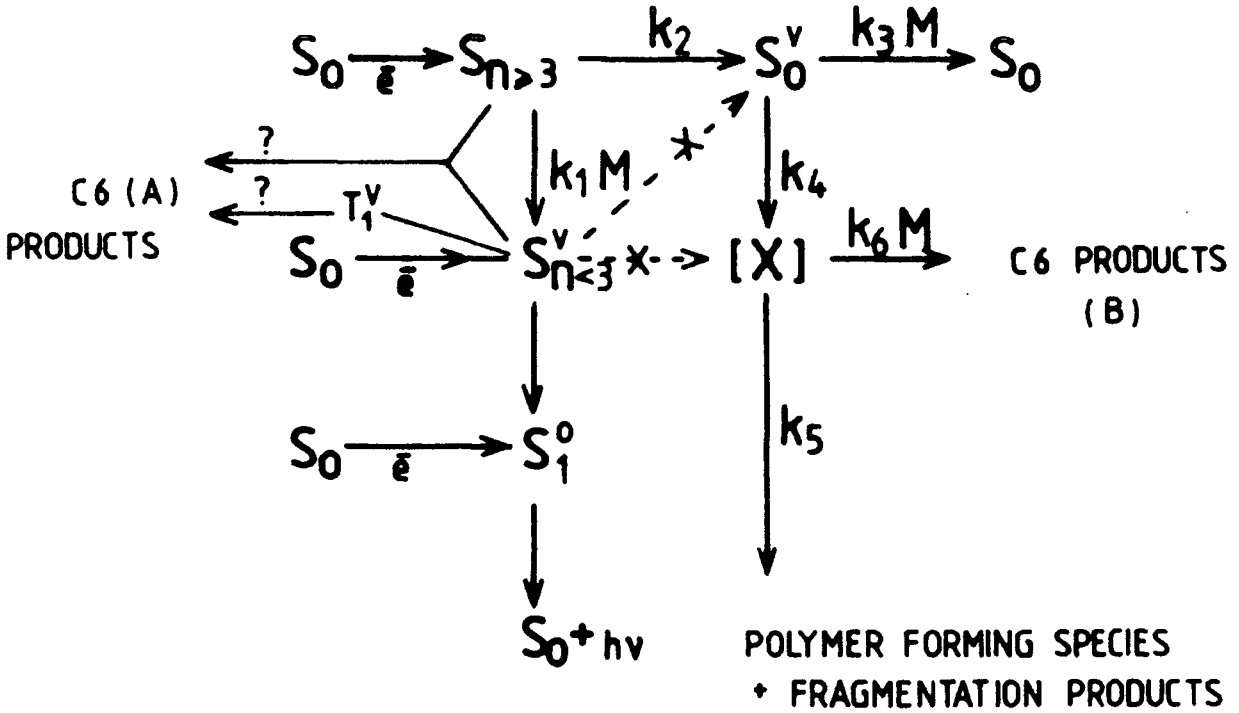

FIGURE 7.13 A generalised scheme for electron impact excitation of B or PFB

porates the features proposed by Ward and Wishnok[12d] for the photolysis of benzene. Electron impact within the plasma will give rise to large numbers of molecular electronically excited states below the ionisation potential directly, or by internal conversion/intersystem crossing. The minor role of the $S_n \rightarrow S_o$ pathways in the plasma of aromatic compounds may be demonstrated by the weak fluorescence decay in the photolysis of perfluorobenzene,[45] in the plasma S_1 states may be formed by direct electron impact excitation. The inclusion of C-6 products A allows for the valence isomers that arise from the S_1 and S_2 states. These states do not directly contribute to the formation of states leading to C-6 products B and the polymer forming species. Evidence for this arises from the lack of photopolymer formation during irradiations at λ>200nm. The exact nature of the intermediate X is at present unknown. However, its existence, postulated by Ward and Wishnok,[12d] is indicated by the pressure independence of C-6 products B *versus* polymer formation.

Confirmatory evidence on the existence of vibrationally highly excited ground state perfluorobenzene molecules, PFB*, is found in the work of K. Yoshihara *et al*[46,47]. They found that PFB, on excitation with a 193nm laser beam, rapidly converted from the S_3 level to the ground electronic state by internal conversion.[46] The lifetime of this state was very dependent on the pressure of inert gas added to the system. At 2 torr pressure of PFB vapour, PFB* had a lifetime of micro seconds, whilst an addition of 20 torr of N_2 collisional deactivation of PFB* resulted in a lifetime of nanoseconds. Work on benzene by the same authors has also shown the presence of vibrationally highly excited ground state benzene molecules following laser excitation.[47]

7.4 Conclusion

Analysis by ESCA and SIMS of the polymer films derived from N vinyl pyrrolidone vapour by both photo irradiation and plasma polymerization indicate that two distinct types of polymer composition are formed. Both closely retain the stoichiometry of the starting monomer, *i.e.* $C_1:N_{0.13}:O_{0.14}$ *c.f.* $C_1:N_{0.16}:O_{0.16}$.

Using a high flow rate of N vinyl pyrrolidone, a film whose surface composition gives the polymer a very high surface energy (with a contact angle of $<5^{o}$) is produced irrespective of the method of polymerization, *i.e.* plasma polymerization, or vacuum UV irradiation.

At a lower flow rate vacuum UV irradiation or plasma polymerization produces a film whose composition bestows the polymer with a lower surface energy (with a contact angle of $\sim 50^{o}$). An exception, however, is the high flow rate polymer produced by UV irradiation which more strongly resembles the latter polymer type. This is believed to be explained by $^{W}/_{FM}$ considerations.

Only vacuum UV irradiation is effective in producing a photopolymer of perfluorobenzene. ESCA analysis of the films formed by vacuum UV irradiation and plasma polymerization of perfluorobenzene and a 1:1 perfluorobenzene/benzene mixture reveal that they are very similar in composition; both containing functional groups not originally present in the monomer, and both retain the C:F stoichiometry of the parent compound.

This suggests that for plasma polymerization, polymer forming species arise from electronically excited states caused

mainly by electron impact of electrons whose energy is in the 6-8eV range. This indicates that for perfluorobenzene radical cation formation, although essential for plasma maintenance and colour, is not involved directly in polymer formation within a plasma.

In conclusion it would appear certainly for perfluorobenzene and N vinyl pyrrolidone that plasma polymerization and vacuum UV photopolymerization are very similar in their mechanistic aspects. Ionization does not need to be invoked in the mechanism of polymer formation within a plasma, rather, the photochemistry of the monomer should be considered.

REFERENCES - Chapter Seven

1. D.O. Cowan and R.L. Drisko, 'Elements of Organic Photochemistry', Plenum Press, N.Y. (1976).

2a. G.B. Kistiakowsky and T.A. Walter, J.Phys.Chem., 72, 3952, (1968).

2b. G. Gee, Trans. Faraday Soc., 34, 712 (1938).

2c. R. Srinivasan, J.Am.Chem.Soc., 82, 5063 (1960).

3. A.N. Wright in 'Polymer Surfaces', D.T. Clark, W.J.Feast (Eds.), Wiley Interscience, London (1978).

4. A.N. Wright, Nature, 215, 935 (1967).

5. A.N. Wright, General Electric Publication, GP-67-0382.

6. J.M. Tibbett, M. Shen and A.T. Bell, Thin Solid Films, 29, 243 (1975).

7. A.N. Wright and R.C. Merrill, U.S.Patent 3 743,532 (1973).

8. I. Haller and R. Srinivasan, J.Chem.Phys. 40, 1992 (1964).

9. R.R. Hentz and M. Burton, J.Am.Chem.Soc., 73, 532 (1951).

10. for example, P.G. Wilkinson, J.Opt.Soc.Am., 45 1044 (1955).

11. R.D. Doepker, J.Phys.Chem., 72, 4037 (1968).

12a. K. Shindo and S. Lipsky, J.Chem.Phys., 45, 2292 (1966).

12b. R.R. Hentz and S.J. Rzad, J.Phys.Chem., 71(12), 4096 (1967).

12c. W.M. Jackson, J.L. Faris and B. Donn, J.Phys.Chem. 71(10), 3346 (1967).

12d. H.R.Ward and J.S. Wishnok, J.Am.Chem.Soc., 90(20), 5353 (1968).

13. From J.E. Wilson and W.A. Noyes, Jr., J.Am.Chem.Soc., 63, 3025, 1941 ref. to S.C. Lind, R. Livingston, J.Am.Chem. Soc. 54 94 (1932).

14. C.A. Jenson and W.F. Libby, J.Chem.Phys., 49, 2831 (1968).

15. A.A. Scala and P. Ausloos, J.Chem.Phys. 49(5), 2282 (1968).

16. O.P. Strausz, P.J. Kozak, G.N.C. Woodall, A.G. Sherwood and H. E. Gunning, Can.J.Chem., 46, 1317 (1968).

17. H. Okabe, J.Opt.Soc.Am. 54(4), 478 (1964).

18. G.A. Corbin, R.E. Cohen and R.F. Baddour, Macromolecules 18(1), 98 (1985).

19. H. Yasuda, Appl. Polym.Sci.Symp. No.22, 241 (1973).

20. M. Bleha and D. Lim, J.Polym.Sci., Part C 23, 15 (1968).

21. I. Haller and P. White, J.Phys.Chem., 67, 1784 (1963).

22. D.T. Clark, Adv.Polym.Sci., 24, 125 (1977).

23. H. Yasuda and T. Hirotsu, J.Polym.Sci., Polym.Chem.Ed., 16, 743 (1976).

24. G.R. Eyre and H.S. Munro, in preparation.

25. J.W.T. Spinks and R.J. Woods in "An Introduction to Radiation Chemistry", John Wiley, N.Y., Chapter 12 (1964).

26. C. Sandorfy, Topics in Current Chem., No.86, Springer-Verlag, N.Y. (1979).

27. R.M. Silverstein, G.C. Bassler and T.C. Morrill, 'Spectrometric Identification of Organic Compounds' 4th Ed., Wiley, N.Y. (1981).

28. C.R. Brundle, M.B. Robin and N.A. Kuebler, J.Am.Chem.Soc., 94(5), 1466 (1972).

29. C. Sandorfy, Atmos.Environ. 10, 343 (1976).

30. R. Gilbert, P. Sauvageau and C. Sandorfy, Canadian J.Chem., 50, 543 (1972).

31. G. Belanger, P. Sauvageau and C. Sandorfy, Chem.Phys.Lett., 3, 649 (1969).

32. I. Haller, J.Am.Chem.Soc., 88, 2070 (1966).

33. D.T. Clark and A. Dilks, J.Polym.Sci., Polym.Chem.Ed., 18, 1233 (1980).

34. J.W. Robinson, (Ed.), C.R.C. Handbook of Spectroscopy, Vol.1, C.R.C. Press, Cleveland, OH. (1974).

35. D.T. Clark and D.B. Adams, Theoret.Chim.Acta (Berlin), 39, 321 (1975).

36. D.T. Clark and M.Z. AbRahman, J.Polym.Sci., Polym.Chem.Ed., 20, 1729 (1982).

37. H.Suhr and G. Rosskamp, Liebigs Ann.Chem., 742, 43 (1970).

38. H. Suhr in 'Techniques and Applications of Plasma Chemistry', J.Hollahan, A.T. Bell (Eds.), Wiley-Interscience, N.Y. (1974), Chapter 2.

39. G.M. Gooseedge and P. Cadman, J.Mat.Sci., 14, 2672 (1979).

40. R.A. Pierotti, J.Phys.Chem., 66, 1810 (1962).

41. M.Z. AbRahman, Ph.D. Thesis, Durham, U.K. (1981).

42. H.S. Munro and C. Till, Thin Solid Films, 131,255 (1985).

43. H.R. Ward, and C.I. Barta, J.Am.Chem.Soc., 90(20), 534 (1968).

44. R. Srinivasan, J.Am.Chem.Soc., 84, 3982 (1962).

45. D. Phillips, J.Chem.Phys., 46, 4679 (1967).

46. T. Ichimura, Y. Mori, N. Nakashima and K. Yoshihara, Chem.Phys.Lett., 104(6), 533 (1984).

47. N. Nakashima, and K. Yoshihara, J.Chem.Phys., 79, 2727 (1983).

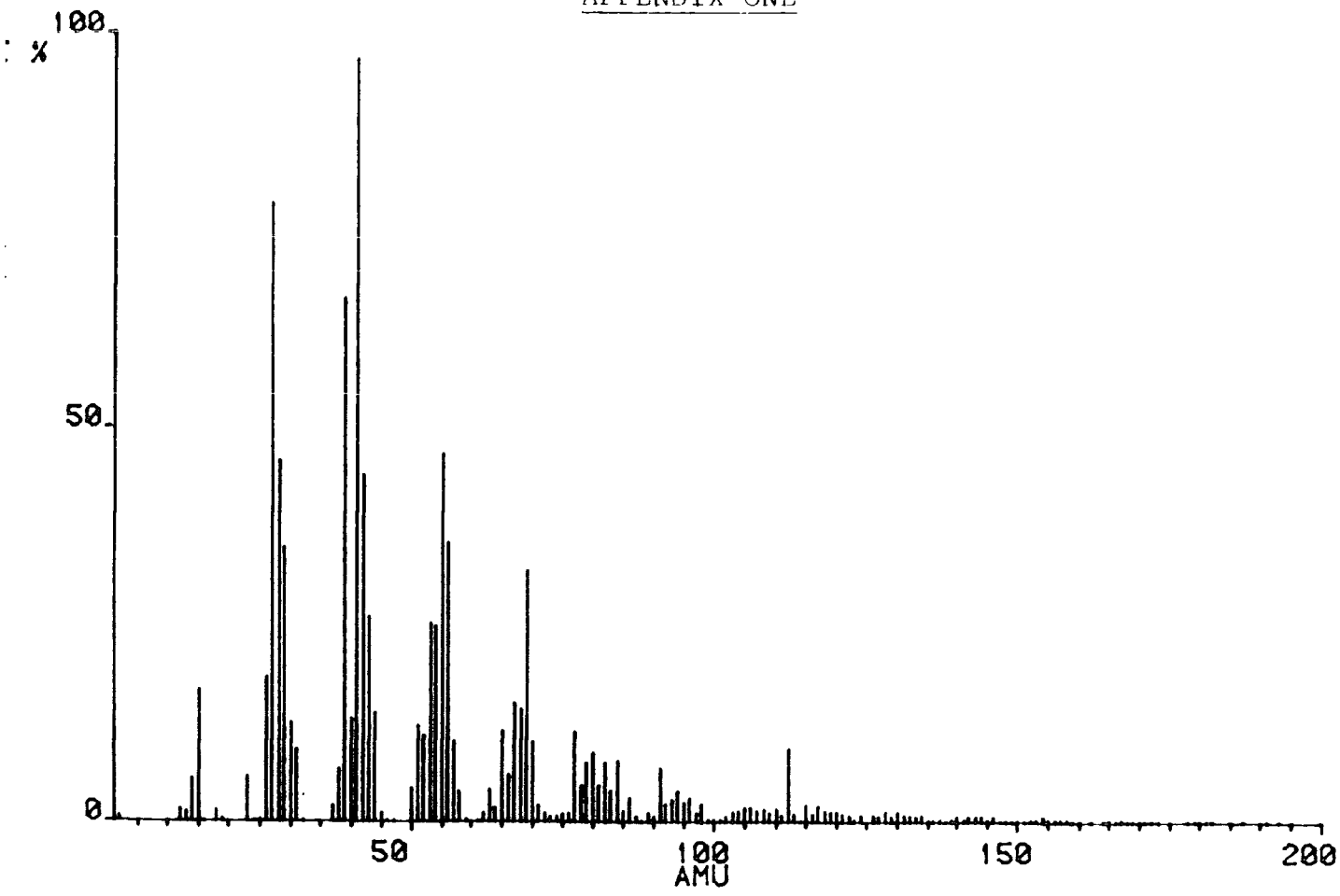

SIMS spectra for UV ($\lambda \geq 200nm$) polymerized NVP under (I) high and (II) low flow rate conditions.

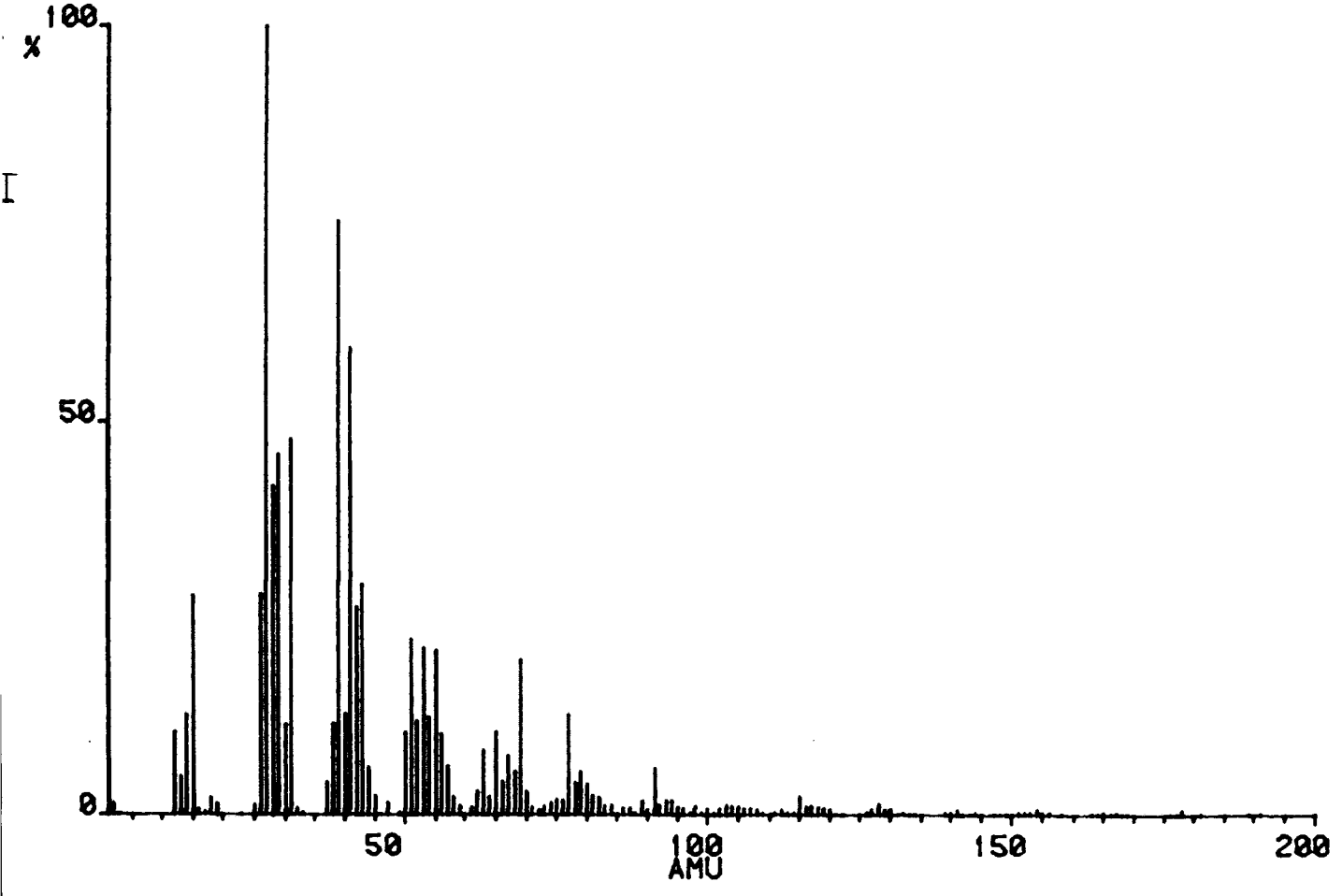

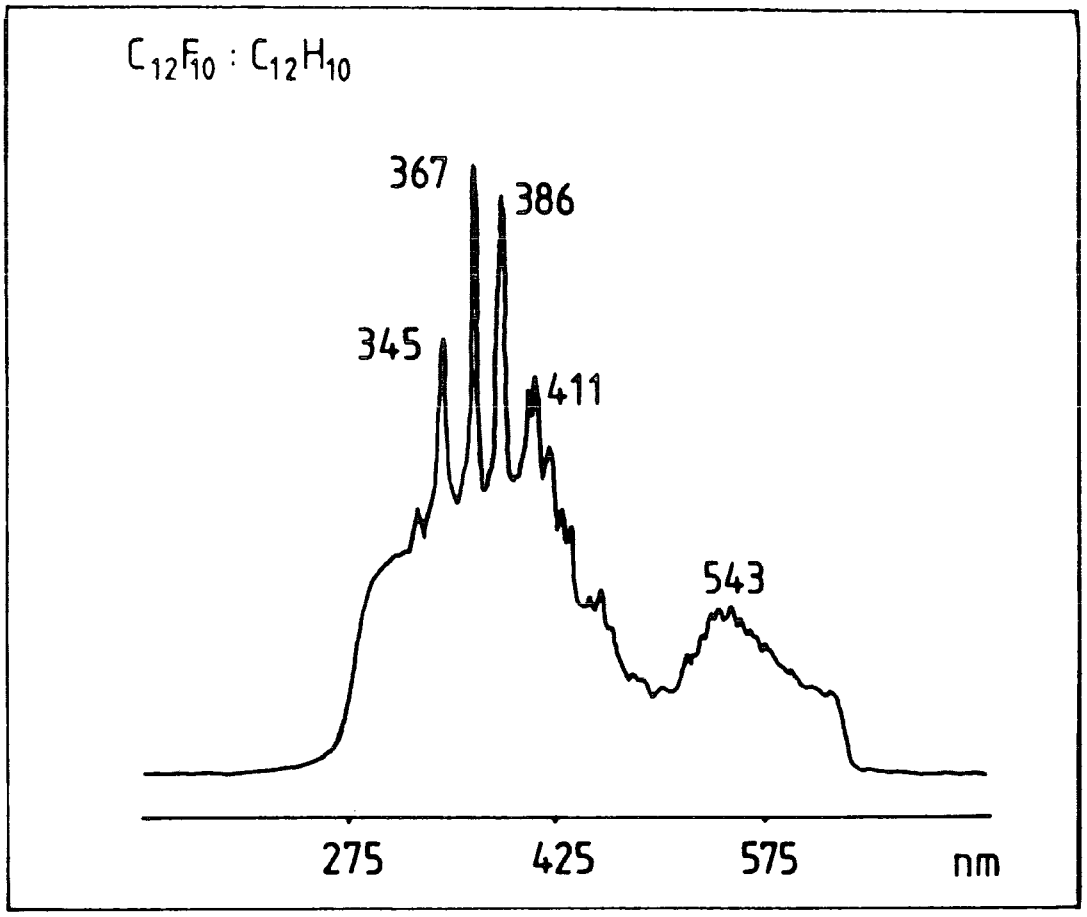
$C_{12}F_{10} : C_{12}H_{10}$
367
386
345
411
543
275
425
575
nm

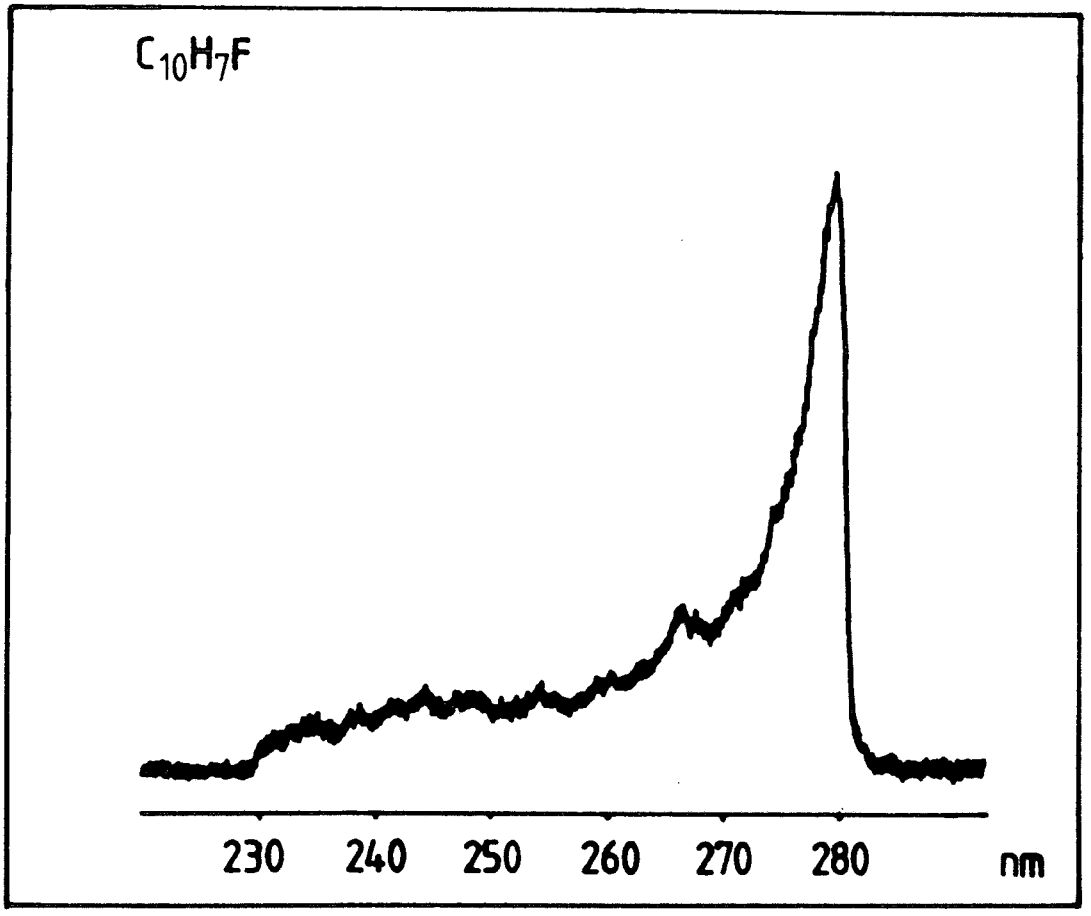
$C_{10}H_7F$
230
240
250
260
270
280
nm

APPENDIX TWO

The sensitivity factor of X, relative to carbon C, can be calculated from the formula:

$$\frac{X}{C} = \frac{\sigma_x^*}{\sigma_c^*} \quad \frac{KE_x^{1.5}}{KE_c^{1.5}}$$

where

σ^* is the corrected photoionisation cross section and KE is the kinetic energy of the photoelectron.

σ^* can be calculated from

$$\sigma^* = \frac{\sigma}{4\pi} \quad (1 - \frac{\beta}{2} (\frac{3}{2} \cos^2\theta - \frac{1}{2})$$

σ = photoionisation cross section

β = an asymmetry parameter of the core level

θ = the angle between photon source and analyser

Both σ and β have tabulated values which can be found in J.Electron.Spec.Related Phenom., 8, 129 (1976)
ibid 8, 389 (1976).

The sensitivity factors used in this thesis are:

$^{c,e}F_{1s}$	x 0.52	$^{e}Si_{2p}$	x 0.97	$^{e}Hg_{4f}$	x 0.16
$^{c,e}O_{1s}$	x 0.55	$^{c}Ge_{3d}$	x 0.52		
$^{e}N_{1s}$	x 0.76	$^{c}Sn_{3d}$	x 0.11		

e = EXPERIMENTAL c = CALCULATED

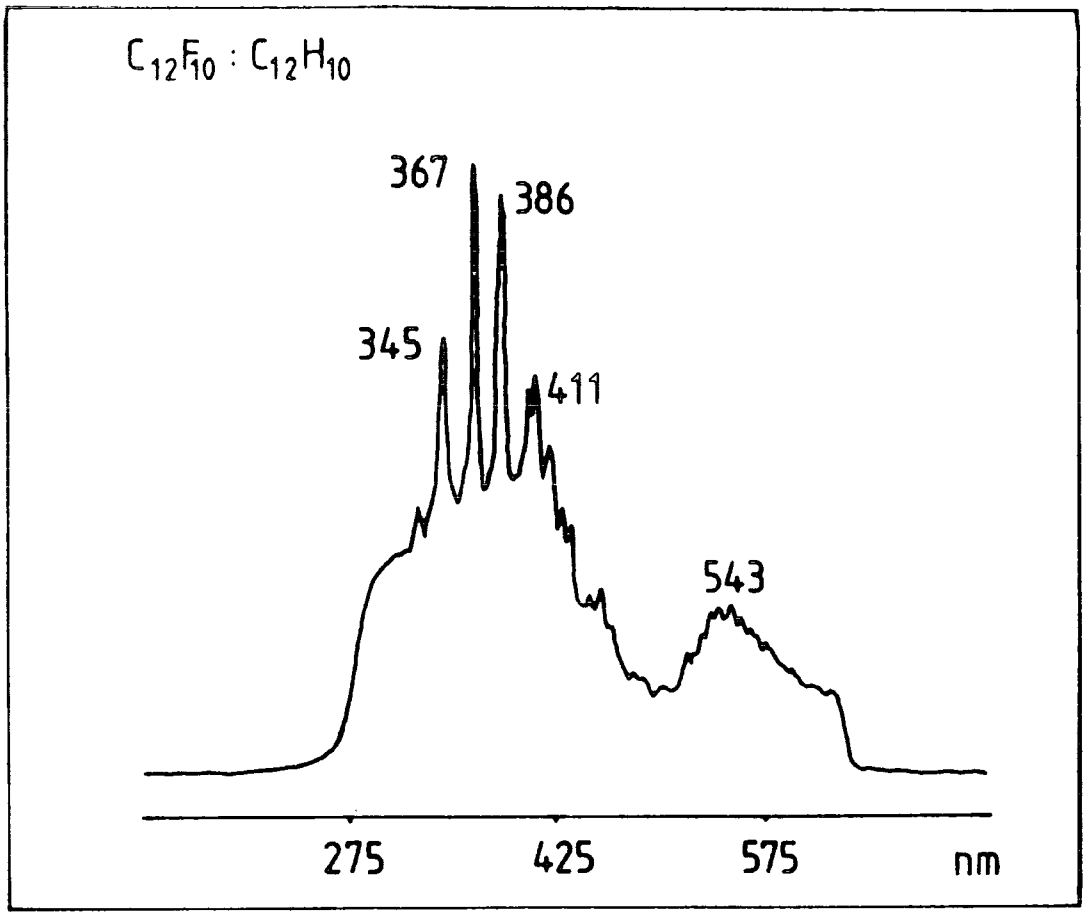
$C_{12}F_{10} : C_{12}H_{10}$
367
386
345
411
543
275
425
575
nm

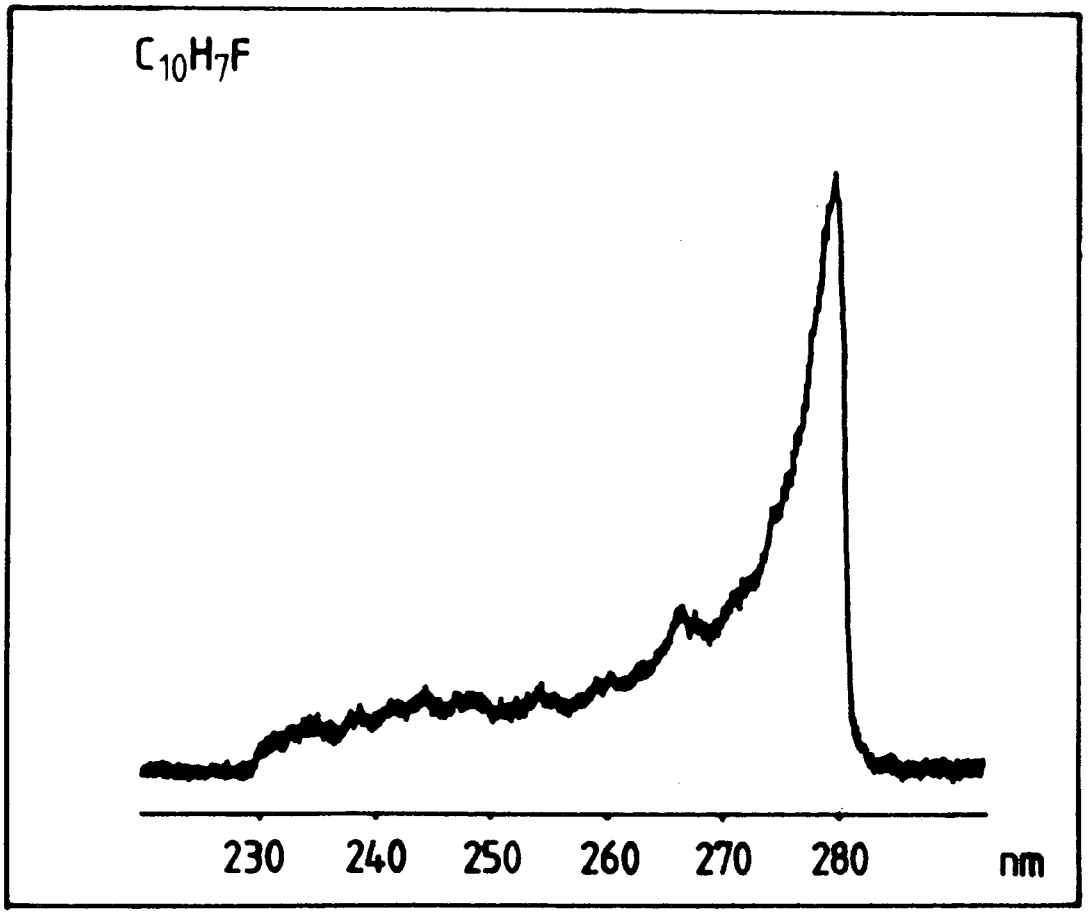
$C_{10}H_7F$
230
240
250
260
270
280
nm

RESEARCH COLLOQUIA, SEMINARS, LECTURES AND CONFERENCES

The Board of Studies in Chemistry requires that each postgraduate research thesis contains an appendix, listing:

(A) all research colloquia, research seminars and lectures arranged by the Department of Chemistry during the period of the author's residence as a postgraduate student;

(B) Lectures organised by Durham University Chemical Society;

(C) all research conferences attended and papers presented by the author during the period when research for the thesis was carried out;

(D) details of the postgraduate induction course.

(A) LECTURES ORGANISED BY DURHAM UNIVERSITY - 1983-1986.

5.10.83 Prof. J.P. Maier (Basel, Switzerland) "Recent approaches to spectroscopic characterization of cations".

12.10.83 Dr. C.W. McLeland (Port Elizabeth, Australia), "Cyclization of aryl alcohols through the intermediacy of alkoxy radicals and aryl radical cations".

19.10.83 Dr. N.W. Alcock (Warwick), "Aryl tellurium (IV) compounds, patterns of primary and secondary bonding".

26.10.83 Dr. R.H. Friend (Cavendish, Cambridge), "Electronic properties of conjugated polymers".

30.11.83 Prof. I.M.G. Cowie (Stirling), "Molecular interpretation of non-relaxation processes in polymer glasses".

2.12.83 Dr. G.M. Brooke (Durham), "The fate of the ortho-fluorine in 3,3-sigmatropic reactions involving polyfluoro-aryl and -hetero-aryl systems".

14.12.83 Prof. R.J. Donovan (Edinburgh), "Chemical and physical processes involving the ion-pair states of the halogen molecules".

10. 1.84 Prof. R. Hester (York)
"Nanosecond Laser Spectroscopy of Reaction Intermediates"

18. 1.84 Prof. R.K. Harris (UEA)
"Multi-nuclear solid state magnetic resonance"

8. 2.84 Dr. B.T. Heaton (Kent)
"Multi-nuclear NMR studies"

15. 2.84 Dr. R.M. Paton (Edinburgh)
"Heterocyclic Syntheses using Nitrile Sulphides"

7. 3.84 Dr. R.T. Walker (Birmingham),
"Synthesis and Biological Properties of some 5-substituted Uracic Derivatives; yet another example of serendipity in Anti-viral Chemotherapy"

21. 3.84 Dr. P. Sherwood (Newcastle)
"X-ray photoelectron spectroscopic studies of electrode and other surfaces"

21. 3.84 Dr. G. Beamson (Durham/Kratos)
"EXAFS: General Principles and Applications"

23. 3.84 Dr. A. Ceulemans (Leuven)
"The Development of Field-Type models of the Bonding in Molecular Clusters"

2. 4.84 Prof. K. O'Driscoll (Waterloo)
"Chain Ending reactions in Free Radical Polymerisation"

3. 4.84 Prof. C.H. Rochester (Dundee)
"Infrared Studies of adsorption at the Solid-Liquid Interface"

25. 4.84 Dr. R.M. Acheson (Biochemistry, Oxford)
"Some Heterocyclic Detective Stories"

27. 4.84 Dr. T. Albright (Houston, U.S.A.)
"Sigmatropic Rearrangements in Organometallic Chemistry"

14. 5.84 Prof. W.R. Dolbier (Florida, USA)
"Cycloaddition Reactions of Fluorinated Allenes"

16. 5.84 Dr. P.J. Garratt (UCL)
"Synthesis with Dilithiated Vicinal Diesters and Carboximides"

22. 5.84 Prof. F.C. de Schryver (Leuven)
"The use of Luminescence in the study of micellar aggregates" and
"Configurational and Conformational control in excited state complex formation"

23. 5.84 Prof. M. Tada (Waseda, Japan)
"Photochemistry of Dicyanopyrazine Derivatives"

31. 5.84 Dr. A. Haaland (Oslo)
"Electron Diffraction Studies of some organometallic compounds"

11. 6.84 Dr. J.B. Street (IBM, California)
"Conducting Polymers derived from Pyrroles"

19. 9.84 Dr. C. Brown (IBM, California)
"New Superbase reactions with organic compounds"

21. 9.84 Dr. H.W. Gibson (Signal UOP, Illinois)
"Isomerization of Polyacetylene"

19.10.84 Dr. A. Germain (Languedoc, Montpellier)
"Anodic Oxidation of Perfluoro Organic Compounds in Perfluoroalkane Sulphonic Acids"

24.10.84 Prof. R.K. Harris (Durham)
"N.M.R. of Solid Polymers"

28.10.84 Dr. R. Snaith (Strathclyde)
"Exploring Lithium Chemistry: Novel Structures, Bonding and Reagents"

7.11.84 Prof. W.W. Porterfield (Hampden-Sydney College, USA)
"There is no Borane Chemistry (only Geometry)"

7.11.84 Dr. H.S. Munro (Durham)
"New Information from ESCA Data"

21.11.84 Mr. N. Everall (Durham)
"Picosecond Pulsed Laser Raman Spectroscopy

27.11.84 Dr. W.J. Feast (Durham)
"A Plain Man's Guide to Polymeric Organic Metals"

28.11.84 Dr. T.A. Stephenson (Edinburgh)
"Some recent studies in Platinum Metal Chemistry"

12.12.84 Dr. K.B. Dillon (Durham)
"^{31}P N.M.R. Studies of some Anionic Phosphorus Complexes"

11. 1.85 Emeritus Prof. H. Suschitzky (Salford)
"Fruitful Fissons of Benzofuroxanes and Isobenzimic azoles (umpolung of o-phenylenediamine)"

13. 2.85 Dr. G.W.J. Fleet (Oxford)
"Synthesis of some Alkaloids from Carbohydrates"

19. 2.85 Dr. D.J. Mincher (Durham)
"Stereoselective Synthesis of some novel Anthracyclinones related to the anti-cancer drug Adriamy and to the Steffimycin Antibiotics"

27. 2.85 Dr. R. Mulvey (Durham)
"Some unusual Lithium Complexes"

6. 3.85 Dr. P.J. Kocienski (Leeds)
"Some Synthetic Applications of Silicon-Mediated Annulation Reactions"

7. 3.85 Dr. P.J. Rodgers (I.C.I. plc. Agricultural Division, Billingham)
"Industrial Polymers from Bacteria"

12. 3.85 Prof. K.J. Packer (B.P. Ltd./East Anglia)
"N.M.R. Investigations of the Structure of Solid Polymers"

14. 3.85 Prof. A.R. Katritzky F.R.S. (Florida)
"Some Adventures in Heterocyclic Chemistry"

20. 3.85 Dr. M. Poliakoff (Nottingham)
"New Methods for detecting Organometallic Intermediates in Solution"

28. 3.85 Prof. H. Ringsdorf (Mainz)
"Polymeric Liposomes as Models for Biomembranes and Cells?"

24. 4.85 Dr. M.C. Grossel (Bedford College, London)
"Hydroxypyridone dyes - Bleachable one-dimensional Metals?"

25. 4.85 Major S.A. Shackelford (U.S. Air Force)
"In Situ Mechanistic Studies on Cendensed Phase Thermochemical Reaction Processes: Deuterium Isotope Effects in HMX Decomposition, Explosives and Combustion"

1. 5.85 Dr. D. Parker (I.C.I. plc. Petrochemical and Plastics Division, Wilton)
"Applications of Radioisotopes in Industrial Research"

7. 5.85 Prof. G.E. Coates (formerly of University of Wymoning, U.S.A.)
"Chemical Education in England and America: Successes and Deficiencies"

8. 5.85 Prof. D. Tuck (Windsor, Ontario)
"Lower Oxidation State Chemistry of Indium"

8. 5.85 Prof. G. Williams (U.C.W. Aberystwyth)
"Liquid Crystalline Polymers"

9. 5.85 Prof. R.K. Harris (Durham)
"Chemistry in a Spin: Nuclear Magnetic Resonance"

14. 5.85 Prof. J. Passmore (New Brunswick, U.S.A.)
"The Synthesis and Characterisation of some Novel Selenium-Iodine Cations, aided by ^{77}Se N.M.R. Spectroscopy"

15. 5.85 Dr. J.E. Packer (Auckland, New Zealand)
Studies of Free Radical Reactions in aqueous solution using Ionising Radiation"

17. 5.85 Prof. I.D. Brown (McMaster University, Canada)
"Bond Valence as a Model for Inorganic Chemistry"

21. 5.85 Dr. D.L.H. Williams (Durham)
"Chemistry in Colour"

22. 5.85 Dr. M. Hudlicky (Blacksburg, U.S.A.)
"Preferential Elimination of Hydrogen Fluoride from Vicinal Bromofluorocompounds"

22. 5.85 Dr. R. Grimmett (Otago, New Zealand)
"Some Aspects of Nucleophilic Substitution in Imidazoles"

4. 6.85 Dr. P.S. Belton (Food Research Institute, Norwich)
"Analytical Photoacoustic Spectroscopy"

13. 6.85 Dr. D. Woolins (Imperial College, London)
"Metal - Sulphur - Nitrogen Complexes"

14. 6.85 Prof. Z. Rappoport (Hebrew University, Jerusalem)
"The Rich Mechanistic World of Nucleophilic Cinylic Substitution"

19. 6.85 Dr. R.N. Mitchell (Dortmund)
"Some Synthetic and NMR - Spectroscopic Studies of Organotin Compounds"

26. 6.85 Prof. G. Shaw (Bradford)
"Synthetic Studies on Imidazole Nucleosides and the Antibiotic Coformycin"

12. 7.85 Dr. K. Laali (Hydrocarbon Research Institute, University of Southern California)
"Recent Developments in Superacid Chemistry and Mechanistic Considerations in Electrophilic Aromatic Substitutions: A Progress Report"

13. 9.85 Dr. V.S. Parmar (University of Delhi),
"Enzyme Assisted ERC Synthesis"

30.10.85 Dr. S.N. Whittleton (University of Durham),
"An Investigation of a Reaction Window"

5.11.85 Prof. M.J. O'Donnell (Indiana-Purdue University),
"New Methodology for the Synthesis of Amino acids"

20.11.85 Dr. J.A.H. MacBride (Sunderland Polytechnic).
"A Heterocyclic Tour on a Distorted Tricycle-Biphenylene"

28.11.85 Prof. D.J. Waddington (University of York),
"Resources for the Chemistry Teacher"

15. 1.86 Prof. N. Sheppard (University of East Anglia),
"Vibrational and Spectroscopic Determinations of the Structures of Molecules Chemisorbed on Metal Surfaces"

29. 1.86 Dr. J.H. Clark (University of York),
"Novel Fluoride Ion Reagents"

12. 2.86 Prof. O.S. Tee (Concordia University, Montreal),
"Bromination of Phenols"

12. 2.86 Dr. J. Yarwood (University of Durham),
"The Structure of Water in Liquid Crystals"

19. 2.86 Prof. G. Procter (University of Salford),
"Approaches to the Synthesis of some Natural Products"

26. 2.86 Miss C. Till (University of Durham),
"ESCA and Optical Emission Studies of the Plasma Polymerisation of Perfluoroaromatics"

5. 3.86 Dr. D. Hathway (University of Durham),
"Herbicide Selectivity"

5. 3.86 Dr. M. Schroder (University of Edinburgh),
"Studies on Macrocycle Complexes"

12. 3.86 Dr. J.M. Brown (University of Oxford),
"Chelate Control in Homogeneous Catalysis"

14. 5.86 Dr. P.R.R. Langridge-Smith (University of Edinburgh),
"Naked Metal Clusters - Synthesis, Characterisation and Chemistry"

9. 6.86 Prof. R. Schmutzler (University of Braunschweig),
"Mixed Valence Diphosphorous Compounds"

23. 6.86 Prof. R.E. Wilde (Texas Technical University),
"Molecular Dynamic Processes from Vibrational Bandshapes"

B. Lectures Organised by Durham University Chemical Society during the period 1983-1986

20.10.83 Prof. R.B. Cundall (Salford)
"Explosives

3.11.83 Dr. G. Richards (Oxford)
"Quantum Pharmacology"

10.11.83 Prof. J.H. Ridd (U.C.L.).
"Ipso-Attack in Electrophilic Aromatic Substitution"

17.11.83 Dr. J. Harrison (Sterling Organic),
"Applied Chemistry and the Pharmaceutical Industry"
"Joint Lecture with the Society of Chemical Industry)

24.11.83 Prof. D.A. King (Liverpool),
"Chemistry in 2-Dimensions"

1.12.83 Dr. J.D. Coyle (The Open University),
"The Problem with Sunshine"

26. 1.84 Prof. T.L. Blundell (Birkbeck College, London)
"Biological Recognition: Interactions of Macromolecular Surfaces"

2. 2.84 Prof. N.B.H. Jonathan (Southampton),
"Photoelectron Spectroscopy - A Radical Approach"

16. 2.84 Prof. D. Phillips (The Royal Institution),
"Luminescence and Photochemistry - a Light Entertainment"

23. 2.84 Prof. F.G.A. Stone F.R.S. (Bristol),
"The Use of Carbene and Carbyne Groups to Synthesise Metal Clusters"
(The Waddington Memorial Lecture)

1. 3.84 Prof. A.J. Leadbetter (Rutherford Appleton Labs.),
"Liquid Crystals"

8. 3.84 Prof. D. Chapman (Royal Free Hospital School of Medicine, London)
"Phospholipids and Biomembranes: Basic Science and Future Techniques"

28. 3.84 Prof. H. Schmidbaur (Munich, F.R.G.),
"Ylides in Coordination Sphere of Metal: Synthetic, Structural and Theoretical Aspects"
(R.S.C. Centenary Lecture)

18.10.84 Dr. N. Logan (Nottingham),
"N_2O_4 and Rocket Fuels"

23.10.84 Dr. W.J. Feast (Durham),
"Syntheses of Conjugated Polymers. How and Why?"

8.11.84 Prof. B.J. Aylett (Queen Mary College, London),
"Silicon - Dead Common or Refined?"

15.11.84 Prof. B.T. Golding (Newcastle-upon-Tyne),
"The Vitamin B_{12} Mystery"

22.11.84 Prof. D.T. Clark (I.C.I. New Science Group),
"Structure, Bonding, Reactivity and Synthesis as revealed by ESCA"
(R.S.C. Tilden Lecture)

29.11.84 Prof. C.J.M. Stirling (University College of North Wales
"Molecules taking the Strain"

6.12.84 Prof. R.D. Chambers (Durham),
"The Unusual World of Fluorine"

24. 1.85 Dr. A.K. Covington (Newcastle-upon-Tyne),
"Chemistry with Chips"

31. 1.85 Dr. M.L.H. Green (Oxford),
"Naked Atoms and Negligee Ligands"

7. 2.85 Prof. A. Ledwith (Pilkington Bros.),
"Glass as a High Technology Material"
(Joint Lecture with the Society of Chemical Industry)

14. 2.85 Dr. J.A. Salthouse (Manchester),
"Son et Lumiere"

21. 2.85 Prof. P.M. Maitlis, F.R.S. (Sheffield),
"What Use is Rhodium?"

7. 3.85 Dr. P.W. Atkins (Oxford),
"Magnetic Reactions"

17.10.85 Dr. C.J. Ludman (University of Durham)
"Some Thermochemical aspects of Explosions"
"A Demonstration Lecture)

24.10.85 Dr. J. Dewing,(U.M.I.S.T.),
"Zeolites - Small Holes, Big Opportunities"

31.10.85 Dr. P. Timms,(University of Bristol),
"Some Chemistry of Fireworks"
(A Demonstration Lecture)

7.11.85 Prof. G. Ertl, (University of Munich),
"Heterogeneous Catalysis",
(R.S.C. Centenary Lecture)

14.11.85 Dr. S.G. Davies (University of Oxford),
"Chirality Control and Molecular Recognition"

21.11.85 Prof. K.H. Jack, F.R.S. (University of Newcastle/Tyne),
"Chemistry of Si-Al-O-N Engineering Ceramics"
(Joint Lecture with the Society of Chemical Industry)

28.11.85 Dr. B.A.J. Clark (Research Division, Kodak Ltd.)
"Chemistry and Principles of Colour Photography"

23. 1.86 Prof. Sir Jack Lewis, F.R.S. (University of Cambridge),
"Some More Recent Aspects in the Cluster Chemistry
of Ruthenium and Osmium Carbonyls"
(The Waddington Memorial Lecture)

30. 1.86 Dr. N.J. Phillips,(University of Technology, Loughborough)
"Laser Holography"

13. 2.86 Prof. R. Grigg (Queen's University, Belfast),
"Thermal Generation of 1,3-Dipoles"
(R.S.C. Tilden Lecture)

20. 2.86 Dr. C.J.F. Barnard,(Johnson Matthey Group Research),
"Platinum Anti-Cancer Drug Development - From
Serendipity to Science"

27. 2.86 Prof. R.K. Harris, (University of Durham),
"The Magic of Solid State NMR"

6. 3.86 Dr. B. Iddon (University of Salford),
"The Magic of Chemistry"
(A Demonstration Lecture)

(C) Research Conferences attended (* indicates Poster presentation)

January 1985 The 4th State of Matter: A challenge for the Future, I.C.I. Symposium, Wilton.

April 1985* Polymer Surfaces and Interfaces, University of Durham.

(D) First Year Induction Course, October 1982

This course consists of a series of one hour lectures on the services available in the department.

1. Departmental organisation
2. Safety matters
3. Electrical appliances and infrared spectroscopy
4. Chromatography and Microanalyais
5. Atomic absorptiometry and inorganic analysis
6. Library facilities
7. Mass spectroscopy
8. Nuclear magnetic resonance spectroscopy
9. Glassblowing technique.